Department of Civil Engineering

Assessment of the Impacts of Long-term Climate Change Variations on Catchment Hydrology

Hashim Isam Jameel Al-Safi

This thesis is presented for the Degree of
Doctor of Philosophy
of
Curtin University

March 2018

DECLARATION

To the best of my knowledge and belief, this thesis contains no material previously published by any other person except where due acknowledgement has been made.

This thesis contains no material which has been accepted for the award of any other degree or diploma in any university.

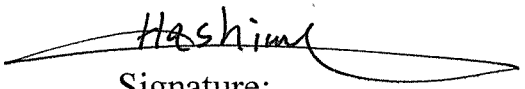

Signature:

Hashim Al-Safi

Date: 21/02/2018

ABSTRACT

Freshwater is one of the most vital resources in Australia and has a rapidly growing value in the economic, environmental and social sectors. Climate change can directly affect the availability of freshwater resources, mainly through changes in precipitation and temperature, and secondarily through changes in vegetation water use. There are clear evidences that climate change will affect the Australian rainfall and temperature trends across the continent. Water scarcity resulting from climate change impact is becoming a growing problem, especially in areas experiencing precipitation reduction and temperature increase. The hydrologic modelling is a widely adopted procedure, used to simulate the possible impacts of future climate changes on local and global scales. Future streamflow projection, using the hydrological modelling approaches, is a key element that can assist authorities and decision makers in a water-related sector for an effective water resources planning and management policies.

This thesis presents an assessment of the impacts of future climate changes on the hydrological characteristics of some local Australian catchments mainly located in New South Wales (NSW) and Western Australia (WA) states and the potential consequences on the availability of future water resources. Five catchments corresponding to five rivers were selected including Harvey River and Richmond River local catchments and three contributing catchments of the Australian Hydrologic Reference Stations namely Harvey River at Dingo Road, Beardy River at Haystack and Goulburn River at Coggan HRSs. The selected catchments are located in the south-western and south-eastern parts of Australia which are expected to be highly vulnerable to the impact of climate change. The key incentives behind the selection of the study area were firstly the selected rivers have received less attention to investigating their hydrological response to the future climate changes. Secondly, the selected catchments support a biodiversity of environmental and ecological communities. Furthermore, the selected rivers represent the main tributaries of surface water supply systems in their catchments. Therefore, assessing the impacts of future climate changes on the hydrological system of these rivers is highly beneficial to draw efficient and sustainable water management strategies in their contributing catchments.

Firstly, two different structured hydrological models, the conceptual modelling approach (HBV model) and the physically-based distributed hydrological model (BTOPMC model) were used to assess the impacts of climate change on flow regimes of the selected local catchments. The two models were calibrated and validated with acceptable modelling performance by using the observed streamflow in line with the observed weather data from the studied catchments. The general performance of the two models were relatively sensible in simulating the historical runoff volume at the three HRSs. The analysis of the results shows that there are no large differences in the modelling performance of the two

models. However, the conceptual model performs better than the distributed model in capturing the observed streamflow across the three contributing catchments (average values of NSE 0.9 versus 0.8).

Secondly, the global-scale future climate signals (monthly mean outputs) of rainfall and temperature were obtained from a multi-model ensemble of several Global Climate Models from the Coupled Model Intercomparison Project phase 3 (CMIP3) and phase 5 (CMIP5) of the Intergovernmental Panel on Climate Change, Fourth and Fifth Assessment Reports (AR4 and AR5). The future data has spanned the current century into three periods including the near future (2016-2035), mid (2046-2065) and late (2080-2099) of the 21st century. A baseline climatic period was also extracted from the multi-model ensemble to be compared with the future climate projections. The global-scale monthly outputs from each GCM were then downscaled into local-scale daily climate projections suitable for local impact assessment studies by using the statistical downscaling approach (LARS-WG5.5 and the BoM-SDM). Based on the downscaled daily mean temperature, the modified Blaney–Criddle method and Hargreaves method are employed to obtain the future Potential Evaporation across the studied catchments.

Overall modelling results of the downscaled GCMs show that the rainfall is anticipated to increase slightly during the near-future (0.3-2.6 %) and decrease during the mid and late century (1.4-23%) for all climate scenarios compared to the baseline period. Potential Evaporation (PE) is also projected to increase during the future periods under all scenarios (4-14.3%) because of the increase in annual mean temperature (0.15-2.4 ^{o}C) relative to the baseline period.

Finally, the two calibrated hydrological models were then forced with the ensemble-mean of the downscaled climate output (rainfall and temperature) to simulate the future daily streamflow at the downstream outlets of the studied catchments. A control run, with baseline climate period, was used to represent current climate status. The results of hydrological modelling of the two models showed positive trends in annual mean streamflow during the near-future and negative trends in the mid and late century under all scenarios compared to the control run.

The outcomes of this study specify that the potential changes in streamflow due to future climate changes could be very significant. The projected streamflow reduction would probably impose additional burdens on the currently available surface water resources and would affect the environmental and ecological communities in the studied catchments. Thus, options for additional water supply sources and adaptive responses would be essential in the future to support the economic and population development and to maintain sustainable ecological communities. The current findings could provide a theoretical basis to the communities and decision makers to manage the usage of future water resources in the selected catchments taking the expected streamflow reduction into account.

ACKNOWLEDGEMENTS

I would like to take this opportunity to express my sincere gratitude to my supervisor, Dr Rnajan Sarukkalige, for his continuous guidance and encouragement throughout this study. Without his advice and active support, this project would not have been possible.

My appreciation is also extended to Dr June Magome for his enormous knowledge and advice during learning the BTOPMC distributed model.

I would like to express my deepest thanks to the Iraqi government for the continuous financial support from the Higher Committee for Education Development in Iraq (HCED Iraq) for this great opportunity to complete my PhD study. I would also like to acknowledge Department of Civil Engineering of Curtin University for providing all sorts of support in conducting this research.

Last but not least, I would like to thank my dearest wife, for her permanent encouragement, understanding and generous support during my PhD study.

LIST OF PUBLICATION

Journal Papers

1- Al-Safi, H. I. J., & Sarukkalige, P. R. (2017). Assessment of future climate change impacts on hydrological behavior of Richmond River Catchment. *Water Science and Engineering*, 10(3), 197-208.

2- Al-Safi, H. I. J., & Sarukkalige, P. R. (2017). Evaluation of the impacts of future hydrological changes on the sustainable water resources management of the Richmond River catchment. *Journal of Water and Climate Change*, 9(1), 137-155.

3- Al-Safi, H. I. J., & Sarukkalige, P. R. (2018). The application of conceptual modelling to assess the impacts of future climate change on the hydrological response of the Harvey River catchment. *Journal of Hydro-environment Research*, (in press).

4- Al-Safi, H. I. J., & Sarukkalige, P. R. (2018). Hydrological impacts of climate change on the future streamflow of three unregulated catchments of the Australian hydrologic reference stations. *Int. J. Hydrology Science and Technology*, (in press).

5- Al-Safi, H. I. J., & Sarukkalige, P. R. (2018). A Conceptual Modelling Approach to Evaluate the Impacts of Climate Change on Future Streamflow in Unregulated Catchments. *Int. J. Hydrology Science and Technology*, (in press).

Papers in peer reviewed conference proceedings

6- Al-Safi, H. I. J., & Sarukkalige, P. R. (2017). Potential climate change impacts on the hydrological system of the Harvey River Catchment. World Academy of Science, Engineering and Technology, *International Journal of Environmental, Chemical, Ecological, Geological and Geophysical Engineering*, 11(4), 310-320.

7- Al-Safi, H. I. J. & Sarukkalige, P. R. (2017). Assessment of climate change impacts on the variability of future streamflow in a selected contributing catchment of the Australian Hydrologic Reference Stations. In: Proceedings of the 16th World Water Congress 'Bridging Science and Policy', Cancun, Mexico, pp.1–19.

TABLE OF CONTENTS

LIST OF FIGURES

LIST OF TABLES

Chapter 1

Research Overview

1.1 Background

Demand for fresh water in the future will be a significant issue due to climate change, ongoing population increase and agriculture and industrial expansion. Hence, many regions around the world are projected to experience a decline in the availability of water resources as a result of urbanizations, global warming and the extreme withdrawals of groundwater. Alternatively, other areas are expected to suffer from extreme weather events due to climate change that is resulting in floods, soil driftage and heat waves. Therefore, a sustainable planning response and potential change in the management of water resources is required to deal with such situations.

Australia could be considered as the driest inhabited continent in the world, with more than 60% of the continent receiving an annual mean rainfall of less than 500 mm (Arthington and Pusey, 2003). Annual mean rainfall across the entire continent is around 455 mm, and the losses of evapotranspiration are enormously higher than the rainfall amount (around 800 mm). Hence, the annual mean runoff comprises only 12 % of rainfall, with 75 % of the Australian continent receiving an annual mean runoff of less than 12.5 mm (Brown et al., 2015).

Climate change will have significant impacts on water availability and the hydrological system of many local catchments within Australia, especially the south-eastern and south-western parts of the continent. Most of the Australian's population and agricultural activities are extremely concentrated in these parts of the continent (Murphy and Timbal, 2008). Therefore, the predicted ecohydrological impacts of climate change require an urgent adaptation and mitigation strategies to protect these catchments from the risk of water scarcity. Perceptive information about the current and future water availability is vital to assure the proper management of the limited water resources. Furthermore, the prediction of future streamflow can help the water sector authorities to optimally manage the usage of future water resources such as domestic, agriculture, industrial, tourism, environmental maintenance and hydropower

generation. A plethora of hydrological studies has been implemented across Australia to improve the accurate perception of climate change and its impacts on water-related sectors. In short, the research-based hydrological knowledge is highly important to efficiently cope with sector-specific impacts of climate change by using the adaptation processes.

1.2 Motivation

Climate change is the universal pressing challenge of the 21st century, and it is significantly capable of influencing all features of the hydrologic cycle. A massive body of scientific evidence has apparently specified that the continuously changing climate is a significant and crucial concern (Stern, 2007). The amplified impacts of climate change on water resources is becoming one of the main anxieties around the world. In Australia, a growing evidence of rapid climate change has already been observed on local scale basins since the early 1970s. According to the recent literature, climate change is going to negatively impact the currently available water resources and freshwater ecosystems in large part of the continent, especially the south-eastern and south-western regions (e.g. Chiew et al., 2009; Vaze and Teng 2011; Bari et al., 2010; McFarlane et al., 2012; Silberstein et al., 2012; Teng et al., 2012; Islam et al., 2014; Al-safi and Sarukkalige, 2017 a, b and c). Therefore, effective water management strategies become essential to cope with water crises.

The impact of climate change on flow regimes can be simulated by utilizing the hydrological modelling procedure to draw the flow generation process and its response to external inputs. Hydrological models are vital tools for simulating the hydrological processes in drainage basins under a changing climate to foster an efficient water resources planning and management strategies (Beven, 2001). Over the past few decades, numerous hydrological models have been developed and put into practice (Bao et al., 2010). They range from conceptual lumped-parameters models, such as the HBV model (SMHI, 2012), to semi-distributed models such as Xin'anjiang model (Zhao, 1992), and the ARNO model (Todini, 1996), to physically-based fully distributed models such as the BTOP model (Takeuchi et al., 2008) and SHE-model (Abbott et al., 1986). In light of the present study, two different structured hydrological models, the conceptual modelling approach (HBV-model) and the physically-based distributed hydrological model (BTOP-model) were used to assess the impacts of climate change on flow regimes of some local Australian catchments.

Future streamflow projection, using the hydrological modelling approaches, is a key element that can assist authorities and decision makers in a water-related sector for an effective water

resources planning and management policies (Nash and Sutcliffe, 1970; Nayak et al., 2005; Sene, 2010; Piotrowski and Napiorkowski, 2011; Zeng et al., 2012). Many hydrological studies have been implemented around the world to address the problem of climate change and its influence on future water demands (e.g. Kundzewicz et al., 2007; Bates et al., 2008; Praskievicz and Chang, 2009; Whitehead et al., 2009; Driessen et al., 2010). Charles et al. (2010) pointed out that a plethora of hydrologic impact studies, with a diversity of Global Climate Models (GCMs) and warming scenarios, has warned from inevitable decline in future rainfall and runoff trends in many parts of Australia, and the currently available water resources will probably not meet the future demands in the continent. In short, the concerns of less water accessibility in many Australian regions need to be carefully addressed to achieve a consistent water management to meet the future water demands in these areas.

This study aims at assessing the hydrological behaviour of some local Australian catchments to the impacts of climate change and the potential consequences on the availability of future surface water resources in these catchments. Five catchments corresponding to five rivers were selected including Harvey River and Richmond River local catchments and three contributing catchments of the Australian Hydrologic Reference Stations namely Harvey River at Dingo Road, Beardy River at Haystack and Goulburn River at Coggan HRSs. The selected catchments are located in the south-western and south-eastern parts of Australia which are expected to be highly vulnerable to the impact of climate change. The key incentives behind the selection of the study area were firstly the selected rivers have received less attention to investigating their hydrological response to the future climate changes. Secondly, the selected basins support a biodiversity of environmental and ecological communities. Furthermore, the selected rivers represent the main tributaries of surface water supply systems in their catchments. Therefore, assessing the impacts of future climate changes on the hydrological system of these rivers is highly beneficial to draw efficient and sustainable water management strategies in their contributing catchments.

1.3 Significance of the research

Almost all climate change impact studies performed within Australia showed that many parts of the continent, especially the south-eastern and south-western parts, are expected to experience a significant rainfall reduction in the next decades and consequently less runoff to the main water streams. In line with the projected climate change, the continuous increase in population, economic and agricultural expansion in these areas need additional amounts of

water to meet future water demands. Therefore, it is highly important to study the future hydrological response of the selected catchments to the expected changes in climatic conditions to ensure the best allocation of the available water resources to counterfort the problem of water deficiency. This study uses the most recent global climate data from the IPCC 5th assessment report (AR5-CMIP5) (Representative Concentration Pathways of the Coupled Model Intercomparison Project Phase 5 CMIP5) in addition to the data from the 4th assessment report (AR4-CMIP3) combined with lumped and distributed model approaches to assess the hydrological behaviour of the selected catchments to the future climatological changes. The recent literature shows significant bias in the General Circulation Models (GCMs) results of the CMIP, especially of the previous generation, i.e. phase 3 (CMIP3). However, due to improvements in the GCMs, a reduction in their bias was expected in the recently released phase 5 (CMIP5). The study also assesses the impact of climate change on the ecology of the catchments and how the local ecosystem will be affected. Hence, this study will contribute to developing new plans for water resources management in the study areas by taking into account the effect of future water deficiency, population growth and economic and agricultural development.

1.4 Aims and Objectives of the study

The main objective of this study is to investigate the impacts of future climate changes on the hydrological system (surface hydrology) of some important local catchments in Australia and its consequence on the availability of future water resources in these catchments. To do this, firstly the observed hydro-meteorological data of the catchments has been collected and analysed. Next, the local scale future climate series were extracted from a range of Global Climate Models (GCMs) under different warming scenarios to assess the uncertainty in climate projections. Then, the future streamflow across the catchment was simulated by using the hydrological modelling approach. And finally, the hydrological response of the catchments to the impact of climate change was assessed by comparing the future and historical streamflow. Moreover, the key aims of the study are as follows:

1. Understanding the hydrological characteristics of the catchments.
2. Analyse the historical climate change patterns in the catchments using the temporal change of climate over the past decades.
3. Modelling and evaluating the projected impacts of climate change on the future streamflow of the catchments by using different hydrological rainfall-runoff models.

4. Assessing the hydrological performance of the modelling process, and then analysing the uncertainty associated with the modelling process.
5. Evaluating the impacts of future climate change on the ecohydrological systems of the studied catchments.
6. Developing recommendations for sustainable water resources management in the studied catchments taking the effect of future climate change into account.

1.5 Thesis Layout

This thesis comprises four main parts, including introduction, methodology, applications and conclusion which are expanded in 8 chapters. Table (1.1) depicts the structure of the thesis. Following is a brief description of each chapter:

Chapter One is mainly focused on the problem and the main motivations for conducting this research study. It also highlights the main aims of the study and thesis layouts.

Chapter Two illustrates a review of the literature on the climate change impacts on catchment hydrology. It introduces the various types of rainfall-runoff hydrological models and provides a comprehensive description of the conceptual and physically-based modelling approaches with the advantages and disadvantages of each approach. The previous studies of climate change impacts on local Australian basins as well as other global basins were reviewed.

Chapter Three illustrates the methodology and datasets used to perform the hydrological modelling across the studied five catchments. It also provides a comprehensive description of the data sets used for the study and different climate models. Hydrological models used in the study (HBV and BTOPMC hydrological models), their structures and important parameters as well as the required input data for each model.

Chapter Four describes the application of HBV conceptual model to perform the hydrological simulation at Harvey River Catchment and Richmond River Catchments.

Chapter Five shows and discusses the hydrological modelling of three unregulated catchments of the Australian Hydrologic Reference Stations (HRSs).

Chapter Six displays the hydrological modelling procedure with the distributed hydrological model (BTOPMC) in three unregulated catchments of the Australian Hydrologic Reference Stations (HRSs).

Chapter Seven illustrates a comparison between the applications of the two hydrological modelling approaches; lumped and distributed in three unregulated catchments of the Australian Hydrologic Reference Stations (HRSs). It also describes the Eco-hydrological applications of the outcome of the hydrological assessment and brings the findings towards development of recommendations for sustainable water resources management

Chapter Eight gives a summary of research results and general reasoned conclusions. Recommendations for future work are also provided in this chapter.

Table (1. 1) Main structure of the thesis

Part 1 Introduction	Chapter One: Research Overview
	Chapter Two: Review of Climate Change Impacts on Catchment Hydrology
Part 2 Methodology	Chapter three: Methodology and Data
Part 3 Applications	Chapter Four: Hydrological Modelling with a Conceptual Model
	Chapter Five: Hydrological Modelling in Unregulated Catchments of the Australian Hydrologic Reference Stations (HRSs) using a Conceptual Model
	Chapter Six: Application of distributed Hydrological Modelling to Unregulated Catchments of the Australian Hydrologic Reference Stations (HRS)
	Chapter Seven: A comparison of conceptual versus distributed hydrological modelling across three catchments of the Australian HRSs network
Part 4 Conclusion	Chapter Eight: Conclusions and Recommendations for the future works

Chapter 2

Review of Climate Change Impacts on Catchment Hydrology

2.1 INTRODUCTION

Climate change is significantly capable of influencing all features of the hydrologic cycle of a catchment. Many regions of the world are adversely affected by climate changes caused by global warming (IPCC, 2007). Global warming is projected to affect rainfall trends and other climate variables, which will be exacerbated in the runoff. The shift in climatic conditions could be highly attributed either to the anthropogenic factors, a probability of more than 90%, (IPCC, 2007) or the greenhouse gas emissions (De Jager and Usoskin, 2006; Stanhill, 2007; Svensmark, 2007). However, few scientists have confidence in natural conditions as the main reason for the current climate behaviour (Santer et al., 2004; Michaels, 2005; Singer and Avery, 2006; Scafetta and West, 2006). The current trends of increasing global warming and its consequences are widely agreed to continue for decades further than the current century even if the rate of present greenhouse emissions are supposed to extremely decline (Seiler et al., 2008; Zareeian et al. 2017; Dehghan et al. 2018; Zareian and Eslamian, 2018).

Water shortage resulting from climate change impact is a growing problem especially in the areas experiencing precipitation reduction and temperature increase (Maleksaeidi et al. 2017). Water scarcity could also result from the continuous economic and population growth and the enlargement in industry and agriculture fields which consumes high quantities of water (Chartres & Varma 2010). The combined impact of climate change and human development significantly affect the accessibility of future water resources. Future climate change predictions have considerable importance for development plans for water resources, agriculture and other water-related sectors (Kebede et al. 2014; Nazif et al. 2017). Hence, estimating the availability of future water resources has grown rapidly in the past decades

because of the changing climate conditions and the increased water demands for urbanisation, agriculture and economic development. In short, knowing future conditions of surface water resources plays a key role in a sustainable water resources planning and management.

Climate change and hydrological variability have been viewed as a certain observation which has attracted the attention of governmental institutions around the world (Bian et al. 2017). For instance, the Intergovernmental Panel on Climate Change in its Fourth Assessment Report (IPCC AR4) (Solomon et al. 2007) explained that the global warming would lead to accelerating melting process of the glacial, affecting global hydrologic cycle, and altering the distribution patterns of the future precipitations. In comparison to the IPCC AR4, the Fifth Assessment Report (AR5) of the IPCC (Hartmann et al. 2014) had a great innovative warning in its late edition of Global Climate Models (GCMs). In addition to the illustration of the possible scenarios of atmospheric radiation forces, it also made bold predictions for the near future climate change impacts that the national and international authorities around the world should seriously be concerned (Bian et al. 2017).

Climate change impact studies normally use the hydrological modelling approach to simulate the daily, monthly and seasonal streamflow characteristics and to predict the combined impact of climate change and other components on the hydrological status of the local catchments (Chiew et al., 2009). The hydrological simulation at catchment scale usually requires the predictions of future climate conditions to simulate the future streamflow at catchment outlet. Future climate series of rainfall and temperature can be extracted from the analysis of Global Climate Models (GCMs) at regional and global scales. According to Zorita and Storch (1999) and Solomon et al., (2007), GCMs are a fair source to extract the local and continental future climate signals. However, the resolution of climate series outputs resulting from the GCMs is too coarse for the direct use in the catchment-scale hydrological modelling and needs to be downscaled before the simulation process (Fowler et al., 2007). Furthermore, the estimation of future water availability always involves uncertainties which could be attributed to the use of different climate scenarios of GCMs, hydrological models and the selection of the downscaling procedure.

There are many types of process-based simulation models ranging from deterministic to stochastic models (Clarke, 1973). The selection of the best simulation approach is mainly based on the purpose of the modelling and the availability of hydro-meteorological data in the catchment. Generally, there are three main types of hydrological models, including conceptual,

physically-based (distributed), and data-driven models (Dawson and Wilby, 2001; Sene, 2010). The main focus of the present study was on the conceptual and physically-based hydrological models. The following sections provide a brief description of these two types of river flow forecasting models.

2.2 CONCEPTUAL HYDROLOGICAL MODELS

Conceptual models are process-based models that utilised the most predominant atmospheric elements such as rainfall, temperature, evapotranspiration losses as well as the soil moisture to represent the physical process of the hydrological cycle. Conceptual rainfall-runoff models principally comprise some linked conceptual storage reservoirs to maintain mass balance. Figure 2.1 explains a schematic structure of a typical conceptual storage and the way they are connected to each other in the hydrological cycle.

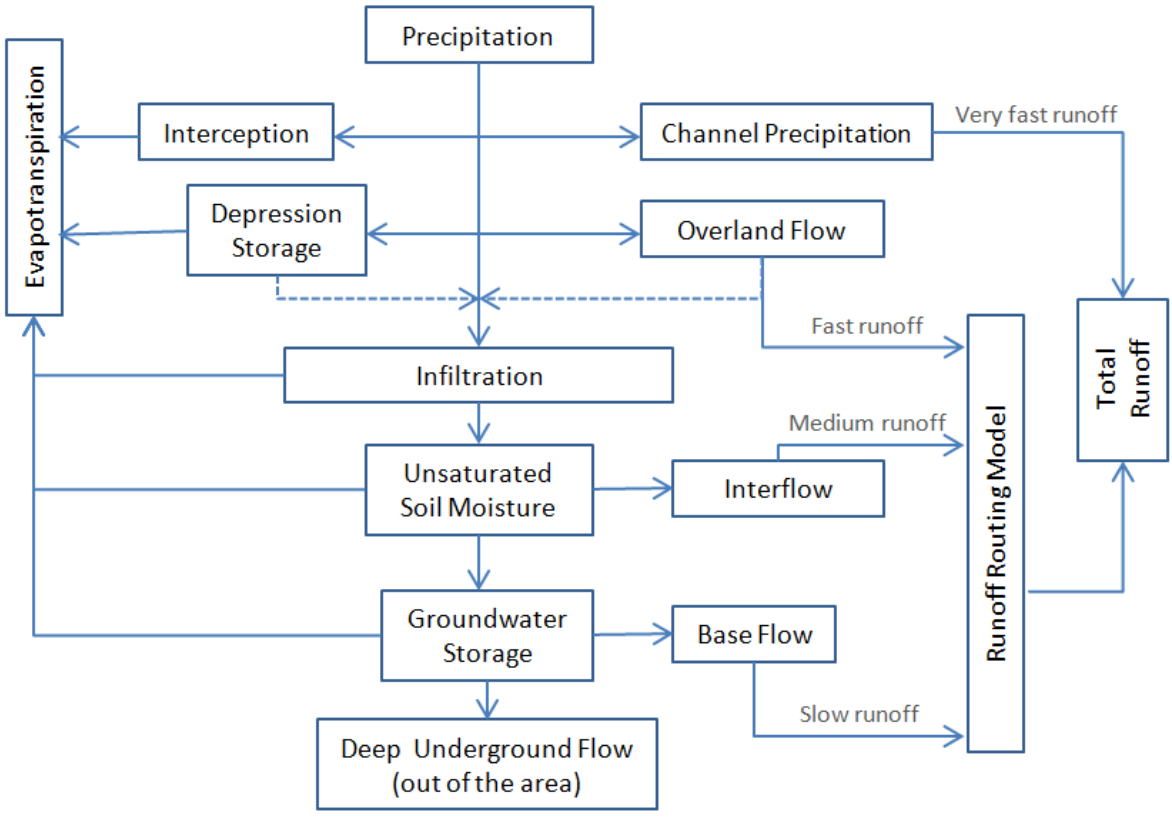

Figure 2.1 Schematic structure of a storage system in conceptual models (Badrzadeh, 2014)

Conceptual models could be of high or less complexity. It is normally ranging from the use of simple mass balance equations for components representing storage in the catchment to coupled nonlinear partial differential equations. Some equations could be simply translated into

programming code for use on a digital computer. However, if the equations cannot be solved analytically, some boundary conditions are normally used to represent the real system, and to define a procedural model in a code form which can be run on the computer by using the numerical analysis techniques (Beven, 2011). Conceptual rainfall-runoff models can be classified into two main types lumped and semi-distributed models (Todini, 1988). The majority of conceptual models are lumped, in which a catchment is treated as a single uniform unit (Refsgaard, 1997). This means that the average values of the hydrometeorological and hydrogeological parameters are taken into account in an input-output system instead of their spatial variation.

Numerous conceptual hydrological models have been developed over the past decades and applied in the hydrological simulation. Some of these models are Stanford Watershed Model (U.S.A) (Crawford and Linsley, 1966), Sacramento (U.S.A) (Burnash et al., 1973), Tank model (Japan) (Sugawara, 1979), HBV model (Sweden) (Bergström, 1976), Xin'anjiang model (China) (Zhao, 1992), IHACRES (Jakeman et al., 1990; Littlewood et al., 1997), SIMHYD (Chiew et al., 2002) and Hydrologic Engineering Center Hydrologic Modeling System HEC-HMS (USA) (U.S. Army Corps of Engineers, 2015). In this study, the most popular Swedish conceptual rainfall-runoff model, HBV, was adopted to assess the impact of climate change on catchment hydrology.

Over the past decades, a considerable number of hydrological impact studies have been implemented in different areas around the world using the conceptual modelling approach. For example, Chiew et al. (2009) utilized the conceptual modelling approach to investigate the impact of climate change on runoff in large part of south-eastern Australia. They forced the calibrated SIMHYD rainfall-runoff model (a simplified version of the daily conceptual rainfall-runoff model HYDROLOG) with the downscaled climate data from an ensemble of 15 GCMs of the Intragovernmental Panel on Climate Change Fourth Assessment Report (IPCC-AR4) to simulate the future streamflow at the study area. The results showed that there could be a high deficiency in the runoff across the study area in the future. In addition, the assessment of the model shows that it can be used with a high confidentiality to predict the impact of climate change on runoff generation.

Driessen et al., (2010) applied the HBV model to assess the hydrological behaviour of the rain-fed Ourthe River catchment in Western Europ to the potential climate change impacts. Outputs from the IPCC climate scenarios (A2, A1B and B1) were used to force the calibrated HBV

model to simulate the future streamflow of the river by the early and late of the 21st century. The simulation results projected a slight increase in streamflow during the start of the century, especially for the B1 scenario. By the late the century, all scenarios revealed negative trends in summer streamflow and positive trends in winter.

Grillakis et al., (2011) assessed the impact of climate on the hydrological behaviour of Spencer Creek catchment located in Southern Ontario, Canada. They forced the three well-known conceptual rainfall-runoff models (HBV, HEC-HMS and Sacramento) with four couples of GCM driven Regional Climate Models under the A2 emission scenario for the period (2040-2069). The precipitation and temperature projections were provided by the North American Regional Climate Change Assessment Program (NARCCAP) climate simulations. Climate projections revealed significant changes in the annual exceedance probability (recurrence interval) of the extreme precipitation, temperature and runoff events. The modelling results also showed increasing tendencies in the mean annual streamflow and slight changes in the seasonal streamflow distribution.

Vaze and Teng (2011) showed that the future streamflow across many local catchments in southeastern Australia is projected to decline within a range of 0-20% by 2030. They used the IPCC-AR4 climate scenarios informed by 15 GCMs under median emission projections (the A1B climate scenario) to force the SIMHYD and Sacramento conceptual rainfall-runoff models to simulate the future streamflow across the catchments. Teng et al. (2012a) also used the climate projections informed by 15 GCMs of the CMIP3 to force five conceptual rainfall-runoff models to simulate the future streamflow across southeastern Australia. They found that the majority of the modelling results indicate a larger reduction in future runoff across the study area by the middle of the 21st century. Another study by Teng et al. (2012b) also revealed a reduction in the future runoff across the southeast and far southwest of the Australian continent.

In another study, McFarlan et al., (2012) also examined the impact of climate change on the water yield demands in south-western Australia by using the conceptual modelling approach. They used the IHACRES and Sacramento rainfall-runoff models driven by 15 GCMs of the IPCC-AR4 under three warming scenarios to simulate the future streamflow. The results showed that there is an expected reduction in streamflow to Perth city by about 25% by 2030 and this percentage is expected to increase to 50% if a dry future climate is experienced. The yield of surface water was estimated to reduce by about quarter, which is approximately the same estimated reduction in runoff. Groundwater yield has estimated to decrease by a small

percentage of 2% under the effect of evapotranspiration and the losses of drainage. The study concluded that the fast population and economic growth together with the current decrease in water yield might result in a reduction in water availability in many cities in south Western Australia including Perth.

Silberstein et al., (2012) also used the conceptual modelling approach, computer simulation, to examine the impact of climate change on future surface water availability in south-western Australia using different global warming scenarios. The results revealed that there could be a decrease in rainfall with a median value of 8% under all scenarios by 2030 which may result in a runoff decline by about quarter. This is projected to cause a reduction in water yield to the main water supply reservoirs in south-western Australia. In addition, the results imply that if future climate predictions occur, the runoff reduction will possibly continue.

Shi et al. (2013) applied the conceptual lumped parameters hydrologic model, Xinanjiang, to simulate the streamflow of the Sancha River, a karst basin in south-west China. The model was calibrated and validated with different efficiency criteria, and the results revealed that the structure of the model and its parameters were highly reasonable to simulate the future hydrologic condition in the basin. The ability of the model to duplicate the streamflow and base flow was the base to evaluate its performance. In addition, the results of separation of hydrograph into the base flow and surface flow showed that the model might be capable of simulating the base flow in such a complicated system.

Zhag et al. (2014) employed the rainfall-runoff modelling, GR4J lumped conceptual model (Perrin et al., 2003), as one approach for predicting different hydrological signatures in ungauged catchments in south-eastern Australia. The results showed that the hydrological modelling approach is not suitable for predicting daily streamflow signatures, but it performs properly in estimating the long-term aggregated signatures. Furthermore, the use of hydrological modelling for simulating flow duration curves in dry catchments will produce poor results as compared with other approaches such as special interpolation and index model which used in the same study.

Islam et al. (2014) used the LUCICAT conceptual rainfall-runoff model to assess the hydrological impact of climate change on Murray Hotham catchment in the south-west of Western Australia under two climate change scenarios A2 and B1 of the IPCC-AR4. The results revealed that there could be a high reduction in rainfall and runoff by the mid and late

of the 21st century as compared with the last century. The results also showed that the reduction in rainfall and runoff was higher in the parts of high rainfall compared to the low rainfall parts. The results were proposed to be used for planning of future water resources in the catchment.

However, the literature of conceptual modelling approach is quite enormous. The majority of the popular hydrologic research centres around the world have developed and applied their own conceptual models for hydrological modelling. Vaze, et al., (2012) pointed out that the most popular conceptual models used in Australia are SMAR (O'Connell et al., 1970), Sacramento (Burnash et al., 1973), IHACRES (Jakeman et al., 1990; Littlewood et al., 1997), SIMHYD (Chiew et al., 2002), GR4J (Perrin et al., 2003) and AWBM (Boughton, 2004). In light of the present study, the most popular European conceptual model Hydrologiska Byrans Vattenbalansavdelning (HBV-model) will be applied to investigate the hydrological impact of climate change on some local Australian catchments. Compare to the physically-based models, conceptual models are more popular, easier to develop and require fewer parameters for the calibration process. However, conceptual models have some limitations which can be summarized as below (Badrzadeh, 2014):

- In lumped-parameter models, catchment is treated as a single spatial unit by adopting the average value of spatially heterogeneous parameters to simulate the various hydrological process. This may affect the accuracy of the modelling results.
- The parameters of a specified conceptual model are optimized based on the unique characteristics of a particular catchment such as climate, catchment size and type, geology, topography, soil type and land cover. Therefore, the developed conceptual models cannot be applied to other catchments.
- Event-based conceptual models are not applicable for ungauged catchments as the calibration process requires a huge amount of data.
- The limitations of physically-based models are almost the same as in the semi-distributed conceptual models such as the massive data requirement and the uncertainty of parameters estimation due to measurement difficulties.
- The use of conceptual models to simulate the complex processes normally includes many assumptions.

2.3 PHYSICALLY-BASED (DISTRIBUTED) HYDROLOGICAL MODELS

Physically-based models, also called “distributed” or “deterministic” hydrological models, can be used to simulate major hydrological processes in river basins mathematically. In these models, the physical process of runoff generation in a catchment are spatially represented by a group of nonlinear partial differential equations. Physically-based models are also capable of reflecting the spatial and temporal distribution of basin hydro-meteorological elements by including different parameters that need to be adjusted either manually or automatically (Du et al. 2013; Zhang et al. 2013). The parameters of the physically-based distributed hydrological models are normally related to specific characteristics of the basin (Takeuchi et al. 2008, Manandhar et al. 2013, Sun et al. 2014). Therefore, the hydrological behaviour of a basin in response to the climate variability strongly relies on the sources of runoff, physical characteristics of the basin, climatic conditions, and the level of anticipated climatic changes (Singh and Bengtsson, 2005).

Over the past few decades, several physically-based distributed hydrological models have been developed and applied in the hydrological simulation. Some of the most popular distributed hydrological models including DHSVM (Wigmosta et al., 1994), MIKE SHE (Refsgaard and Storm, 1995), IHDM (Calver and Wood, 1995), DBSIM (Garrote and Bras, 1995), SWAT (Arnold et al.,1998; Gassman et al., 2007), TOPKAPI (Todini and Ciarapica, 2001; Liu and Todini, 2002), GBHM (Yang et al., 2002), HMS (Yu, 2000), and the grid-based Xin’anjiang model (Li et al., 2006a, Wang et al., 2007b; Li and Zhang, 2008; Yao et al., 2009). In this study, a physically based distributed hydrological model developed at the University of Yamanashi (Japan) based on the block-wise use of the original TOPMODEL and the Muskingum–Cunge routing method (YHyM/BTOPMC) (Takeuchi et al., 1999, 2008) was adopted to assess the impact of climate change on catchment hydrology.

A plethora of hydrological impact studies have been performed by applying the distributed models. For instance, Phan et al., (2010) used the grid-based distributed BTOPMC hydrological model to evaluate the hydrological response of the Kone River basin in Central Vietnam to the changes in climate conditions by the 2030s. Climate outputs from the Coupled Model Intercomparison Project phase 3 (CMIP3) under the A1B scenario of the Japanese MRI GCM were used to represent the future climate. The modelling results revealed a positive trend in the future streamflow of the Kone River compared to the reference period (1980-1999). The study also showed that the water volume during the flood season is projected to decrease by about

18.6% and increase by around 90.0% during the low flow season relative to the reference period.

Manandhar et al., (2013) also employed the BTOPMC hydrological model to assess the hydrological behaviour of the snow-fed Kali Gandaki River Basin (KGRB) in Western Nepal under changing climatic conditions. The modelling results revealed that the mean annual streamflow is projected to increase by 2.4%, 3.7%, and 5.7% following an increase of 1, 2, and 3 ^{o}C in annual mean temperature compared to the reference scenario. The study also showed that the monsoon and pre-monsoon season's maximum, minimum, and seasonal streamflows are also projected to increase with temperature rise.

Demaria et al., (2013) investigated the potential impacts of climate change on the Mataquito River basin in central Chile by applying the grid-based Variable Infiltration Capacity (VIC) hydrological model (Liang et al., 1994). Climate projections from a multi-model ensemble of 12-GCMs from the Coupled Model Intercomparison Project Phase 3 (CMIP3) and Phase 5 (CMIP5) were used to run the model for future streamflow projections by the end of the 21st century. Simulation results indicate that future climate conditions will probably shift the location of snow line to higher elevations and reduce the number of days with precipitation falling as snow. Results also projected an increase in the extreme events (precipitation and streamflow) during the wet months and a decrease in the low flow conditions during the warm months.

Brown et al., (2015) utilized the physically-based Soil and Water Assessment Tool (SWAT) hydrological model to investigate the impact of the prolonged drought (1997–2009) resulting from the changing climate conditions on streamflow in two sub-catchments in south-eastern Australia. Results show a substantial decline in annual mean streamflow compared to the long-term average. Also, the assessment of baseflow contributed by the model showed a mix of over and underestimation depending on catchment and season. The study suggests that the adopted SWAT model will neither be applicable for local climate change impact studies in the catchments nor the assessment of land management and land-use change impact on streamflow.

Bian et al., (2017) applied the well-known distributed hydrological soil vegetation model (DHSVM) to assess the impact of climate change on future streamflow of Tuotuo River basin, China. They employed climate output from six GCMs of the CMIP5 model under three Representative Concentration Pathways (RCPs) scenarios to represent three future periods

including the 2020s, 2050s and 2080s. The downscaled climate outputs revealed a rise in mean annual temperature, ranged between -0.66-6.68 ^{o}C, and a change in mean annual precipitation ranged between -1.18-66.14% compared to the observations. The modelling results also show that the seasonal streamflow is projected to increase during the future periods compared to the observations.

Although the deterministic models can improve our understanding of the hydrological system by representing the interaction of the spatial-temporal variables, they are considered as very costly and time-consuming tools (Chau et al., 2005). They normally require a large amount of data, such as catchment physical characteristics and meteorological parameters to represent sub-surface and surface runoff generation and routing processes. Therefore, the numerical solutions such as finite element, finite difference and boundary conditions are normally adopted to solve the complex equations of the hydrological process (Gosain et al., 2009). The key difficulties of the physically-based distributed hydrological models could be summarized below:

- Distributed models cannot exactly represent the hydrological process in a catchment because of the difficulty of measuring and understanding catchment characteristics such as soil parameters and determine their temporal variation over the time (Liu et al., 2011).
- The solution of descriptive catchment equations normally includes some difficulties. This means that even the numerical techniques may not be effective because of the complexity of nonlinear partial differential equations.
- They are costly, and time-consuming tools as they require a substantial amount of input data and preparation time for the setting up processes such as measuring an extensive set of parameters from the field, appropriate software and training time.
- In the distributed models, the grid size governs the accuracy of the modelling process. Grid-scale normally covers a wider area compared to the more homogenous site-specific scale which is normally used to measure the hydrological data.
- Since the complex numerical simulations consume more time, therefore the physically-based distributed models may not be appropriate for real-time flood forecasting.
- The predictions of the Physically-based models include a high level of uncertainty as there are many possible sources of error in calibrating the model (Huang and Liang, 2006).

In short, despite the above limitations, physically-based hydrological models are still an effective tool for providing spatial information of the hydrological parameters at catchment and basin scales. They also provide valuable outcomes for effective water management strategies such as assessing water storage within the catchment in addition to the streamflow prediction (O'Connor, 2006).

In the current study, two different structured hydrological models, the conceptual modelling approach (HBV-model) and the physically-based distributed hydrological model (BTOP-model) were used to assess the impacts of climate change on flow regimes of some local Australian catchments.

Chapter 3

Methodology and Data

3.1 Hydrological Modelling Approaches

3.1.1 Introduction

In this study, two different structured hydrological models, the conceptual modelling approach (HBV-model) and the physically-based distributed hydrological model (BTOP-model) were used to assess the impacts of climate change on the flow regimes of some local Australian catchments. In this chapter, the concept of each model, its structure and parameters and the important equations connecting these parameters are described in more details. The required input data for each hydrological model are also explained briefly, followed by a detailed description of the downscaling techniques used in this study.

3.1.2 The HBV Hydrological Model

The Hydrologiska Byrans Vattenbalansavdelning (HBV) model, firstly established in Sweden, is a semi-distributed conceptual rainfall-runoff model widely used in catchment hydrology (SMHI, 2012). This means that the whole basin can be divided into different elevation and vegetation zones as well as into different sub-basins. It is also possible to run the model separately for several sub-basins and then add the contributions from all sub-basins. Calibration, as well as forecasts, can be made for each sub-basin separately. For basins of considerable elevation range, a subdivision into elevation zones can also be made. This subdivision is made for the snow and soil moisture routines only. Each elevation zone can further be divided into different vegetation zones (forested and non-forested areas).

The model utilizes the daily rainfall, air temperature, and the long-term monthly mean potential evapotranspiration as input data to simulate the daily streamflow at basin outlet (Bergstrom, 1995; SMHI, 2012). Figure (3.1) illustrates a basic schematic structure of the HBV model as well as the required input and output data. Observed streamflow record is used to calibrate the model, and to verify its correctness before a runoff forecast. Lindstrom et al., (1997) reported that the HBV model had proven its high performance in many regions around the world with a diversity of climatic conditions where different versions of the model were successfully applied to perform the hydrological modelling. In this study, the latest version of the Integrated Hydrological Model System (IHMS 6.3, HBV version 7.3) (SMHI, 2012) was adopted to perform the hydrological modelling. In addition to the hydrological forecasting, the model was also effectively used in many water resources related fields such as data quality control, broadening of runoff records, estimation of missing data and groundwater simulation (SMHI, 2012).

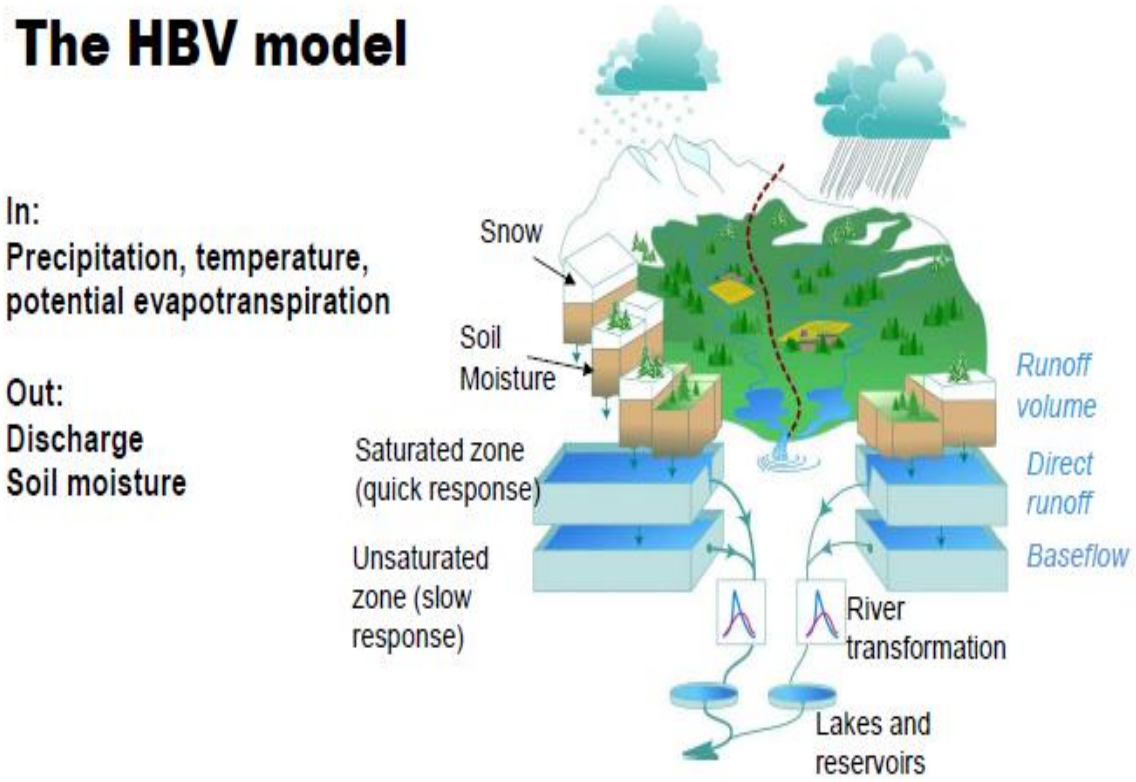

Figure (3.1) Basic schematic structure of the HBV model with required input data and output parameters.

3.1.2.1 The motivations of using the HBV model

The purpose of adopting the HBV model in the present study was due to two main incentives. Firstly, the simplicity of the input data and the robust and flexible model structure have demonstrated the reliable performance of the model in solving water resource problems (SMHI 2012). Secondly, daily streamflow prediction offers a comprehensive idea of the hydrological changes and the status of future water resources in the study area. This could help the decision makers to draw efficient water management strategies for the studied catchments. In addition, the model has been widely applied in Europe to predict the potential impacts of climate change on a verity of river catchments and basins and has proven its applicability and its well performance. Some of these applications include (Grillakis et al., 2010; Teutschbein and Seibert, 2012; Geris et al., 2015; Photiadou et al., 2016). Furthermore, the model has also been successfully applied in many catchments around the world to assess the impact of climate change on local and global scales basins (e.g. Normand et al., 2010; Jia and Sun, 2012; Kebede et al., 2014; Yu et al., 2014).

3.1.2.2 Model structure and parameter description

The HBV model includes four main modules including precipitation routine, soil moisture, river routing and response routine (Lindström et al., 1997). Figure (3.2) provides a detailed description of the four routines, their parameters and the important equations connecting these parameters. Basically, the HBV model uses three storage reservoirs to describe the mechanism of water balance (Figure 3.1) including soil moisture storage, storage of the upper zone and lower zone storage. Therefore, the general water balance equation becomes as shown in equation (1) (Lidén and Harlin, 2000).

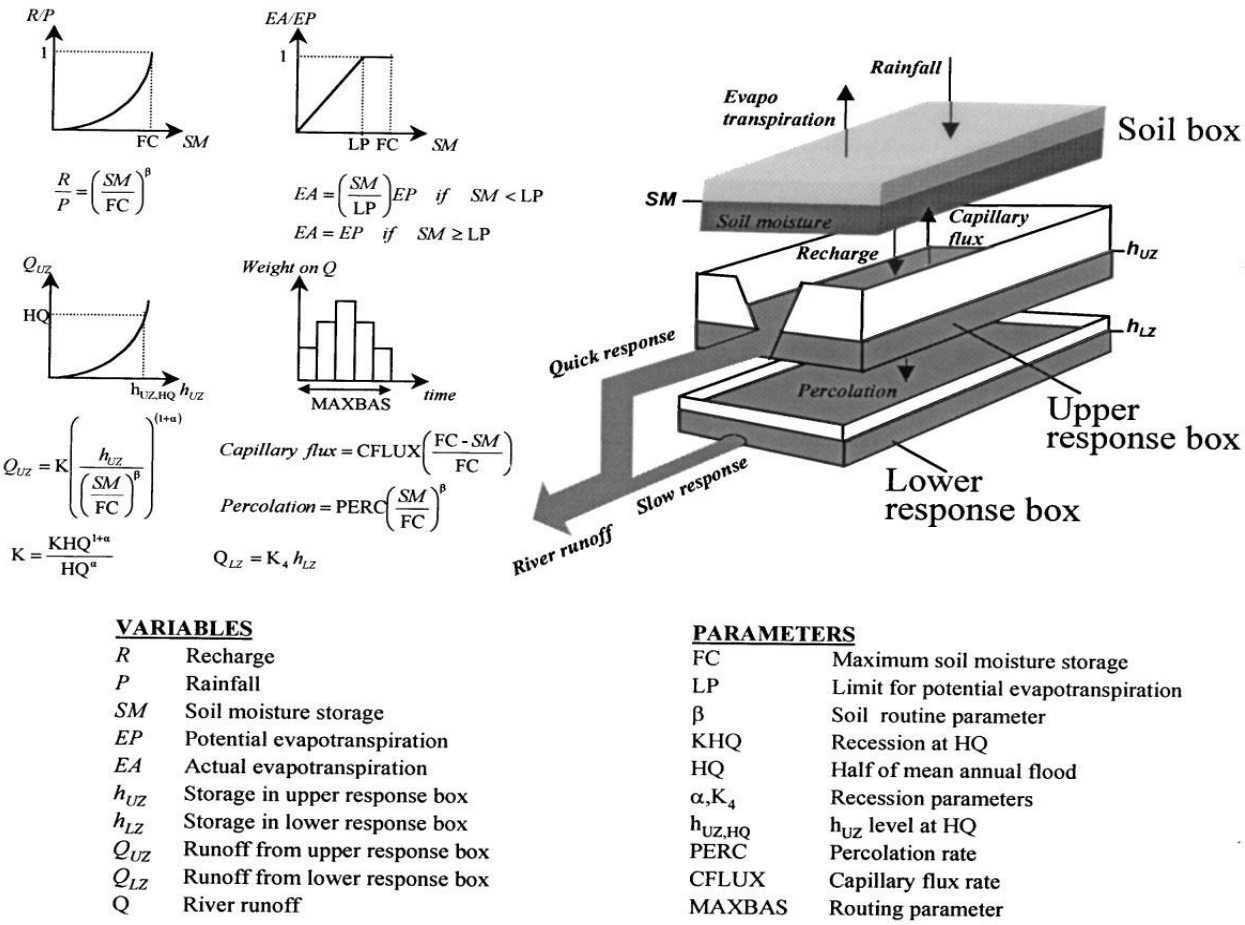

VARIABLES

R	Recharge
P	Rainfall
SM	Soil moisture storage
EP	Potential evapotranspiration
EA	Actual evapotranspiration
h_{UZ}	Storage in upper response box
h_{LZ}	Storage in lower response box
Q_{UZ}	Runoff from upper response box
Q_{LZ}	Runoff from lower response box
Q	River runoff

PARAMETERS

FC	Maximum soil moisture storage
LP	Limit for potential evapotranspiration
β	Soil routine parameter
KHQ	Recession at HQ
HQ	Half of mean annual flood
α, K_4	Recession parameters
$h_{UZ,HQ}$	h_{UZ} level at HQ
PERC	Percolation rate
CFLUX	Capillary flux rate
MAXBAS	Routing parameter

Figure (3.2) The principal structure and parameters of the HBV model when applied on catchments without snow (Lidén & Harlin, 2000).

$$P - E - L \pm \Delta S = Q \qquad (3.1)$$

Where P, E, L, ΔS and Q are the rainfall, evapotranspiration, losses to groundwater systems or nearby catchments, water storage change and runoff excess from the basin correspondingly.

The precipitation routine in the current work was represented by the rainfall only because there is no snow in the selected catchments. The soil moisture (SM) routine, which gives an indication about soil moisture storage in the catchment, depends on the parameters Field Capacity (FC), BETA (β) and the Limits of Potential evapotranspiration (LP) as shown in equation (3.2). The extreme soil storage volume of the catchment is represented by the parameter FC. The correlation between SM and FC can be used to estimate the actual evapotranspiration based on the available soil moisture (equation 3.3) (Kebede *et al.*, 2014). The parameter β governs the relative involvement of precipitation to the runoff volume at a

specified deficiency of soil moisture. The shape of potential evapotranspiration curve is governed by the parameter LP (Abebe *et al.*, 2010). Finally, the surplus water of the soil moisture routine is transformed through the response routine to be released into the catchment through two connected reservoirs (h_{UZ} and h_{LZ}). These reservoirs are connected together by a filtration rate (PERC) in which water percolates from the (h_{UZ}) to the (h_{LZ}) at a constant proportion as shown in (Fig. 3.1). The channel flow hydraulics (runoff) can be described by the transformation function parameter (MAXBAZ) which calculates the outflow from the catchment (equations 3.4, 3.5 and 3.6) (Kebede *et al.*, 2014).

$$\frac{Recharch}{P_t} = \left(\frac{SM_t}{FC}\right)^{BETA} \quad (3.2)$$

$$EA = EP\ minimum\ \left(\frac{SM_t}{FC\ .\ Lp}\ , 1\right) \quad (3.3)$$

$$Q_{GW}(t) = K_2.\ S_{LZ} + K_1.\ S_{UZ} + K_o\ maximum\ (S_{UZ} - S_{LZ}\ ,\ 0) \quad (3.4)$$

$$QC\ (t) = \sum_{i=1}^{MAXBAZ} C(i).\ Q_{GW}(t - i + 1) \quad (3.5)$$

$$C(i) = \int_{i=1}^{i} \frac{2}{MAXBAZ} - \left|u - \frac{MAXBAZ}{2}\right| . \frac{4}{MAXBAZ^2}\ du \quad (3.6)$$

Where P_t is the precipitation at the time (t), EA is the actual evapotranspiration and EP is the potential evapotranspiration. Q_{GW} is the recharge from the groundwater portion, QC is the computed discharge and K_i is the recession constant.

3.1.2.3 Calibration procedure – model parameters

The following steps can describe the calibration process of the HBV model (manual method):

- Assign values to parameters not to be calibrated.
- Adjust model parameters affecting the precipitation/runoff volume including Rfcf (rainfall correction factor), Sfcf (snowfall correction factor).
- Adjust model parameters affecting the snow including Tt (Threshold temperature for precipitation), cfmax (factor for snowmelt).
- Adjust model parameters affecting the soil routine (and runoff volume) including FC (maximum soil water storage), beta (soil parameter), ecorr (correction factor for potential evaporation).

- Finally adjust model parameters affecting the shape of the hydrograph including khq (recession coefficients), perc (percolation to lower response box), k4 (recession from lower response box) and maxbaz (transformation function).

Figure (3.3) illustrates the manual calibration process of the HBV model.

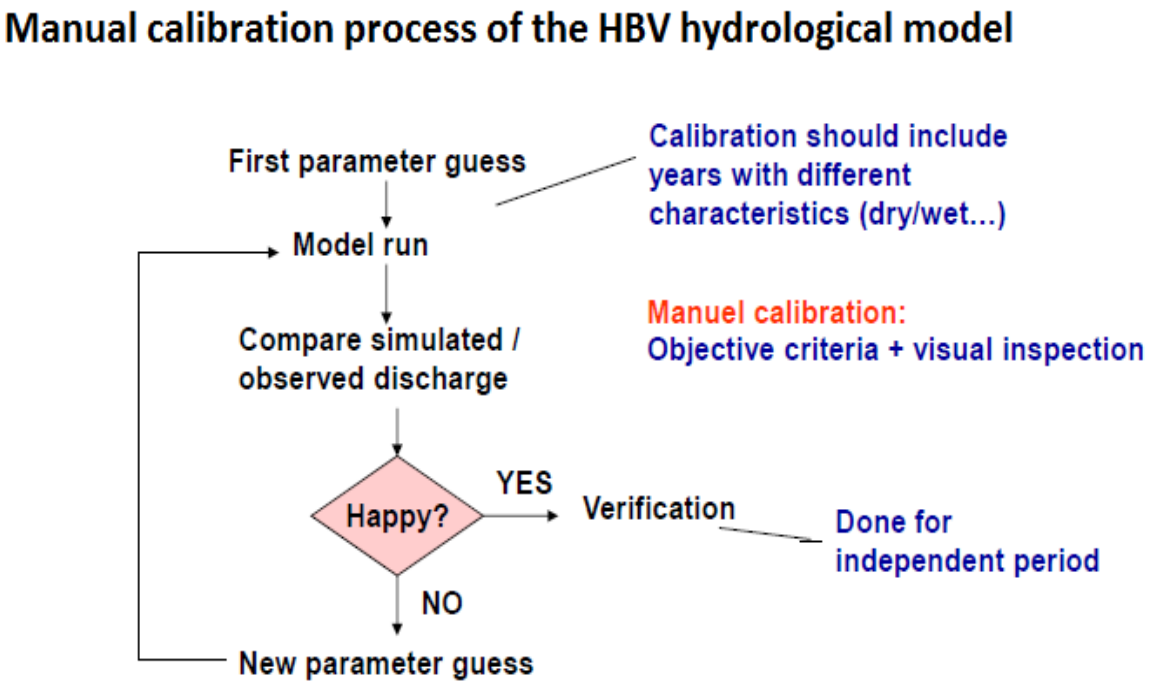

Figure (3.3) A sketch showing the manual calibration process of the HBV model.

3.1.3 BTOPMC Hydrological Model

A physically based distributed hydrological model developed at the University of Yamanashi (Japan) based on the block-wise use of the original TOPMODEL and the Muskingum–Cunge routing method (YHyM/BTOPMC) (Takeuchi et al., 1999, 2008) is adopted in this study. The BTOPMC model has been successfully applied in numerous regions around the world, especially in the Asian Monsoon area, and has proven its applicability and its well performance (e.g. Takeuchi et al., 1999; Ao et al., 2003; Shrestha et al., 2007; Hapuarachchi et al., 2008; Silva et al., 2010; Manandhar et al. 2013). The model has been derived from the concept of the original TOPMODEL, which depends on the topographic index and geographic elements, to extend the applicability of the TOPMODEL for large river basins by dividing them into several blocks (Ao 2000; Shrestha et al., 2007). A comparison between the basic control units of the original TOPMODEL and the BTOP model are presented in Figure (3.4). In the BTOPMC

model, the entire catchment is divided into several grid cells to maintain the spatial heterogeneity within the catchment. Simultaneously, the grid cells are regrouped into several blocks to preserve the relatively simple model structure. The topographic index (γ_i) of a specified grid cell (i) is calculated from equation (3.7).

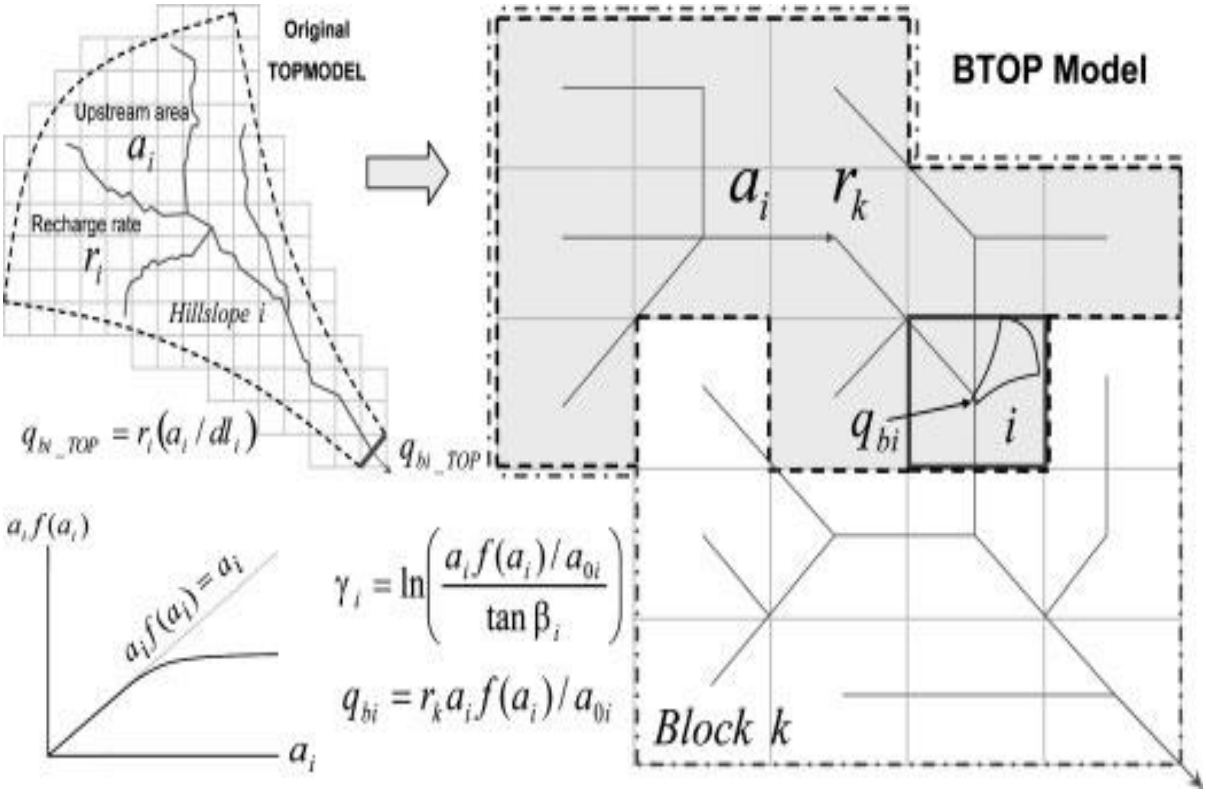

Figure (3.4) A comparison between the basic control units of the original TOPMODEL and the BTOP model (Takeuchi et al. 2008)

$$\gamma_i = \ln(\alpha_i / \tan\beta_i) \qquad (3.7)$$

Where, α_i is the drainage area per unit length of contour, and $\tan\beta_i$ is the slope of the grid cell (i).

The main characteristics of the YHyM/BTOPMC model are as follows (Takeuchi et al. 2008):

1- The whole basin is divided into some blocks (sub-basins) each of which may comprise some hillslopes. The sub-surface water is supposed to be shared within each hillslope rather than between sub-basins.
2- When reaching the steady state condition (soil moisture equals the field capacity), the streamflow resulting from the effective rainfall over a sub-basin (or block) releases either

as overland flow from each saturated grid cell, or as sub-surface flow to a local stream segment schemed in each grid cell in the block, or both.

3- At the steady state condition, sub-surface flow from each grid cell is equal to the recharge rate in a block (assumed homogeneous over a block) times the effective contributing area of the grid cell i. The effective contributing area is known as the product of total upstream area and the effective contributing area ratio. The ratio of the net upstream catchment area that contributes to the discharge from the grid cell i to the total upstream area (ai) is defined as the effective contributing area ratio f (ai) ($0 \leq f(ai) \geq 1$). Through this relationship, the topographic index γ in the BTOPMC is re-defined using the effective contributing area ai f(ai):

$$q_{bi} = [\, a_i \, f(a_i).\, rk] \,/\, a_{0i} \tag{3.8}$$

$$\gamma_i = ln \frac{a_i \, f(a_i)/a_{0i}}{tan_{\beta i}} \tag{3.9}$$

where q_{bi} (m/day) is the specific base flow of the grid cell i to the local stream segment per unit grid cell area (rather than per unit contour line), rk (m/day) is the spatially homogeneous recharge rate over the block k, $a_i f(a_i)$ (m^2) is the effective contributing area of the grid cell (a fraction of its drainage area), and a_{0i} (m^2) is the area of the grid cell i.

4- The simulated discharge at the outlet of a grid cell is expressed in terms of the saturation deficit of the outlet grid cell:

$$q_{bi} = D_i \tan \beta_i \, exp(-SD_i/m) \tag{3.10}$$

Where D_i (m/day) is the groundwater discharge-ability, SD_i(m) is the saturation deficit in the unsaturated zone. The subscript i refers to the grid cell i, and average block value is used for m, the discharge decay factor. This contradicts the original TOPMODEL in which a coefficient of transmissivity T_0 has been used. This modification allows groundwater flow from each grid cell in the BTOPMC rather than only from the hillslope outlet, which has been the case with TOPMODEL. The groundwater hydraulic gradient in a grid cell is assumed to be parallel to the land surface (inter-grid slope). In a large grid cell, however, the inter-grid slope may not be directly related to local flow pathways or hydraulic gradients. Hence the local variation of hydraulic gradients is mostly accounted for in the new parameter, the groundwater discharge-ability.

The groundwater discharge-ability D_i may be considered as a parameter that expresses the potential of groundwater to discharge to the surface of the grid cell i. It is considered as a function of the texture of land surface layer of a grid cell, i.e. topographical roughness, geological complexity, surface types etc. If there are cliffs, ground breaks, depression ponds and the like, groundwater generation to surface water should occur much more easily than in the case of a flat uniform surface. The slope of the surface is also a decisive factor, which is accounted for by the term $\tan\beta_i$.

5- Streamflow produced at each grid cell flows into a local stream segment for that cell. Streamflow is then routed via an open channel from any upstream origin to the basin outlet.

It can be seen that the basic blocks assumptions of the BTOPMC model concerning areal water balance, flow generation and flow routing are different from the original TOPMODEL (Takeuchi et al. 2008). However, all the basic forms of the mathematical equations of the TOPMODEL are still the same. The runoff generation process from a topography dominant sloping basin is still totally dependent on the topographic index, which is re-defined. Here the sloping basin is a basin where the topography forms a unique stream network, as was defined in Falkenmark and Chapman (1989).

The BTOPMC model utilized the block average saturation deficit instead of the average catchment value that is proposed in the TOPMODEL to calculate local saturation deficit. A core module, the runoff generation module, comprises four sub-models including topographic, runoff generation, parameter calibration, and flow routing (Takeuchi et al., 1999; Ao et al., 2003). The catchment's topographic characteristics such as catchment boundary, grid area, river slope and length, flow accumulation and direction are created by the topographic sub-module using the digital elevation map (DEM). Runoff is produced based on the extended TOPMODEL concept (Beven and Kirkby 1979), and flow routing is performed by applying the modified Muskingum-Cunge method (Zhou et al., 2006). In streamflow routing calculation, the river cross section is supposed to be rectangular, and river width B (in meters) is approximately calculated from (Equation 3.11). The equivalent Manning's roughness coefficient of a grid cell is estimated from equation (3.12).

$$B(i) = C\sqrt{A(i)} \tag{3.11}$$

$$n_i = n_o(k)\,[\tan\beta_i / \tan\beta_o(k)]^{1/3} \tag{3.12}$$

Where C is a constant and equal to 10, A is the drainage area in (km^2) (Lu et al., 1989), n_o and tan β_o are the equivalent roughness coefficient and slope at the outlet of sub-catchment k respectively. It should be noted here that n_o is a model parameter that's need to be calibrated.

The vertical profile of each grid-cell in the BTOPMC model consists of four key zones including vegetation, root, unsaturated, and saturated (groundwater aquifer) zones as illustrated in Figure 3.5 (Takeuchi et al., 2008). In the beginning, the rainfall is intercepted by the canopy in the vegetation zone for evaporation, and then the root zone receives the remaining rainfall. To clearly depict the hydrological processes in the unsaturated zone, it is further divided into gravity drainage zone (active area) and inactive area. The soil water storage between the field capacity and the wilting point is represented by the root zone and inactive area. Net rainfall is supposed to penetrate into the root zone until reaching the field capacity, and vegetation can use only the fraction in the root zone. The soil water content between saturation and field capacity is represented by the gravity drainage zone which receives the surplus water from the root zone (q_{rz}). Once the soil moisture in the gravity drainage zone touches its amplitude, the overland flow (q_{of}) occurs (equation 3.13). The base flow (q_b) (equation 3.14) is nonlinearly released from the saturation zone which receives groundwater recharge (q_v) from the gravity drainage zone. The sum of the overland flow (q_{of}) and the base flow (q_b) per unit length of contour line represents the runoff from a grid cell to the local schematic stream reach.

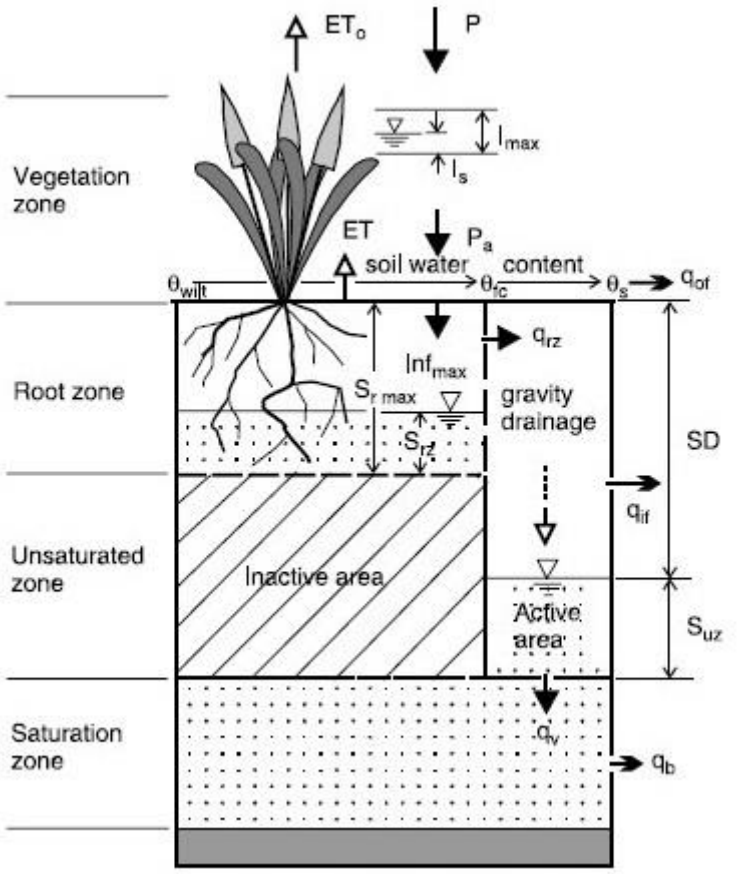

Figure (3.5) A schematic structure of BTOPMC model for runoff generation at each grid-cell (Takeuchi et al., 2008)

Where P is the gross rainfall, ETo is the interception evaporation, Imax is the interception storage capacity, I is the interception state, Infmax is the infiltration capacity, Pa is the net rainfall on the land surface, ET is the actual evapotranspiration, Srmax is the storage capacity of the root zone, S_{rz} is the soil moisture state in root zone, SD is soil moisture deficit in unsaturated zone, S_{uz} is the soil moisture state in unsaturated zone, q_{of} is the overland runoff, qif is the saturation excess runoff, q_v is the groundwater recharge, and q_b is groundwater release. θ_{wilt}, θ_{fc}, θ_s are soil water content at wilting point, field capacity and saturation respectively (Takeuchi et al., 2008).

$$q_{of}(i, t) = \{S_{uz}(i, t) - SD(i, t)\} \quad (3.13)$$

$$q_b(i, t) = T_o(i) \text{ Exp } [\frac{-SD(i,t)}{m(k)}] \tan \beta_i \quad (3.14)$$

Where T_o is the saturation soil transmissivity, and m (k) is the discharge decay factor of sub-basin k.

The potential evapotranspiration, either from the interception (PET0) or soil water in the root zone (PET), is computed based on the Shuttleworth-Wallace (S-W) model developed by Zhou et al., (2006) by utilizing the global data sets. The interception evaporation $ET_o(t)$ is considered as the less of PET0, and the intercepted water from the canopy $I_s(t)$ (Equation 3.15). While the actual evapotranspiration is considered as the less of PET and water in the root zone. For more information about the BTOPMC model, please refer to (Takeuchi et al. 2008).

$$ET_o(t)\,\Delta t = \min\{I_s(t), PET0(t)\,\Delta t\} \quad (3.15)$$

3.2 Input Data

3.2.1 Observed Climate Data

The observed daily hydro-meteorological data of rainfall, temperature and discharge and the long-term monthly mean potential evapotranspiration were obtained from the Australian Bureau of Meteorology, and the quality of data has been checked with high priority. Weather stations were selected within the studied catchments and nearby locations considering the availability of long-term data. Spatial distribution of rainfall and temperature data across the contributing catchments was implemented by applying Thession polygon method.

3.2.2 Future Climate Data

Climate scenarios derived from the coupled atmosphere-ocean general circulation models can be used in line with the process-based models for global and local scales impact assessment studies. However, climate predictions from GCMs always involve uncertainties that result from using different climate scenarios (Fu et al., 2007). Therefore, an ensemble analysis combining multiple GCM projections and quantifying the probability of future climate is usually adopted to make a more reliable future regional climate change scenarios. For the present study, the global-scale future climate signals (monthly mean outputs) were obtained from a multi-model ensemble of several GCMs from the Coupled Model Intercomparison Project phase 3 (CMIP3) and phase 5 (CMIP5) of the Intergovernmental Panel on Climate Change Fourth and Fifth Assessment Reports (AR4 and AR5) respectively under different warming scenarios.

3.2.2.1 CMIP3 Dataset

The global-scale future rainfall and temperature (monthly mean outputs) were extracted from a multi-model ensemble of seven GCMs of the CMIP3 (Table 3.1) under three climate scenarios A2, A1B, and B1 which belong to the IPCC-AR4. These models effectively

reproduce the observed historical mean annual rainfall and the daily rainfall distribution across south-east Australia based on a combined score rank provided by Vaze et al., (2011). Next, the global-scale outputs from each GCM were transferred (downscaled) into daily local-scale climate projections suitable for regional impact assessment studies by using the LARS-WG 5.5 stochastic weather generator (detailed description is provided in paragraphs 3.3). The ensemble mean of the downscaled seven-GCMs was then derived and adopted in streamflow simulation. The future data has spanned the current century into three periods including the near future (2016-2043), mid (2044-2071) and late (2072-2099). A baseline climatic period of 40 years (1971-2010) was also extracted from the multi-model ensemble to be compared with the future climate projections.

Table 3.1 the seven GCMs of the CMIP3 model included in the present study

Model Abbreviation	Institute	Country	Grid resolution
CSIRO-Mk3.0	Commonwealth Scientific and Industrial Research Organisation	Australia	1.9 × 1.9°
INMCM	Institute for Numerical Mathematics	Russia	5 × 4°
HADCM3	UK Meteorological Office	UK	2.5 × 3.75°
CNRM	Me´te´o-France/Centre National de Recherches Me´te´orologiques	France	2.8 × 2.8°
MPI-ECHAM5	Max-Planck Institute for Meteorology	Germany	1.9 × 1.9°
GFDL 2.0	Geophysical Fluid Dynamics Lab	USA	2.0 × 2.5°
CCCMA-T47	Canadian Centre for Climate Modelling and Analysis	Canada	3.8 × 3.7°

According to the Special Report on Emissions Scenarios (IPCC, 2000), A2 scenario represents a very heterogeneous world with continuous population growth, slow economic and technological development, and the average CO_2 emission is proposed to reach 850 ppm by the end of this century. On the other hand, B1 scenario refers to a convergent world with a global population that peaks by the mid of the 21st century and decreases afterwards with a rapid economic and technological development. For the B1 scenario, the average concentration of CO_2 emission will firstly increase at the same rate of the A2 scenario and then reduces near the mid-century and end at 550 ppm (IPCC, 2000). Whereas the A1B scenario represents a balance status across all energy sources.

3.2.2.2 CMIP5 Dataset

Future climate signals (rainfall and temperature at monthly scale) were extracted from a multi-model ensemble of eight GCMs of the CMIP5 under three emission scenarios (Representative Concentration Pathways) (RCP2.6, 4.5 and 8.5) which belong to the IPCC-AR5. These scenarios are defined as concentration pathways of human radiative activities which will cause Green House Gas emissions of 2.6, 4.5, and 8.5 Wat/m^2 by the end of the 21st century (Moss et al., 2010). In the CMIP5 dataset, the RCPs 2.6, 4.5, and 8.5 correspond to the emission scenarios B1, A1B and A2 of the CMIP3 respectively (Deng et al., 2016; Onyutha et al., 2016). According to Taylor et al., (2012), RCPs are mitigation scenarios that assume policy actions will be taken to achieve certain emission targets. For CMIP5, four RCPs (2.6, 4.5, 6.0 and 8.5) have been formulated that are based on a range of projections of future population growth, technological development, and societal responses. The labels for the RCPs provide a rough estimate of the radiative forcing in the year 2100 (relative to preindustrial conditions). For example, the radiative forcing in RCP8.5 increases throughout the twenty-first century before reaching a level of about 8.5 W/m^2 at the end of the century. In addition to this "high" scenario, there are two intermediate scenarios, RCP4.5 and RCP6, and a low so-called peak-and-decay scenario, RCP2.6, in which radiative forcing reaches a maximum near the middle of the twenty-first century before decreasing to an eventual nominal level of 2.6 W/m^2.

Table (3.2) provides a detailed description of the eight GCMs incorporated into the multi-model ensemble. According to the Australian Bureau of Meteorology and the CSIRO, these models represent the best eight GCMs out of 40 GCMs of the CMIP5 model (CSIRO and BoM, 2015). They have been selected according to specific criteria to effectively investigate the Australian future climate predictions, particularly for the impact assessment studies. The basis for selecting these models as the best among the CMIP5 models can be found in (https://www.climatechange inaustralia.gov.au/en/support-andguidance/faqs/eight-climate-models-data/). Collier et al., (2011) showed that the CMIP5 represents an unparalleled approach to quality control data (datasets of consistent format) extracted from a range of globally acknowledged climate models to generate a dataset archive which can be easily analyzed. Furthermore, Taylor et al. (2012) explained that the CMIP5 is a globally matched effort for utilizing GCMs and Earth System Models to provide a climatic dataset which can be used efficiently for hydrological analysis of local and global scales. As in the CMIP3 dataset, three future time periods, including the near future (2016-2035), mid (2046-2065) and late (2080-2099) of the 21st century were selected to represent the future climatic conditions.

Furthermore, a baseline climatic period was also extracted from the multi-model ensemble to be compared with the future climate projections.

Table 3.2 The eight CMIP5 GCMs of the IPCC AR5 used in the present study

CMIP5 model ID (name)	Institute	Global average atmosphere resolution (km)
ACCESS1.0	CSIRO-BOM, Australia	210×130
CanESM2	CCCMA, Canada	310×310
CNRM-CM5	CNRM-CERFACS, France	155×155
GFDL-ESM2M	NOAA, GFDL, USA	275×220
CESM1-CAM5	NSF-DOE-NCAR, USA	130×100
HadGEM2-CC	MOHC, UK	210×130
MIROC5	JAMSTEC, Japan	155×155
NorESM1-M	NCC, Norway	275×210

Next, the global scale monthly outputs of rainfall and temperature (from each GCM of the CMIP5) were downscaled into local-scale daily climate projections (point-specific data) suitable for regional impact assessment studies by using the LARS-WG5.5. The ensemble mean of the downscaled 8-GCMs was then derived and adopted in this study.

3.2.2.3 Calculations of future potential evapotranspiration

Potential Evapotranspiration (PET) values are not included in the simulated dataset (i.e. the future and baseline periods). Hence, the monthly mean PET values need to be calculated to make the HBV model applicable for the future and baseline periods. Depending on the downscaled daily mean temperature, two methods were utilized to calculate the potential evapotranspiration for the future and baseline periods and as follows:

a- The modified Blaney-Criddle Method (Doorenbos and Pruitt, 1977)

This method computes the potential evapotranspiration by utilizing the daily mean temperature (T_{mean}) and the average daily percentage of annual daytime hours (Equation 3.16).

$$PET = C[P(0.46 * T_{mean} + 8] \quad (3.16)$$

PET denotes to the monthly average crop evapotranspiration (mm/d). C is a correction factor depends on sunshine hours, minimum relative humidity, and daytime wind speed. P is the daily mean proportion of yearly daylight periods (in hours), and Tmean refers to the daily mean temperature (°C).

b- Hargreaves Method (Hargreaves and Samani, 1985)

Hargreaves (1994) tested this method in a wide range of climatological conditions by using some high-quality lysimeter data whose obtained as nearly accurate results as Penman-Monteith in estimating ET_o. Thus, the use of the Hargreaves method (Equation 3.17) is highly recommended when reliable data are lacking (Alkaeed et al. 2006) as in the case of the present study.

$$ET_o = 0.0023\ (T_{mean} + 17.8)(\ T_{max} - T_{min})\ R_a \qquad (3.17)$$

Where ETo is the reference crop evapotranspiration (mm/day). T_{max} and T_{min} are the daily maximum and minimum air temperature (°C). T_{mean} is the average daily air temperature (°C) calculated as the average of T_{max} and T_{min}. R_a is the extra-terrestrial radiation [MJ m^{-2} day^{-1}] which computed from information on the location of the site and time of the year.

3.3 Downscaling Techniques

Climate data is the key input for regional and global scales impact assessment studies, and they can be extracted from the analysis of Global Climate Models (GCMs) results. Zorita and Von Storch (1999) and Solomon et al., (2007) pointed out that GCMs represent a suitable data source for extracting the regional and global future climate signals. However, the spatial and temporal scales of the outputs resulting from the GCMs are too coarse to be applied directly to local-scale impact assessment studies. Therefore, the GCMs outputs need to be downscaled to a finer scale to be used effectively as input to the rainfall-runoff models. Many downscaling techniques are globally available to extract the local-scale climate outputs from the GCMs including statistical downscaling (Charles et al., 2004; Fowler et al., 2007), dynamic downscaling (Gordon and O'Farrell, 1997; Nunez and McGregor, 2007) and weather generators (Semenov and Barrow, 1997). In this study, the statistical downscaling technique will be adopted.

3.3.1 Long Ashton Research Station Weather Generator version 5.5 (LARS-WG5.5)

The Long Ashton Research Station Weather Generator version 5.5 (LARS-WG5.5), a highly popular stochastic weather generator (Semenov and Stratonovitch, 2010), is used in the present work to compute the local-scale rainfall and temperature from the ensemble mean of the GCMs outputs. LARS-WG5.5 is a statistical downscaling model (Wilks and Wilby, 1999) used to

generate local-scale daily weather data required for climate change impact studies. Semenov and Barrow (1997) explained that the magnitude and periodic sequence of the main climate features had been efficiently simulated by the LARS-WG model. This downscaling technique provides cross-validation for the generated data which has significantly improved the simulation of extreme weather events (Semenov and Stratonovitch, 2010). Accordingly, it has been successfully applied in many local impact assessment studies in diverse climates and has proven its applicability and its high performance, where bias corrections or any other adjustments are not required (Semenov and Stratonovitch, 2010; Gunawardhana et al., 2015).

The process of weather generation using the (LARS-WG5.5) includes three key stages (Semenov et al., 2002):

- **Model calibration:** the model analyses the daily observed weather parameters (rainfall, min and max temperature and solar radiation) of a specified location during a baseline period to determine their statistical characteristics. Then, it creates a set of calibrated probability distribution parameters for that site to be stored in two parameter files.
- **Model validation:** the created parameter files are then used to generate synthetic climate data having the same statistical characteristics as the original observed data. The validity of the model is examined by comparing the statistical characteristics of the observed and synthetic data to evaluate the suitability of the LARS-WA to simulate future weather data for that site. Then, the model calculates relative change factors for each month considering the data in the baseline and GCMs projections.
- **Climate Scenarios generation:** the relative change factors are then used with the calibrated parameters to produce daily climate scenarios for the site in consideration that are compatible with the GCM projections and the observations (Wilks and Wilby, 1999).

The model utilises a Semi-Empirical Probability Distribution (SED) to estimate probability distributions of dry and wet series of daily climate parameters (Semenov et al., 2002). SED is defined as a separate histogram that has a constant number of intervals of flexible lengths. The wet days are expressed as the days with precipitation of more than 0.0 mm. The LARS-WG5.5 uses 23 intervals to describe the shape of the SED compared to the ten intervals of the earlier versions (Semenov and Stratonovitch, 2010). This offers diverse distributions of weather statistics (rainfall and temperature) to be simulated more accurately. The simulation of daily temperature statistics (min and max) is governed by the status of the day whether it is wet or dry. A good record of daily observed weather (minimum of 20 years) is required to obtain

robustly site-specific weather parameters which are used later to produce the synthetic future data (Semenov and Barrow, 1997). In this study, 40 years of daily continuous observed weather data are incorporated into the LARS-WG5.5 to create the calibrated weather parameters.

3.3.2 The Australian Bureau of Meteorology Statistical Downscaling Model (BoM-SDM)

The Australian Bureau of Meteorology (BoM) has developed a Statistical Downscaling Model (BoM-SDM) based on the idea of a meteorological analogue approach introduced by (Timbal and McAvaney, 2001). The model was based on the principle that the regional climate is governed by two factors including the large-scale climatic variables (predictors) and local physiographic characteristics (predictands). Firstly, the model has been applied to ten regions across the Australian continent to simulate six surface predictands including daily minimum and maximum temperatures, dew-point minimum and maximum temperatures, total rainfall and pan evaporation. With the enormous development of the application of SDMs, the BoM-SDM has been extended to cover most of the Australian continent. To enable easy access to downscaling projections across a wider user community, a graphical user interface (GUI) has been developed to provide climate projections across the southern half of the Australian continent (Timbal et al., 2008).

The ability of the model to capture the observed climate has been checked through several studies (e.g. Timbal, 2004; Timbal and Jones, 2008) to verify its applicability to predict the shift in future climate signals as a result of the global warming. The model was also found to well produce the daily variations between the recorded and the reassembled climate series and also its ability to capture the long-term trend of the recorded climate and the inter-annual variability (Timbal et al., 2008). Furthermore, a comparison between the downscaled projections from the BoM-SDM and the direct model outputs was found to be consistent when averaged back on a scale relevant to climate model resolution (Timbal et al., 2008a). More details about the BoM-SDM and the Graphical User Interface (GUI) can be found in (Timbal et al., 2008).

The BoM-SDM has been employed in this study to compute the local-scale daily rainfall and temperature (point-specific climate projections) from the global-scale monthly outputs for the baseline and the future periods. The downscaling approach depends on relationships between the large-scale climate variables (predictors) and the station record variables (predictands).

Based on the availability of high-quality local climate observations, the future local-scale climate variables are derived by matching preceding weather observations (i.e. analogous situations) to the present weather-state (Timbal et al., 2008).

3.4 Summary

In this chapter, the background theory of two hydrological models, HBV conceptual model and BTOPMC distributed model, with special references to their application in hydrological modelling and streamflow forecasting, was briefly reviewed. The detailed structure and parameters of each model were illustrated in more details. The dataset (observed hydrometeorological record) required to run, calibrate and validate each model was also described in details. In addition, future climate data under different scenarios of the CMIP3 and CMIP5, which used to force the hydrological models for future streamflow simulation, were reviewed. The methods of calculating the Potential Evapotranspiration (PET) for the baseline and future periods were also discussed. Finally, the downscaling techniques which were used to extract the local scale future climate series of rainfall and temperature from the different scenarios of GCMs were explained.

Chapter 4

Hydrological Modelling with a Conceptual Model

Extended from:

Al-Safi, H. I. J., & Sarukkalige, P. R. (2017). Evaluation of the impacts of future hydrological changes on the sustainable water resources management of the Richmond River catchment. Journal of Water and Climate Change, (in press).

Al-Safi, H. I. J., & Sarukkalige, P. R. (2018). The application of conceptual modelling to assess the impacts of future climate change on the hydrological response of the Harvey River catchment. Journal of Hydro-environment Research, (in press).

4.1 Introduction

Over the last 40 years, the South-West of Western Australia (SWWA) has experienced a drier climate which has badly affected the amounts of runoff to the main rivers in the area (Barron et al., 2011). Southeast Australia has also experienced a prolonged dry spell similar to the one that began around 1970 in the SWWA (Indian Ocean Climate Initiative 2002; Power et al., 2005). Many researchers have reported and demonstrated this change in climate conditions (e.g. Bari et al., 2010; Vaze and Teng 2011; Vaze et al., 2011; Silberstien et al., 2012; McFarland et al., 2012 and Islam et al., 2014). According to McCarthy (2001), Perth and its surrounding areas are highly vulnerable to a water supply deficiency in the next decades as a result of future climate variations. A reduction in winter rainfall of around 20% has resulted in more than 40% decline in annual mean discharge flows to the main supplying reservoirs in Perth and its outskirts (Indian Ocean Climate Initiative, 2002). Furthermore, most of Australia's population and agricultural activities are extremely concentrated in the southeastern part of the continent (Murphy and Timbal, 2008). The rapid economic and population growth in line with the current water reduction in the area have raised concerns about future water availability and its sufficiency. Therefore, efficient and sustainable water resources management approaches need to be applied by water planners and decision makers in the region to overcome these

issues. Assessments of the impacts of climate change on water resources are vitally important for sustainable water resources management.

Conceptual modelling procedure has been widely used in climate change impact studies and future streamflow predictions. Tian et al. (2013) utilized the conceptual modelling approach (HBV, GR4J and Xinanjiang models) to assess the impact of climate change on river high flows in Jinhua River basin for the near future (2011–2040). The daily scale climate projections from the PRECIS model (Providing REgional Climates for Impacts Studies) under the A1B climate scenario were used to run the three hydrological models for future streamflow predictions. Both bias-corrected and raw precipitation data from the PRECIS model were used to force the hydrological models. Results show that the annual maximum streamflow simulated by the three hydrological models are higher by using the raw precipitation from PRECIS than by bias-corrected precipitation at any return period. Yu et al. (2014) investigated the impact of changing climate conditions on streamflow draught in Tseng-Wen Reservoir Catchment in Southern Taiwan. The A1B and B1 climate scenarios, of the CMIP3, from many GCMs, were used to force the HBV conceptual model to simulate the future streamflow for the periods (2010–2045) and (2081–2100). They found that future streamflow tends to decrease during the dry periods and increase during the wet periods.

The CMIP5 climate data (Taylor et al. 2012) and the (HBV) conceptual model (SMHi 2012) have also been widely used in climate change impact assessment studies around the world, at catchment and global scales. For instance, Sperna et al. (2013) investigated the impact of climate change informed by a multi-model ensemble of the CMIP5 on the extremes streamflow of the Meuse River Basin. They utilized the HBV model to formulate the future streamflow of the river which provides a comprehensive insight into the variations in discharge extremes. Bouaziz et al. (2014) assessed the impact of future climate changes on the annual water yield of the Rhine River basin. They also forced the HBV model with the downscaled climate outputs extracted from an ensemble of 31 GCMs of CMIP5 to simulate the future discharge of the river. Szépszó et al. (2014) and Photiadou et al. (2016) also utilized the HBV lumped-parameter model forced by a multi-model ensemble of the CMIP3 and CMIP5 to study the hydrological response of the Rhine River basin under the impacts of future climate change.

In this chapter, the predicted impact of climate change on future streamflow is assessed for the near-future (2016-2035), mid (2046-2065) and late (2080-2099) of the 21st century at Richmond River catchment and for the mid and late century at the Harvey River catchment.

There were many motivations behind the selection of the study area for this research project. The Peel-Harvey Estuarine System has a considerable ecological, recreational, commercial and scientific importance in South Western Australia. Its fringing environment comprises ecologically important wetlands and lakes that have been placed on the list of Wetlands of International Importance (Environmental Protection Authority, 2008). The Estuarine system also has a valuable commercial and recreational waterway which has improved the urbanisation development and tourist industry. On the other hand, Richmond catchment comprises popular tourist places such as Ballina and supports a continuously growing population attracted by the region's coastal lifestyle. Furthermore, it holds extensive agricultural and wetlands which consume high quantities of water. Hence, assessing the impact of future climate changes on the hydrological system of the catchments is of high environmental and ecological importance.

A multi-model ensemble of eight GCMs from the recently released GCMs of the IPCC-AR5 (i.e. CMIP5) under three Representative Concentration Pathways (RCPs) (2.6, 4.5 and 8.5) was used to extract the global-scale future climate signals across the catchments. The LARS-WG5.5 stochastic weather generator was employed to compute the local-scale future daily rainfall and temperature from each GCM of the multi-model ensemble by incorporating the daily observed climate data. The ensemble mean of the eight-GCMs was then derived to represent the mean value of future rainfall and temperature over the catchment. Next, the mean values of the daily downscaled climate data were used to force the Hydrologiska Byrans Vattenbalansavdelning (HBV) conceptual model to simulate the future daily streamflow at Casino and Clifton Park gauging stations on Richmond and Harvey Rivers respectively. Daily future streamflow forecasting can provide a comprehensive image about the availability of future water resources in the catchments. Thus, the outcomes of this research study could deliver effective water management policies for the study area to overcome the problem of low water accessibility in the future.

4.2 Study area

4.2.1 Harvey River catchment

The Peel-Harvey catchment is located about 80 kilometres south of Perth city in Western Australia. It extends over an approximate area of 1.15 million hectares around the Serpentine, Harvey and Murray River systems (Figure 4.1) (Kelsey et al., 2010). The catchment area has a growing economic, environmental and cultural importance in Western Australia. The Peel Region is distinguished by its waterways and wetlands, which are recognised by international

treaties as the most important waterbird sites in southwestern Australia. The Peel is also one of Western Australia's fastest developing regions, with much recent land use change as well as a large demand for future urbanisation, particularly in the areas close to the ocean and estuaries (Kelsey et al., 2010). For the present study, the main focus area was the Harvey River catchment which stretches from the latitude of 32.35°-33.15° S and longitude of 115.40°–116.10° E with an approximate total drainage area of 1329 km^2 (Figure 4.1). The climate of the catchment is Mediterranean with a summer season tends to be hot-dry and winter season tends to be cool-wet. The temperature is nearly ranged between 10 to 18o C in the winter, and it approximately between 18 to 31° C in the summer and sometimes reaches 40° C (Kelsey et al., 2010). The mean annual rainfall increases from about 750 mm on the coast to 1050 mm on the Darling Scarp and then decreases east of the scarp to about 400 mm at the catchment's eastern boundary (Kelsey et al., 2010). The period between May and October normally holds 80% of the yearly total rainwater falling on the catchment.

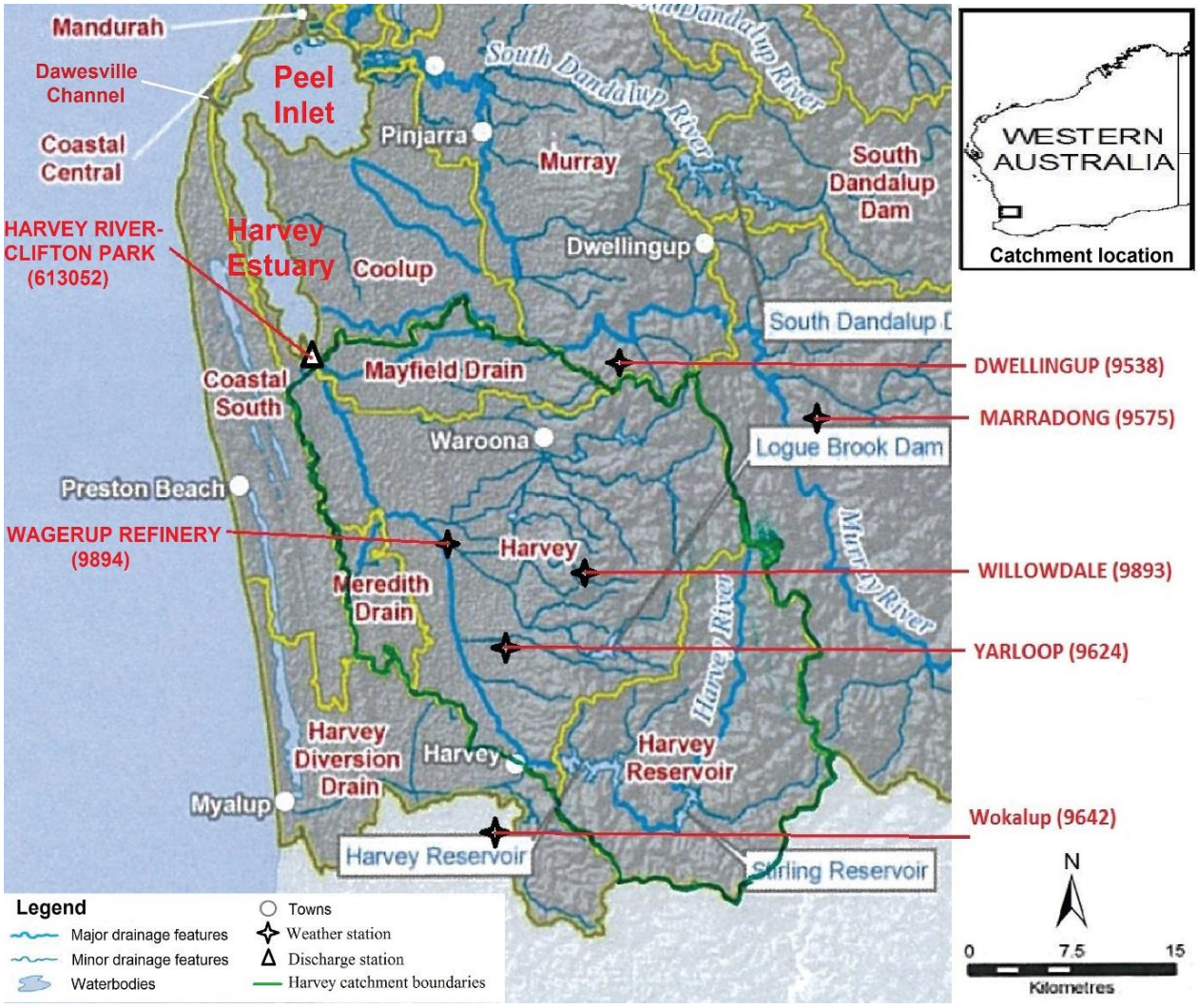

Figure 4.1 Harvey River Catchment with the weather and streamflow gauging stations

4.2.2 Richmond River catchment

The Richmond catchment, with an approximate area of 7000 km^2, is located in the distant north part of NSW, Australia. It extends from the Border Ranges in the north to the Richmond Ranges in the west and south with a variable elevation ranges between more than 1000 meters above sea level near the Border Ranges to few meters above sea level near the coastal floodplain. The catchment includes a diversity of natural sceneries such as world heritage, rainforest, agricultural lands and coastal estuaries. The area also comprises popular tourist places such as Ballina and supports a continuously growing population attracted by the region's coastal lifestyle. In the present work, the area upstream to the Casino gauging station (Figure 4.2) was taken into consideration. It extends over an approximate drainage area of 1790 km2 and stretches from the latitude of 28.22°–29.05°S and longitude of 152.15°–153.15°E. The catchment has Mediterranean climatic conditions with a relatively warm dry summer, approximately ranged between 27-30° C and moderate cold winter, nearly ranged between 19-20° C (CSIRO and BoM 2007). The period between November and April holds the peak rainfall which is approximately ranged between 1350–1650 mm/year in the catchment's coastal areas. However, the interior areas receive the lowest amount of precipitation which is under 800 mm/year at Armidale (CSIRO and BoM, 2007).

Figure 4.2 Richmond River catchment with the hydro-meteorological stations (Source: Department of Primary Industries, Water, NSW, 2016)

4.3 Datasets and hydrological modelling

4.3.1 Observed Climatic data

For the Harvey River catchment, the recorded climate and streamflow data were obtained from seven hydro-meteorological stations (Figure 4.1). Daily observations of rainfall and temperature from six weather stations (Table 4.1) are available for the period (1961-2015). Also, the high-quality daily streamflow record at Clifton Park gauging station on Harvey River

for the period (1983-2015) was used in the model calibration and validation processes. The observed average monthly mean potential evapotranspiration values from two weather stations Dwellingup and Wokalup (Table 4.1) were also included in the modelling process. Whereas, for the Richmond River catchment, the daily observed rainfall, temperature and discharge were obtained from eight hydro-meteorological stations (Table 4.1) over a period of 43 years (1972-2014). The locations of the hydro-meteorological stations are illustrated in (Figure 4.2). In addition, the observed average monthly mean values of potential evapotranspiration from the Tabulam (Muirne) weather station (Table 4.1) were also included in the hydrological simulation.

Table (4.1) Locations of the hydrological and meteorological stations

	Hydro meteorological Stations:	Station No.	Latitude (S^o)	Longitude (E^o)	Altitude (m)	Observed Parameter(s)
Harvey River catchment	Dwellingup	9538	32.71	116.06	267	Rainfall, Temperature and evapotranspiration
	Marradong	9575	32.86	116.45	250	Rainfall
	Wagerup Refinery	9894	32.92	115.92	65	Rainfall
	Willowdale	9893	32.92	116.01	320	Rainfall
	Wokalup	9642	33.13	115.88	30	Rainfall, Temperature and evapotranspiration
	Yarloop	9624	32.96	115.90	30	Rainfall
	Harvey River - Clifton Park	613052	32.82	115.74	20	Discharge
Richmond River catchment	Bentley	58078	28.78	153.11	29	Rainfall
	Green Pigeon	58113	28.47	153.09	210	Rainfall
	Loadstone	58141	28.41	152.98	160	Rainfall
	Old Bonalbo	57085	28.57	152.59	290	Rainfall
	Tabulam post office	57018	28.89	152.57	130	Rainfall
	Tabulam (Muirne)	57095	28.76	152.45	555	Rainfall, Temperature and Evapotranspiration
	Murwillumbah	58158	28.34	153.38	8	Temperature
	Richmond River – Casino	203004	28.86	153.05	20	Discharge

4.3.2 Future climate data

Three future time periods including the near future (2016-2035), mid (2046-2065) and late (2080-2099) of the current century were selected to represent the future climatic conditions across the Richmond catchment. While for the Harvey catchment, only the mid and late century were selected. Future climate signals of rainfall and temperature at monthly scale were extracted from a multi-model ensemble of eight GCMs (Table 3.2) from the Coupled Model

Intercomparison Project phase 5 (CMIP5) of the IPCC Fifth Assessment Report (AR5) under three Representative Concentration Pathways (RCP2.6, RCP4.5 and RCP8.5). A baseline climatic period of continuous 40 years (1971-2010) was also extracted from the multi-model ensemble. It was used to force the calibrated HBV model to obtain the streamflow at catchment outlet for a control run to be compared with the future streamflow. Next, the global-scale monthly outputs were transferred (downscaled) into daily local-scale climate projections (for each GCM) suitable for regional impact assessment studies by using the LARS-WG 5.5 stochastic weather generator (detailed description is provided in paragraph 3.3.1). To reduce the uncertainties in the GCMs projections, the ensemble mean of the 8-GCMs was derived and adopted. Depending on the downscaled daily mean temperature, the Hargreaves Method (Hargreaves and Samani, 1985) (Equation 3.17) is employed to obtain the Potential Evapotranspiration (PE) across the two catchments for the baseline and future periods.

The future climate data from the Coupled Model Intercomparison Project phase 3 (CMIP3) of the IPCC Fourth Assessment Report (AR4) from a variety of GCMs (Table 3.1) and climate scenarios were also used in this research project. The impact of climate change on future streamflow of the two catchments was assessed for same future periods in two separate studies (Al-Safi and Sarukkalige, 2017a and 2017b).

4.3.3 Hydrological modelling

The hydrological simulation was performed by applying the HBV conceptual model to simulate the future daily streamflow at the catchments outlets. A detailed description of the HBV model is provided in chapter three (paragraph 3.1.2).

4.4 Results

4.4.1 HBV Model calibration, validation and parameter estimation

Daily observed streamflow record with a variety of hydrological regimes is required to calibrate and validate the HBV model in a more accurate way. For the Harvey catchment, observed daily streamflow at Clifton Park gauging station on Harvey River was available for a period 33 years (1983-2015). While, for the Richmond catchment, daily streamflow observations at Casino gauging station on Richmond River were available for 43 years (1972-2014). Vaze et al., (2010) reported that the recent discharge record from the south-eastern Australian catchments could be used effectively to calibrate the rainfall-runoff models to represent the current

prolonged drought across the region and to predict the future climate change impact on the local catchments. Since there was only one gauging station at the outlet of each catchment with a daily streamflow record, therefore, each catchment was treated as a single spatial unit during the calibration and validation periods as well as during the simulation of future streamflow.

Before starting the calibration process, the Harvey and Richmond catchments were divided into five and three elevation zones respectively of different areal fractions to laps rainfall and temperature with elevation (using the parameters pcalt and tcalt). It was proposed that rainfall will increase by 10% and temperature will decrease by 0.61^{o} C with each 100 m elevation increment (Seibert, 2005). By presenting this adjustment, the reliance of precipitation and temperature on topography, which is present in the atmospheric forcing data, is reintroduced in the lumped model simulation. For the Harvey and Richmond catchments, the HBV model was firstly run for an initial state of one year (1983-1984) and (1972-1973) respectively with the observed rainfall, temperature and monthly mean potential evapotranspiration to initialize the system. At Clifton Park gauging station, the HBV-model was manually calibrated for a period of 20-years (1984-2003) and validated for the rest of the recorded period (2004-2015). While at Casino gauging station, the model was manually calibrated and validated for the periods (1973-2000) and (2001-2014) respectively. Driessen et al., (2010) suggested that long-time calibration period is useful to simulate large data set of future scenarios. Therefore, a calibration period of almost twofold the validation period is adopted in this study. The calibration and validation periods were selected to represent a compromise between a longer period that would better account for climate variability and a shorter period that would better represent current development.

Eleven parameters are included in the calibration and validation processes (Table 4.2). SMHI (2012) explained that the method of evaluating the results during the calibration process is considered of great importance. Hence, the modelling performance was evaluated using three criteria of efficiency including Nash-Sutcliffe efficiency (NSE) (Nash and Sutcliffe, 1970), relative volume error (VE) and the coefficient of determination (R^2) (Equations 4.1, 4.2 and 4.3). A satisfactory modelling performance was acquired during the calibration and validation processes across the two catchments (Table 4.3) which indicates that the model can be used effectively to simulate the future streamflow at the two gauging stations. Figure (4.3) illustrates the results of the observed and simulated discharges at Clifton Park and Casino gauging stations for the calibration and validation periods. Through the visual inspection of Figure (4.3), it can

be seen that the simulated discharge is fairly captured the observed discharge for the calibration and validation periods except for some periods of low flow simulations. This could be attributed to the simple conceptual structure of the HBV model which only includes a single groundwater storage responsible for the runoff generation.

$$NSE = 1 - \frac{\sum (QC-QR)^2}{\sum (QR-QR_{mean})^2} \quad (4.1)$$

$$VE = \frac{\sum (QR-QC)}{\sum (QR)} X\,100 \quad (4.2)$$

$$R^2 = \frac{[\sum_{i=1}^{n}(QR-QR_{mean})(QC-QC_{mean})]^2}{\sum_{i=1}^{n}(QR-QR_{mean})^2 \cdot \sum_{i=1}^{n}(QC-QC_{mean})^2} \quad (4.3)$$

Where QC is the computed discharge, QR is the recorded discharge. QR_{mean} and QC_{mean} are the means recorded and computed discharges over the calibration period.

Table 4.2 HBV model parameters and their optimal values resulting from the calibration and validation periods across the two catchments

Parameter	Symbol	Unit	Optimal value Harvey Catchment	Optimal value Richmond Catchment
Rainfall correction factor	rfcf	-	0.65	1.1
Elevation correction factor for precipitation	pcalt	1/100m	0.1	0.1
Temperature lapse	tcalt	º C/100m	0.6	0.6
Maximum of soil moisture zone	FC	mm	650	500
Limit for potential evapotranspiration	Lp	-	0.5	0.5
Shape coefficient	Beta	-	1.5	1.5
General correction factor for potential evapotranspiration	ecorr	-	0.9	0.8
Recession coefficient for upper response box	Khq	1/day	1	0.8
Recession coefficient for lower response box	K4	1/day	0.1	0.1
Maximum percolation capacity	Perc	mm/day	1	3
Routing parameter	Maxbaz	day	1	1

Table 4.3 HBV model performance during the calibration and verification periods

	Process	NSE	VE %	r^2
Harvey River Catchment	**Calibration**	0.89	3.6	0.81
	Validation	0.85	4.7	0.78
Richmond River Catchment	**Calibration**	0.92	4.0	0.84
	Validation	0.90	4.8	0.81

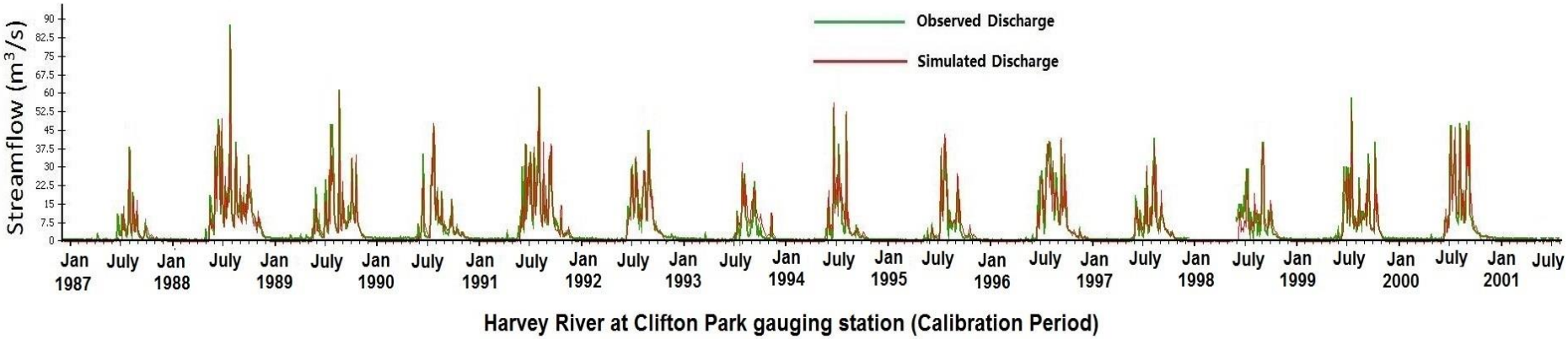

Harvey River at Clifton Park gauging station (Calibration Period)

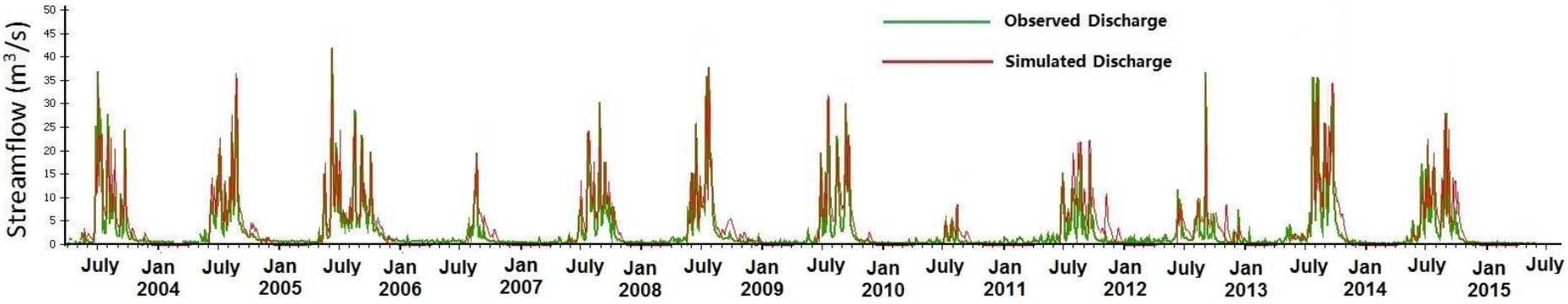

Harvey River at Clifton Park gauging station (Validation Period)

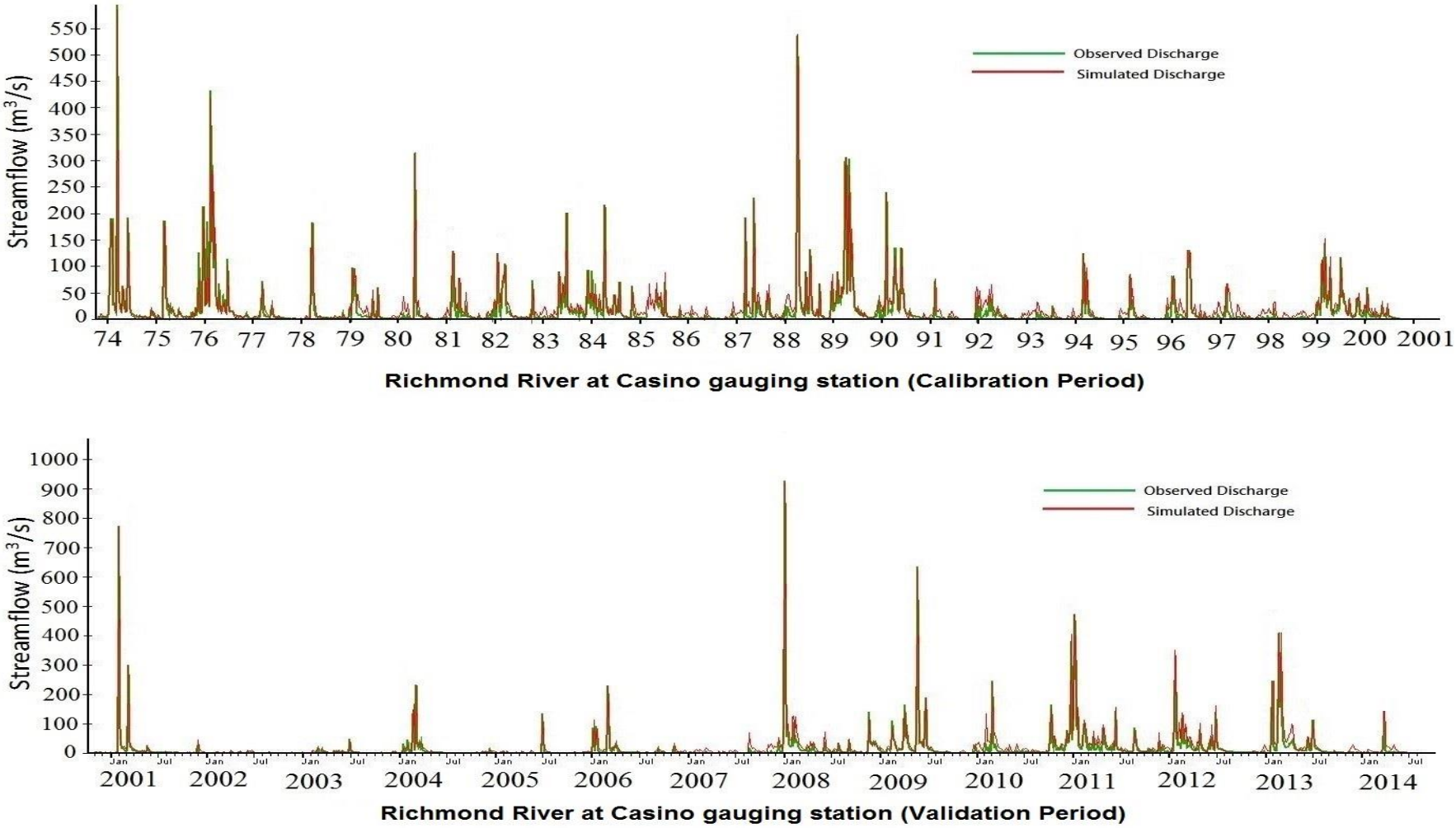

Figure 4.3 Daily observed and simulated streamflow at Clifton Park and Casino gauging stations for the calibration and validation periods.

4.4.2 Performance of the LARS-WG5.5 model

The ability of the LARS-WG to capture the observed climate should be checked before generating the future climate series of rainfall and temperature required for climate impact assessment. As mentioned earlier, 40 years of observed daily precipitation, minimum and maximum temperature, (1961-2000) for the Harvey catchment and (1972-2011) for the Richmond catchment, were used to calibrate and validate the LARSE-WG model. The modelling performance was assessed by relating the probability distributions of the generated (synthetic) climate data with those resulting from the observations.

For the rainfall time series, two characteristics were used including monthly mean rainfall and standard deviation (Figure 4.4). While for the temperature time series, the min and max monthly mean statistics were taken into account (Figure 4.5). Furthermore, the Kolmogorov-Smirnov (K-S) test is performed to compare the seasonal probability distributions for the lengths of the wet/dry periods (Table 4.4). The K-S goodness-of-fit test is also adopted to assess the equality of the daily distributions of rainfall, min and max temperature calculated from the observed and simulated data series (Tables 4.5 and 4.6). The test computes a p-value which gives an indication of the possibility that the observed and generated datasets may have come from the same distribution. A very small p-value (corresponding to a high K-S value) indicates that the synthetic data belongs to a distribution different from that of the observed climatic data, and therefore, it should be rejected. While a large p-value means that the differences between the observed and generated climate statistics for the variable in consideration are too small and there is no indication to reject the generator. Semenov et al., (2002) recommended that a p-value of 0.01 can be used as the acceptable significance limit of the model results. They explained that the basis for using a higher level of statistical significance than the conventional 0.05 level is due to the fact that the level of p-value to be considered as significant is subjective and depends on the importance of a very close fit for the model application.

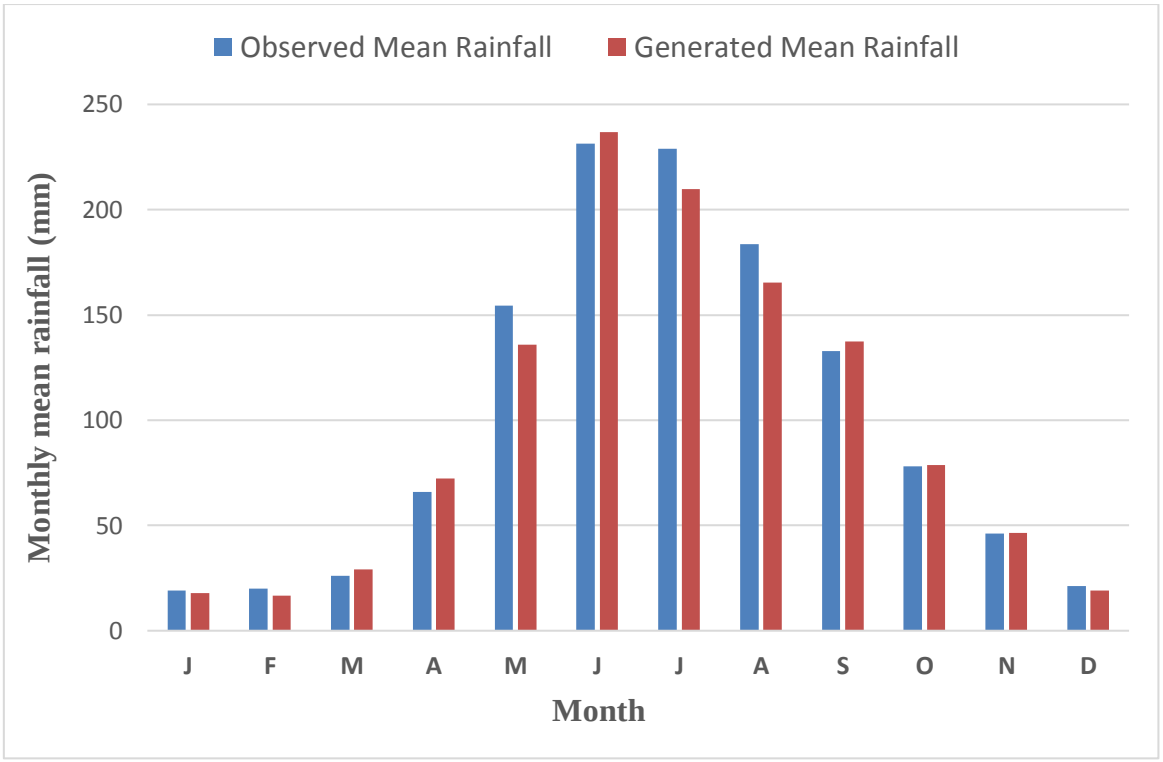

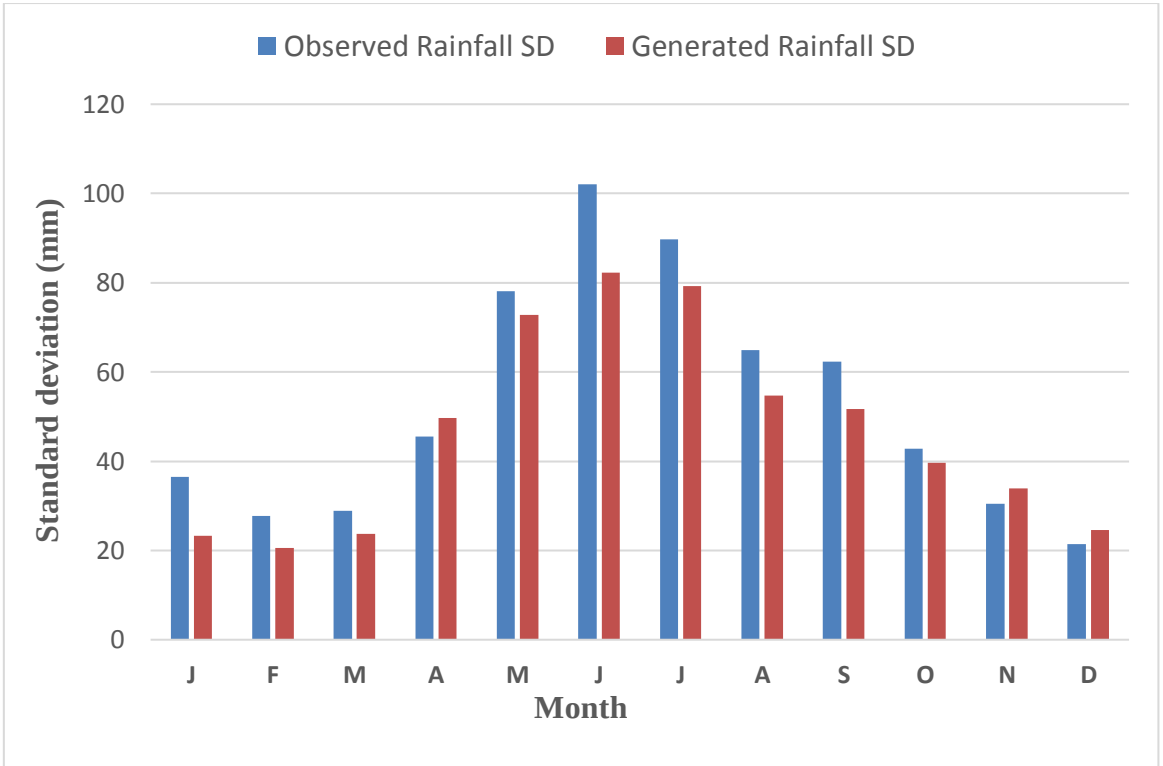

(a) Harvey River Catchment

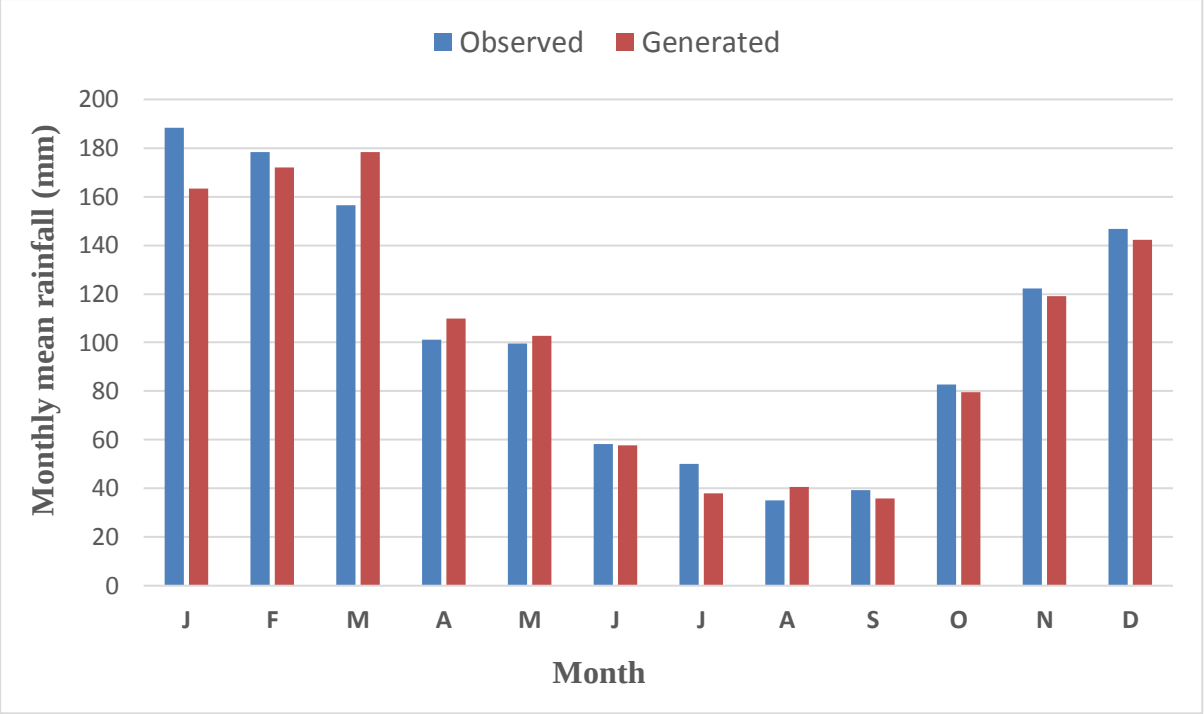

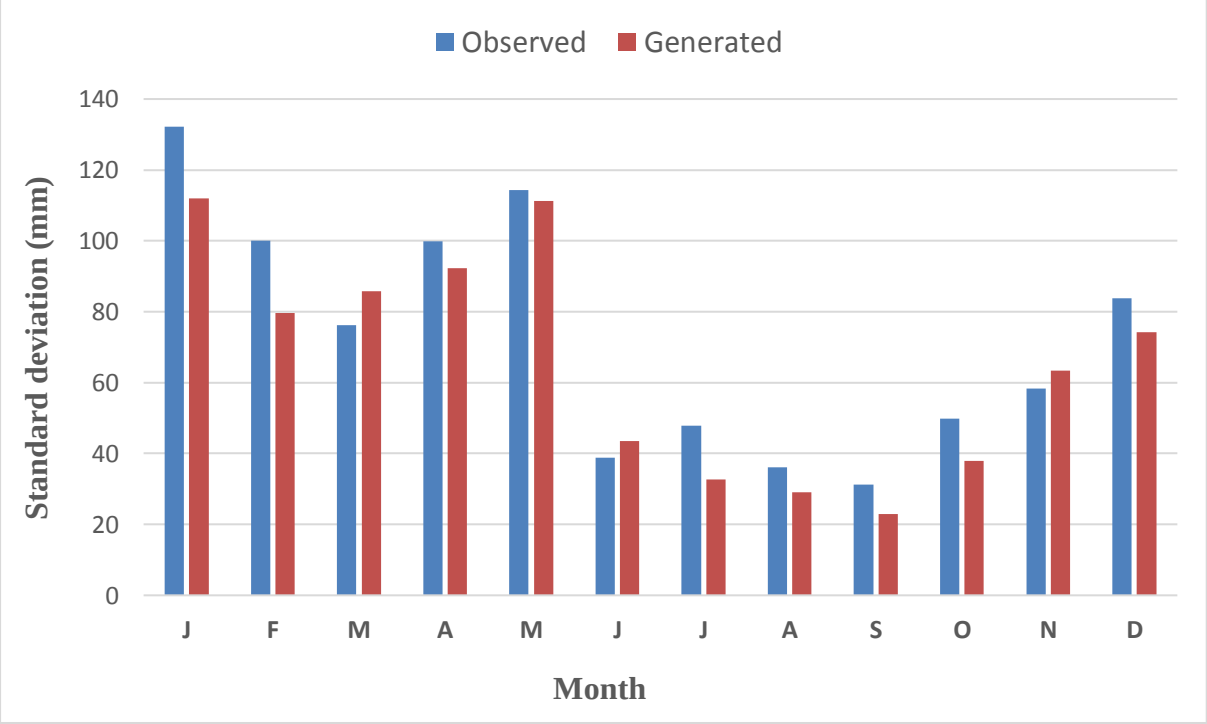

(b) Richmond River Catchment

Figure (4.4) A comparison between the observed and generated rainfall time series across the two catchments

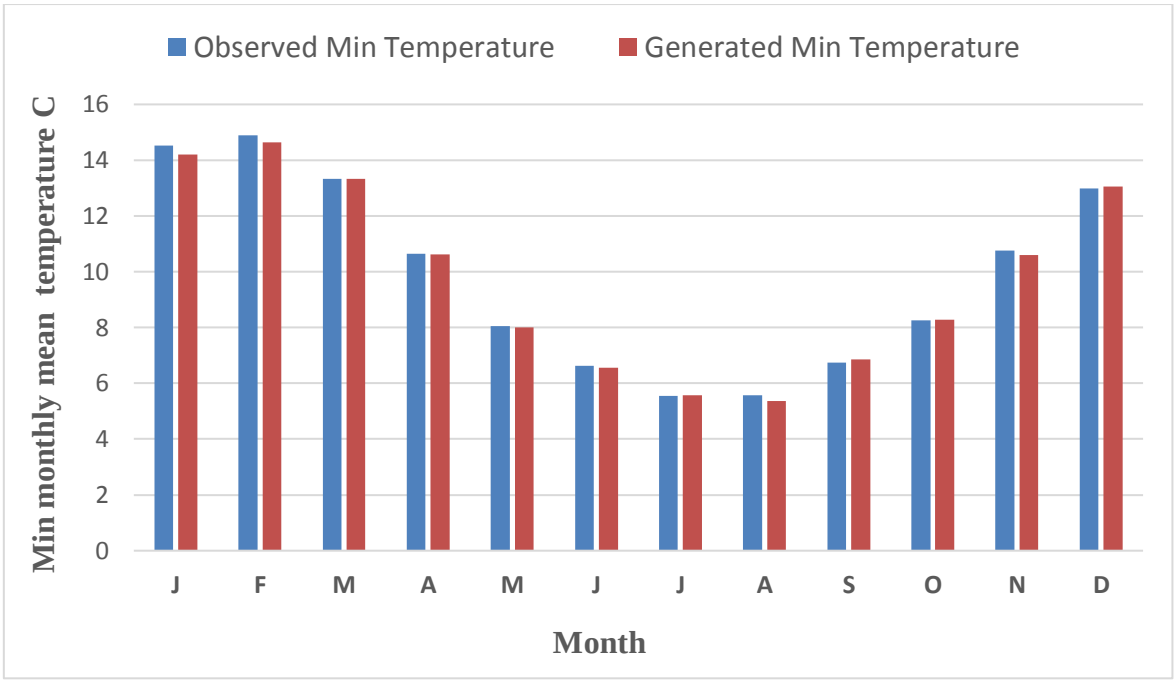

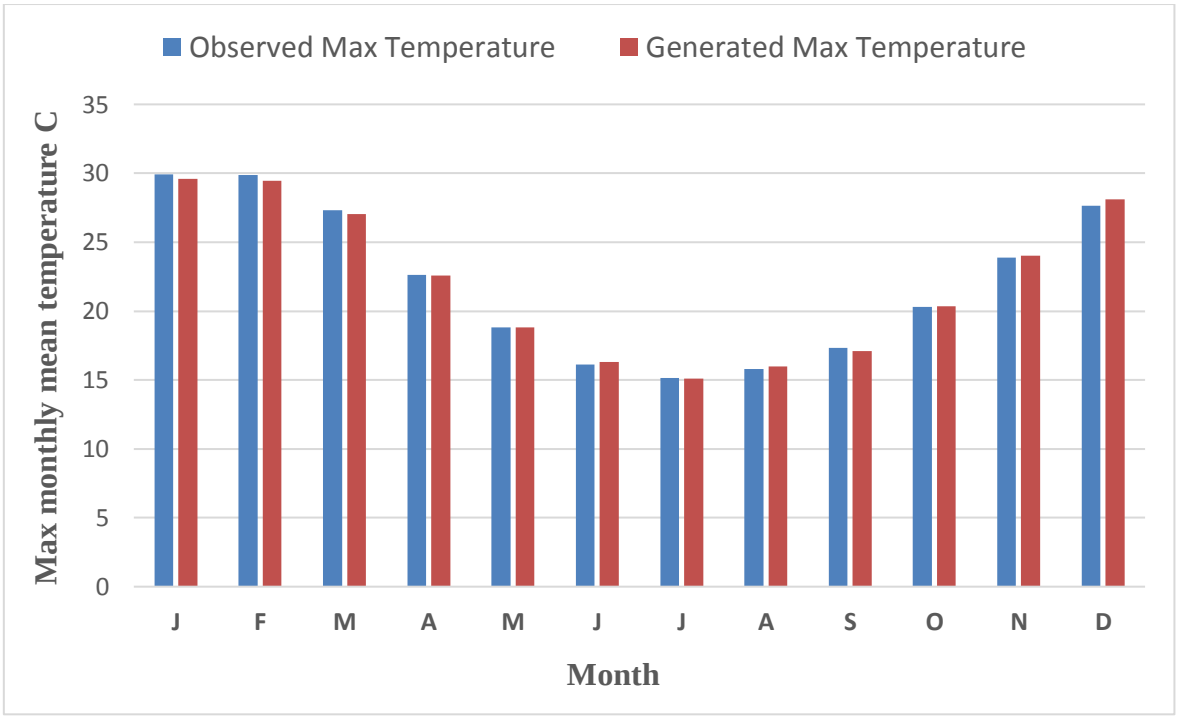

(a) Harvey River Catchment

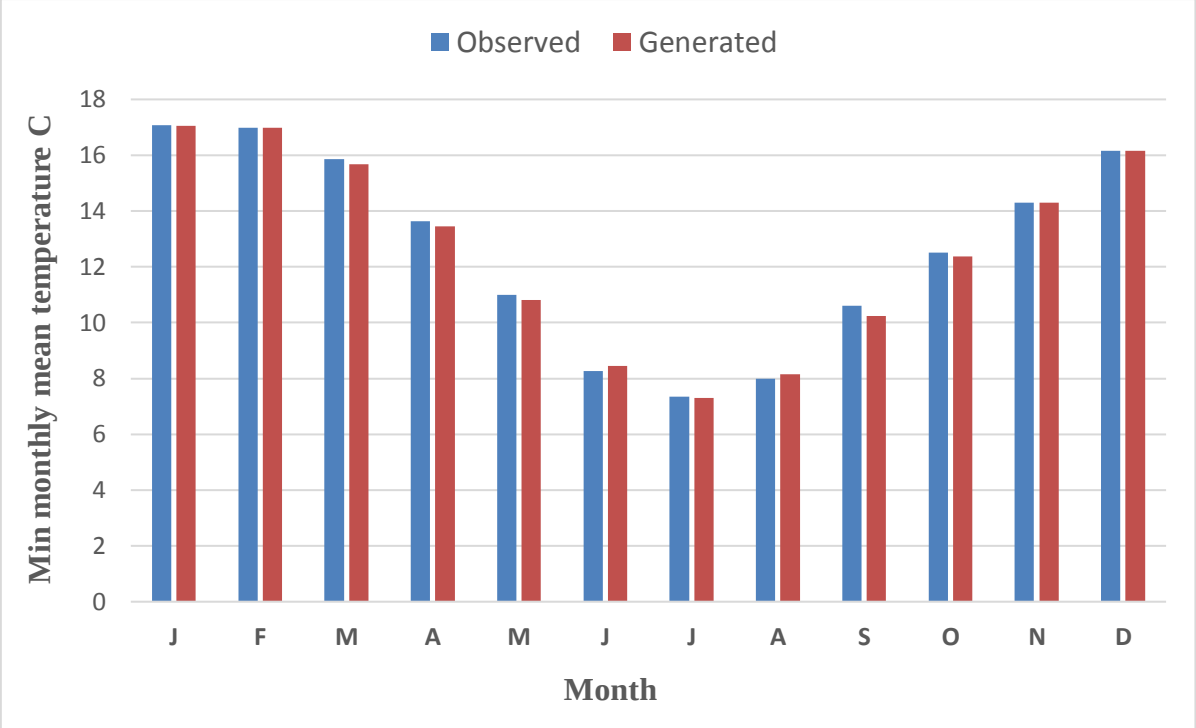

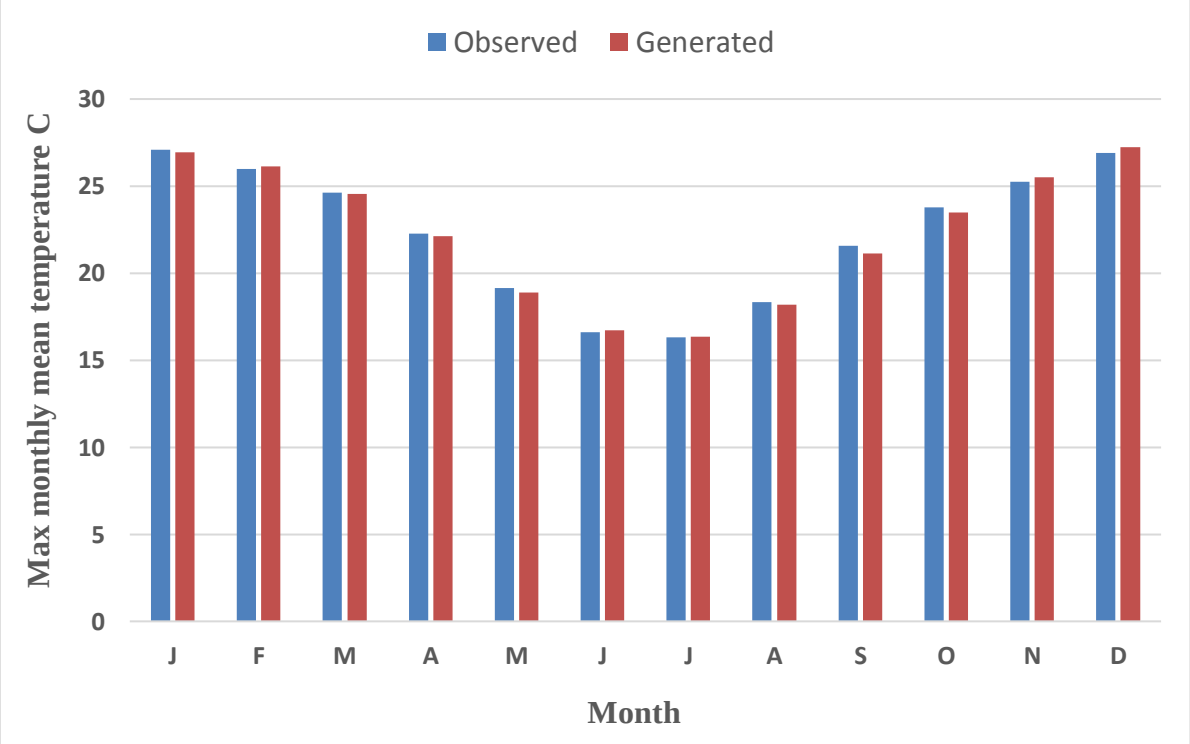

(b) Richmond River Catchment

Figure (4.5) A comparison between the observed and generated Temperature time series across the two catchments

Table (4.4) Kolmogorov-Smirnov test results for seasonal wet/dry series distributions

	Season	Event	No. of tests (N)	K-S Test	P-value	Assessment
Harvey River Catchment	**Dec/Jan/Feb**	Wet	12	0.09	0.981	Very good fit
		Dry	12	0.084	1.000	Perfect fit
	Mar/Apr/May	Wet	12	0.175	0.843	Very good fit
		Dry	12	0.036	1.000	Perfect fit
	Jun/Jul/Aug	Wet	12	0.103	0.928	Very good fit
		Dry	12	0.032	1.000	Perfect fit
	Sep/Oct/Nov	Wet	12	0.047	1.000	Perfect fit
		Dry	12	0.032	1.000	Perfect fit
Richmond River Catchment	**Dec/Jan/Feb**	Wet	12	0.08	1.000	Perfect fit
		Dry	12	0.218	0.644	Good fit
	Mar/Apr/May	Wet	12	0.037	0.992	Perfect fit
		Dry	12	0.041	1.000	Perfect fit
	Jun/Jul/Aug	Wet	12	0.154	0.741	Good fit
		Dry	12	0.031	0.994	Perfect fit
	Sep/Oct/Nov	Wet	12	0.051	1.000	Perfect fit
		Dry	12	0.084	1 .000	Perfect fit

Table (4.5) Kolmogorov-Smirnov test results for daily rainfall distributions (in each month)

	Month	No. of tests (N)	K-S Test	P-value	Assessment
Harvey River Catchment	**Jan**	12	0.083	1.000	Perfect fit
	Feb	12	0.108	0.999	Perfect fit
	Mar	12	0.072	1.000	Perfect fit
	Apr	12	0.13	0.984	Very good fit
	May	12	0.265	0.341	Good fit
	Jun	12	0.142	0.962	Very good fit
	Jul	12	0.231	0.514	Good fit
	Aug	12	0.197	0.714	Good fit
	Sep	12	0.039	1.000	Perfect fit
	Oct	12	0.037	1.000	Perfect fit
	Nov	12	0.027	1.000	Perfect fit
	Dec	12	0.064	1.000	Perfect fit
Richmond River Catchment	**Jan**	12	0.111	0.980	Perfect fit
	Feb	12	0.109	0.989	Perfect fit
	Mar	12	0.175	0.860	Very good fit
	Apr	12	0.049	1.000	Perfect fit
	May	12	0.051	1.000	Perfect fit
	Jun	12	0.172	0.863	Very good fit
	Jul	12	0.210	0.667	Good fit
	Aug	12	0.162	0.914	Perfect fit
	Sep	12	0.235	0.519	Good fit
	Oct	12	0.141	0.960	Perfect fit
	Nov	12	0.049	0.987	Perfect fit
	Dec	12	0.120	0.999	Perfect fit

Table (4.6) K-S test results for distributions of the daily minimum and maximum temperature (in each month)

	Month	No. of tests (N)	Daily Minimum Temperature			Daily Maximum Temperature		
			K-S Test	P-value	Assessment	K-S Test	P-value	Assessment
Harvey River Catchment	**Jan**	12	0.158	0.913	Perfect fit	0.106	0.998	Perfect fit
	Feb	12	0.106	0.998	Perfect fit	0.106	0.999	Perfect fit
	Mar	12	0.106	0.998	Perfect fit	0.106	0.998	Perfect fit
	Apr	12	0.053	1.000	Perfect fit	0.053	1.000	Perfect fit
	May	12	0.105	0.999	Perfect fit	0.053	1.000	Perfect fit
	Jun	12	0.106	0.998	Perfect fit	0.053	1.000	Perfect fit
	Jul	12	0.053	1.000	Perfect fit	0.053	1.000	Perfect fit
	Aug	12	0.106	0.998	Perfect fit	0.053	1.000	Perfect fit
	Sep	12	0.053	1.000	Perfect fit	0.053	1.000	Perfect fit
	Oct	12	0.105	0.999	Perfect fit	0.053	1.000	Perfect fit
	Nov	12	0.106	0.998	Perfect fit	0.053	1.000	Perfect fit
	Dec	12	0.106	0.998	Perfect fit	0.053	1.000	Perfect fit
Richmond River Catchment	**Jan**	12	0.106	0.998	Perfect fit	0.106	0.998	Perfect fit
	Feb	12	0.106	0.998	Perfect fit	0.053	1.000	Perfect fit
	Mar	12	0.106	0.998	Perfect fit	0.053	1.000	Perfect fit
	Apr	12	0.106	0.998	Perfect fit	0.106	0.998	Perfect fit
	May	12	0.106	0.998	Perfect fit	0.105	0.999	Perfect fit
	Jun	12	0.053	1.000	Perfect fit	0.053	1.000	Perfect fit
	Jul	12	0.053	1.000	Perfect fit	0.053	1.000	Perfect fit
	Aug	12	0.053	1.000	Perfect fit	0.106	0.998	Perfect fit
	Sep	12	0.158	0.913	Perfect fit	0.106	0.998	Perfect fit
	Oct	12	0.106	0.998	Perfect fit	0.106	0.998	Perfect fit
	Nov	12	0.105	0.999	Perfect fit	0.053	1.000	Perfect fit
	Dec	12	0.106	0.998	Perfect fit	0.053	1.000	Perfect fit

The simulated rainfall and temperature statistics are in good agreement with those of the recorded statistics as illustrated in Figures (4.4) and (4.5). Table (4.4) also demonstrates the good performance of the LARS-WG model in simulating the seasonal distributions of the wet and dry spells. In addition, the daily distributions of rainfall, minimum and maximum temperature (in each month) (Tables 4.5 and 4.6) also verify the excellent modelling performance. It can be seen that all p-values in Tables (4.4, 4.5 and 4.6) are more than 0.01 (i.e. 99% confidence level) and the results of the assessment columns ranged between good and perfect fit. This could be attributed to the fact that the LARS-WG generates random data which is comparable to the observed data in its statistical properties only. Furthermore, the high-quality observed climate data of the baseline period could also be a reason for the reasonable agreement between the observed and synthetic climate series. It also found that the performance of the LARS-WG was satisfactory through the t and F tests which compared the mean and variance values of two-time series. The seasonal distributions of the wet/dry spells

and the daily rainfall, minimum and maximum temperature distributions are very important when using the model results in impact assessment studies (Osman et al., 2014). These properties were properly fitted for the observed and synthetic climate series which highlights the good performance of LARS-WG simulation. Therefore, the calibrated parameters of the LARS-WG can be incorporated properly with the RCP scenarios to generate the future rainfall and temperature series for climate impact assessment across the two catchments.

In short, 40 years of continuous daily observed weather data from many sites (weather stations) across the two catchments were incorporated into the LARS-WG5.5 to create the calibrated weather parameters. Next, the grid climate outputs resulting from each GCM of the 8-GCMs multi-model ensemble that are covering the two catchments were also incorporated with the calibrated parameters to generate local-scale daily time series of rainfall and temperature for the future and baseline periods. Finally, the ensemble mean of the local-scale climate outputs was then derived and used to force the calibrated HBV model to simulate the discharge at the catchments outlet (Clifton Park and Casino discharge stations).

4.4.3 Future climate projections

The projected climate (rainfall, temperature and evapotranspiration) of the future periods was compared with the baseline climate (1971-2010) as illustrated in Table (4.7). Almost all GCMs predict a reduction in mean annual rainfall and a rise in temperature and potential evapotranspiration across the two catchments under all scenarios during the mid and late century. For the Richmond catchment, the ensemble mean of the downscaled eight-GCMs shows a positive trend in rainfall amounts and a rise in temperature and potential evapotranspiration values during the near future. A significant variation in rainfall prediction between different scenarios, especially for the late century, were observed.

Table (4.7) Changes in the mean annual climate of the future scenarios relative to the baseline period across the two catchments. (The values of the RCPs represent the ensemble mean of 8-GCMs)

Harvey River catchment	Variable	Observed (1961-2015)	Baseline period (1971-2010)	Changes in mean annual values compared to the baseline period								
				2016-2035			2046-2065			2080-2099		
				RCP 8.5	RCP 4.5	RCP 2.6	RCP 8.5	RCP 4.5	RCP 2.6	RCP 8.5	RCP 4.5	RCP 2.6
	P (mm/year)	1165	1126	-	-	-	-5.9%	-10.9%	-6.7%	-14.1%	-23.0%	-7.6%
	T (Cº)	16.1	17.0	-	-	-	+0.6 Cº	+0.31 Cº	+0.15 Cº	+1.81 Cº	+1.2 Cº	+0.32 Cº
	PET (mm/year)	1431	1473	-	-	-	+10.7%	+9.8%	+8.6%	+14.1%	+12.8%	+10.0%

Richmond River catchment	Variable	Observed (1972-2014)	Baseline period (1971-2010)	Changes in mean annual values compared to the baseline period								
				2016-2035			2046-2065			2080-2099		
				RCP 8.5	RCP 4.5	RCP 2.6	RCP 8.5	RCP 4.5	RCP 2.6	RCP 8.5	RCP 4.5	RCP 2.6
	P (mm/year)	1209	1180	+5.0%	+2.8%	+4.5%	-0.2%	-0.4%	-2.0%	-3.0%	-8.5%	-5.3%
	T (Cº)	17.5	18.0	+0.2 Cº	+0.4 Cº	+0.4 Cº	+1.3 Cº	+1.4 Cº	+1.1 Cº	+2.4 Cº	+1.9 Cº	+1.6 Cº
	PET (mm/year)	1553	1601	+0.8%	+2.8%	+2.9%	+4.5%	+5.8%	+4.4%	+8.6%	+5.9%	+5.1%

Note: (+) means increase, (-) means decrease

For the Harvey River catchment, the mid-century mean annual rainfall is projected to decline by 6.7%, 10.9% and 5.9% under the RCP2.6, RCP4.5 and RCP8.5 respectively. By the end of the century, there could be a further decline in the mean annual rainfall of 7.6%, 23.0% and 14.1% under the same scenarios correspondingly. On the other hand, rainfall is projected to increase during the near future across the Richmond River catchment with an annual mean increment of 5%, 2.8% and 4.5% under the scenarios RCP8.5, RCP4.5 and RCP2.6 respectively. Conversely, by the mid-century, the annual mean rainfall is projected to decline by 0.2%, 0.4% and 2.0% under the scenarios RCP8.5, RCP4.5 and RCP2.6 correspondingly. While by the end of the century, the average declines in the mean annual rainfall are projected to be 8.6%, 5.9% and 5.1% under the same scenarios respectively. A graphical comparison between the baseline and future predicted rainfall across the two catchments is presented in Figure (4.6).

The decline in rainfall amounts across the two catchments could be attributed to the fact that the whole distribution is shifted to lower values by the mid and late of the current century. Another possible explanation for the rainfall decline is the lack of high-intensity rainfall events during the future periods. For instance, in the Harvey catchment, the 90^{th} rainfall percentile during the mid-century is projected to decline by 1%, 7% and 2% under the RCP2.6, RCP4.5 and RCP8.5 respectively compared to the baseline period (Figure 4.7). Toward the end of the century, the decline in the 90^{th} rainfall percentile is anticipated to be 2%, 20% and 10% under the same scenarios correspondingly. Similarly, in the Richmond catchment, the 90^{th} rainfall percentile during the mid and late of the century shows a noticeable decline ranged between 1-11% (Figure 4.7). The maximum rainfall values are also expected to decline during the mid and late of the century with a range of 10-19%.

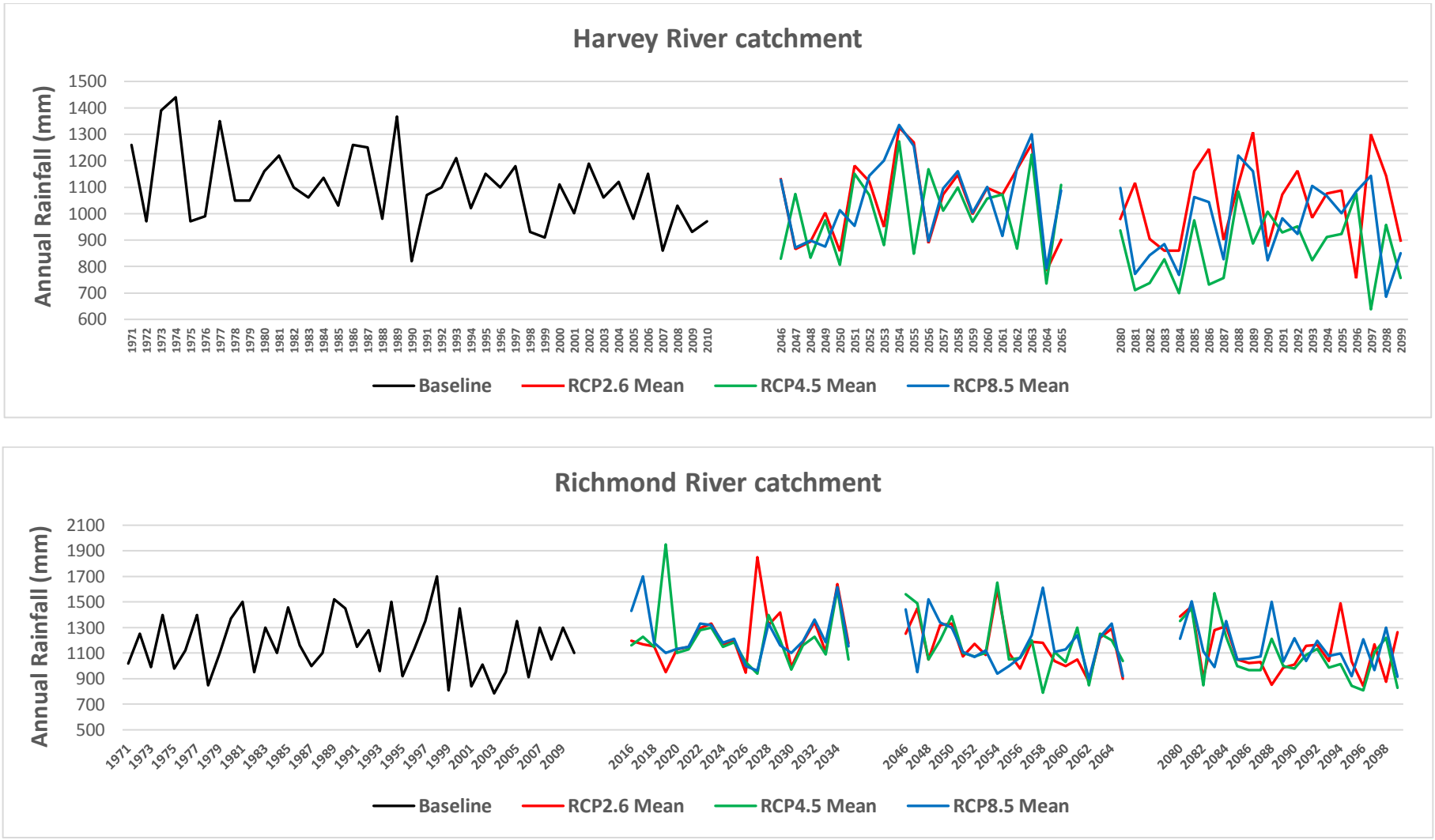

Figure (4.6) A comparison between the baseline and future annual rainfall across the two catchments under the three climate scenarios. The simulated rainfall is the ensemble mean of 8-GCMs.

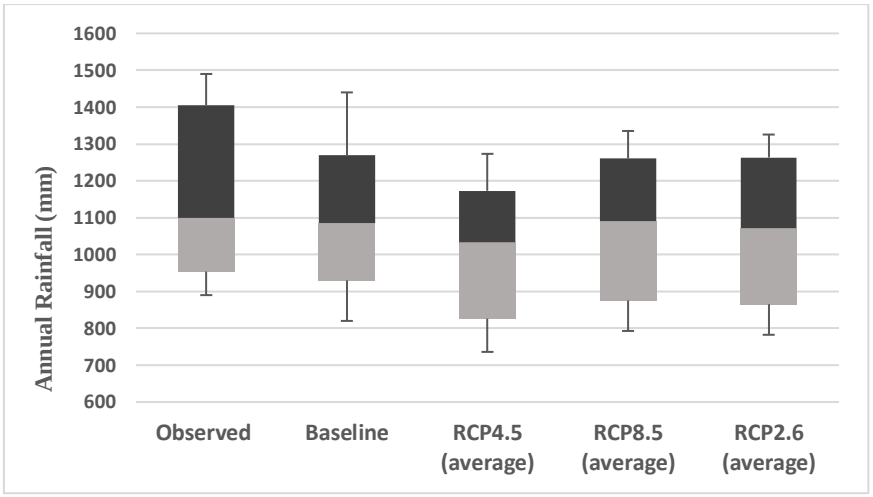

(a) Harvey River catchment during the mid-century

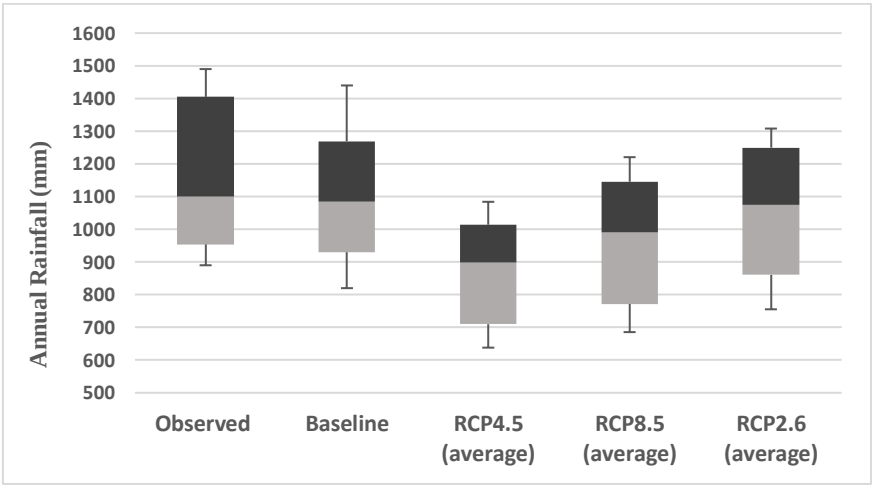

(b) Harvey River catchment during the late-century

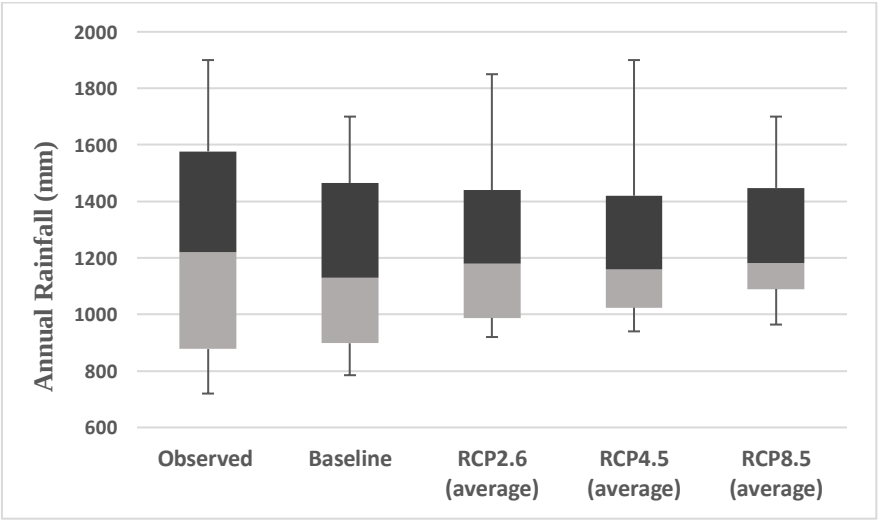

(c) Richmond River catchment during the near future

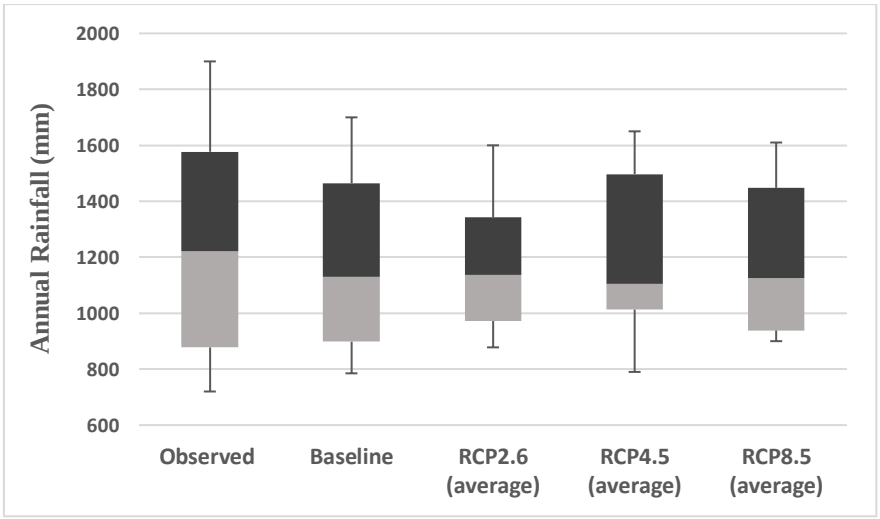

(d) Richmond River catchment during the mid-century

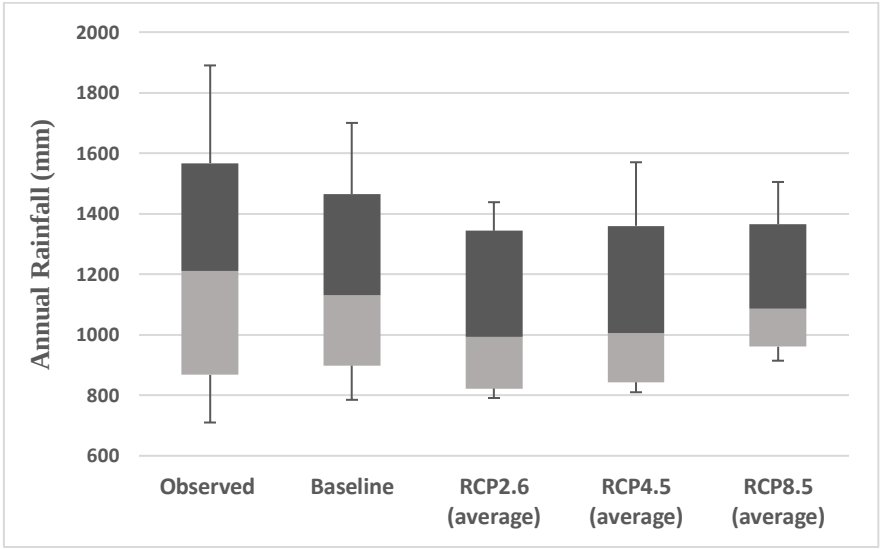

(e) Richmond River catchment during the late-century

Figure (4.7) The 10th, 50th and 90th percentiles of annual rainfall for the observed, baseline and future periods. The bars represent the errors in the minimum and maximum annual rainfall percentiles. The simulated rainfall of the baseline and future periods is the ensemble mean of 8-GCMs.

On the other hand, the mean annual temperature across the two catchments show positive trends under all climate scenarios during the future periods (Table 4.7). The projected rise in temperature values is anticipated to increase the annual mean Potential Evapotranspiration (PET) across the two catchments in the future (Table 4.7). The sole rise of air temperature could increase the additional energy available for driving soil water and intercepted water for

evaporation or transpiration. Consequently, the combined impact of rainfall reduction and potential evapotranspiration increase by the mid and late of the century could adversely affect the future streamflow across the two catchments.

4.4.4 Future streamflow projections

After the calibration process, the HBV model was forced with the ensemble mean of the downscaled climate data to simulate the future daily streamflow at Clifton Park and Casino gauging stations on Harvey and Richmond Rivers respectively. The model was also forced with the downscaled climate data of the baseline period (1971-2010) to simulate the daily streamflow at the tow stations for a control run. The differences between the two simulations represent the impact of climate change on the hydrological system of the Harvey and Richmond catchments. Vaze et al., (2010) pointed out that the rainfall-runoff models calibrated over a period of more than 20 years could be used effectively in impact assessment studies, conditioned that the annual mean rainfall in the simulated period shouldn't be more than 15% drier or 20% wetter than the calibration period. As the simulated future annual mean rainfall over the two catchments is within the above limits relative to the observed annual mean rainfall over the calibration periods (Table 4.7), then the calibrated HBV model can be used efficiently for regional scale impact assessment. The variations of annual mean streamflow statistics of the future climate scenarios relative to the control run at the two gauging stations are presented in Table (4.8). It clearly shows that for the two catchments, the response to the anticipated climate change is obvious through the decline in the future annual mean streamflow at Clifton Park and Casino gauging stations by the mid and late-century.

Further, Figure (4.8) illustrates a graphical comparison between the control run and the streamflow resulting from the future scenarios. While Figure (4.9) shows the minimum, 10^{th}, 50^{th}, 90^{th} and maximum streamflow percentile statistics at the two gauging stations for the observed, baseline and the scenarios of the future periods.

Table (4.8) Changes in annual mean streamflow statistics (m^3/s) of the future climate scenarios relative to the control run at Clifton Park and Casino gauging stations. The values of all RCPs represent the ensemble mean of 8-GCMs

	Variable	Control Run (1981-2010)	Changes in mean annual runoff compared to the control run (%)								
			(2016-2035)			(2046-2065)			(2080-2099)		
			RCP 2.6	RCP 4.5	RCP 8.5	RCP 2.6	RCP 4.5	RCP 8.5	RCP 2.6	RCP 4.5	RCP 8.5
Harvey River at Clifton Park	**Q Min.**	1.5	-	-	-	-13	-7	-7	-53	-27	0
	Q10	1.96	-	-	-	-18	-8	-8	-54	-34	-8
	Q50	4.3	-	-	-	-16	-7	-7	-56	-23	-9
	Q90	10.0	-	-	-	-50	-42	-45	-65	-53	-45
	Q Max.	11.2	-	-	-	-45	-36	-35	-55	-36	-37
	Q Mean	4.8	-	-	-	-27	-17	-19	-52	-33	-23

	Variable	Control Run (1971-2010)	Changes in mean annual runoff compared to the control run (%)								
			(2016-2035)			(2046-2065)			(2080-2099)		
			RCP 2.6	RCP 4.5	RCP 8.5	RCP 2.6	RCP 4.5	RCP 8.5	RCP 2.6	RCP 4.5	RCP 8.5
Richmond River at Casino	**Q Min.**	4.5	+16	+24	+29	-9	-7	-4	-13	-16	-11
	Q10	11.0	+7	+15	+26	-20	-20	-11	-19	-28	-19
	Q50	17.7	+7	+10	+18	-2	-5	-4	-14	-24	-11
	Q90	32.9	+1	+1	+6	-17	-14	-11	-15	-16	-16
	Q Max.	42.0	+10	+12	+10	-17	-14	-14	-12	-14	-14
	Q Mean	17.9	+15	+16	+23	-4	-3	-1	-7	-15	-4

Note: (+) means increase, (-) means decrease

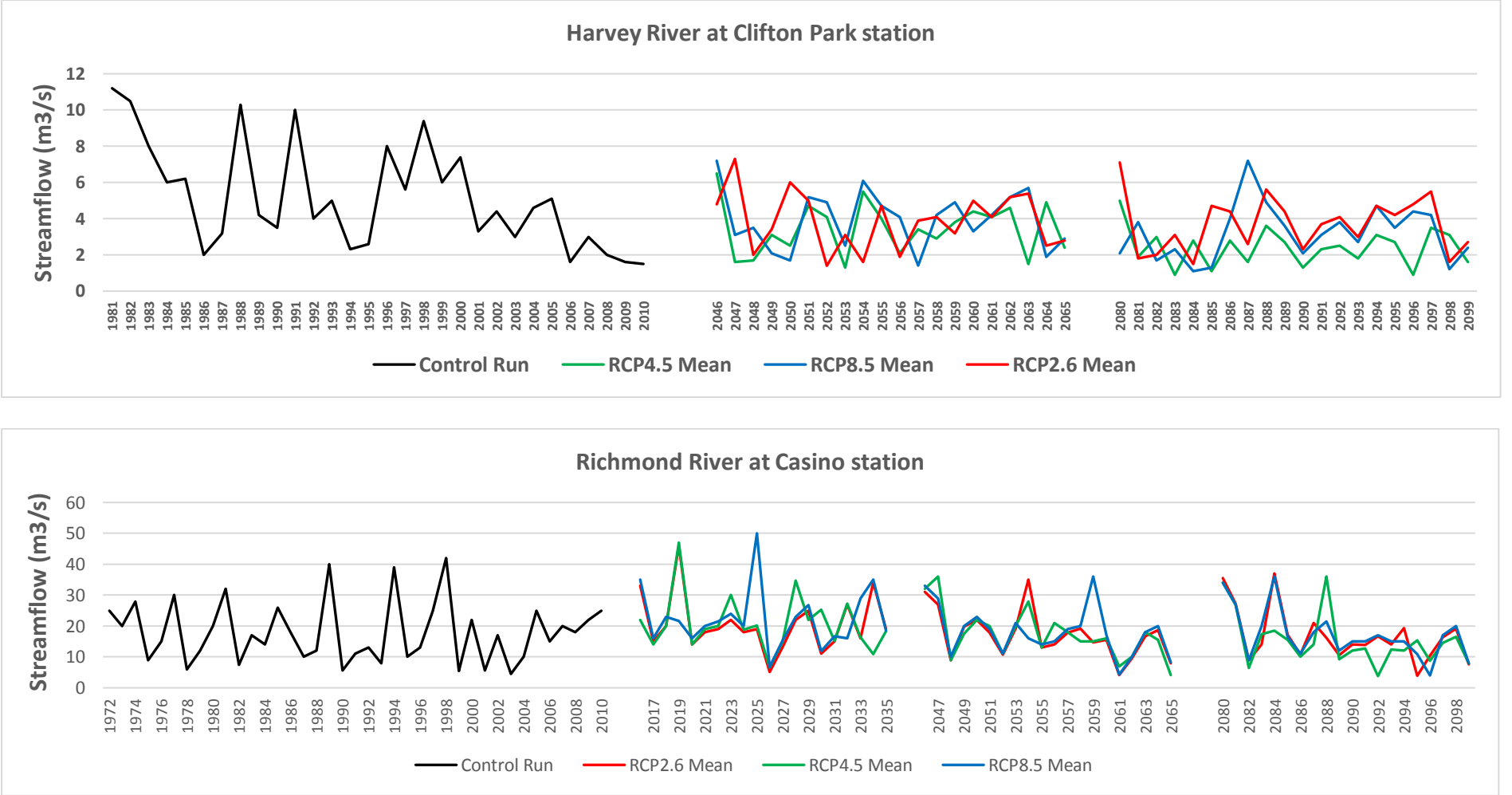

Figure (4.8) Annual mean streamflow variations of future climate scenarios relative to the control run. The average simulated discharge is the ensemble mean of 8-GCMs.

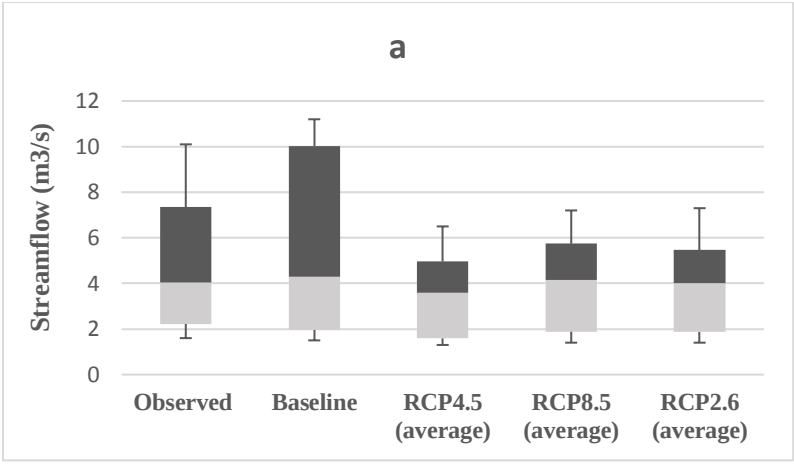
a
Streamflow (m3/s)
12
10
8
6
4
2
0
Observed
Baseline
RCP4.5 (average)
RCP8.5 (average)
RCP2.6 (average)

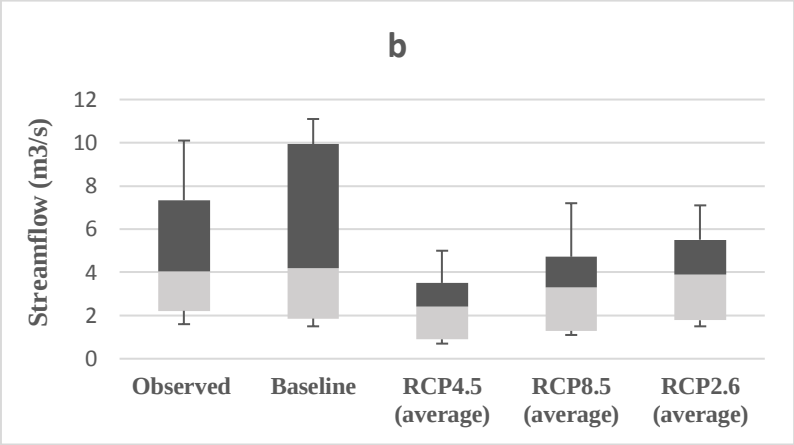
b
Streamflow (m3/s)
12
10
8
6
4
2
0
Observed
Baseline
RCP4.5 (average)
RCP8.5 (average)
RCP2.6 (average)

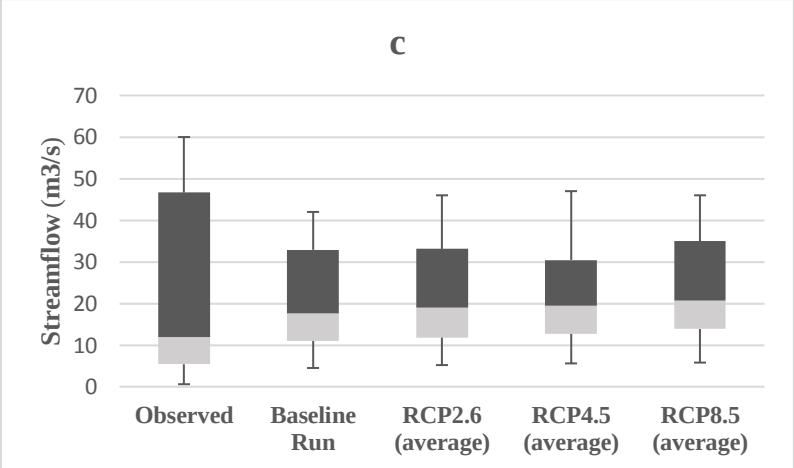
c
Streamflow (m3/s)
70
60
50
40
30
20
10
0
Observed
Baseline Run
RCP2.6 (average)
RCP4.5 (average)
RCP8.5 (average)

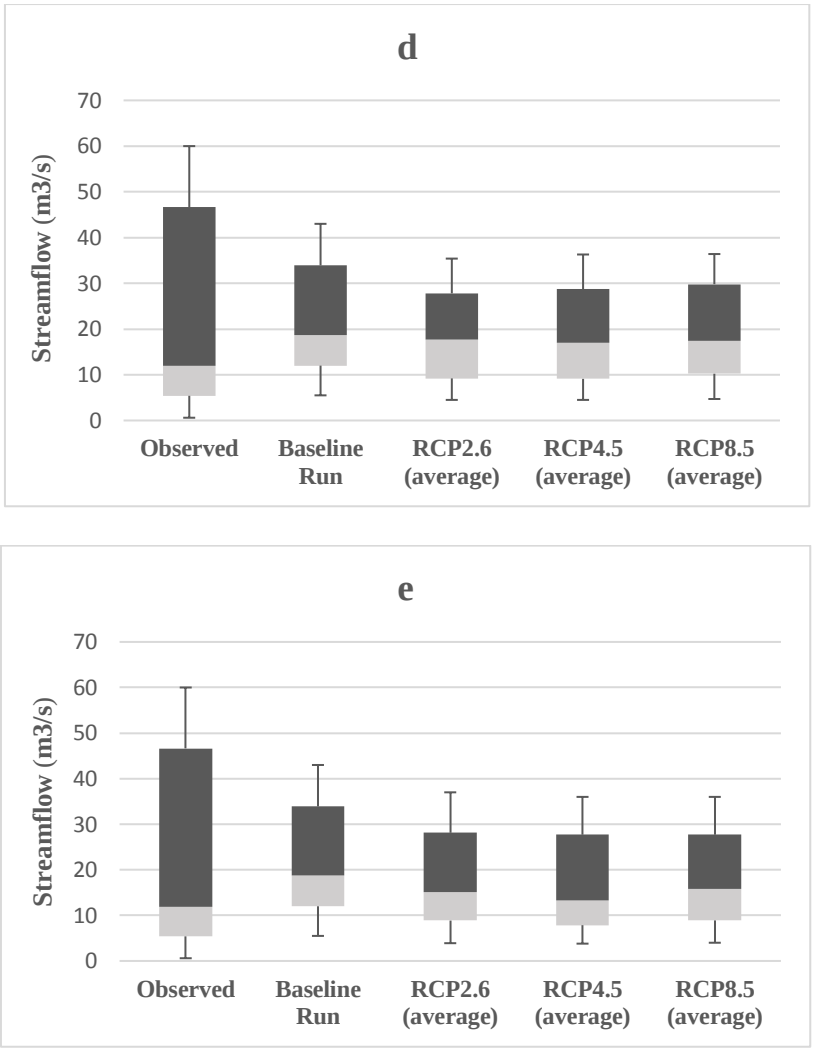

Figure (4.9) The 10th, 50th and 90th percentiles of annual mean streamflow for the observed, baseline and future periods. (a) and (b) at Clifton Park gauging station, (c), (d) and (e) at Casino gauging station. The bars represent the errors in the minimum and maximum annual streamflow percentiles. The simulated streamflow of the baseline and future periods is the ensemble mean of 8-GCMs.

At Clifton Park gauging station, there is a substantial variation in projected streamflow declines between different emission scenarios. Compared to the control run, the low flows (Qmin and Q10) are projected to decrease under all scenarios during the mid and late of the 21st century. The projected decline ranged between 7% (for the RCP8.5 and RCP2.6 during the mid of the century) and 54% (for the RCP4.5 by the end of the century). The medium flow (Q50) also revealed a decreasing tendency under all scenarios during the future periods, ranged between 7% and 56% relative to the control run. In addition, the high flows (Q90 and Q max) are also projected to decrease significantly in the future under all scenarios with a range of 35-65%

compared to the control run (Table 4.8). Furthermore, the mean annual discharge is expected to decrease under all scenarios during the future periods (Figures 4.8). A possible explanation for the future streamflow decline is the rainfall reduction during the mid and late of the current century as well as the increase in evapotranspiration (Table 4.7).

Future streamflow at Casino gauging station shows considerably varied tendencies compared to the control run as illustrated in Table (4.8). For the near-future period (2016-2035), mean annual rainfall revealed positive trends under all scenarios compared to the baseline period (Table 4.7). Therefore all streamflow statistics are projected to increase relative to the control run. The minimum flows (Q min and Q10) show relatively higher positive trends, ranged between 7-29%, than the maximum flows (Q max and Q90) which have a range of 1-12%. A possible explanation for this phenomena is the natural behaviour of the HBV model which sometimes over or underestimates the minimum and maximum flows. The conceptual structure of the HBV model is relatively simple with only one single groundwater storage responsible for the runoff generation. The median (Q50) and annual mean (Qmean) flows also show positive trends ranged from 7-18% and 15-23% respectively. This could be explained as a consequence of the relative increase in the annual mean rainfall during the start of the century.

By the mid of the century, all climate scenarios show relatively less annual mean rainfall and higher potential evapotranspiration compared to the baseline period (Table 4.7). Hence, all streamflow statistics measured at Casino discharge station show decline tendencies relative to the control run. The minimum flows are expected to decrease with a range of 4-20%. The same is applicable for the maximum flows which ranged between 11-17%. The annual mean streamflow is also anticipated to decline by 4%, 3% and 1% under the RCP2.6, RCP 4.5 and RCP8.5 climate scenarios correspondingly. Similarly, toward the end of the century, all streamflow statistics are projected to decline under all scenarios relative to the control run. This could be attributed to the fact that the annual mean rainfall under all climate scenarios is expected to decline substantially relative to the baseline period, and the potential evapotranspiration is also projected to increase as a result of the relative rise in the annual mean temperature (Table 4.7). The declining percentage of the minimum and maximum flows is expected to range between (11%-28%) and (12%-16%) respectively. While the decline in the annual mean streamflow is projected to reach 7%, 15% and 4% under the scenarios RCP2.6, RCP4.5 and RCP8.5 compared to the control run. The RCP4.5 climate scenario shows a higher

reduction in the annual mean streamflow because it corresponds to the higher annual rainfall reduction (8.5%) relative to the baseline period (Table 4.7).

4.5 Discussion

The trend analysis of the observed annual mean streamflow at Clifton Park and Casino gauging station (Figure 4.10) revealed a decreasing tendency over the time. At Clifton Park station, the long-term annual streamflow has declined by around two thirds, from 6.2 m^3/s to 2.1 m^3/s, since the early 1980s until 2014. At Casino gauging station, the long-term annual streamflow has almost declined to the half, from 25 m^3/s to 12 m^3/s, since the early 1970s until 2014. The trend analysis at the two stations confirmed evidence of changes in hydrological responses consistent with observed changes in rainfall over the past decades (Figure 4.11). Furthermore, Figure (4.12) also explains the flow duration curves of the decadal mean recorded streamflow at Clifton Park and Casino stations over the periods (1982-2017) and (1970-2017) respectively which demonstrates the streamflow variations over the time. Hence, in addition to the global warming, the projected decline in the future streamflow could also be credited to the natural climate variations. Based on the above analysis, the results specify that the potential changes in streamflow due to global warming could be very significant. Therefore, assessing the impacts of climate change on the hydrological system of the Harvey and Richmond catchment is highly beneficial since it may influence the seasonal or long-term water availability.

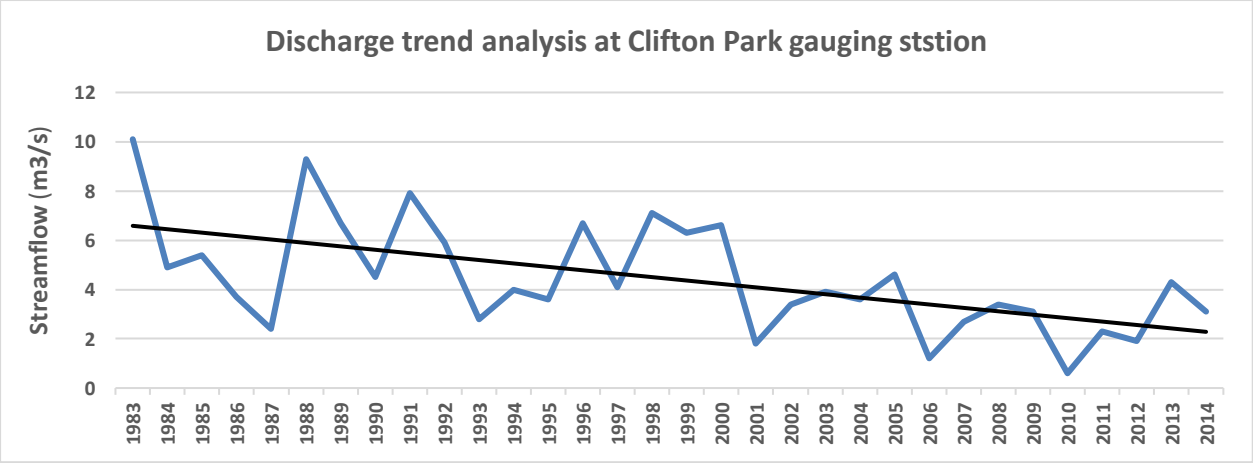

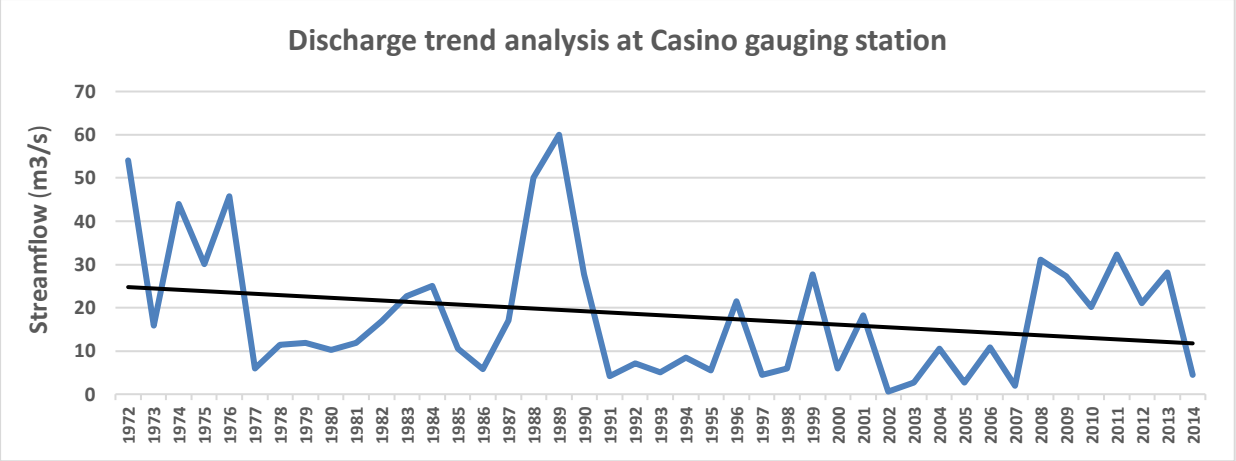

Figure (4.10) step-change analysis of the observed streamflow at Clifton Park and Casino gauging stations

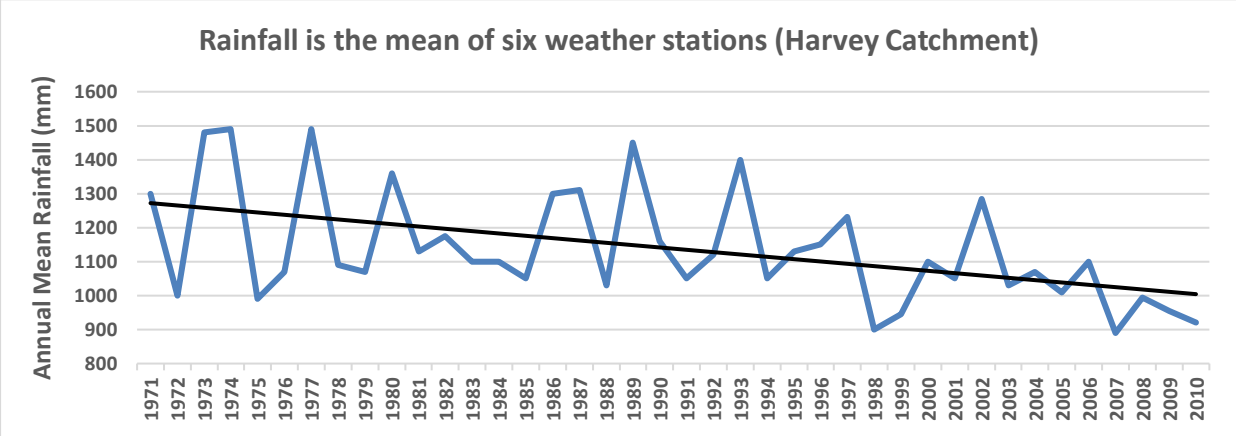

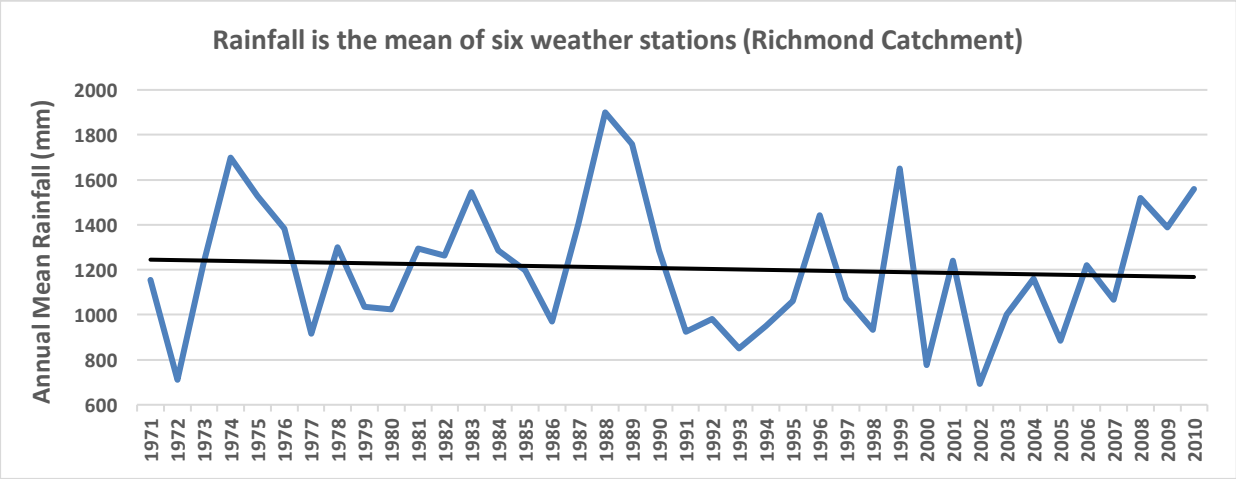

Figure (4.11) Rainfall trend analysis across the two catchments

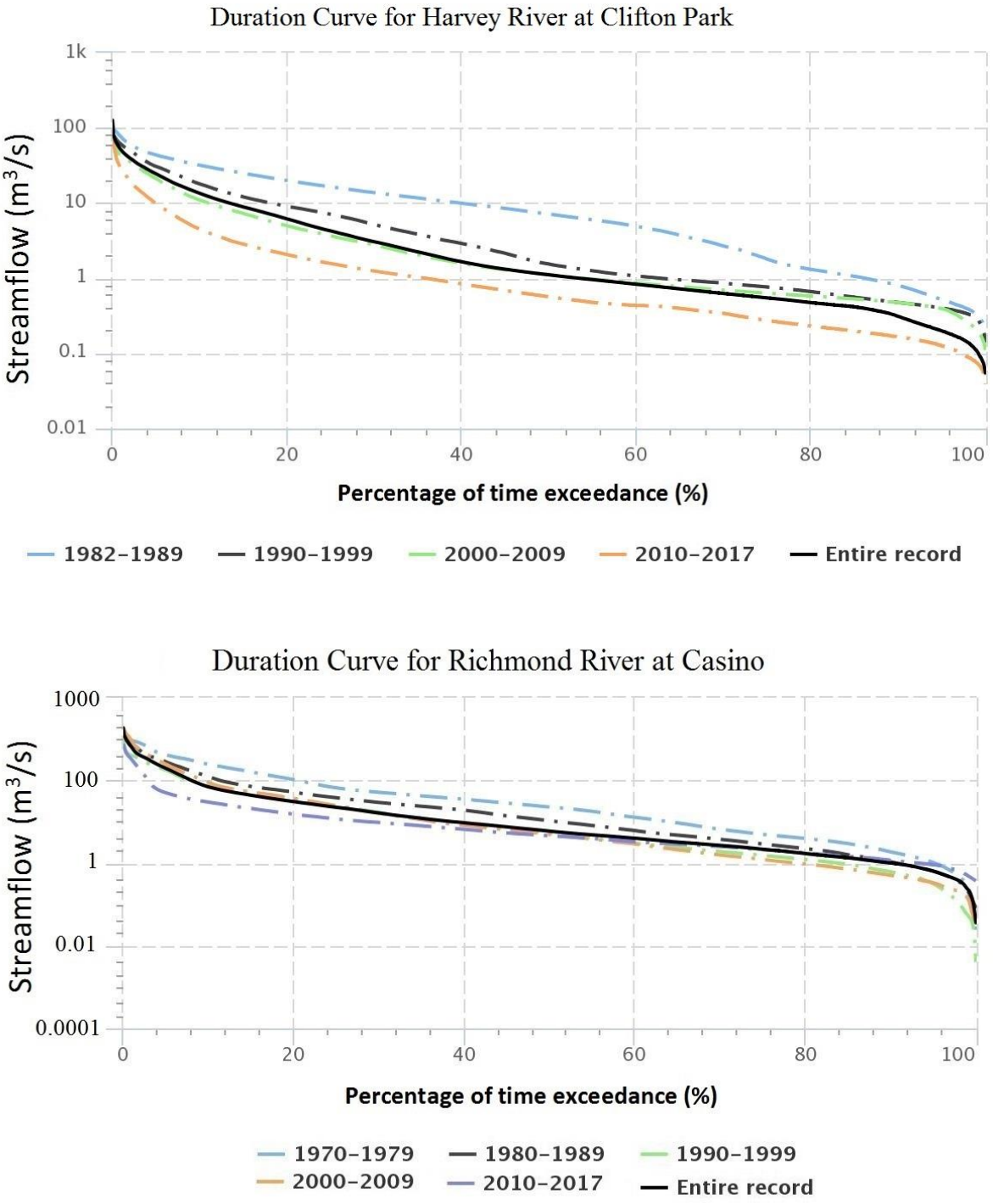

Figure (4.12) Decadal streamflow duration curves at Clifton Park and Casino gauging stations

The outcomes of the present study are well-matched with other previous studies which have been conducted in other South-Eastern and South-Western Australian catchments and revealed an evident decline in future streamflow. However, this study used the most recent global climate data from the IPCC 5th assessment report (AR5-CMIP5) compared to the 4th assessment

report (AR4-CMIP3) data which have been utilised in the previous studies. For example, Chiew et al., (2009) utilized the conceptual rainfall-runoff modelling approach, SIMHYD model, forced by 15 GCMs of the AR4 to investigate the impact of climate change on runoff in large part of south-east Australia. The results showed that there could be a high deficiency of runoff across the study area in the near future. Also, the assessment of the modelling approach showed that it could be used with a high confidentiality to predict the impact of climate change on runoff generation. Bari et al., (2010) explained that the runoff trends in the Serpentine catchment (in Western Australia) are projected to decrease by the mid and late of the 21st century with a range of 45-69% following a decline in annual rainfall which ranged between 12% and 24%. They forced the LUCICAT semi-distributed model with the downscaled climate outputs from 11 GCMs of the CMIP3 under the A2 and B1 scenarios to simulate the future runoff in the catchment. McFarlane et al., (2012) and Silberstein et al., (2012) utilized the conceptual modelling approach (Sacramento and IHACRES models) driven by the downscaled climate outputs from the AR4 to simulate the future runoff in many basins across South Western Australia. They found that the streamflow trends across the study area are projected to decrease during the 2030s because of a predicted decline in the annual precipitation over the area. Islam et al., (2014) repeated the same procedure as in (Bari et al., 2010) to assess the impact of climate change on the future streamflow in Murray–Hotham catchment in Western Australia. They also found that the runoff trends are expected to decrease by a range of 31% - 74% for the mid and late of the 21st century as a result of a decline in annual rainfall which ranged between 11.6% and 23.6%. Cheng et al., (2014) also reported that the future runoff is projected to decrease in Glendon Brook River catchment in the south-east of NSW. They utilized the hydrological modelling procedure (WAVES eco-hydrological model) forced by the downscaled climate series informed by 12 GCMs to simulate the future discharge at the catchment outlet. In addition, the more recent studies by the researchers of the CSIRO and the Australian Bureau of Meteorology have confirmed that the rainfall-runoff trends in most parts of south-eastern Australia are projected to decline through the mid and late of the 21st century (CSIRO and BoM, 2015).

The expected streamflow decline at the outlet of the Harvey River catchment, measured at Clifton Park gauging station, will possibly reduce the flows received by the Peel-Harvey Estuary (total area of 133 km^2) (Figure 4.1). Since the Harvey River discharges directly to the Harvey Estuary and the water in the estuary is primarily riverine, therefore any reduction in the flow amount of the River will badly affect the quantities of water received by the Estuary. As

the depth of the Estuary is quite shallow (up to 2m for the deepest point), and more than 50% of its area has a depth of only 0.5m (Kelsey et al., 2010), this will affect the aquatic life and the environmental status of the lagoon. The estuary is an internationally important habitat for waterbirds and migratory wading birds, in which tens of thousands of waterbirds gather annually with more than 80 species (Environmental Protection Authority, 2008). The growing environmental and economic importance of the estuary (such as water demands for drinking and agricultural production, parasite control, commercial fishing, foreshore development and access, boat use and moorings and jetties) have placed additional burdens on the estuarine system.

A possible solution to overcome the expected streamflow decline in the Harvey River, which will directly affect the estuary, is to store more water in the Harvey and Stirling Reservoirs during the period between May and October (rainy period) to be used later (on demand) to feed the estuary. The capacity of the Harvey and Stirling Reservoirs is approximately 56 Giga-litres each (Water and Rivers Commission, 2000; South West Attraction, 2017), which is capable of covering the projected streamflow decline in the Harvey River. Under the Stirling-Harvey Redevelopment Scheme, Stirling Reservoir will be used to supply drinking water to Harvey, Perth, Mandurah, Goldfields and Agricultural area water supply schemes as part of the Integrated Water Supply System (IWSS) (Water and Rivers Commission, 2000). Furthermore, the water from the Harvey Reservoir will be used solely for irrigation, and the increased storage of the new Harvey Dam will reduce the need for releases from Stirling Reservoir. Therefore, enough water can be stored to offset the declining river flow without changing the management priorities of the two reservoirs. Hence, this study could help the local community of the Harvey catchment to manage the usage of future water resources in the region.

On the other hand, as the Richmond catchment holds an increasing population growth in line with the highly intensive agricultural lands and tourist places, the expected streamflow reduction will negatively impact the future water resources in the area. Thus, long-term development plans in the area should take into consideration the potential future climate change. This requires sustainable and efficient water management strategies to be applied in the catchment to overcome the problem of water scarcity. The outcomes of the present study could help the local community of the Richmond River catchment to manage the usage of future water resources in the region.

4.6 Summary and conclusions

The HBV conceptual rainfall-runoff model was successfully used to simulate the hydrological response of the Harvey and Richmond catchments to the impact of future climate change for the near future (2016-2035), mid (2046-2065) and late (2080-2099) of the 21st century. Future rainfall and temperature climatic series (monthly scale) were extracted from a multi-model ensemble of eight GCMs of the CMIP5 under three Representative Concentration Pathways (RCP2.6, RCP4.5 and RCP8.5) of the IPCC (AR5). The LARS-WG5.5 downscaling technique was used to generate daily local-scale rainfall and temperature from each GCM of the 8-GCMs multi-model ensemble. The model was found to perform very well in capturing the observed rainfall and temperature climate statistics, and it can reasonably be used to predict the daily climate series for catchment-scale impact assessment. The ensemble mean of the 8-GCMs was then derived and adopted for streamflow simulation. The HBV model was applied to perform the hydrological modelling to simulate the future daily streamflow at the catchments outlet. The model shows a good performance during the calibration process which verifies its applicability to describe the future hydrological status of the two catchments. Overall modelling results show that rainfall is projected to increase in the near future across the Richmond catchment compared to the baseline period (1971-2010). Towards the mid and late of the century, annual mean rainfall shows negative trends under all climate scenarios across the two catchments. Potential Evapotranspiration is also projected to increase across the two catchments under all scenarios during the future periods as a result of the increase in annual mean temperature relative to the baseline period.

Compared to the control run, the projected mean annual streamflow measured at Clifton Park discharge station on Harvey River shows noticeable reduction tendencies under all scenarios during the mid-century ranged between 17-27% following a decline of 5.9-10.9% in mean annual rainfall. By the end of the century, all scenarios revealed a substantial reduction in the mean annual streamflow ranged between 23-52% following a decline of 7.6-23.0% in the mean annual rainfall. On the other hand, the annual mean streamflow measured at Casino gauging station on Richmond River is projected to increase under all scenarios during the near future with a range of 15-23% following an increase of 2.8-5.0% in the annual mean rainfall. By the mid-century, the annual mean streamflow is projected to decline under all climate scenarios with a range of 1-4% following a decline of 0.2-2.0% in the annual mean rainfall. Toward the end of the century, all scenarios revealed a decline in the annual mean streamflow ranged

between 4-15% following a reduction of 3.0-8.5% in the annual mean rainfall. This reduction in the annual streamflow will possibly seriously impact the sufficiency of future surface water resources and influence the aquatic and environmental life of the Harvey and Richmond Rivers system.

The following conclusions from this investigation study could be drawn as below:

1. The trend analysis of the annually observed streamflow confirmed evidence of changes in hydrological responses consistent with observed changes in climate over the past decades.
2. The outcomes of this assessment study specify that the potential changes in streamflow due to global warming could be very significant.
3. The study highlighted the similar outcomes with other previous studies that have been conducted in many south-western and south-eastern Australian catchments and revealed noticeable rainfall-runoff reduction tendencies.
4. The findings could assist the authorities and communities of the Harvey and Richmond Rivers catchments to manage the future water resources in the catchments such as irrigation, domestic and even drinking taking into consideration the low flow situation.
5. The findings may assist the water managers of the Peel-Harvey estuary region to protect the health of the ecosystem from the risk of water reduction.
6. The results could also be significant to preserve the extensive wetland complexes in the lower Richmond River, such as Tuckean Swamp on the Richmond floodplain and Ballina Nature Reserve which protects wide areas of mangroves and saltmarsh communities, from the risk of streamflow reduction.

Chapter 5

Hydrological Modelling in Unregulated Catchments using a Conceptual Model

Extended from:

Al-Safi, H. I. J., & Sarukkalige, P. R. (2018). A Conceptual Modelling Approach to Evaluate the Impacts of Climate Change on Future Streamflow in Unregulated Catchments. Int. J. Hydrology Science and Technology, (in press).

Al-Safi, H. I. J. & Sarukkalige, P. R. (2017). Assessment of climate change impacts on the variability of future streamflow in a selected contributing catchment of the Australian Hydrologic Reference Stations. In: Proceedings of the 16th World Water Congress 'Bridging Science and Policy', Cancun, Mexico, pp.1–19.

5.1 Introduction

The long-term investigation of the observed streamflow trends can provide vital information for sustainable water resource management. However, the effect of various environmental factors and land use changes either naturally or under human activities (such as land clearing, farms, dams and reservoirs) can highly affect the characteristics of the catchment and consequently influence the state of water flow. Hence, the Australian Bureau of Meteorology (BoM) has collected data for a network of Hydrologic Reference Stations (HRSs) from state agencies to study the variability of streamflow over the time in the corresponding catchments of these stations. Hydrologic Reference Stations, 222 sites in total, represent an important source of high-quality and continuous streamflow data across Australia (Zhang et al. 2016). Figure (5.1) shows the locations of the HRSs network and its long-term streamflow trends across the Australian continent (BoM, 2015:p.2) All sites of the HRSs network have been carefully chosen and prioritized according to three specific criteria (Turner et al., 2012). Firstly, the contributing catchments of the selected sites are unaffected by the land-use change and local water resources regulations. Secondly, they hold a long-term, high-quality discharge

record, and lastly, the selected stations signify all hydro-climatic areas within Australia. A valuable streamflow statistics and trend analysis products are freely available in the web portal of the HRSs (Zhang et al., 2014a). Furthermore, a periodic reviewing and information updating are normally applied to the HRSs web portal biennially to maintain a high-quality discharge data. Briefly, the HRSs network represents 'living gauges' for streamflow monitoring and climate change investigation in the contributing catchments.

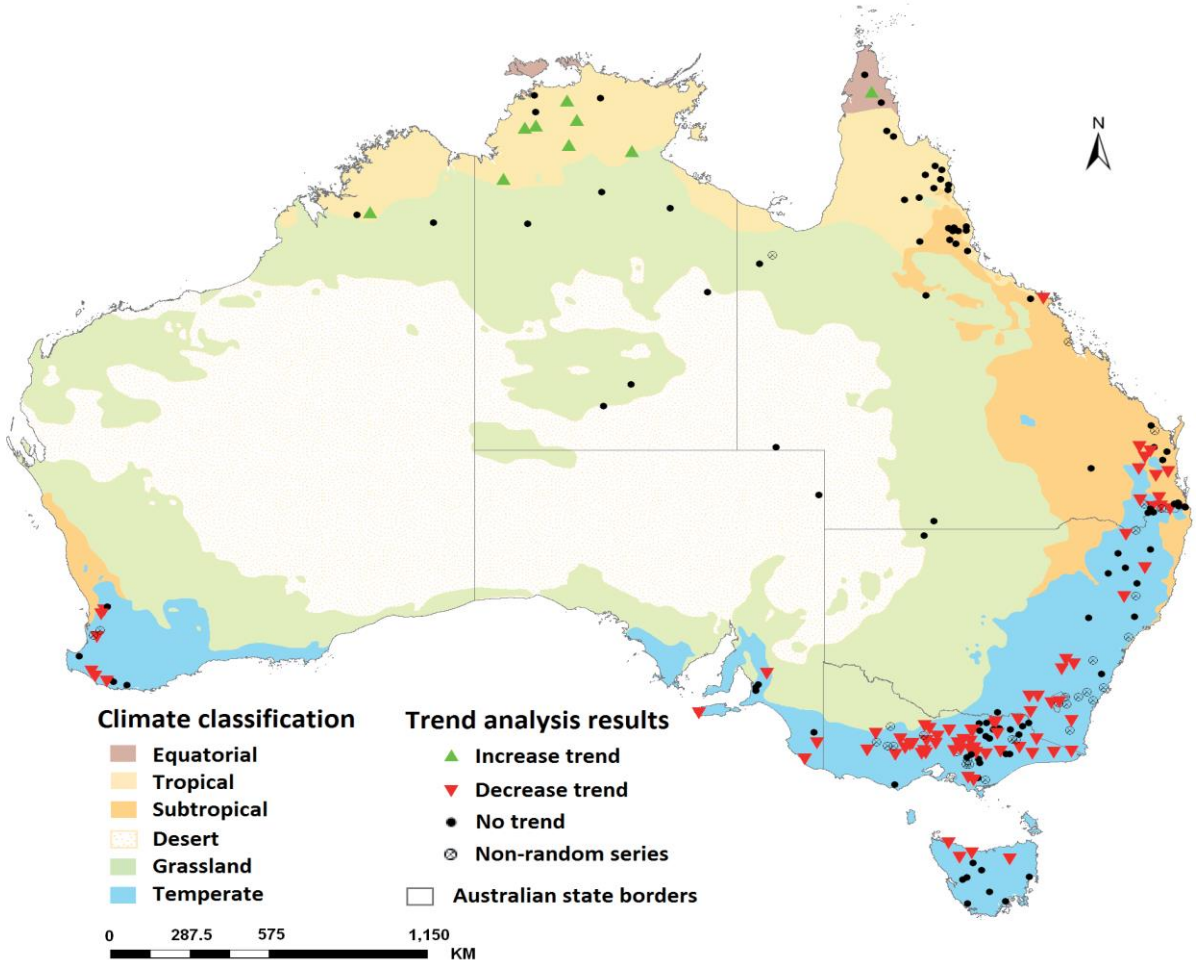

Figure 5.1 HRSs network sites and its long-term streamflow trends (BoM, 2015:p.2)

Few studies were conducted to date to investigate the long-term streamflow variability in the HRSs network (e.g. Turner et al., 2012; Zhang et al.; 2014 and Zhang et al., 2016), and some rivers have received a close attention very recently. The majority of findings revealed reduction trends in mean annual streamflow in most stations of south-eastern and south-western Australia. These studies, however, focused on examining the streamflow trends for the past and current time and no attention was paid to the impacts of climate change on the future streamflow in the HRSs network. Hence, the present study aims at assessing the impacts of

future climate changes on the local streamflow of three different sized contributing catchments of the Australian HRSs. The key incentives behind the selection of the study area are firstly the selected rivers have received less attention to investigating their hydrological response to the future climate changes. Secondly, Beardy and Harvey Rivers basins support a biodiversity of environmental and ecological communities. Furthermore, Harvey and Goulburn Rivers represent the main tributaries of surface water supply systems in their catchments. Therefore, assessing the impacts of future climate changes on the hydrological system of these rivers is highly beneficial to draw efficient and sustainable water management strategies in their contributing catchments.

This chapter of the thesis mainly highlights the application of a conceptual lumped-parameter (HBV model) to estimate the impact of climate change on the future runoff across three contributing catchments of the Australian HRSs; Harvey River (Dingo Road HRS), Beardy River (Haystack HRS) and Goulburn River (Coggan HRS). The study also uses a multi-model ensemble of eight-GCMs of the most recent climate scenarios (CMIP5 of the IPCC-AR5) to explore the future runoff under a changing climate and develops some recommendations to manage the usage of the future water resources in these catchments. The ensemble mean of the downscaled future climate variables of rainfall and temperature under two Representative Concentration Pathways (RCP 4.5 and RCP 8.5) was used to force the calibrated HBV model to simulate the daily streamflow at the three HRSs for the mid (2046-2065) and late (2080-2099) of the 21st century. The outcomes of this study could deliver valuable water management strategies for the selected catchments to effectively manage the projected water deficiency in these regions.

5.2 Study Area

Three different sized catchments corresponding to three HRSs were selected including Harvey-River at Dingo Road station in Western Australia, Beardy-River at Haystack and Goulburn River at Coggan stations in New South Wales as shown in Figure (5.2). The selected catchments nearly represent a range of climatic conditions and biophysical characteristics (e.g., latitude, longitude, elevation, land use type and soil type) across the Australian continent. This will provide an effective evaluation of the HBV model performance across the studied catchments.

Figure 5.2 Locations of the Hydrologic References Stations with their corresponding catchments

5.2.1 Harvey River at Dingo Road HRS (station ID 613002)

The corresponding catchment of this station is located around 130 km south of Perth City (Figure 5.2). It stretches between the latitude of 32.55º-33.05º S and longitude of 116.02º116.26º E with an entire drainage area of 148 km^2. Harvey River discharges directly to the Harvey Estuary and is considered as the main tributary to the Peel-Harvey Estuarian water system. The River also supports Harvey and Stirling reservoirs, which are considered as the main water supply sources to the Perth metropolitan. The Harvey River catchment has a temperate climate with a summer season tend to be hot-dry, the temperature fluctuates between 18-28º C and sometimes reaches 40º C, and a winter season tends to be cool-wet, with a temperature range of around 10 to 18º C (Peel-Harvey Catchment Council, 2012). The period between April and October nearly holds 90% of the total annual rainwater with an approximate mean annual rainfall of 900 mm (Peel-Harvey Catchment Council, 2012). The mean annual evaporation across the catchment is normally going above the mean annual precipitation, and it approximately reaches 1460 mm.

5.2.2 Beardy River at Haystack HRS (station ID 416008)

The corresponding catchment of this station is located in the far northern part of NSW (Figure 5.2). It stretches from 29.11^{o} to 29.30^{o} Southern latitude and from 151.18^{o} to 151.50^{o} Eastern longitude and holding an approximate drainage area of 908 km^{2}. Beardy River basin supports a biodiversity of environmental and ecological communities and some rare birds and plants. The climate of the catchment is temperate with a relatively warm dry summer, the temperature approximately ranges between 27-30^{o} C, and cool moderate winter, the temperature nearly ranges between 19-20^{o} C (CSIRO and BoM, 2007). The rainfall distribution over the catchment is extremely seasonal in which the summer season holds the maximum rainwater volumes due to the activity of summer storm, while the other seasons of the year hold the minimum amounts of rainfall. The average monthly summer precipitation is around 100 mm, and it decreases to 40-50 mm during the period between April and September (Green et al., 2012). The mean annual evaporation in the catchment is higher than the mean annual precipitation and ranged between 1200 and 2000 mm (Green et al., 2012).

5.2.3 Goulburn River at Coggan HRS (station ID 210006)

The corresponding catchment extends over 3402 km^{2} area (BoM, 2017) (the majority are national parks, forest and wasteland areas) (Figure 5.3). It also forms the whole western part of the Hunter River catchment (the largest coastal catchment in NSW). The Goulburn River is a major branch of the Hunter River which drains around 50% of the Hunter catchment and donates nearly quarter of the mean Hunter River flow (NSW Department of Infrastructure, Planning and Natural Resources, 2002). The Goulburn River catchment stretches from 31^{o}48` to 32$^{o}$51` Southern latitude and from 149^{o}40` to 150$^{o}$36` Eastern longitude. The climate of the catchment is subhumid to temperate and varies with elevation and ocean proximity (Krogh et al., 2013). As the Goulburn River catchment is relatively located far away from the ocean, it receives the lowest annual rainfall (around 620mm) compared to the eastern part of the Hunter catchment which receives around 1600mm. The rainfall in the catchment is seasonally distributed in which the summer is the wettest season in the year (December to February), and the annual evaporation normally exceeds the annual rainfall to reach more than 1300mm, and it varies with temperature variations (Krogh et al., 2013).

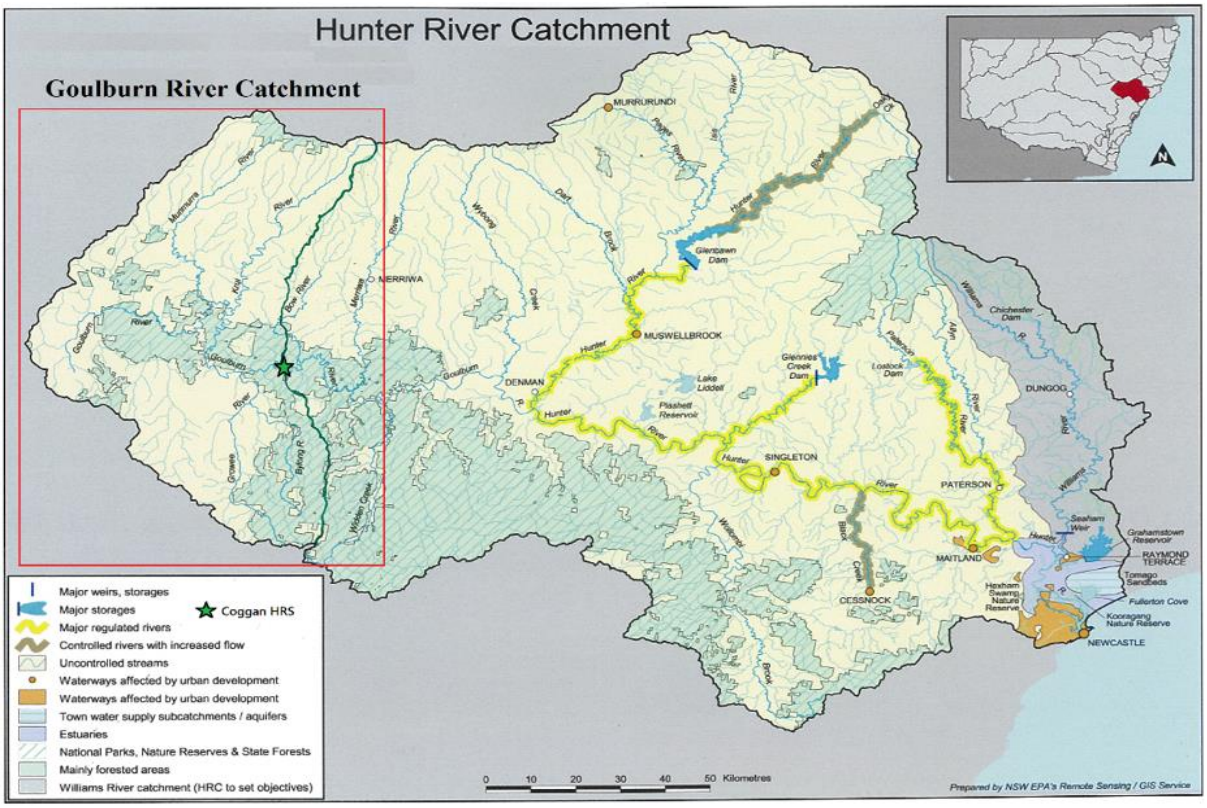

Figure 5.3 Location of Goulburn River catchments within Hunter River catchment

5.3 Datasets and hydrological modelling

5.3.1 Observed datasets

Daily hydro-meteorological observations of rainfall, temperature and discharge and the long-term monthly mean potential evapotranspiration from the three contributing catchments were obtained from the Australian Bureau of Meteorology, and the quality of data was checked with higher priority. Weather stations (Table 5.1) were selected within the contributing catchments and nearby locations considering the availability of long-term data. Also, the high-quality streamflow record was collected from the three HRSs including Dingo Road, Haystack and Coggan located at the outlet of each catchment. Figure (5.4) illustrates the locations of the hydro-meteorological stations across the three contributing catchments. For the Harvey River catchment, the observed daily mean rainfall, temperature and discharge and the long-term monthly mean potential evapotranspiration were available for the period (1982-2014). While for the Beardy and Goulburn catchments, the daily mean recorded rainfall, temperature and discharge and the long-term monthly mean potential evapotranspiration were available for 40 years (1975-2014). The average areal precipitation and temperature over the three catchments were obtained from Thiessen polygon method.

Table 5.1 Locations of the hydro-meteorological stations with the observed parameters

	Station Name	Latitude (S°)	Longitude (E°)	Station No.	Altitude (m)	Observed Parameter
Harvey River Catchment	Marradong	32.86	116.45	9575	250	Rainfall
	Yourdamung Lake	33.20	116.28	9960	240	Rainfall
	Willowdale	32.92	116.01	9893	320	Rainfall
	Wokalup	33.13	115.88	9642	30	Temperature and Evaporation
	Harvey River at Dingo Road	33.086	116.039	613002		Discharge
Beardy River Catchment	Ashford (Burrabogie)	29.40	151.41	54046	750	Rainfall
	Ashford (Springvale)	29.34	151.29	54045	578	Rainfall
	Emmaville (Strathbogie)	29.46	151.48	56029	735	Rainfall
	Emmaville Post Office	29.44	151.60	56009	890	Rainfall
	Tenterfield (kookynie)	29.27	151.86	56194	930	Rainfall
	Deepwater Post Office	29.70	151.69	56008	970	Temperature and Evaporation
	Pindari Dam	29.39	151.24	54104	462	Temperature and Evaporation
	Beardy River at Haystack	29.218	151.383	416008		Discharge
Goulburn River Catchment	Bylong (Bylong Road)	32.52	150.08	62102	328	Rainfall
	Bylong (Heatherbrae)	32.36	150.10	62080	230	Rainfall
	Cassilis Post Office	32.01	149.98	62005	395	Rainfall
	Ulan Water	32.28	149.74	62036	420	Rainfall
	Wollar (Barrigan St)	32.36	149.95	62032	366	Rainfall
	Wollar (Maree)	32.43	149.95	62056	410	Rainfall
	Gulgong Post Office	32.36	149.53	62013	475	Rainfall, Temperature and Evaporation
	Merriwa (Roscommon)	32.19	150.17	61287	375	Temperature and Evaporation
	Nullo Mountain AWS	32.72	150.23	62100	1130	Temperature and Evaporation
	Goulburn River at Coggan	32.344	150.101	210006		Discharge

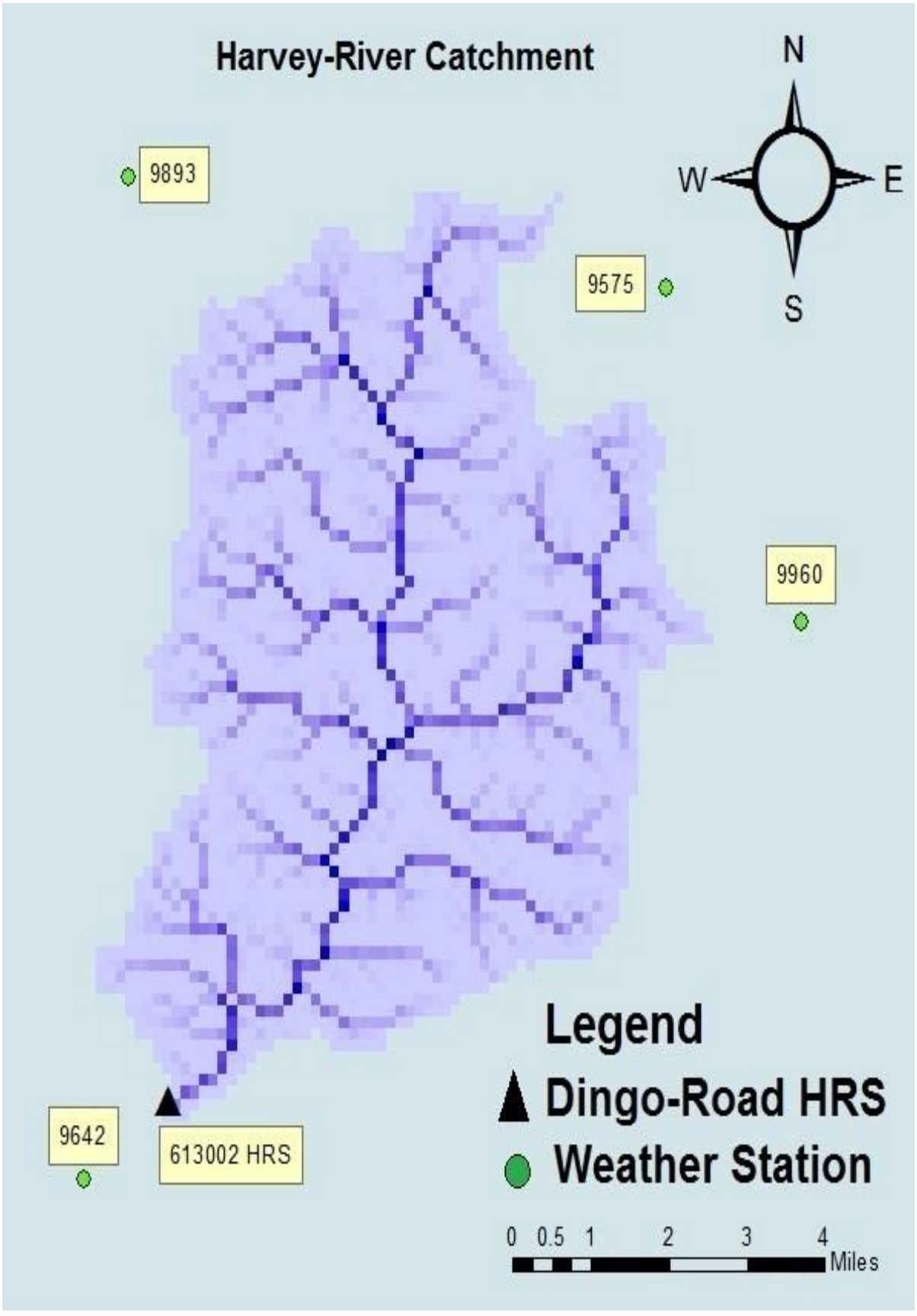

(a) Harvey River catchment

(b) Goulburn River catchment

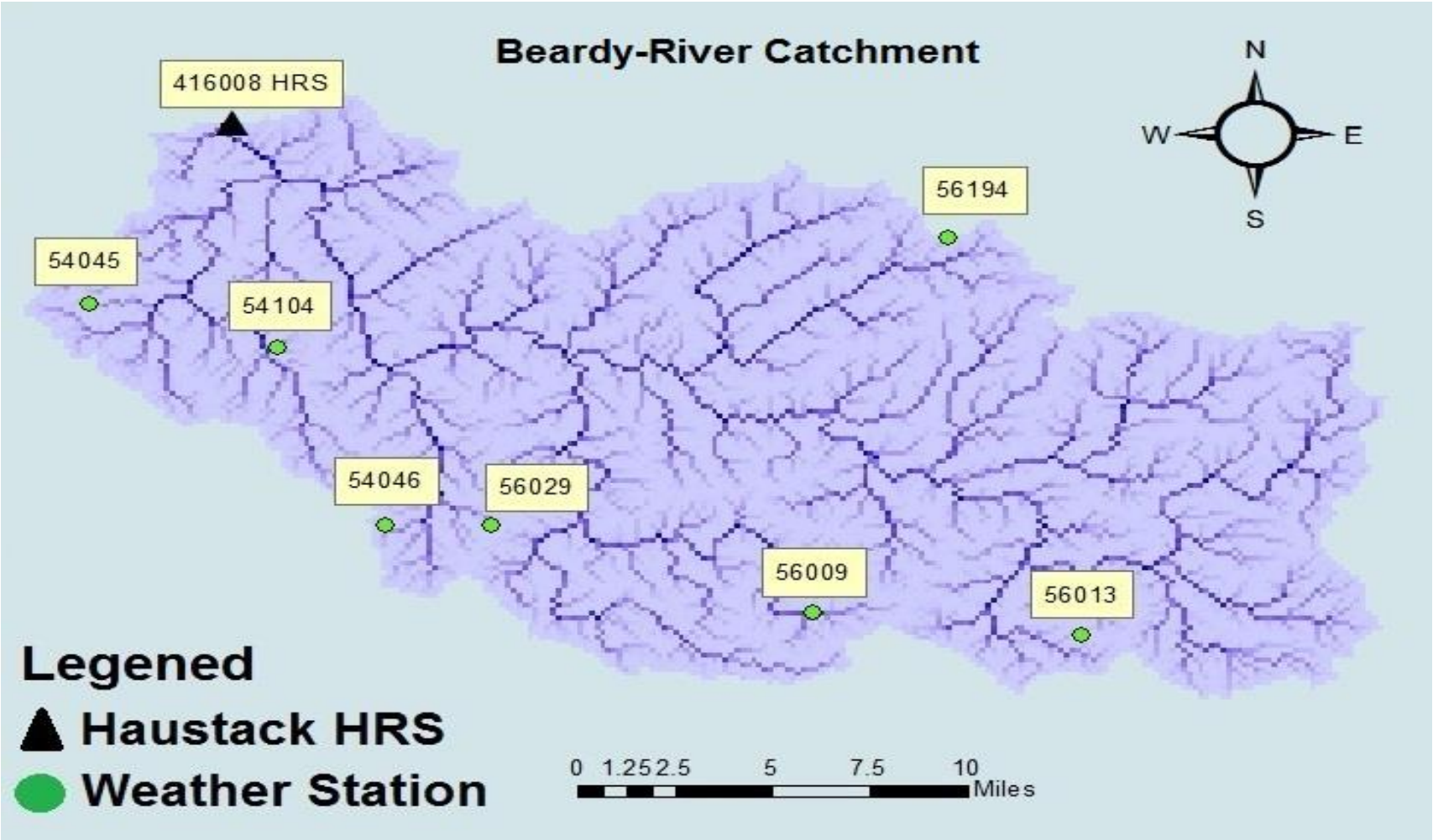

(c) Beardy River catchment

Figure 5.4 Streamflow network (with the hydro-meteorological stations) of the three contributing catchments

5.3.2 Future climate data

In this study, the global-scale future rainfall and temperature (monthly mean outputs) were extracted from a multi-model ensemble of eight-GCMs of the CMIP5 (Table 3.2) under two RCPs (RCP4.5 and RCP8.5) which belongs to the IPCC-AR5. Two 20-year periods, the mid (2046-2065) and late (2080-2099) of the 21st century, were selected to represent the future climatic conditions. A baseline climate period of 33-years (1982-2014) for the Harvey catchment and 40-years (1975-2014) for the Beardy and Goulburn catchments was also extracted from the multi-model ensemble to represent the current climate. The baseline periods were selected depending on the available observed climate forcing data across the three catchments to enable a fair comparison between the observed and historical climate on the one hand and the observed and simulated discharges on the other hand. Next, the global-scale monthly outputs (of each GCM) were downscaled into local-scale daily climate projections (point-specific data) suitable for regional impact assessment studies. A statistical downscaling model developed by the Australian Bureau of Meteorology (BoM-SDM) was adopted to compute the regional scale future climate signals (a detailed description of the downscaling procedure is provided in paragraph 3.3.2). The ensemble mean of the eight-GCMs was then derived and adopted for streamflow simulation. Using the downscaled daily mean temperature, the Potential Evapotranspiration (PET) across the contributing catchments (for the baseline and future periods) was calculated by employing the modified Blaney-Criddle method (Equation 3.16) (Doorenbos and Pruitt, 1977).

5.3.3 Hydrological modelling

The hydrological simulation was performed by applying the HBV conceptual model to simulate the future daily streamflow at the three HRSs. A detailed description of the HBV model is provided in chapter three (paragraph 3.1.2).

5.4 Results and Discussion

5.4.1 HBV Model calibration, validation and parameter estimation

To calibrate and validate the HBV model, the daily observed streamflow data (in line with the observed daily rainfall, temperature, and monthly mean potential evapotranspiration) should be available with a variety of hydrological regimes. In the current study, daily streamflow observations from Dingo Road, Haystack and Coggan HRSs were available for the periods (1982-2014), (1975-2014) and (1975-2014) respectively. Vaze et al., (2010) claimed that the

recent streamflow records from the south-eastern Australian catchments could be used effectively to calibrate the process-based models to represent the current prolonged drought across the region and to predict the future climate change impact on the local catchments where the large majority of climate models predict a drier future across the region. For the three contributing catchments, the HBV model was firstly run for an initial state of one year to initialize the system. At Dingo Road-HRS, the model was manually calibrated for 22-years (1983-2004) and validated for the rest of the recorded period (2005-2014). While at Haystack and Coggan HRSs, the HBV model was manually calibrated for a 29-year period (1976-2004) and validated for the rest 10-years (2005-2014). The calibration and validation periods were selected to represent a compromise between a longer period that would better account for climate variability and a shorter period that would better represent current development.

Eleven parameters are included in the model calibration and validation processes. The resulting sets of optimal parameters and the order in which they were optimized for the three contributing catchments are presented in Table (5.2). Assessing the modelling performance during the calibration process is an important issue (SMHI, 2012). Therefore, the modelling performance was evaluated by using three criteria of efficiency including Nash-Sutcliffe efficiency (NSE) (Nash and Sutcliffe, 1970), relative volume error (VE) and the coefficient of determination (R^2) (Equations 4.1, 4.2 and 4.3). The calibration and validation processes revealed an acceptable modelling performance (Table 5.3) which indicates that the model could be used successfully to simulate the future daily streamflow at the three HRSs. Figure (5.5) illustrates a comparison between the observed and simulated hydrographs at the three HRSs for a selected calibration and validation periods. It clearly shows that the simulated discharge fairly captures the observed discharge at the three HRSs.

Table (5.2) HBV model parameters and their optimal values for the calibration period at the three contributing catchments

Parameter	Symbol	Unit	Optimal value Harvey catchment	Optimal value Beardy catchment	Optimal value Goulburn catchment
Rainfall correction factor	rfcf	-	0.8	0.9	0.8
Elevation correction factor for precipitation	pcalt	1/100m	0.1	0.1	0.1
Temperature lapse	tcalt	^{o} C/100m	0.6	0.6	0.6
Maximum of soil moisture zone	FC	mm	400	500	250
Limit for potential evaporation	Lp	-	0.7	0.5	0.8
Shape coefficient	Beta	-	1.5	2	3
General correction factor for potential evaporation	ecorr	-	0.9	0.9	0.85
Recession coefficient for upper response box	Khq	1/day	0.25	0.8	0.9
Recession coefficient for lower response box	K4	1/day	0.04	0.09	0.07
Maximum percolation capacity	Perc	mm/day	1.1	0.9	0.9
Routing parameter	Maxbaz	day	0.07	1.1	0.5

Table (5.3) HBV model performance during the calibration and verification periods for the Three HRSs

Hydrologic Reference Stations	Calibration			Validation		
	NSE	**VE (%)**	**R^2**	**NSE**	**VE (%)**	**R^2**
Beardy River at Haystack	0.92	-3.9	0.91	0.90	-4.1	0.89
Harvey River at Dingo Road	0.87	-4.2	0.83	0.85	4.4	0.81
Goulburn River at Coggan	0.9	3.8	0.85	0.88	4.2	0.82

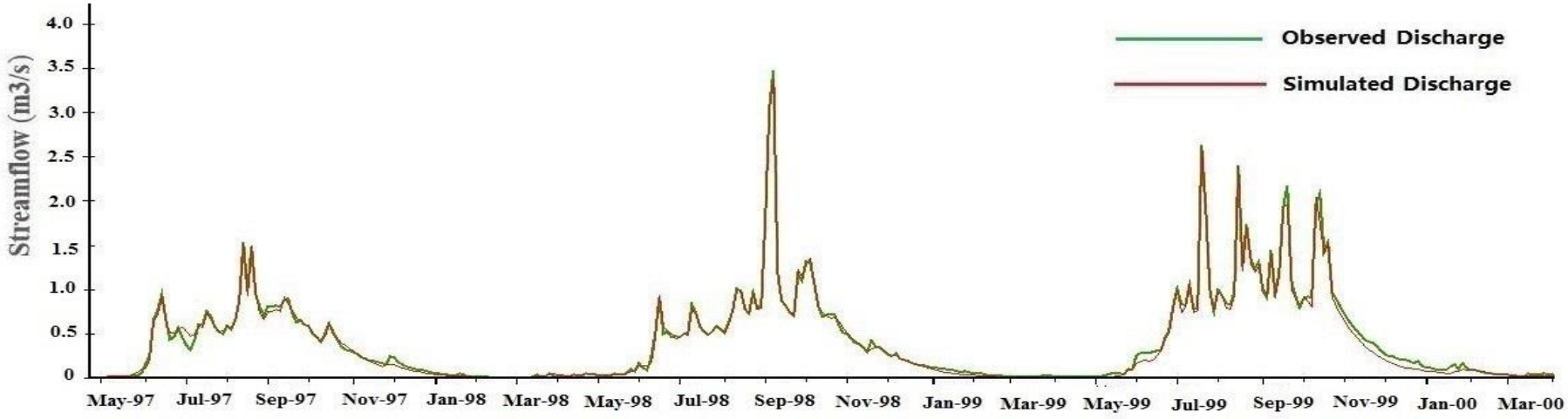

Harvey River at Dingo-Road (Calibration Period)

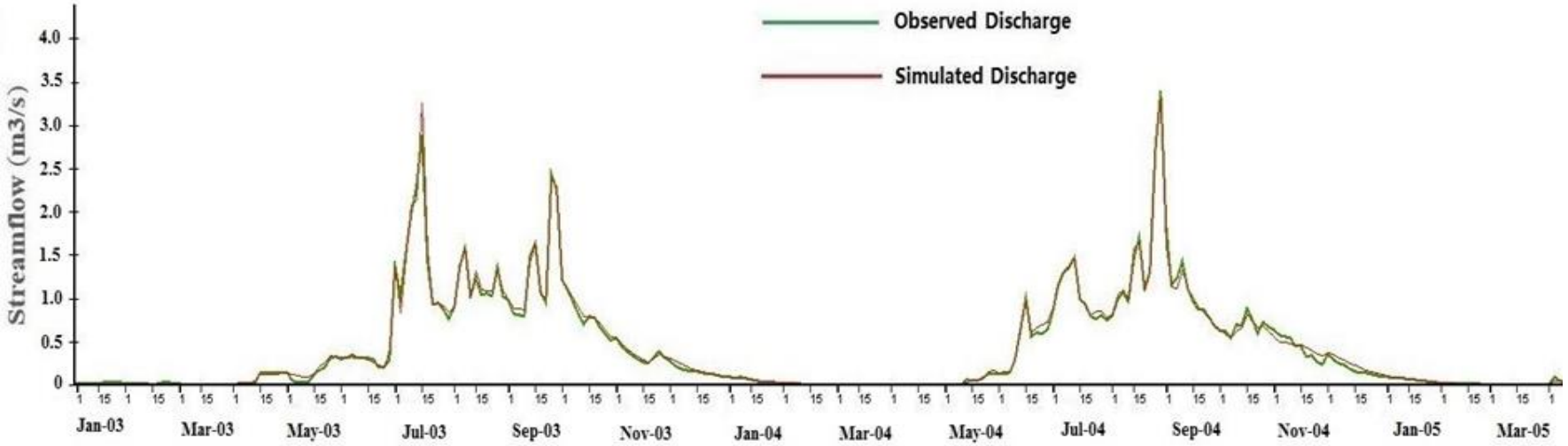

Harvey River at Dingo-Road (Validation Period)

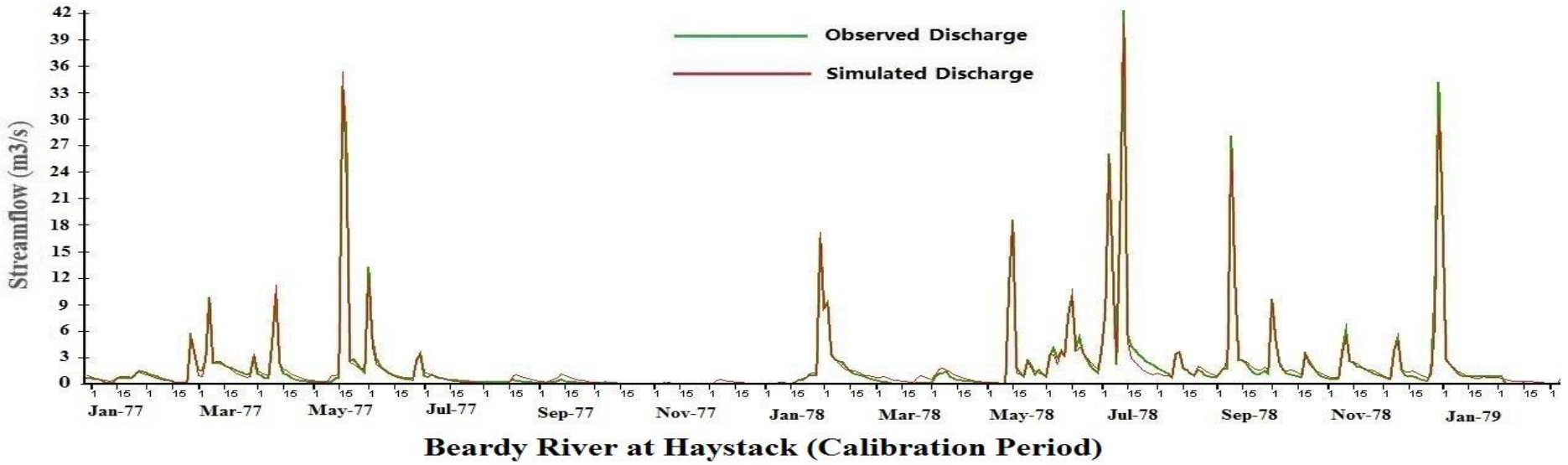

Beardy River at Haystack (Calibration Period)

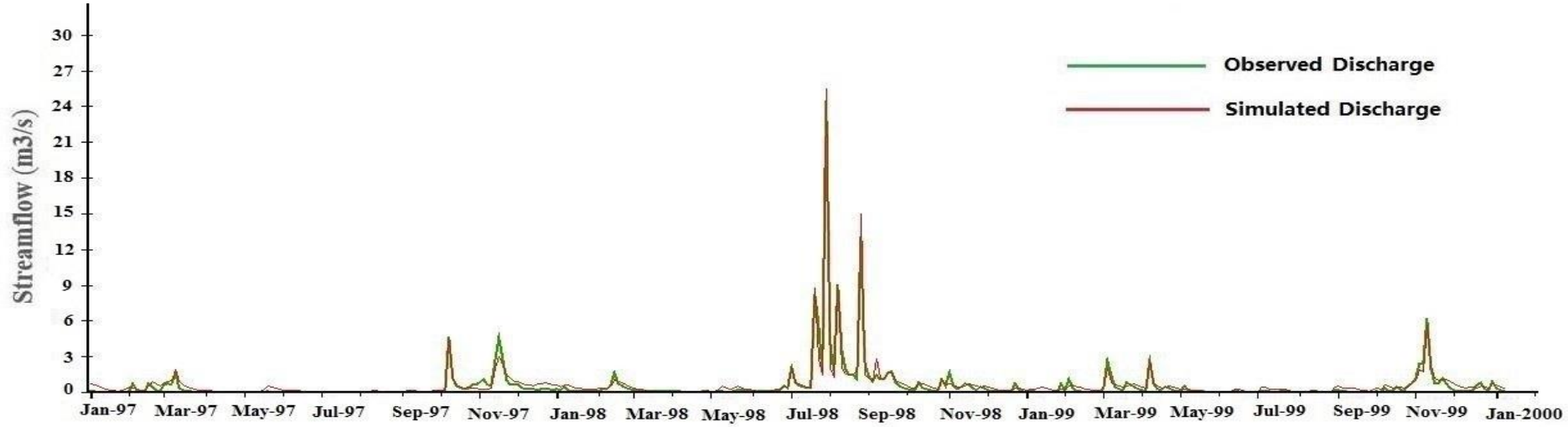

Beardy River at Haystack (Validation Period)

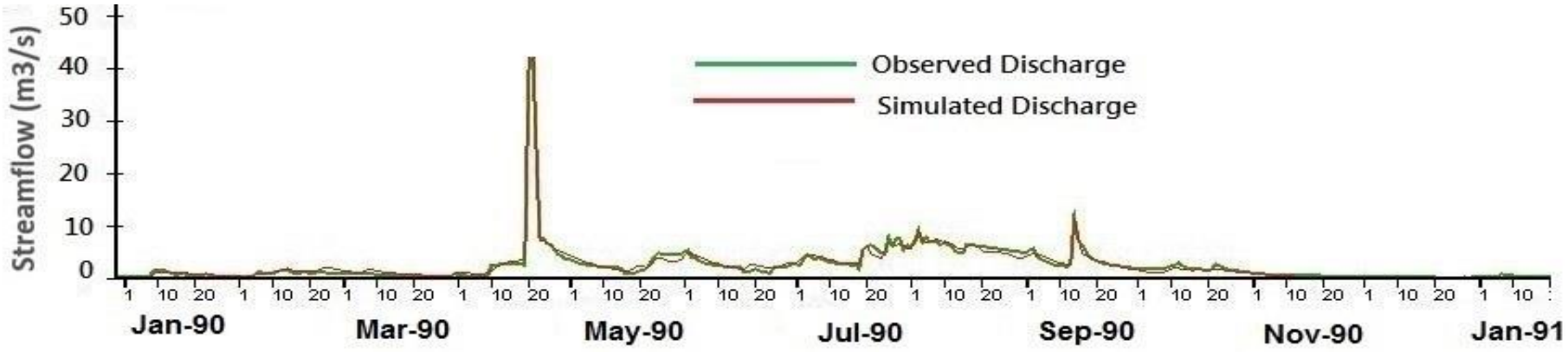

Goulburn River at Coggan (Calibration Period)

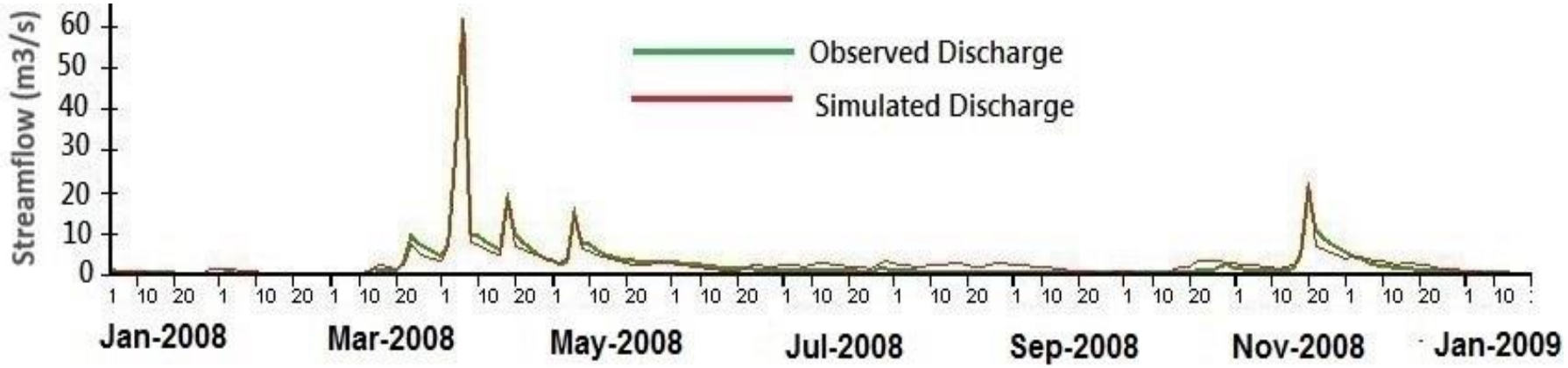

Goulburn River at Coggan (Validation Period)

Figure (5.5) Daily observed and simulated streamflow at the three HRSs for the calibration and validation periods.

5.4.2 Future climate predictions

Future climate series of rainfall, temperature and potential evapotranspiration across the three contributing catchments were compared with the baseline climate, and the changes in mean annual values are illustrated in Table (5.4). Almost all GCMs show a clear decline in mean annual rainfall and an increase in temperature and potential evapotranspiration values during the future periods under the RCP4.5 and RCP8.5 climate scenarios. For the Harvey River catchment, the mid-century rainfall is projected to decline by 7.4% and 9.1% under the scenarios RCP4.5 and RCP 8.5 respectively (Figure 5.6). By the late-century, the rainfall decline is projected to reach 7.6% and 12.2% under the same scenarios correspondingly. In the same manner, the rainfall across the Beardy River catchment also shows a negative trend during the mid and late of the current century compared to the baseline period (Figures 5.6). The rainfall reduction during the mid-century is anticipated to be 2.9% and 5.5% under the RCP4.5 and RCP8.5 scenarios respectively. Towards the end of the century, the decrease in mean annual rainfall is projected to reach 9.2% and 1.3% under the same scenarios correspondingly. Similarly, the mid-century mean annual rainfall across the Goulburn River catchment is projected to decline by 3.9% and 7.0% under the RCP4.5 and RCP8.5 scenarios respectively (Figures 5.6). By the late-century, there could be a 4.7% and 7.8% rainfall decline under the same scenarios correspondingly. The reduction in mean annual rainfall across the three contributing catchments could be a consequence of shifting the whole distribution into lower values by the mid and late of the current century. The reduction in mean annual rainfall could also be attributed to the lack of high rainfall events during the future periods.

Table (5.4) Changes in the mean annual climate of the future scenarios relative to the baseline period across the three studied catchments. (The values of the RCPs represent the ensemble mean of 8-GCMs)

	Variable	Observed (1982-2014)	Baseline climate (1982-2014)	Changes in mean annual values compared to the baseline period			
				(2046-2065)		(2080-2099)	
Harvey River catchment				**RCP 4.5**	**RCP 8.5**	**RCP 4.5**	**RCP 8.5**
	P (mm/year)	1010	985	-7.4%	-9.1%	-7.6%	-12.2%
	T (Cº)	16.2	16.81	+0.4 ºC	+0.8 ºC	+0.7 ºC	+1.2 ºC
	PE (mm/year)	1442	1510	+8.3%	+9.7%	+12.4%	+13.7%

	Variable	Observed (1975-2014)	Baseline climate (1975-2014)	Changes in mean annual values compared to the baseline period (%)			
				(2046-2065)		(2080-2099)	
Beardy River catchment				**RCP 4.5**	**RCP 8.5**	**RCP 4.5**	**RCP 8.5**
	P (mm/year)	795	760	-2.9%	-5.5%	-9.2%	-1.3%
	T (Cº)	15.6	16.1	+0.6 ºC	+1.0 ºC	+0.7 ºC	+1.5 ºC
	PE (mm/year)	1536	1602	+9.3%	+10%	+13.0%	+14.2%
Goulburn River catchment	P (mm/year)	625	635	-3.9%	-7.0%	-4.7%	-7.8%
	T (Cº)	16.1	16.7	+0.4 ºC	+0.8 ºC	+0.6 ºC	+1.2 ºC
	PE (mm/year)	1477	1542	+8.3%	+9.6%	+11.0%	+13.5%

Note: (+) means increase, (-) means decrease

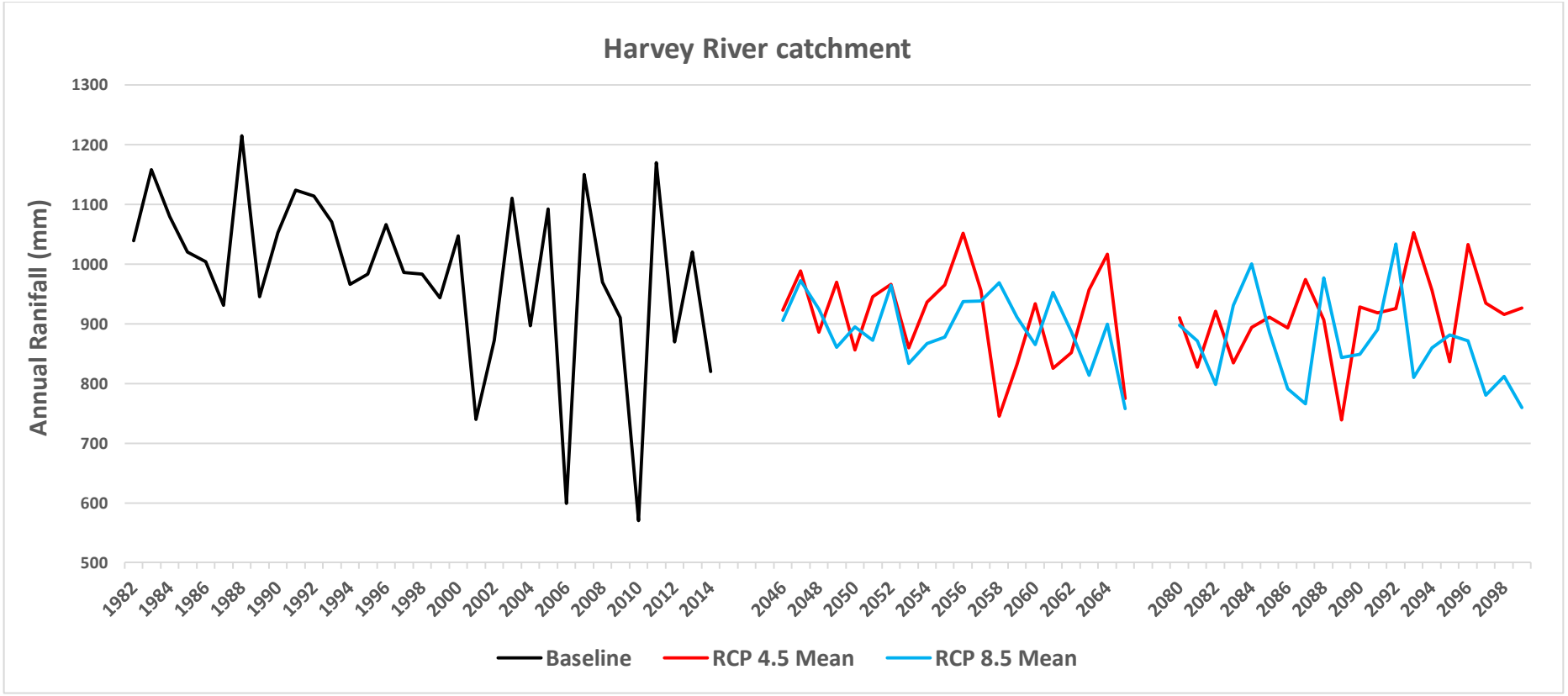
Harvey River catchment
Annual Ranifall (mm)
1300
1200
1100
1000
900
800
700
600
500
1982
1984
1986
1988
1990
1992
1994
1996
1998
2000
2002
2004
2006
2008
2010
2012
2014
2046
2048
2050
2052
2054
2056
2058
2060
2062
2064
2080
2082
2084
2086
2088
2090
2092
2094
2096
2098
Baseline
RCP 4.5 Mean
RCP 8.5 Mean

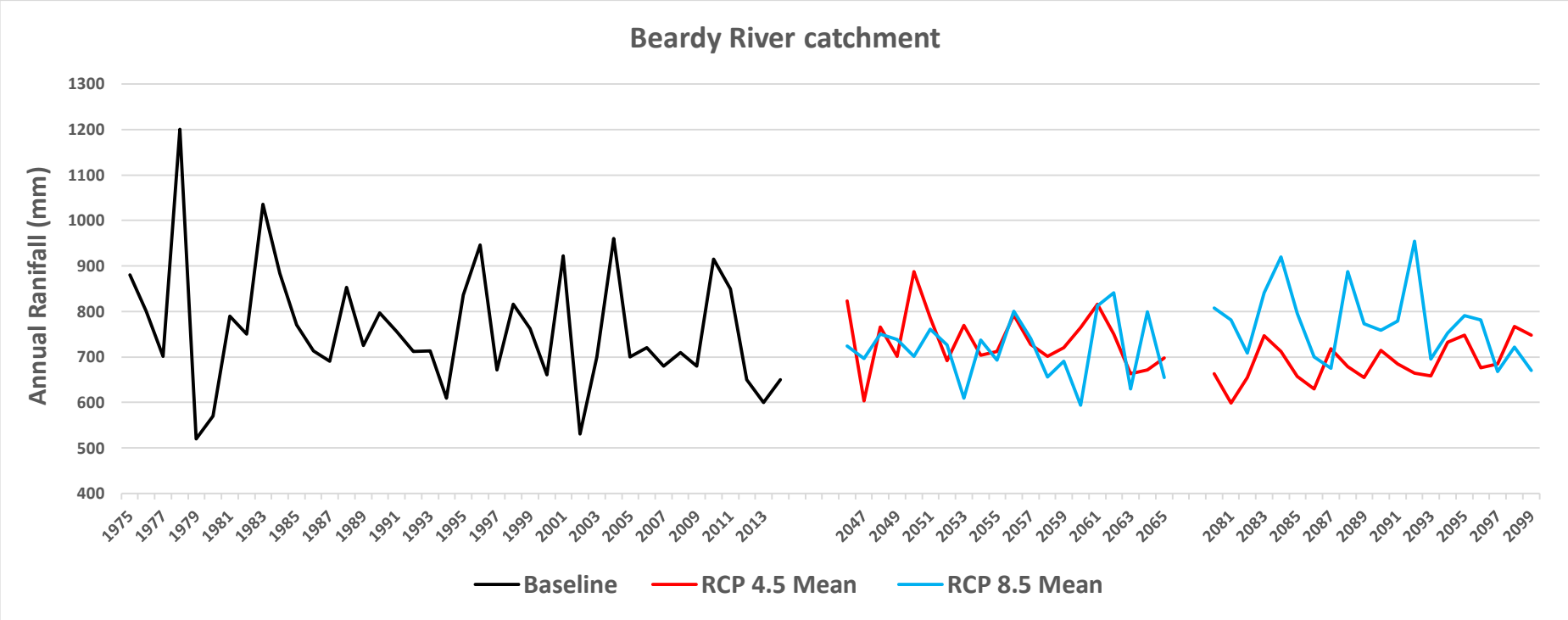
Beardy River catchment
Annual Ranifall (mm)
1300
1200
1100
1000
900
800
700
600
500
400
1975 1977 1979 1981 1983 1985 1987 1989 1991 1993 1995 1997 1999 2001 2003 2005 2007 2009 2011 2013
2047 2049 2051 2053 2055 2057 2059 2061 2063 2065
2081 2083 2085 2087 2089 2091 2093 2095 2097 2099
Baseline
RCP 4.5 Mean
RCP 8.5 Mean

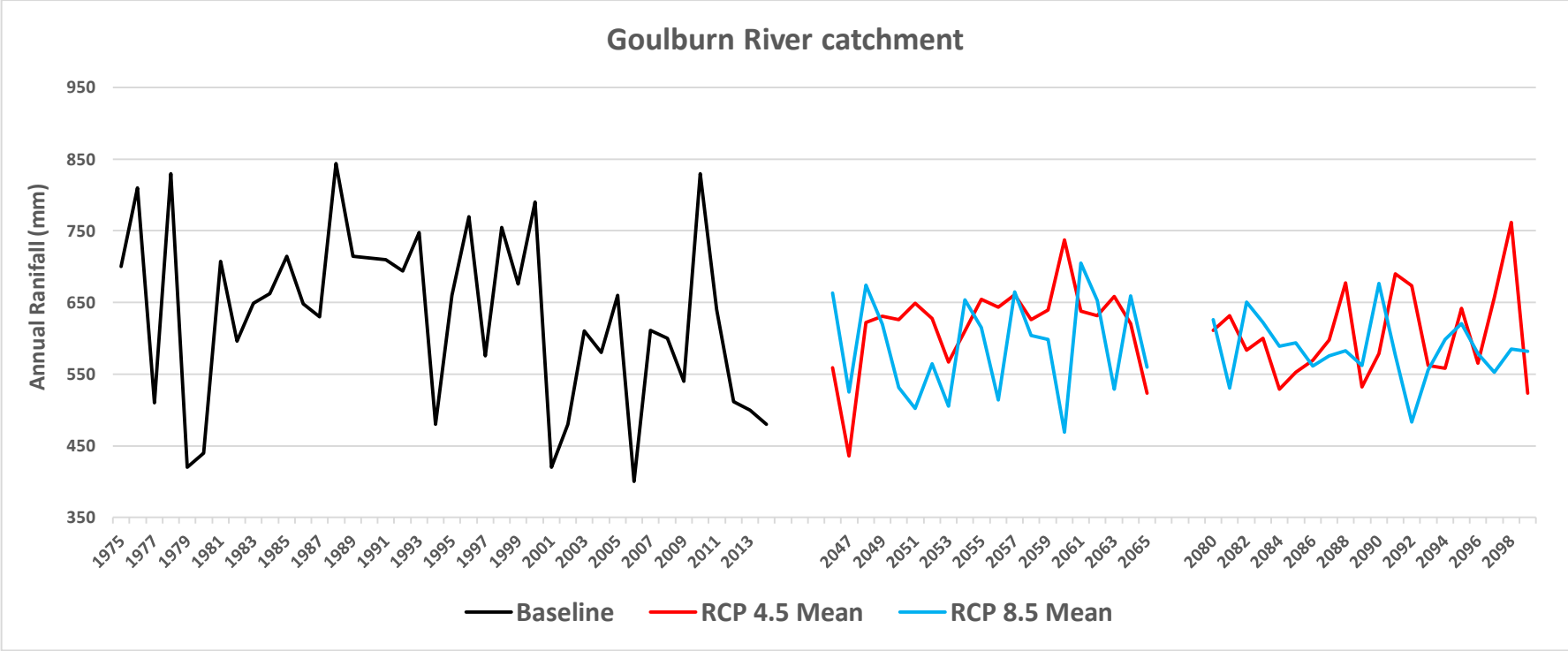

Figure (5.6) Annual mean rainfall of the baseline and future scenarios across the three contributing catchments. The simulated rainfall is the ensemble mean of 8-GCMs.

On the other hand, potential evaporation across the contributing catchments is projected to increase for all scenarios during the future periods relative to the baseline period (Table 5.4). For the Harvey River catchment, the increase in potential evaporation ranged between 8.3% and 13.7% under the RCP4.5 and RCP8.5 scenarios during the mid and late-century. For the Beardy River catchment, the increase in potential evaporation ranged between 9.3% and 14.2% under the same scenarios of the two future periods. While for the Goulburn River catchment, the expected increment in potential evaporation ranged between 8.3% and 13.5% under the two scenario during the future periods. This is a consequence of the expected rise in future mean annual temperature resulting from the high CO_2 emissions. Increasing atmospheric CO_2 levels will alter the behaviour of vegetation and land cover and atmosphere feedback, impacting evaporation and therefore runoff (Betts et al., 2007). The expected rise in future air temperatures may impact rainfall, potential evaporation and climate-runoff relationship in ways that are different from past observations (Chiew et al., 2014). The sole rise of air temperature also increases the additional energy available for driving soil water and intercepted water for evaporation or transpiration (Al-Safi and Sarukkalige, 2017b). In other words, the higher temperature should naturally increase potential evaporation through an increase in vapour pressure deficit, thereby increasing actual evaporation and reducing runoff under the same rainfall conditions (Chiew et al., 2014). Therefore, the combined impact of rainfall reduction and potential evaporation increase by the mid and late-century could adversely affect the future runoff across the contributing catchments of the three HRSs.

5.4.3 Future runoff projections

After the calibration process, the HBV model was forced with the ensemble mean of the downscaled future climate series to simulate the future daily streamflow at the three HRSs for the mid and late this century. The model also forced with the downscaled climate data of the baseline period to simulate the daily streamflow at the three HRSs for a control-run to be compared with the future streamflow. The differences between the two simulations represent the projected impact of climate change on the hydrological system. A detailed summary of the mean annual streamflow for the baseline and the scenarios of the future periods at the three HRSs is presented in Table (5.5). Figure (5.7) illustrates a graphical representation of the simulated mean annual streamflow at the three HRSs under the RCP4.5 and RCP8.5 climate scenarios. Further, Figure (5.8) shows the 25^{th} and 75^{th} streamflow percentile statistics at the three HRSs for the mid and late-century under the RCP4.5 and RCP8.5 scenarios.

Table (5.5) Changes in annual mean streamflow statistics (m^3/s) of the future climate scenarios relative to the control run at the three HRSs. The values of all RCPs represent the ensemble mean of 8-GCMs

HRSs	Variable	Observed streamflow (1982-2014)	Control run (1982-2014)	Changes in mean annual runoff compared to the control run (%)			
				(2046-2065)		(2080-2099)	
				RCP 4.5	RCP 8.5	RCP 4.5	RCP 8.5
Harvey River at Dingo Road	Q Min.	0.3	0.23	-13	-13	-13	-21
	Q25	0.6	0.6	-33	-33	-53	-66
	Q50	1.1	0.9	-31	-.44	-52	-61
	Q75	1.1	0.9	-30	-44	-52	-61
	Q Max.	1.8	1.7	-23	-23	-29	-35
	Q Mean	0.88	0.8	-31	-37	-48	-60
Beardy River at Haystack	Q Min.	0.6	0.6	0	0	0	0
	Q25	0.8	0.9	-11	-11	-3	-5
	Q50	1.15	1.2	-8	-4	-6	-4
	Q75	2.025	1.9	-4	-27	-31	-4
	Q Max.	5.6	4.6	-15	-37	-28	-19
	Q Mean	1.73	1.68	-1	-24	-16	-11
Goulburn River at Coggan	Q Min.	1.0	0.9	-11	-22	-11	-11
	Q25	1.6	2.4	-4	-54	-33	-33
	Q50	3.1	2.95	-10	-37	-36	-40
	Q75	5.1	4.3	-26	-40	-30	-53
	Q Max.	8.1	8.5	-45	-40	-49	-45
	Q Mean	3.7	3.3	-18	-39	-30	-42

Note: (-) means decrease.

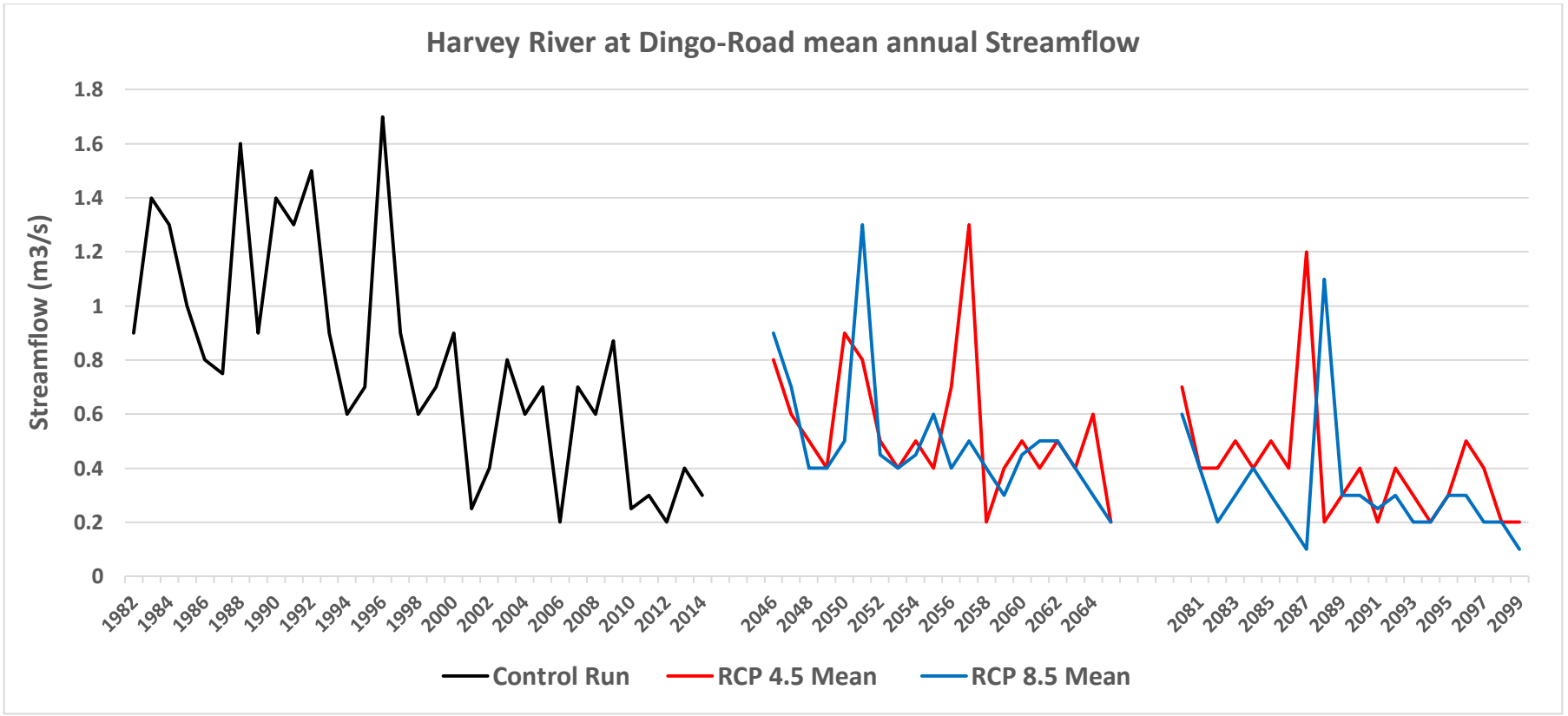
Harvey River at Dingo-Road mean annual Streamflow
Streamflow (m3/s)
1.8
1.6
1.4
1.2
1
0.8
0.6
0.4
0.2
0
1982
1984
1986
1988
1990
1992
1994
1996
1998
2000
2002
2004
2006
2008
2010
2012
2014
2046
2048
2050
2052
2054
2056
2058
2060
2062
2064
2081
2083
2085
2087
2089
2091
2093
2095
2097
2099
Control Run
RCP 4.5 Mean
RCP 8.5 Mean

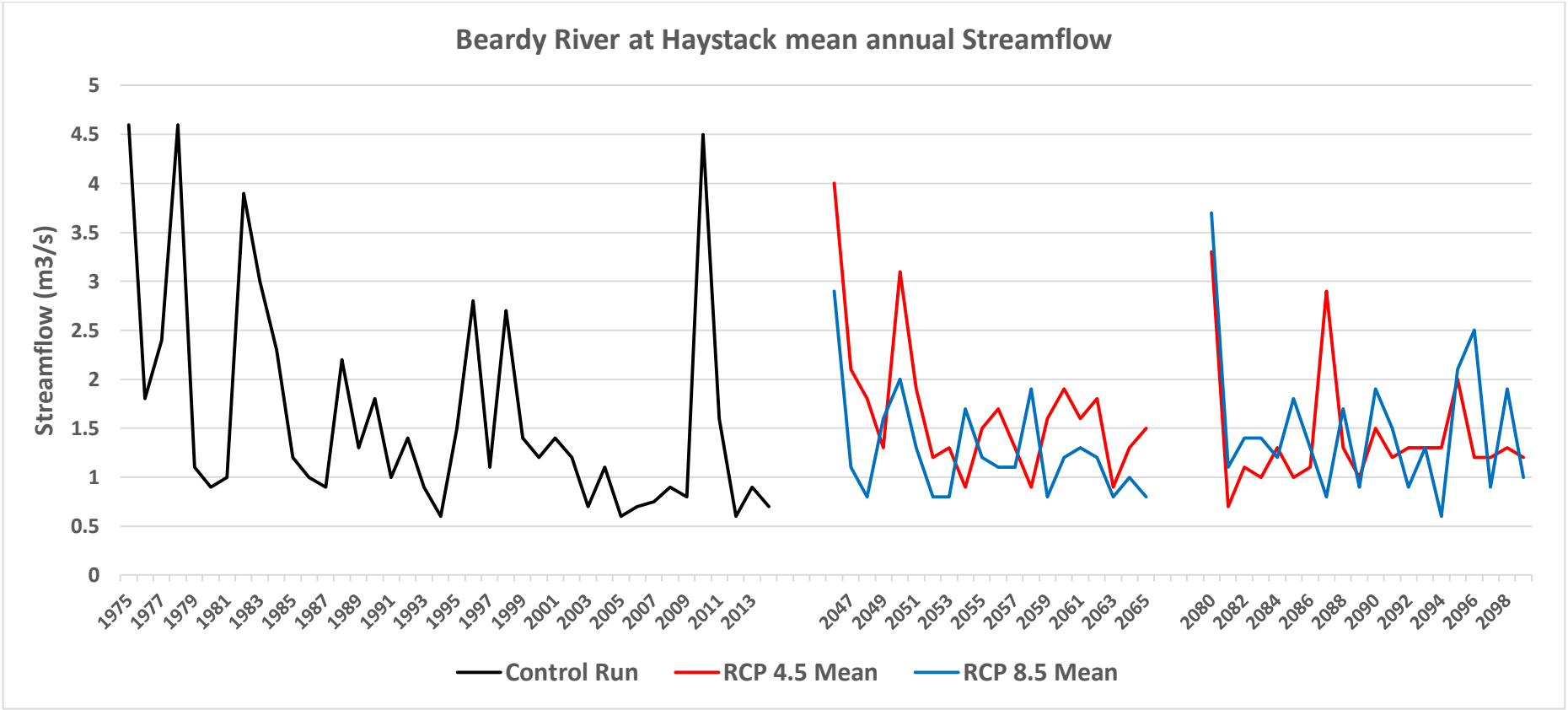
Beardy River at Haystack mean annual Streamflow
Streamflow (m3/s)
5
4.5
4
3.5
3
2.5
2
1.5
1
0.5
0
1975 1977 1979 1981 1983 1985 1987 1989 1991 1993 1995 1997 1999 2001 2003 2005 2007 2009 2011 2013
2047 2049 2051 2053 2055 2057 2059 2061 2063 2065
2080 2082 2084 2086 2088 2090 2092 2094 2096 2098
Control Run
RCP 4.5 Mean
RCP 8.5 Mean

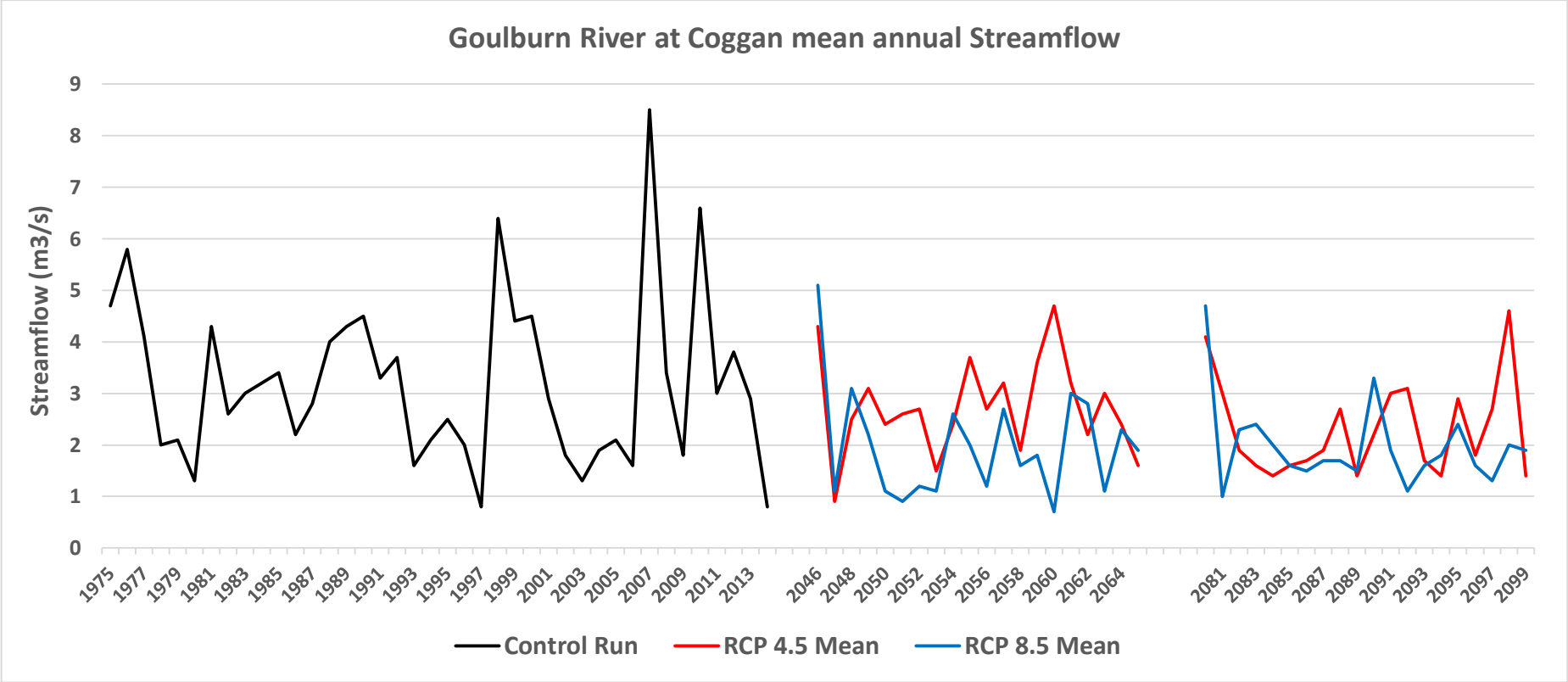

Figure (5.7) Annual mean streamflow variations of the future climate scenarios relative to the control run at the three HRSs. The average simulated discharge is the ensemble mean of 8-GCMs.

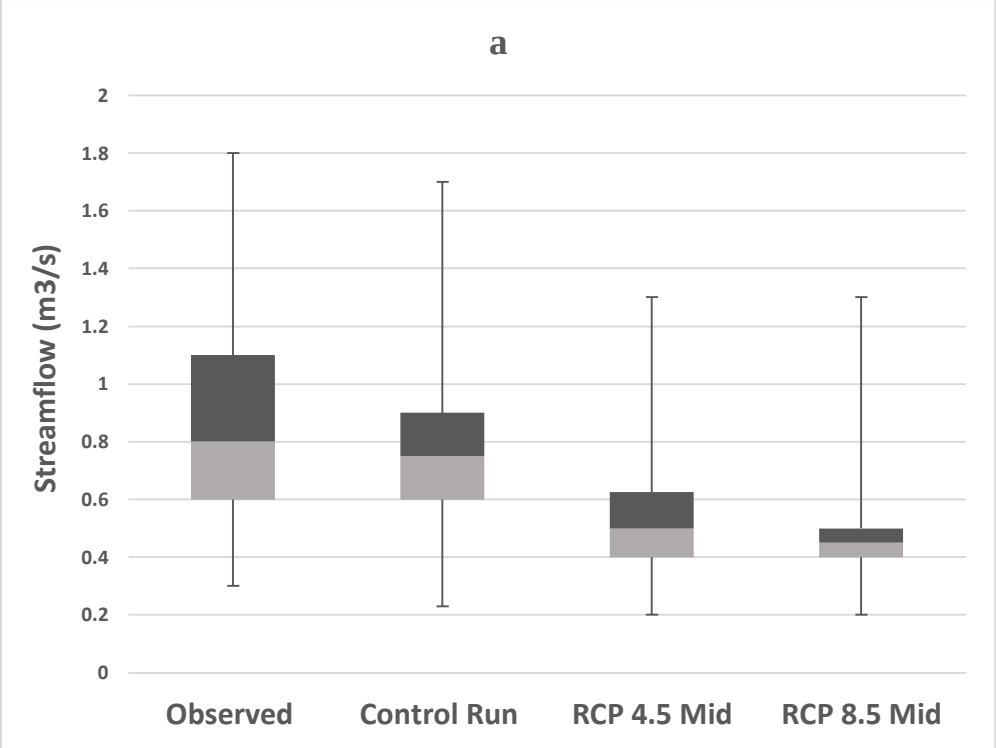
a
Streamflow (m3/s)
2
1.8
1.6
1.4
1.2
1
0.8
0.6
0.4
0.2
0
Observed
Control Run
RCP 4.5 Mid
RCP 8.5 Mid

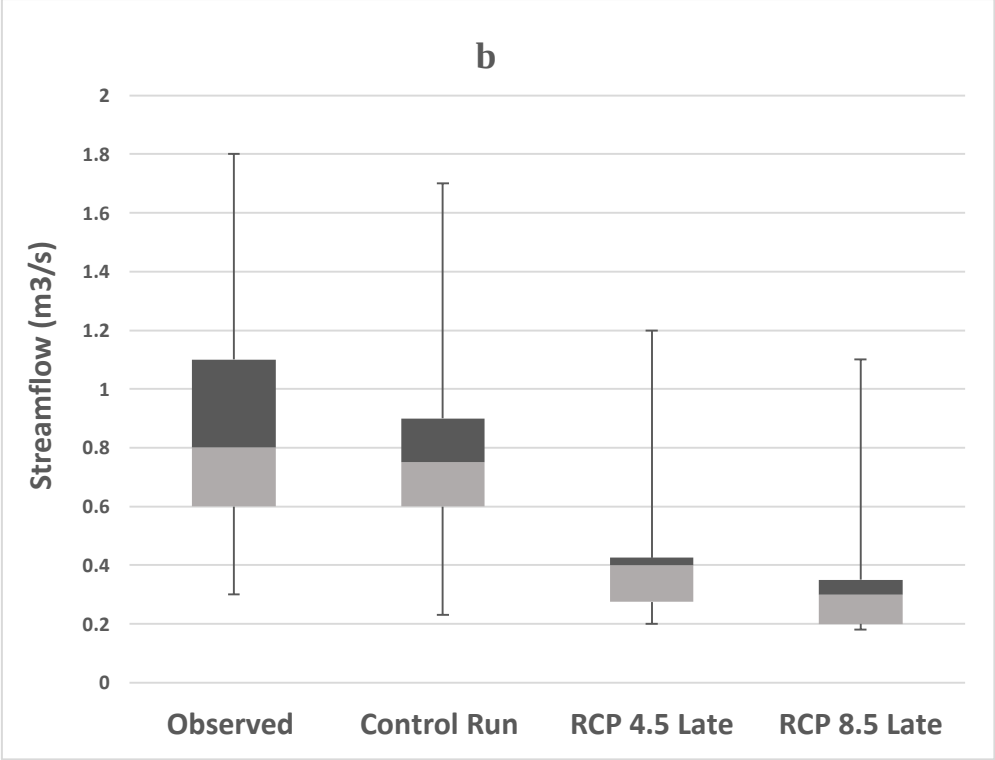
b
Streamflow (m3/s)
2
1.8
1.6
1.4
1.2
1
0.8
0.6
0.4
0.2
0
Observed
Control Run
RCP 4.5 Late
RCP 8.5 Late

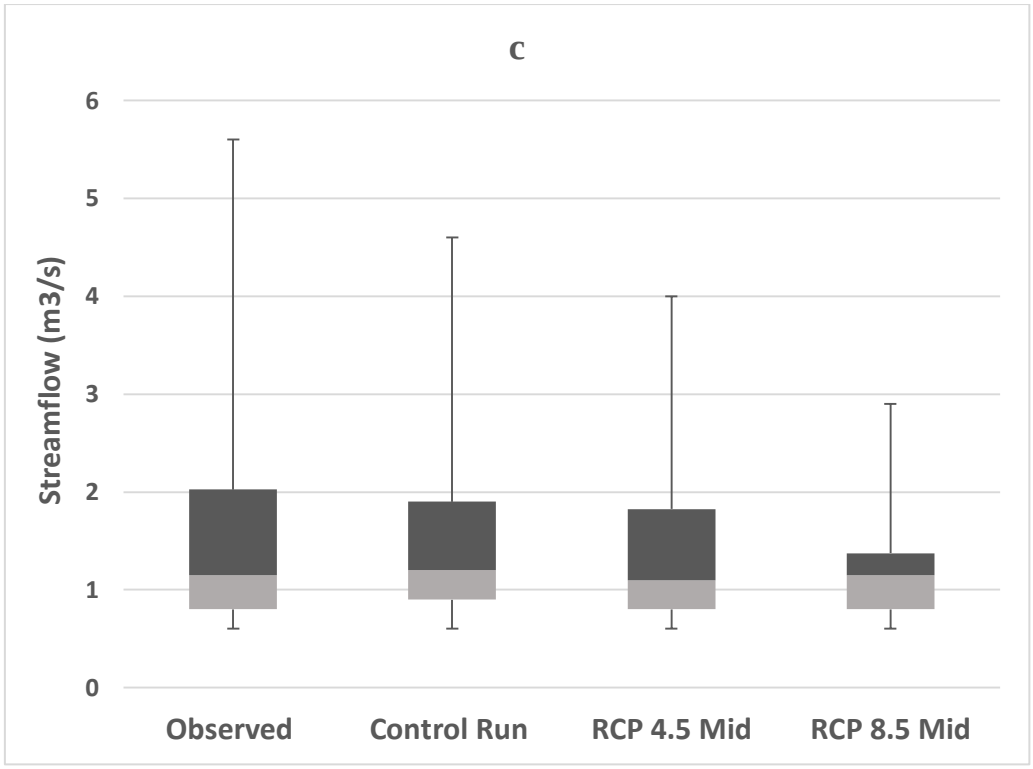
c
Streamflow (m3/s)
0
1
2
3
4
5
6
Observed
Control Run
RCP 4.5 Mid
RCP 8.5 Mid

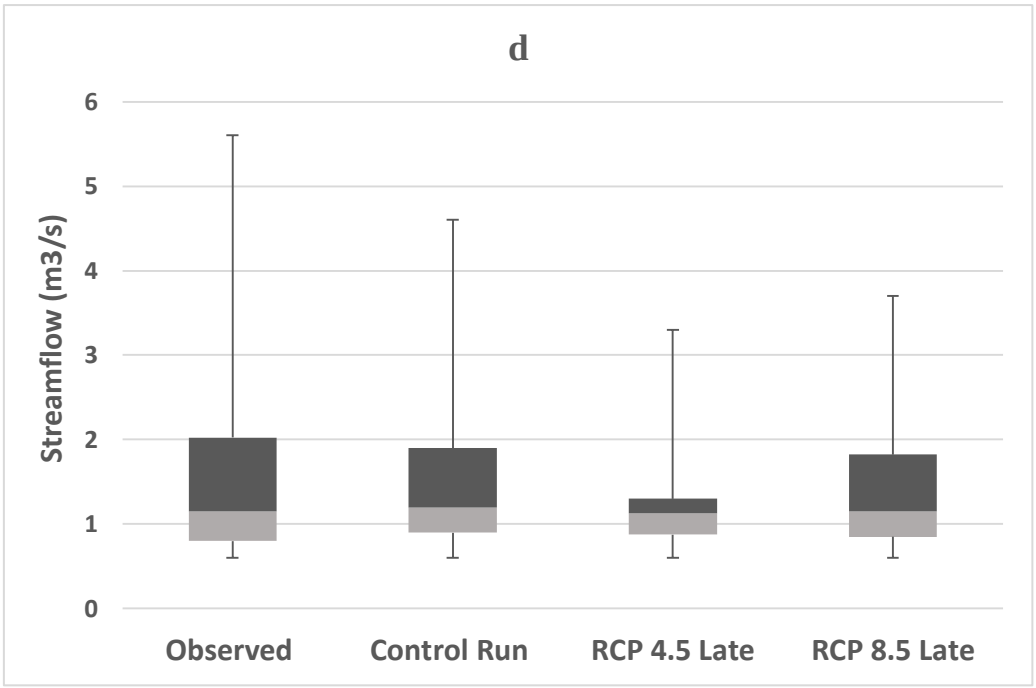
d
Streamflow (m3/s)
0
1
2
3
4
5
6
Observed
Control Run
RCP 4.5 Late
RCP 8.5 Late

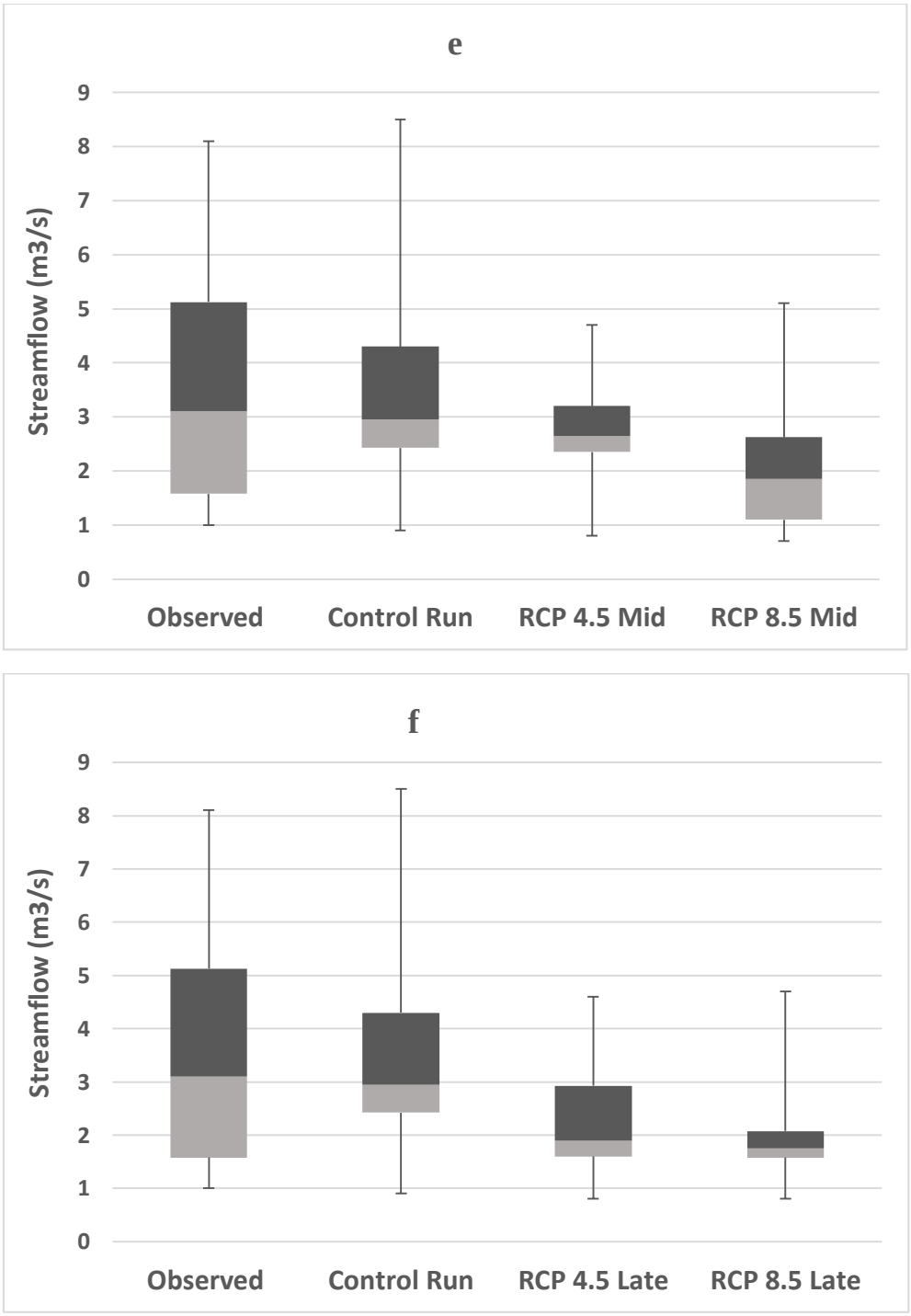

Figure (5.8) The 25th and 75th streamflow percentile statistics for the observed, control run and the future periods. (a) and (b) at Dingo-Road HRS, (c) and (d) at Haystack HRS, (e) and (f) at Coggan HRS The bars represent the errors in the minimum and maximum annual streamflow percentiles. The simulated streamflow of the control-run and future periods is the ensemble mean of 8-GCMs.

Table (5.5) and Figures (5.7) clearly show the responses of the three HRSs to the projected climate change impact through the decline in all future streamflow statistics measured at Dingo Road, Haystack and Coggan HRSs. The decline in streamflow trends could be attributed to the rainfall reduction during the mid and late of the century as well as the increase in potential evapotranspiration across the catchments.

At Dingo Road HRS, a substantial decline in streamflow amounts (especially during the late-century) is projected in the contributing catchment under the RCP4.5 and RCP8.5 climate scenarios compared to the control run. During the mid-century, the mean annual streamflow is projected to decrease by 31% and 37% under the RCP4.5 and RCP8.5 respectively. By the end of the century, the mean annual streamflow decline is anticipated to reach 48% and 60% for the same scenarios correspondingly. The minimum streamflow statistics expressed as (Qmin and Q25) also show negative trends during the future period ranged between 13% and 66% under the two future scenarios (Figure 5.8). Similarly, the maximum streamflow statistics expressed as (Q75 and Qmax) are also anticipated to decline by a range of 23% and 61% under both scenarios during the mid and late-century Figure (5.8). The step-change analysis of the observed mean annual streamflow at Dingo Road HRS showed a reduction trend over the time. The long-term annual streamflow trend has noticeably declined since the early 1970s until 1993 (the step-change year) after which the median annual streamflow has reduced from around 36 GL per water year to 23 GL per water year (Figure 5.9b). Furthermore, since the year 2000, the annual streamflow at Dingo Road HRs was below the long-term average (Figure 5.9a). Durrant and Byleveld (2009) confirmed this negative trend when examined the post-1975 streamflow data at twenty-nine locations within south-west Western Australia and found decreasing trends in most of these locations. Therefore, the reduction tendencies in the average streamflow of the Harvey River are expected to continue in the future.

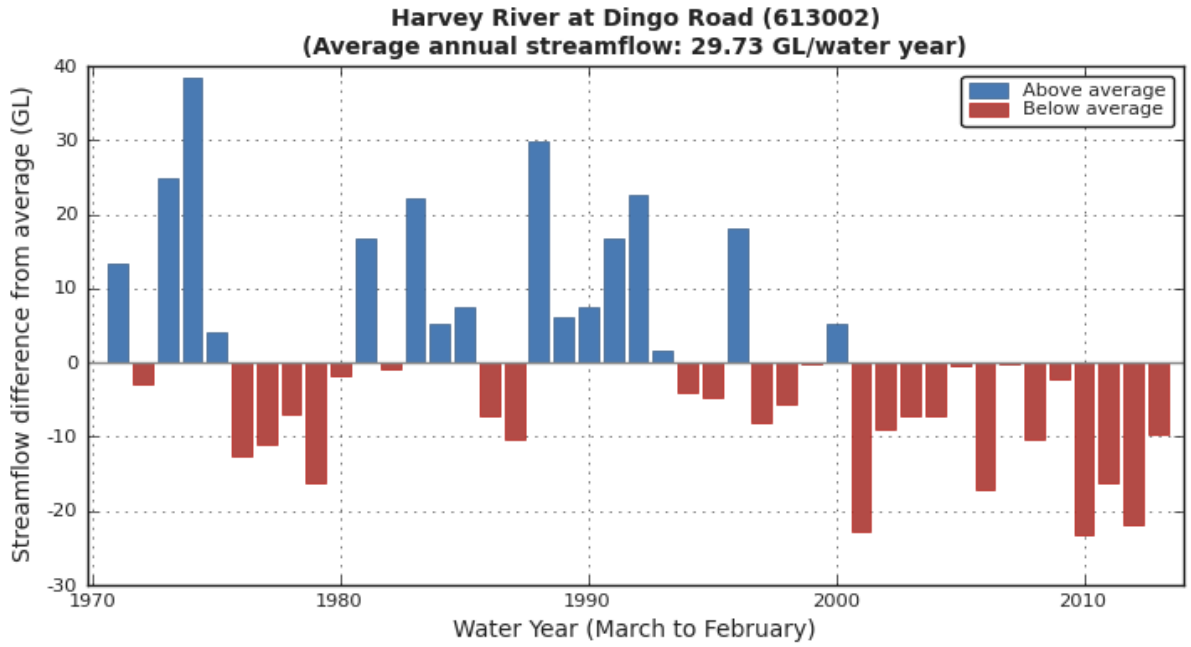

(a)

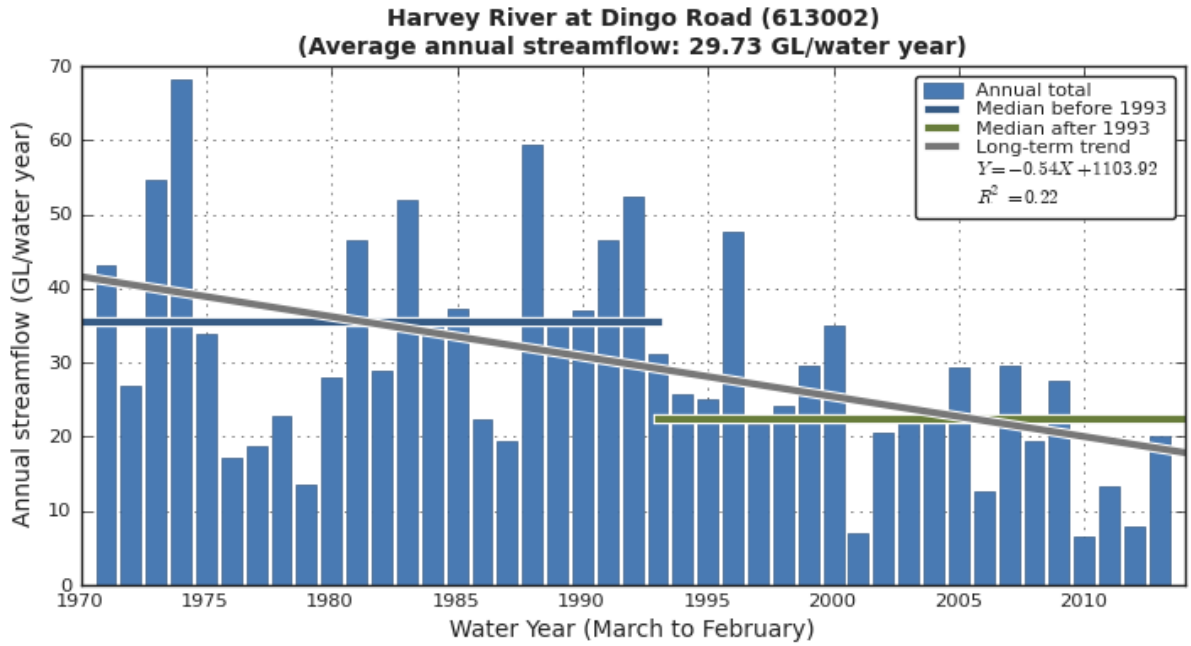

(b)

Figure (5.9) (a) Long-term mean annual streamflow variations (compared to the average), and (b) trend analysis at Dingo Road HRS on Harvey River (BoM, 2017).

As the streamflow of the Harvey River is anticipated to decline in the future, this would severely affect the quantities of water received by the Harvey Estuary. The estuary is an internationally important habitat for waterbirds and migratory wading birds, in which tens of thousands of waterbirds gather annually with more than 80 species (Environmental Protection

Authority, 2008). The depth of the Peel-Harvey Estuarine system (total area of 133 km^2) is relatively shallow (up to 2m for the deepest point), and more than 50% of its area has a depth of only 0.5m (Kelsey et al., 2010). Therefore, any reduction in the flow amount of the Harvey River will affect the aquatic life and the environmental status of the lagoon. In short, the growing environmental and economic importance of the Peel-Harvey estuarine system (such as water demands for drinking and agricultural production, commercial fishing, foreshore development and access, boat use and moorings and jetties) have placed additional burdens on the currently available water of the system. Furthermore, the projected reduction in the flow amount of the Harvey River would also reduce the quantities of water received by the Stirling and Harvey Reservoirs which represent the main water supply sources to the Perth Metropolitan. As the population and the economic development in Perth and its outskirts is in continuous growth, this would increase the competition for the currently available water resources in the area. Therefore, options for additional water supply sources in the future would be necessary to support the economic and population development in the area.

At Haystack HRS, the future streamflow in the contributing catchment is also anticipated to decrease under the two studied scenarios relative to the control run (Table 5.5). The mid-century mean annual streamflow is projected to decrease by 1% and 24% under the RCP4.5 and RCP8.5 respectively. Towards the end of the century, the decline in mean annual streamflow is anticipated to reach 16% and 11% under the same scenarios correspondingly. The minimum flows (Qmin and Q25) are also projected to decline with a range of (0-11%) during the mid and late of the current century under both climate scenarios. Similarly, the maximum flows (Qmax and Q75) are expected to decrease with a range of (4%-37%) under both scenarios during the future periods (Table 5.5). The step-change analysis of the long-term annual streamflow trend at Haystack HRS has also shown a reduction trend over the time (Figure 5.10b). Since the early 1970s, the median annual streamflow has declined from 50 GL per water year to around 35 GL per water year after year of step-change (2000). Furthermore, since the year 2000, the annual streamflow at Haystack Road HRs was below the long-term average (Figure 5.10a), except the year 2010 when the annual streamflow was above the long-term average. Therefore, the reduction tendencies in the average streamflow of the Beardy River are expected to continue in the future.

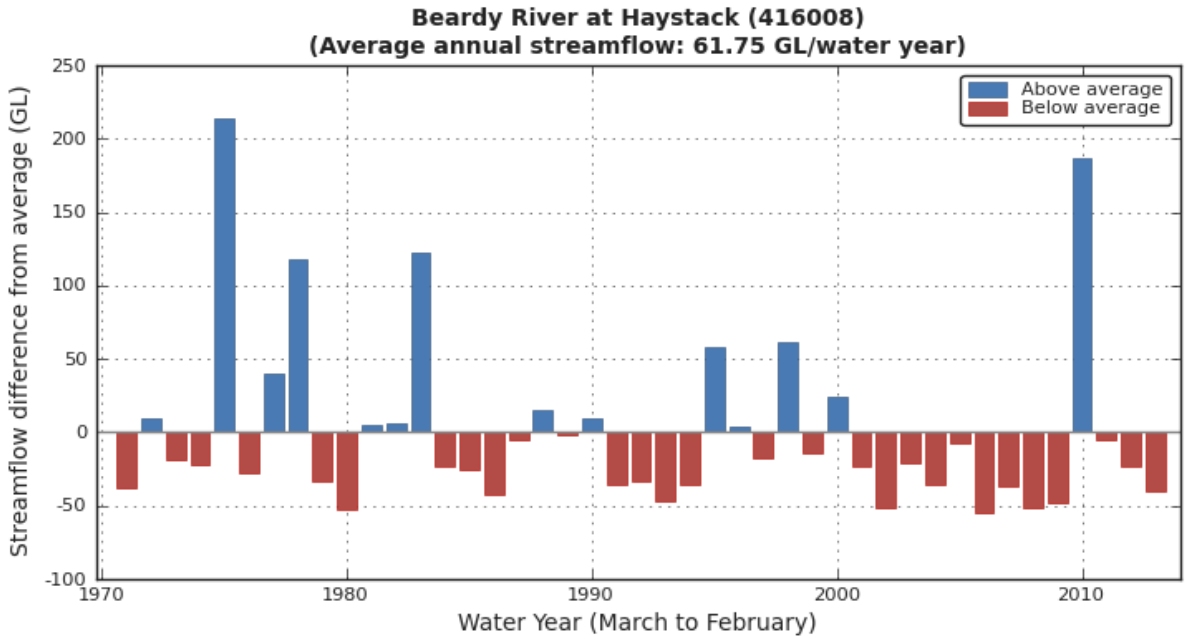

(a)

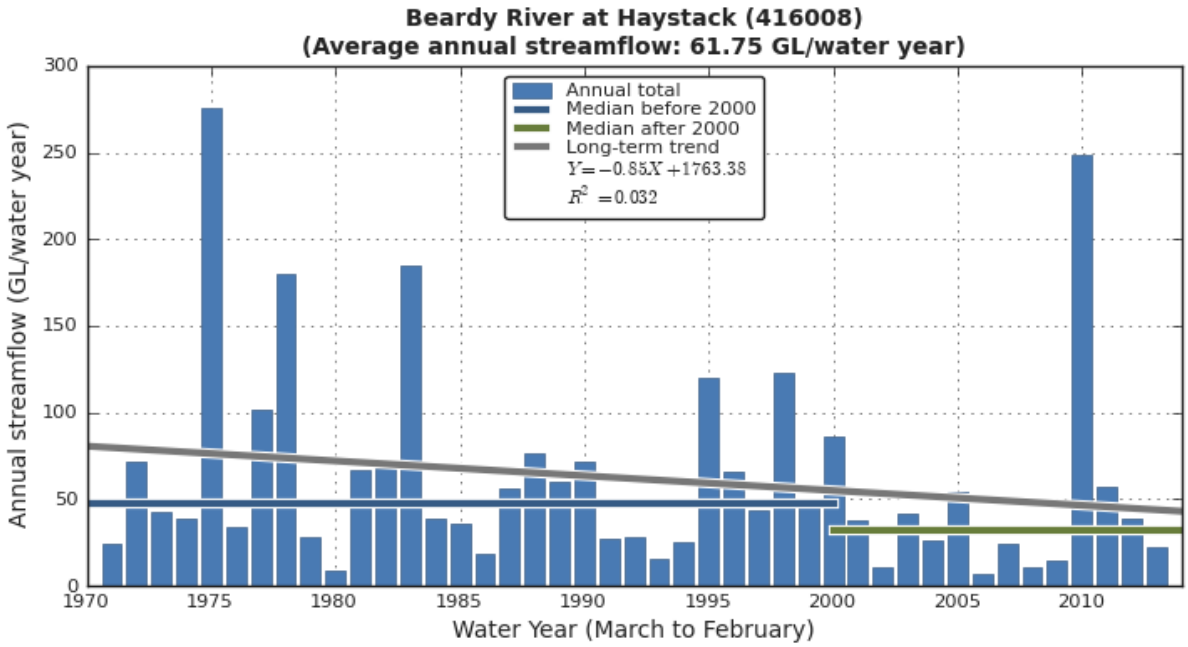

(b)

Figure (5.10) (a) Long-term mean annual streamflow variations (compared to the average), and (b) trend analysis at Haystack HRS on Beardy River (BoM, 2017).

The Beardy River region is rich in rare flora and fauna and some rare plants such as the MacNutt's wattle, velvet wattle and Torrington pea. The region also supports a variety of endangered birds such as the glossy black-cockatoo, brown treecreeper, swift parrot, and a few marsupials, including the spotted-tailed quoll and squirrel glider (NSW government, the Office

of Environment and Heritage, 2016). Therefore, the expected streamflow reduction would adversely impact the environmental and ecological communities of the Beardy-River system particularly the Beardy-River Hill Catchment.

At Coggan HRS, the future streamflow is also anticipated to decrease in the contributing catchment relative to the control run (Table 5.5). For the mid-century, the mean annual streamflow is projected to decline by 18% and 39% under the scenarios RCP4.5 and RCP8.5 respectively. By the end-century, the anticipated decline in the mean annual streamflow will be 30% and 42% under the same scenarios correspondingly. The minimum flows (Qmin and Q25) also show high reduction tendencies under both scenarios ranged between 4% and 54% during the mid and late-century relative to the control run (Figure 5.8). Alike, the maximum flows (Qmax. and Q75) reviled substantial negative trends under the two scenarios ranged between 26% and 53% for the mid and late-century compared to the control run (Figure 5.8). The step-change analysis of the historical (observed) mean annual streamflow at Coggan HRS revealed a decreasing trend over the time. The long-term annual streamflow trend has declined since the early 1950s until the year of step change (1978) after which the median annual streamflow has reduced to the half (from around 80 GL per water year to 40 GL per water year) (Figure 5.11).

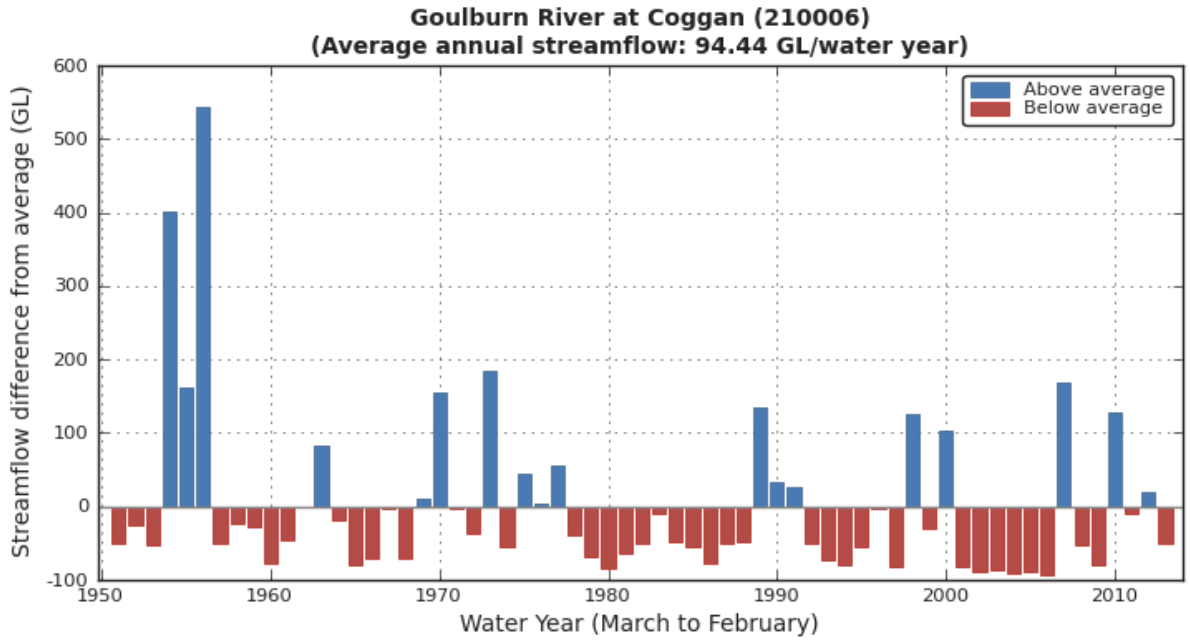

(a)

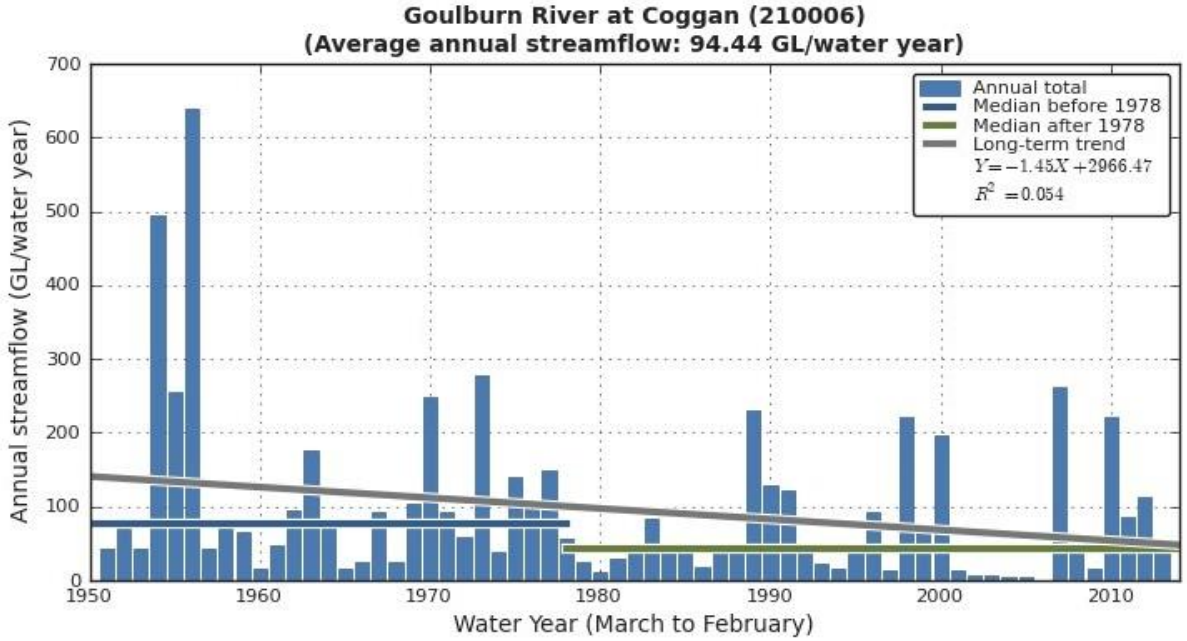

(b)

Figure (5.11) (a) Long-term mean annual streamflow variations (compared to the average), and (b) trend analysis at Coggan HRSs on Goulburn River (BoM, 2017)

Goulburn River is the right bank tributary to the Hunter-River in NSW, Australia. It drains approximately 50% of the Hunter catchment and donates nearly quarter of the mean Hunter River flow. Water in the Hunter basin is the main source for power generation, irrigation and agriculture, stock manufacturing, coal mining and public water supplies. As the Goulburn River flow is projected to decrease due to future climate changes, this would effectively impose further limitations on the surface water supply systems in the Hunter River basin.

The outcomes of the present study are in good agreement with the streamflow reduction trend provided by the Australian-BoM through the step-change analysis (Figures 5.9 - 5.11). The findings from step-change analysis confirmed evidence of changes in hydrological responses consistent with the observed climate changes over the past decades. The current outcomes are also support other previous studies that implemented in other south-eastern and south-western Australian catchments and revealed a decline in the future streamflow (e.g. Chiew et al., 2009; Vaze and Teng, 2011; Bari et al., 2010; McFarlane et al, 2012; Silberstein et al., 2012; Teng et al., 2012; Islam et al., 2014). However, these studies have been conducted by utilizing climate scenarios from different IPCC-AR4 GCMs to force a variety of conceptual models to simulate the historical and projected streamflow across the studied basins. In light of this study, two RCPs informed by the ensemble mean of 8-GCMs of the IPCC-AR5 were used to force the

conceptual hydrological model (HBV) to simulate the historical and future streamflow at three contributing catchments of the Australian HRSs network.

Finding of this study may help the communities and decision makers to manage the usage of future water resources in the contributing catchments taking the decline in future streamflow into consideration. From the viewpoint of water management, choices for additional sources of water supply in the future require considering the use of groundwater, improved surface water yield through better land use management, demand management, water reuse and desalination. The anticipated drier climate could also change the flow regimes and harm the biodiversity of the studied basins, and therefore adaptive responses would be necessary to maintain sustainable ecological communities.

5.5 Modelling uncertainty and its implications

Climate change impact studies carried out at catchment scale always involve uncertainties that result from using different scenarios of GCMs, hydrological models and the selection of the downscaling procedure. According to Minville et al. (2008) and Hughes et al. (2011), GCMs are the main source of uncertainty in climate change impact assessment. To minimize this type of uncertainty, the present study uses the downscaled outputs from a multi-model ensemble of the most appropriate 8-GCMs that efficiently represent the Australian future climate conditions. The multi-model ensemble method enables the analysis of a combination of future climate signals that extracted from a combination of GCMs to better represent the future climate variations in the study area which is valuable for water resources management (Coulibaly, 2008). The type of the hydrological model used in the impact assessment also highly affects the modelling results. The type of the model (lumped, distributed and semi-distributed), modelling structures, assumptions, limitations and parameter uncertainties significantly affect the results of hydrological modelling (Surfleet et al., 2012). Nawarathna et al. (2001) explained that the successful application of the lumped and semi-distributed hydrologic models conditioned that the characteristics of the river basin stay stable over the time. As the selected contributing catchments are unaffected by the land use change and local water resources regulations, the HBV conceptual model was successfully applied to perform the hydrological modelling in the studied catchments. In addition, some of the local-scale impact assessment studies perform the hydrological modelling depending on the variability of rainfall only and neglect the effect of temperature and evaporation. Fu et al. (2007) criticized

this assumption and demonstrated the nonlinearity response of runoff to the rainfall variations and the effect of temperature and evaporation needs to be taken into consideration as well. Therefore, the effect of future climate variability in the present work was considered by using the downscaled rainfall, temperature and evapotranspiration across the studied catchments under two different climate scenarios. Furthermore, the selection of the downscaling procedure plays a key role in climate change impact assessment because of the limitations associated with each method of downscaling (Minville et al., 2008 and Coulibaly, 2008).

5.6 Summary and Conclusions

The effect of climate change impacts on the future streamflow variability during the mid (2046-2065) and late (2080-2099) of the current century was investigated for three contributing catchments of the Australian HRSs, including Harvey River catchment in Western Australia, Beardy and Goulburn catchments in New South Wales. The Australian HRSs network represents an important source of high-quality continuous streamflow data across the continent that enables better analysis of the long-term streamflow trends. The HBV conceptual model was used in this study to perform the hydrological modelling in the selected sites. Daily observations of rainfall, temperature and discharge and the long-term monthly mean potential evapotranspiration from the hydro-meteorological stations of the contributing catchments were used to calibrate and validate the HBV model prior to the streamflow prediction. The calibration and validation results revealed a good modelling performance which indicates that the model could be used successfully to simulate the future discharge at the three HRSs. The global-scale future climate signals of rainfall and temperature (monthly mean outputs) were extracted from a multi-model ensemble of 8-GCMs of the CMPI5 under two Representative Concentration Pathways, RCP4.5 and RCP8.5 which belongs to the IPCC-AR5. These models represent the best 8-GCMs out of 40 GCMs of the CMIP5 that can be used effectively to investigate the Australian future climatic conditions, especially for the impact assessment studies. The global-scale monthly outputs (of each GCM) were then downscaled by using a Statistical Downscaling Model developed by the Australian-BoM (BoM-SDM) using the analogue approach. The ensemble mean of the eight-GCM was then derived and adopted in streamflow simulation. The quality of future climate data has been checked with higher priority by the Australian-BOM before applying it for the catchment scale impact assessment. Nearly all GCMs predict a decline in mean annual rainfall and an increase in temperature and potential evapotranspiration across the three contributing catchments in the future. The calibrated HBV

model was then forced with the ensemble mean of the downscaled daily rainfall and temperature from the baseline (control run) and the future periods to simulate the daily streamflow at the three HRSs. Results show negative trends in the future streamflow measured at Dingo Road, Haystack and Coggan HRSs under the two studied scenarios relative to the control run.

For the Harvey River catchment, the mid-century mean annual streamflow is projected to decline by 31% and 37% under the RCP4.5 and RCP8.5 respectively following a decline of 7.4% and 9.1% in mean annual rainfall. By the late-century, there could be a 48% and 60% decline in mean annual streamflow under the RCP4.5 and RCP8.5 correspondingly following a decline of 7.6% and 12.2% in mean annual rainfall. For the Beardy River catchment, the mid-century mean annual rainfall is projected to decline by 2.9% and 5.5% under the RCP4.5 and RCP8.5 scenarios respectively, and the corresponding mean annual streamflow reduction is anticipated to be 1% and 24%. Toward the end of the century, the mean annual rainfall is predicted to decrease by 9.2% and 1.3% under the RCP4.5 and RCP8.5 respectively, and the corresponding projected reduction of mean annual streamflow will be 16% and 11%. Similarly, the mid-century mean annual streamflow across Goulburn catchment is projected to decline by18% and 39% under the RCP4.5 and RCP8.5 respectively following a decline of 3.9% and 7% in mean annual rainfall. By the late-century, there could be a 30% and 42% decline in mean annual streamflow under the RCP4.5 and RCP8.5 correspondingly following a decline of 4.7% and 7.8% in mean annual rainfall.

In conclusion, this study highlights the similar outcomes of other previous studies which have been conducted in other south-eastern and south-western Australian catchments and revealed reduction tendencies in rainfall and runoff series. The projected streamflow reduction would badly impact the current surface water resources and would influence the environmental and ecological communities of the catchments. Therefore, the current findings could help the communities and decision makers to manage the future water resources in the contributing catchments taking the low flow situation into consideration.

Chapter 6

Hydrological Modelling in Unregulated Catchments using a Distributed Model

Extended from:

Al-Safi, H. I. J., & Sarukkalige, P. R. (2018). Hydrological impacts of climate change on the future streamflow of three unregulated catchments of the Australian hydrologic reference stations. Int. J. Hydrology Science and Technology, (in press).

6.1 Introduction

There are clear evidence that the climate change will affect the Australian climatic conditions by changing the trends of rainfall and temperature across the continent. The Australian climate is considered of high variability in which enormous areas of the continent are having arid and semi-arid climatic conditions (Barron et al., 2011). Since the mid-1990s, noticeable increasing trends of temperature and decreasing trends of rainfall were observed in south-eastern Australia which adversely impacted the availability of water resources in the area (Pittock, 2003, Murphy and Timbal, 2008). This shift in climatic behaviour, which is quite similar to the one that began around 1970 in the SWWA, was widely acknowledged by many researchers (e.g. Cai and Cowan, 2008; Chiew et al., 2009; Vaze et al., 2011; Teng et al., 2012). Accordingly, the problem of water scarcity in Australia has drawn the attention of many researchers to investigate this matter for planning and control purposes.

The majority of the hydrologic studies which have been conducted across the south-eastern and south-western Australian catchments revealed a high rainfall reduction trends, increasing temperature trends and declines in streamflow propensities. For instance, a reduction in winter

rainfall of around 20% has resulted in more than 40% decline in annual mean discharge flows to the main supplying reservoirs in Perth and its outskirts (Indian Ocean Climate Initiative, 2002). Cai and Cowan, (2008) also pointed out that the late outman rainfall over the south-east Australian catchments has reduced by around 40% during the period between 1950-2006 compared to its long-term seasonal average. Bari et al., (2010) showed that the runoff trends in the Serpentine catchment (in Western Australia) are projected to decrease in the future following an expected decline in annual rainfall across the catchment. Chiew et al., (2009) and Vaze and Teng (2011) showed that the future rainfall-runoff tendencies in most parts of south-east Australia are anticipated to decline as a result of climate change. A study by Teng et al., (2012) also demonstrated the streamflow reduction across the south-east Australian catchments. Consequently, the expected decline in future runoff needs a significant planning response and potential change in water resources management.

In this study, the hydrological response of three contributing catchments of the Australian HRSs, Harvey River at Dingo Road station in Western Australia, Beardy River at Haystack and Goulburn River at Coggan stations in New South Wales, is assessed for the mid (2046-2065) and late (2080-2099) of the 21st century. The physically based distributed hydrological model (BTOPMC) is adopted to perform the hydrological modelling in the study areas. The downscaled future climate signals of rainfall and temperature were extracted from a multi-model ensemble of eight Global Climate Models of the Coupled Model Inter-comparison Project phase 5 (CMIP5) under two Representative Concentration Pathways, RCP4.5 and RCP8.5. The ensemble mean of the eight-GCMs was then derived and used to force the calibrated BTOPMC model for daily streamflow prediction. The results of this study could deliver valuable water management strategies for the studied catchments to address the problem of water deficiency.

6.2 Study Area

In this chapter, the same catchments that have been used in chapter five are used here. The selected catchments well represent a range of climatic conditions and geophysical characteristics (e.g., latitude, longitude, elevation, land use type and soil type) across the Australian continent. This will provide an effective evaluation of the BTOPMC model performance across the studied catchments. A detailed description of the locations, climate and other characteristics of the three catchments is provided in section (5.2).

6.3 Methodology

6.3.1 Datasets and sources

In this study, different datasets were collected from various sources and used as input into the BTOPMC model as illustrated in Table (6.1). Observed hydro-meteorological data including the daily scale rainfall, temperature, and discharge from the contributing catchments of the three HRSs were obtained from the Australian Bureau of Meteorology. Weather stations (Table 6.2) were selected within the contributing catchments and nearby locations considering the availability of long-term data. Also, the high-quality streamflow data were collected from the three HRS including Dingo Road, Haystack and Coggan located at the outlet of each catchment. The temporal distribution of the hydro-meteorological data is presented in Table 6.1 and used to calibrate and validate the BTOPMC model prior to the streamflow prediction. Spatial distribution of rainfall and temperature data was implemented by the BTOPMC model by applying the Thession polygon method.

A detailed description of the physical and vegetation data of the three contribution catchments is presented in Table 6.1. Global datasets were employed whenever local data sets were unobtainable. The different spatial resolution of the raster datasets could produce a compatibility problem while using them with the model; therefore, all raster data were set to a unique spatial resolution of 30''x 30'' (90m x 90m) before inputting them into the model. Digital Elevation Map data was extracted from the SRTM dataset (Jarvis et al., 2008) and used as input to the BTOPMC model. The DEM data performed very well in generating the streamflow network of the three catchments and hence used as the topography data in this study. Soil map of the study area was extracted from the Harmonized World Soil Database (HWSD) (FAO, 2012). The soil data contain 6998 soil types according to the FAO classification, of which only nine dominant soil types are distributed in the studied catchments. Related soil properties and textures were also obtained from the HWSD including different percentages of sand, clay, and loam (Table 6.3). The land cover data was extracted from the Global Land Cover Characteristics Database of the United States Geological Survey – International Geosphere-Biosphere Programme (USGS–IGBP) (USGS, 2011). The land cover data comprise 17 types depending on the IGBP classification system, of which only 13 types are available in the studied catchments (Table 6.4). The topography and streamflow networks generated by the BTOPMC model using SRTM dataset for the three contributing catchments are displayed in Figures (6.1 and 6.2) respectively. The FAO soil types and the IGBP land

cover maps of the three contributing catchments are illustrated in Figures (6.3 and 6.4) correspondingly. The Normalized Difference Vegetation Index (NDVI) data were extracted from the Distributed Active Archive Center—Global Inventory Modelling and Mapping Studies and used to compute evapotranspiration using Shuttleworth-Wallace method.

Table 6.1 Sources and details of data used in the BTOPMC model application for the three contributing catchments

Data Type	Data Description	Original Spatial Resolution	Data Source	Remarks
Physical data	Digital Elevation Map (DEM)	3"x3" (90mx90m)	Jarvis et al. (2008)	Global Shuttle Radar Topography Mission data by the CGIAR Consortium for Spatial Information (http://srtm.csi.cgiar.org/SELECTION/inputCoord.asp)
	Soil Map	3"x3" (90mx90m)	FAO (2012)	Harmonized world soil database (FAO/IIASA/ISRIC/ISSCAS/JRC, 2012)
	Soil properties (texture)	----------		
	Land Cover Map	30"x30" (1km x 1km)	USGS (2011)	Global Land Cover Characteristics Database (Version 2.0) (http://landcover.usgs.gov/landcoverdata.php)
Vegetation data	Normalized Difference Vegetation Index NDVI	30"x30" (1km x 1km)	Tucker et al. (2010)	Global monthly data by Distributed Active Archive Center—Global Inventory Modelling and Mapping Studies (DAAC- ISLSCP II GIMMS) (https://daac.ornl.gov/ISLSCPII/guides/gimms_ndvi_monthly_xdeg.html), input for the Shuttleworth-Wallace model
Meteorological data	Rainfall (mm)	Point data	Australian Bureau of Meteorology	Three stations for Harvey Catchment, Daily scale data (1982-2014). Five stations for Beardy Catchment and seven stations for Goulburn Catchments. Daily scale data (1975-2014).
	Mean Temperature ^{o}C			One station for Harvey Catchment at a daily scale (1982-2014). Two stations for Beardy Catchment and three stations for Goulburn Catchments at a daily scale (1975-2014)
	Cloud cover (tenth)	0.5 x 0.5 degree (50 x 50 km)	CRU 2.0 data sets from IPCC (2011)	Global monthly data used for potential evaporation calculation, input for the Shuttleworth-Wallace model (http://www.ipcc-data.org/obs/get_30yr_means.html)
	Daylight duration (h)			
	Diurnal temperature range ^{o}C			
	Extraterrestrial radiation (MJ day^{-2} m^{-2})			
	Vapour pressure (kPa)			
	Wind speed (m/s)			
Hydrological Data	Daily observed streamflow	Gauged	Australian Bureau of Meteorology	Dingo-Road HRS for Harvey Catchment at a daily scale (1982-2014). Haystack HRS for Beardy Catchment and Coggan HRS for Goulburn Catchment at a daily scale (1975-2014)

Table 6.2 Locations of the hydro-meteorological stations with the observed parameters

	Station Name	Latitude (S^o)	Longitude (E^o)	Station No.	Observed Parameter
Harvey River Catchment	Marradong	32.86	116.45	9575	Rainfall
	Yourdamung Lake	33.20	116.28	9960	Rainfall
	Willowdale	32.92	116.01	9893	Rainfall
	Wokalup	33.13	115.88	9642	Temperature
	Harvey-River at Dingo Road	33.086	116.039	613002	Discharge
Beardy River Catchment					
	Ashford (Burrabogie)	29.40	151.41	54046	Rainfall
	Ashford (Springvale)	29.34	151.29	54045	Rainfall
	Emmaville (Strathbogie)	29.46	151.48	56029	Rainfall
	Emmaville Post Office	29.44	151.60	56009	Rainfall
	Tenterfield (kookynie)	29.27	151.86	56194	Rainfall
	Deepwater Post Office	29.70	151.69	56008	Temperature
	Pindari Dam	29.39	151.24	54104	Temperature
	Beardy-River at Haystack	29.218	151.383	416008	Discharge
Goulburn River Catchment					
	Bylong (Bylong Road)	32.52	150.08	62102	Rainfall
	Bylong (Heatherbrae)	32.36	150.10	62080	Rainfall
	Cassilis Post Office	32.01	149.98	62005	Rainfall
	Ulan Water	32.28	149.74	62036	Rainfall
	Wollar (Barrigan St)	32.36	149.95	62032	Rainfall
	Wollar (Maree)	32.43	149.95	62056	Rainfall
	Gulgong Post Office	32.36	149.53	62013	Rainfall, Temperature
	Merriwa (Roscommon)	32.19	150.17	61287	Temperature
	Nullo Mountain AWS	32.72	150.23	62100	Temperature
	Goulburn-River at Coggan	32.344	150.101	210006	Discharge

Table 6.3 Soil properties and distribution of soil textures according to the HWSD

Soil FAO ID/Soil Type		Texture	(% area)		
			Clay	Sand	Silt
Harvey Catchment	5875	Sandy_Clay_Loam	20.98	66.15	12.87
	6029	Sandy_Loam	10.93	74.88	14.19
Beardy Catchment	5903	Sandy_Loam	19.30	57.39	23.31
	6003	Loamy_Sand	5.41	83.76	10.82
	6097	Clay	64.14	24.38	11.49
	6116	Sandy_Loam	19.41	63.43	17.16
Goulburn Catchment	5863	Sandy_Loam	14.55	71.12	13.33
	5892	Sandy_Clay_Loam	24.43	52.98	22.59
	6097	Clay	64.14	24.38	11.49
	6116	Sandy_Loam	19.41	63.43	17.16
	6195	Sandy_Loam	19.37	68.30	12.33

Table 6.4 Land cover classification and root depths according to IGBP

IGBP classification ID	Land cover type	Root Depth (m)
1	Evergreen Broadleaf Forest	2.5
2		2.5
3	Deciduous Broadleaf Forest	2.5
4		2.5
5	Mixed Forest	2.0
6	Closed shrublands	1.0
7	Open shrublands	1.0
8	Woody Savannas	1.0
9		1.0
10	Grasslands	0.5
11		1.0
12	Croplands	0.7
14	Cropland and Natural Vegetation Mosaic	1.0

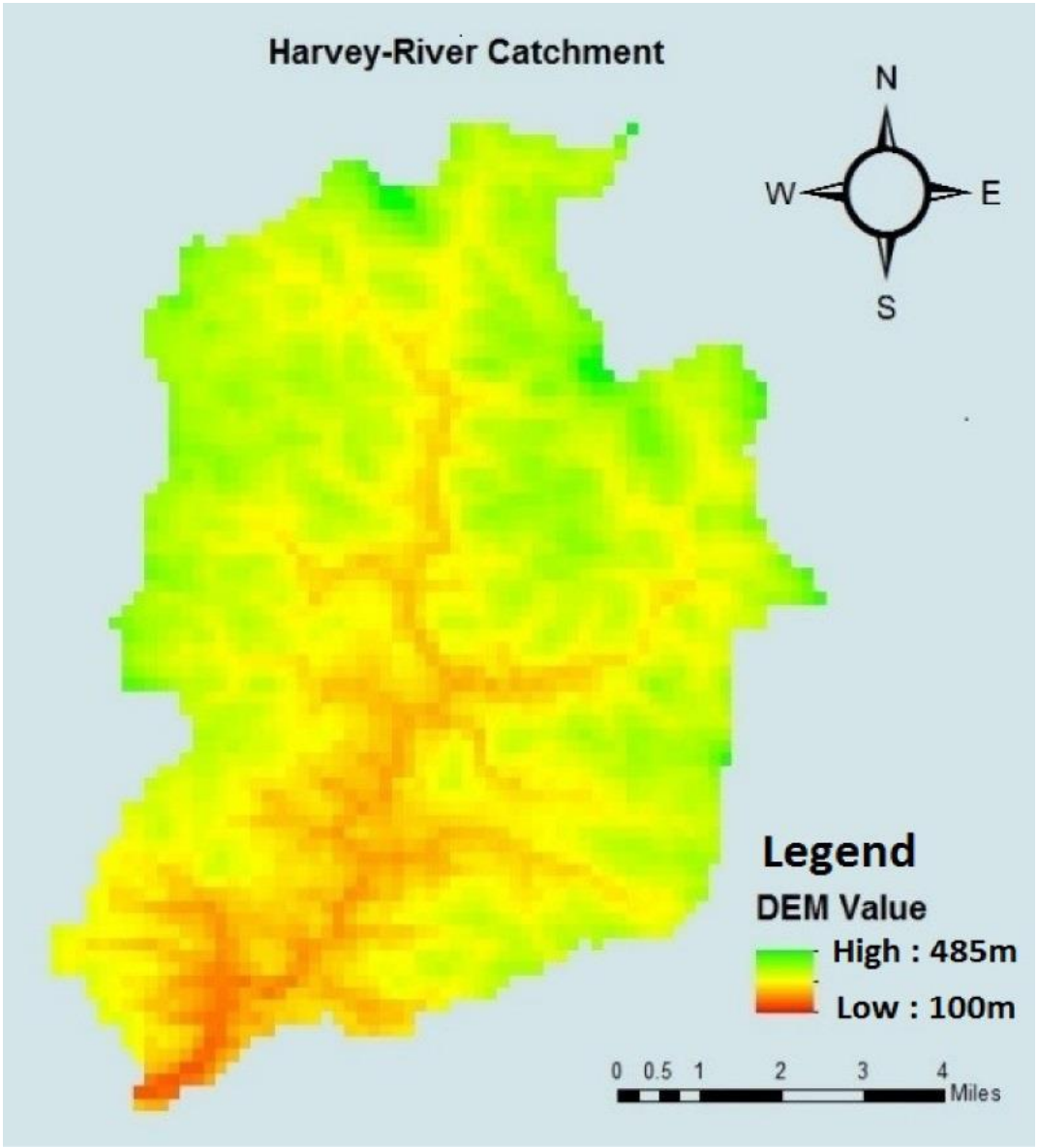

(a) Harvey River catchment

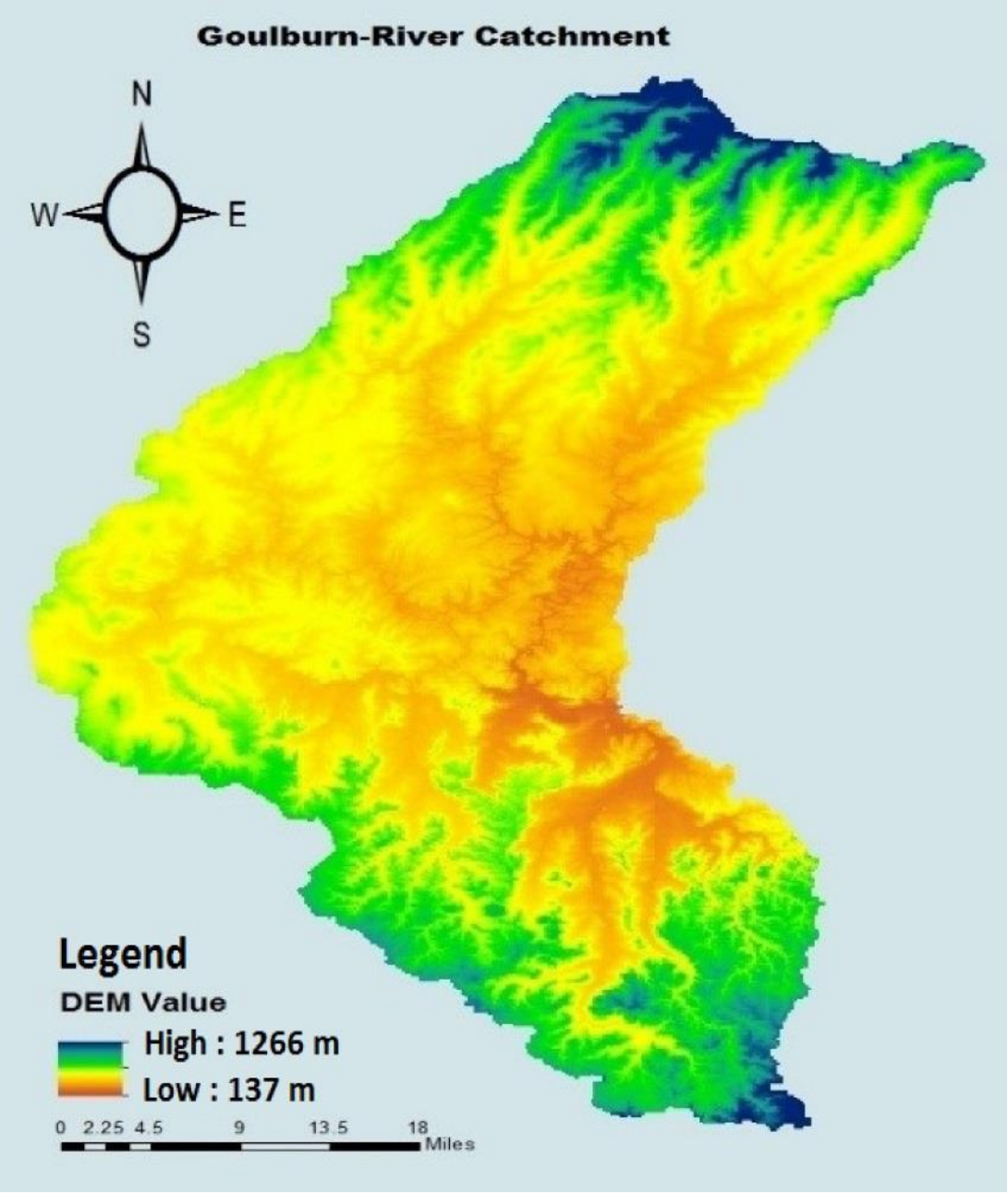

(b) Goulburn River catchment

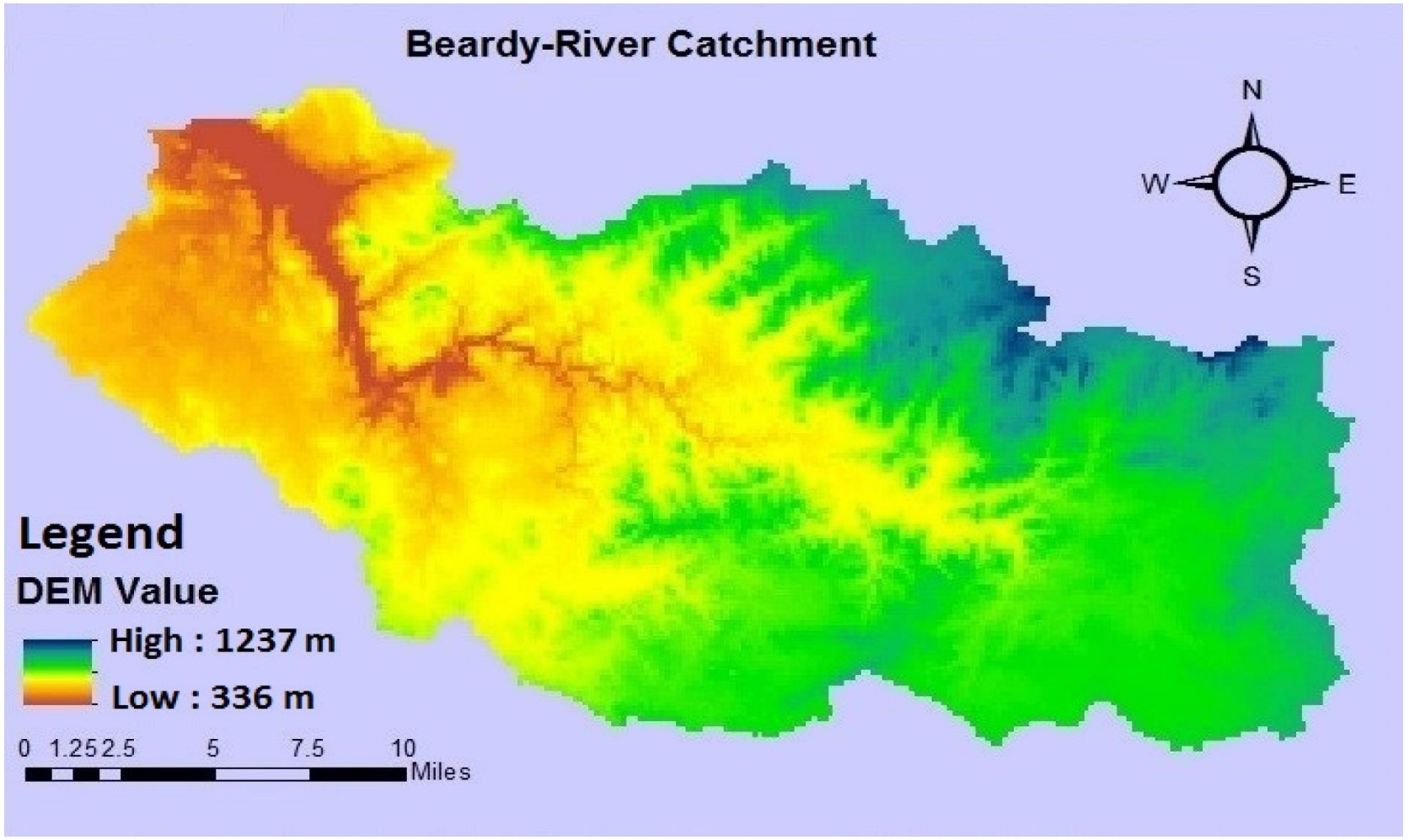

(c) Beardy River catchment

Figure 6.1 Topography of the three contributing catchments

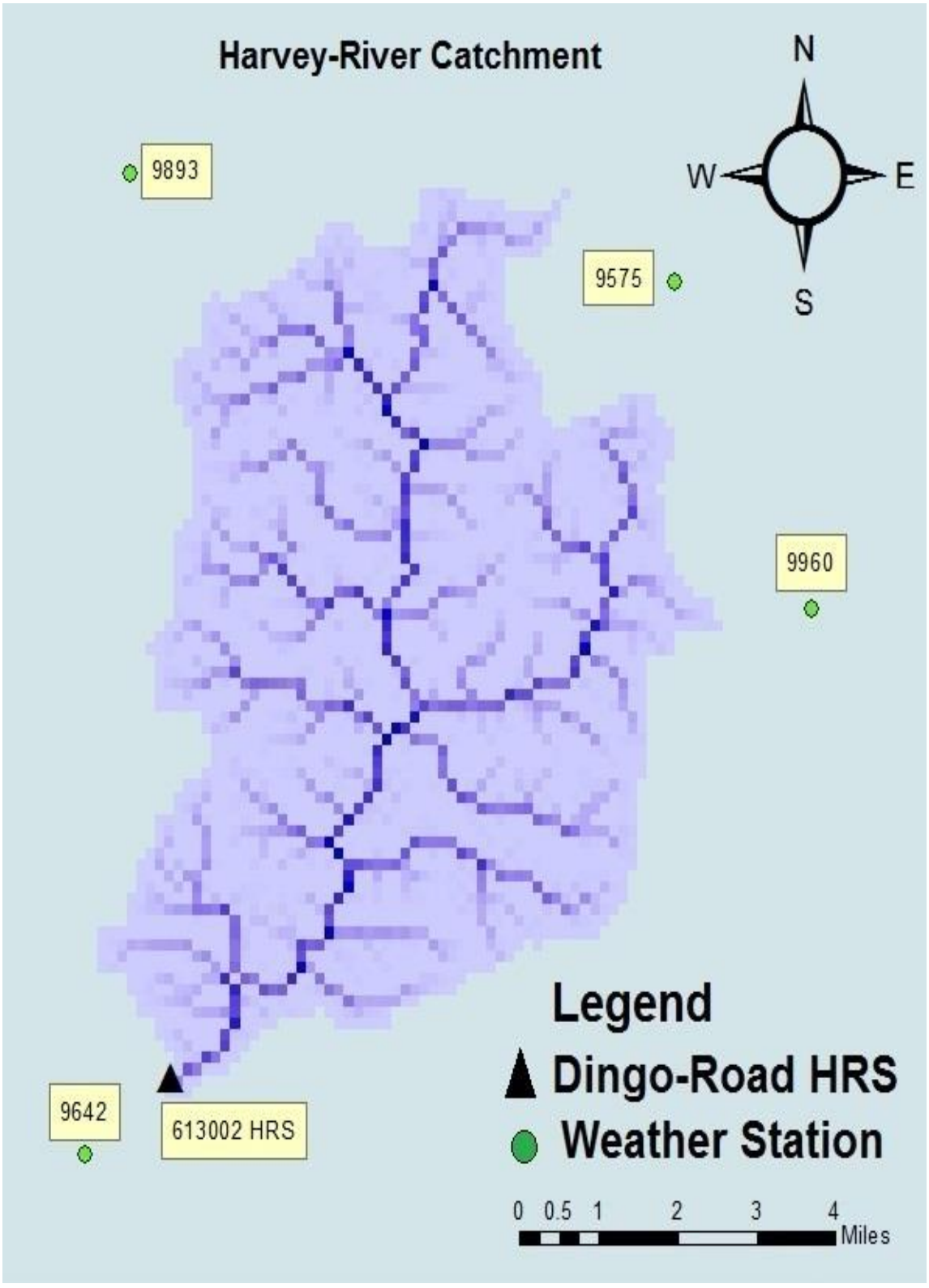

(a) Harvey River catchment

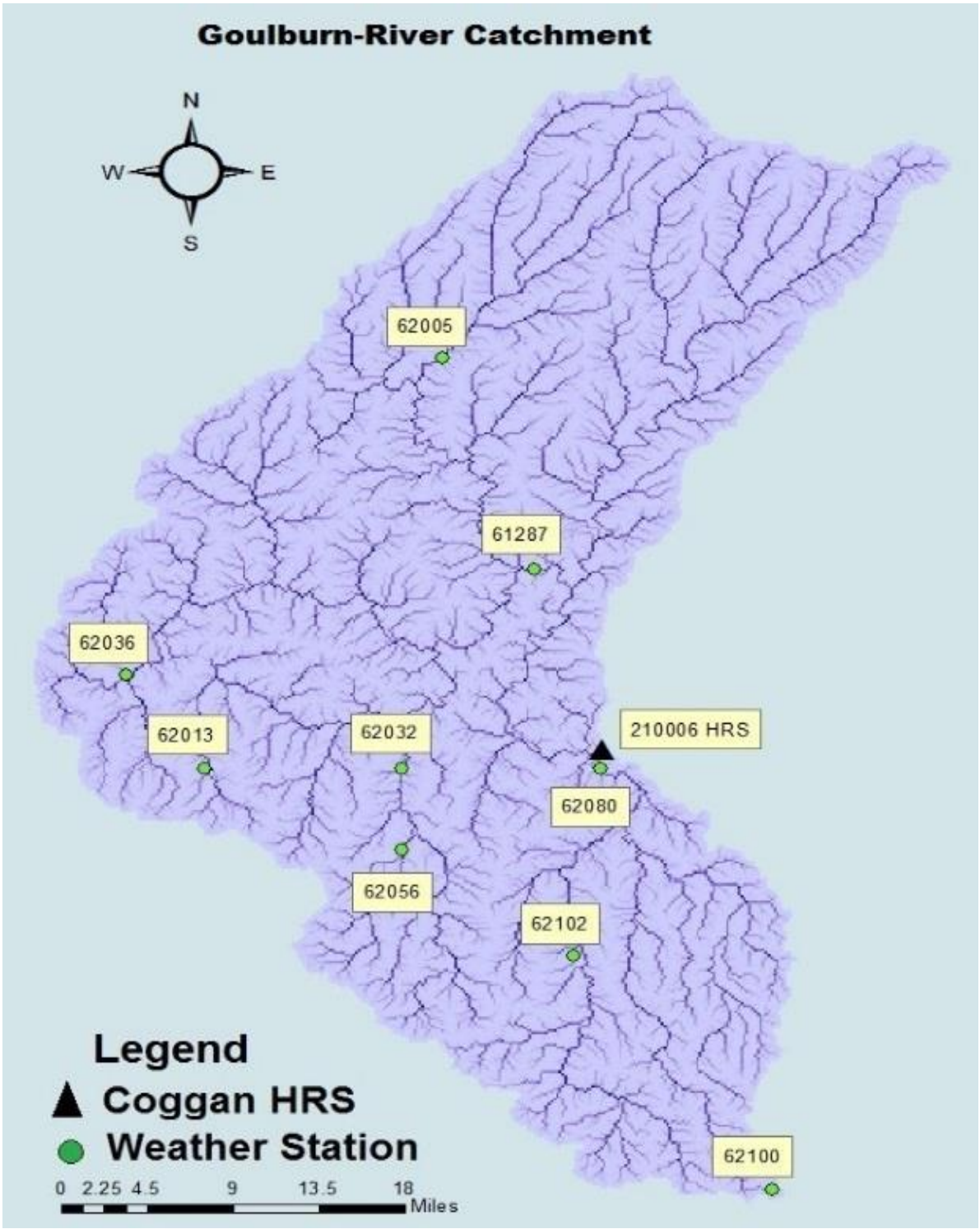

(b) Goulburn River catchment

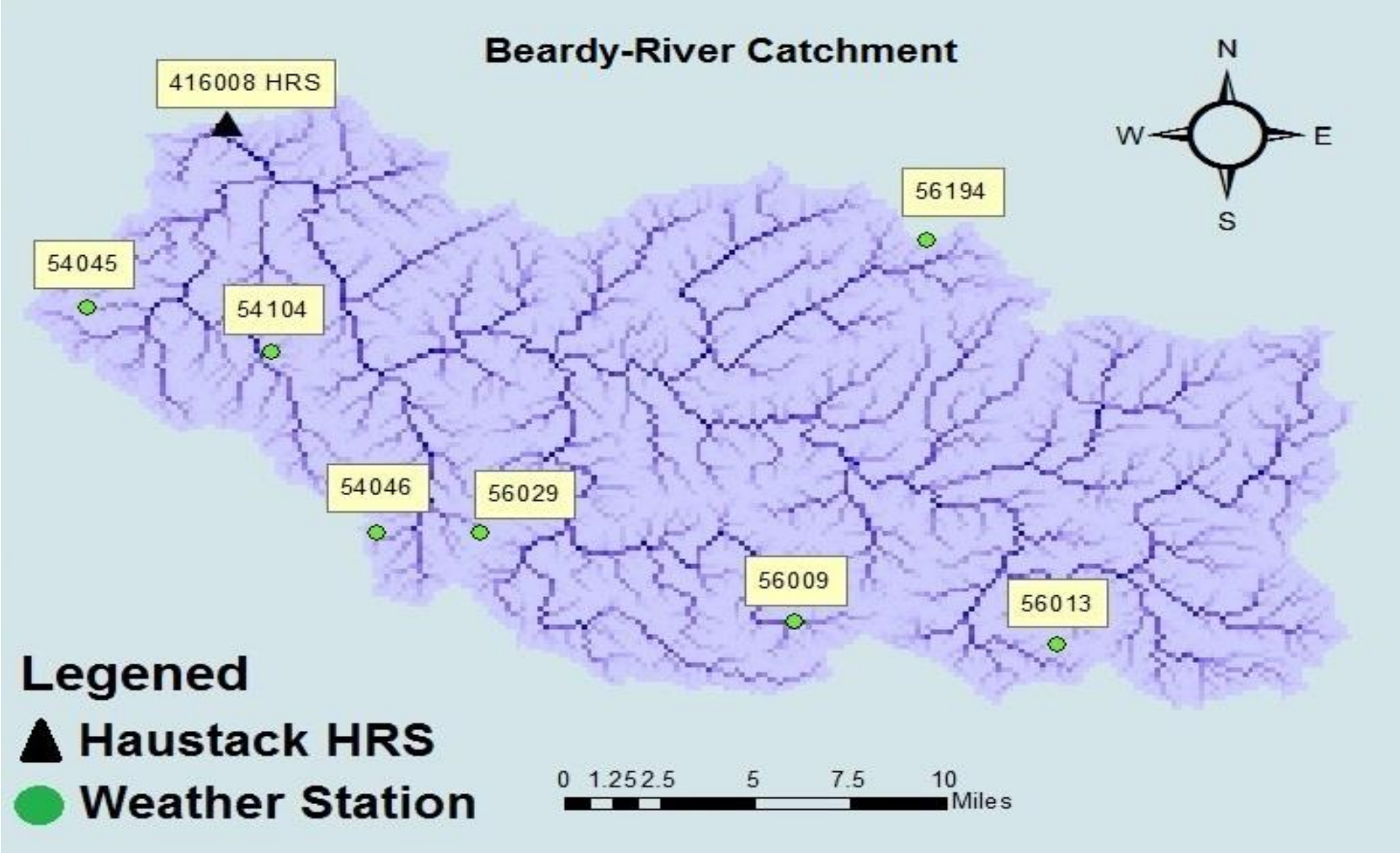

(c) Beardy River catchment

Figure 6.2 Streamflow network (with the hydro-meteorological stations) of the three contributing catchments

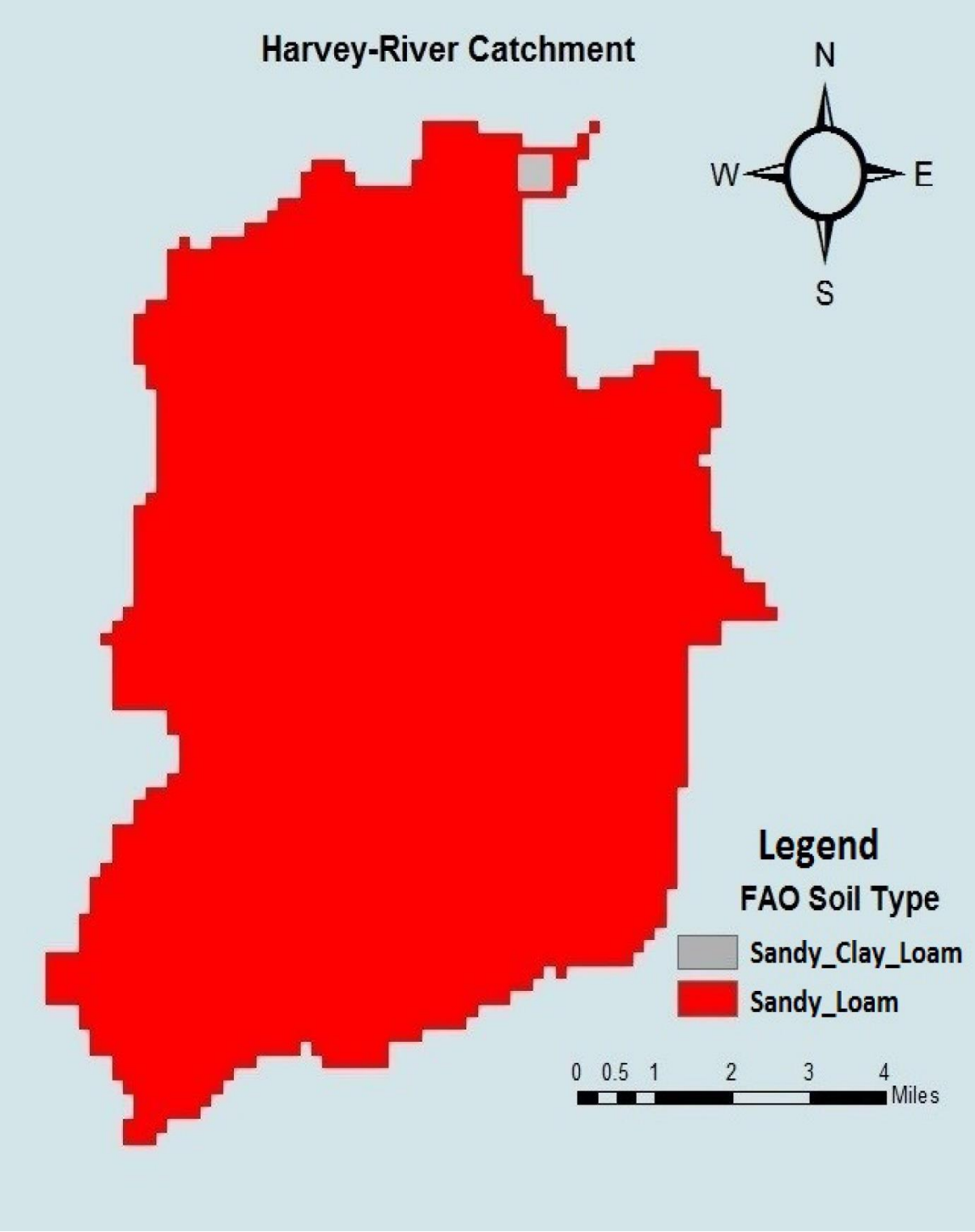

(a) Harvey River catchment

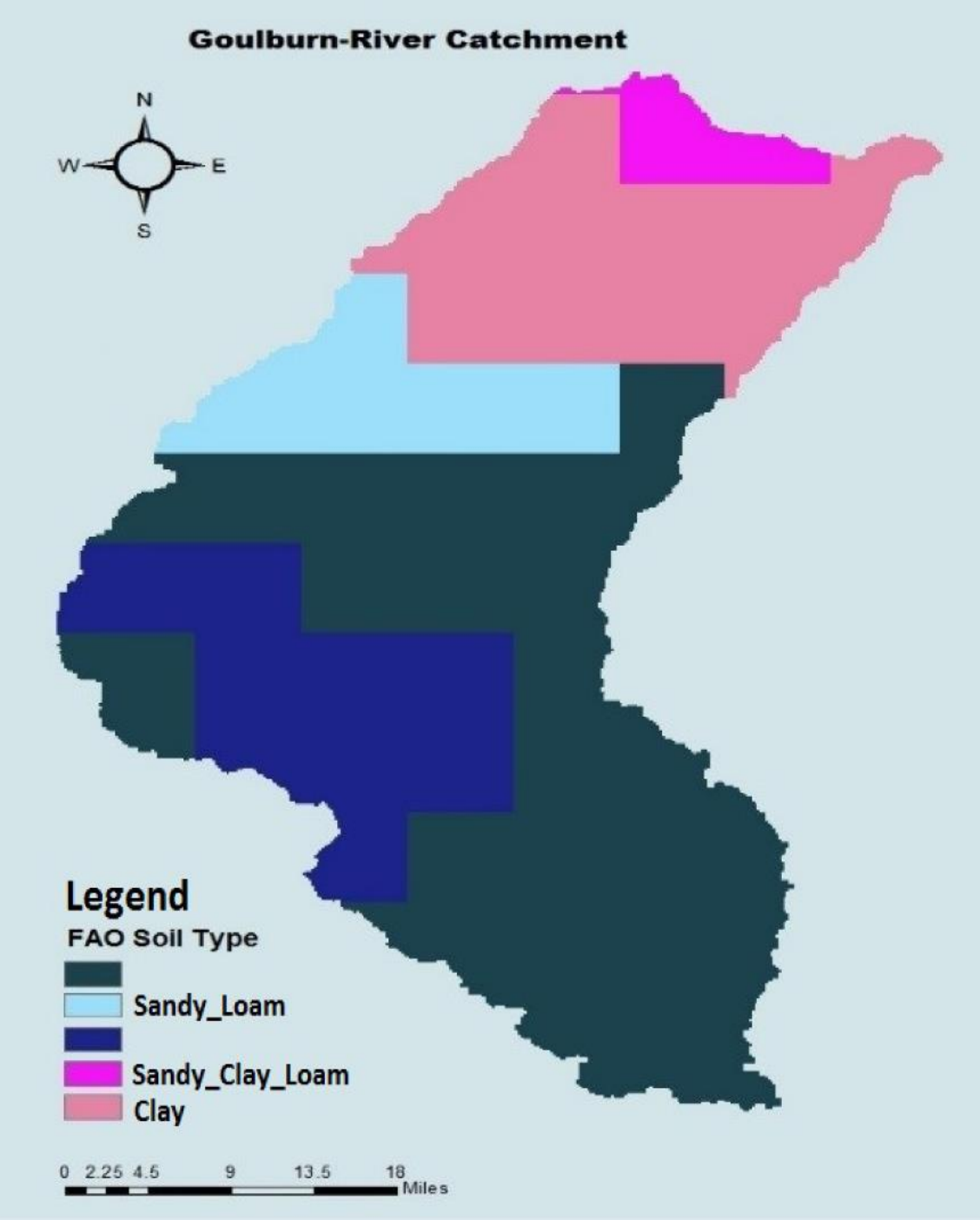

(b) Goulburn River catchment

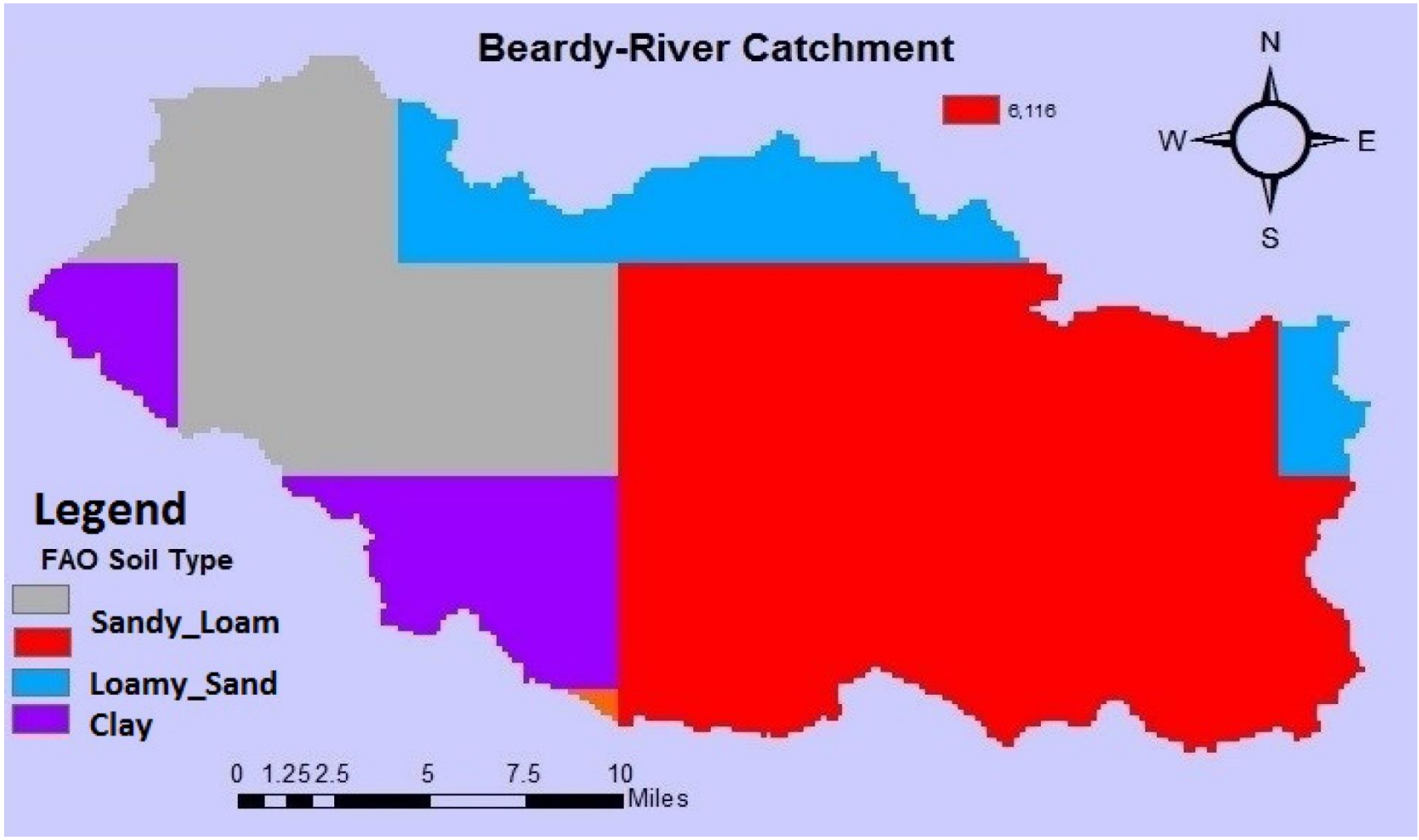

(c) Beardy River catchment

Figure 6.3 Soil types of the three contributing catchments

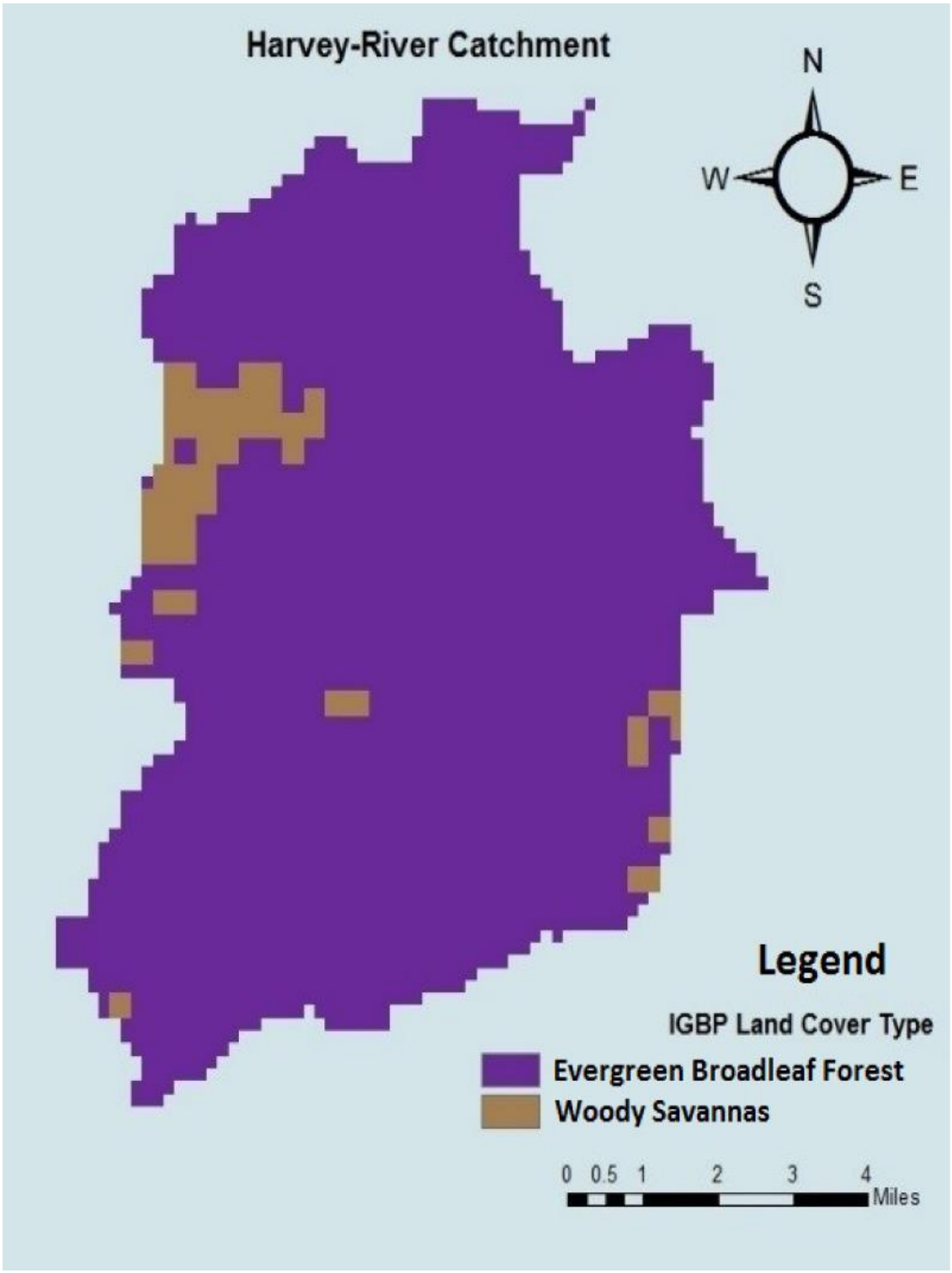

(a) Harvey River catchment

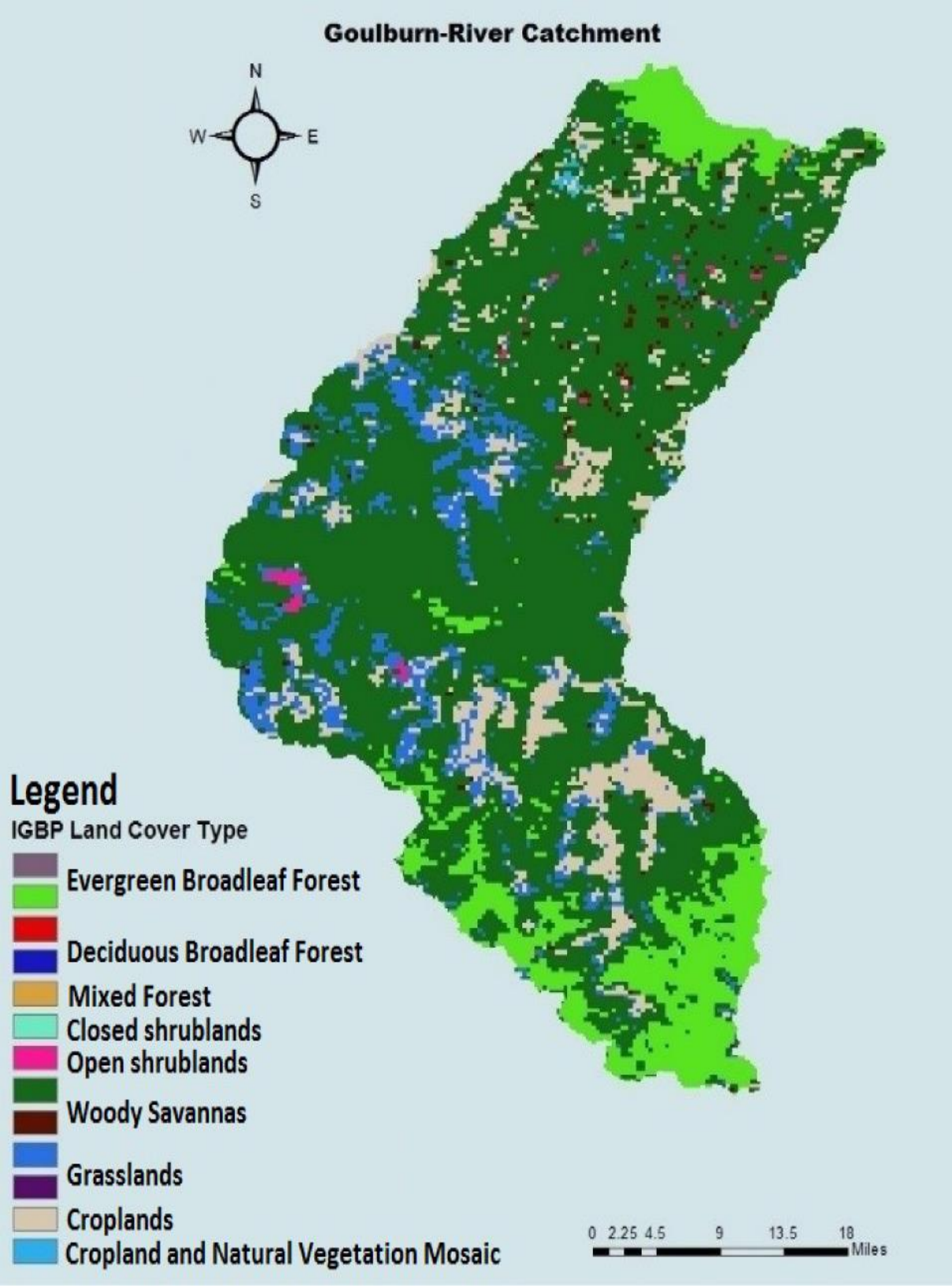

(b) Goulburn River catchment

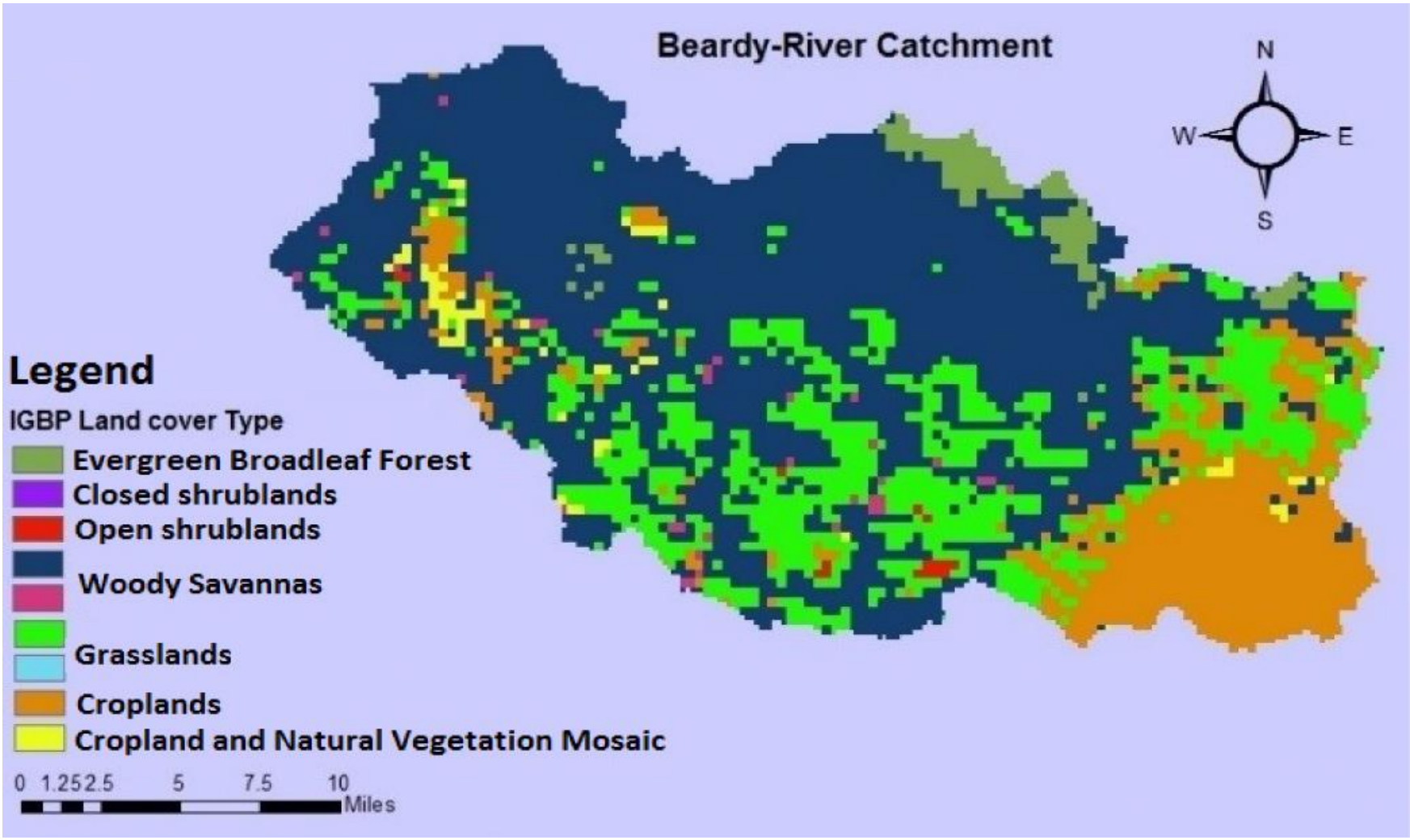

(c) Beardy River catchment

Figure 6.4 Land cover maps of the three contributing catchments

6.3.2 The Future Scenarios of Climate Change

The global-scale monthly future climate signals of rainfall and temperature were extracted from a multi-model ensemble of eight-GCMs of the CMIP5 (Table 3.2) under two RCPs (RCP4.5 and RCP8.5) to cover the mid (2046-2065) and late (2080-2099) of the current century. The data were then downscaled by using a Statistical Downscaling Model developed by the Australian Bureau of Meteorology (BoM-SDM) using an analogue approach (Timbal et al., 2008) and the quality of data has been checked with higher priority (a detailed description of the downscaling procedure is provided in paragraph 3.3.2). The final spatial and temporal resolutions of the downscaled data are 5x5 km (approximately 0.05^{o}x0.05^{o}) and 24 hours respectively which are suitable for the local-scale impact assessment studies. To reduce the uncertainties in the GCMs projections, the ensemble mean of the downscaled climate data was derived and used as input into the BTOPMC model to simulate the future daily streamflow at the three HRS. A baseline climatic periods of 33-years (1982-2014) for the Harvey catchment and 40-years (1975-2014) for the Beardy and Goulburn catchments were also extracted from the multi-model ensemble. The baseline periods were selected depending on the available streamflow records at the three HRSs to enable a fair comparison between the observed and historical discharges.

6.3.3 Hydrological simulation

In this chapter, the physically based distributed hydrological model (BTOPMC) is utilized to perform the hydrological modelling to simulate the future daily streamflow at the three HRSs. A detailed description of the BTOPMC model is provided in chapter three (paragraph 3.1.3).

6.4 Results and Discussion

6.4.1 BTOPMC model calibration and validation

The upstream area of each HRS was used for the BTOPMC model application. The daily observed streamflow, rainfall and temperature measured at the hydro-climatological stations of the three contributing catchments and the spatially distributed monthly average potential evapotranspiration calculated from the Shuttleworth–Wallace method were included in the calibration and validation processes. At Harvey River Catchment, the model was calibrated for the period (1982-2004) and validated for the rest of the recorded period (2005-2014). While at Beardy and Goulburn Rivers Catchments, the model was calibrated for 30-years (1975-2004) and validated for the rest 10-years (2005-2014). Green et al., (2006) pointed out that long

calibration period almost captures a good climate variability which is beneficial to obtain adequate validation results. Vaze et al., (2010) also explained that the recent streamflow records from the south-eastern Australian catchments can be used effectively to calibrate the process-based models to represent the current prolonged drought across the region and to predict the future climate-change impact on the local catchments where the large majority of climate models predict a drier future across the region. Five model parameters were included in the calibrated process (Table 6.5). The values of model parameters were estimated using the manual calibration procedure with a proper understanding of underlying physical processes and expected output. The Nash-Sutcliffe Efficiency (NSE) and Volume Ratio (VR) (Equations 4.1 and 6.1) were used to evaluate the modelling performance. The modelling performance results during the calibration and validation processes are presented in (Table 6.6). The values in Table (6.6) represent the best result chosen after performing several trials, which indicates that the BTOPMC model could be used successfully to simulate the future daily streamflow at the three HRS. Figure (6.5) illustrates a comparison between the daily observed and simulated hydrographs at the three HRS. It clearly shows that the simulated discharge can fairly reproduce the timing and degree of the observed discharge at each station. The high performance of the calibrated model at daily scale justifies its applicability to assess the impacts of future climate changes on the hydrological behaviour of the corresponding catchments of the three HRSs.

$$VR = \frac{\sum Qc}{\sum QR} \times 100 \qquad 6.1$$

Where QC and QR are the simulated and observed discharges.

Table 6.5 Model parameters and their optimal values for the calibration period at the three contributing catchments

Parameter	Unit	Description	Range	Optimal Values		
				Harvey Catchment	**Berdy Catchment**	**Goulburn Catchment**
D_o	m/day	Ground Water Dischargeability	0.01–2.0	Sand = 0.1 Silt = 0.05 Clay = 0.05	Sand = 0.12 Silt = 0.06 Clay = 0.07	Sand = 0.14 Silt = 0.05 Clay = 0.06
m	-----	Decay factor of transmissivity	0. 01–0. 1	0.1	0.075	0.073
n_o	-----	Block average Manning's coefficient	0. 01–0. 8	0.01	0.014	0.019
S_{rmax}	m	Maximum root zone storage	0.0001–0.8	0.25	0.3	0.32
α	-----	Drying function parameter	−10–10	5	6	6.5

Table 6.6 Model performance during the calibration and verification periods at the three HRS

Hydrologic Reference Stations	Calibration		Validation	
	NSE	**VR**	**NSE**	**VR**
Dingo-Road	0.76	96.2%	0.74	114.3%
Haystack	0.79	97.6%	0.77	109.3%
Coggan	0.83	102.4%	0.8	107.6%

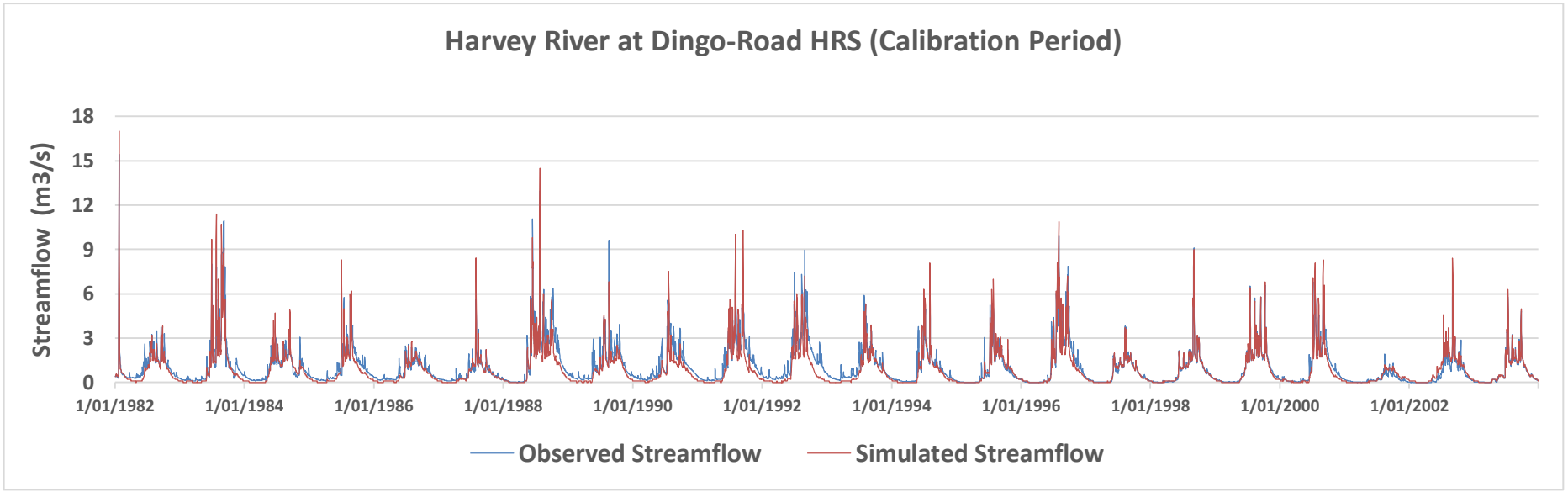
Harvey River at Dingo-Road HRS (Calibration Period)
Streamflow (m3/s)
18
15
12
9
6
3
0
1/01/1982
1/01/1984
1/01/1986
1/01/1988
1/01/1990
1/01/1992
1/01/1994
1/01/1996
1/01/1998
1/01/2000
1/01/2002
Observed Streamflow
Simulated Streamflow

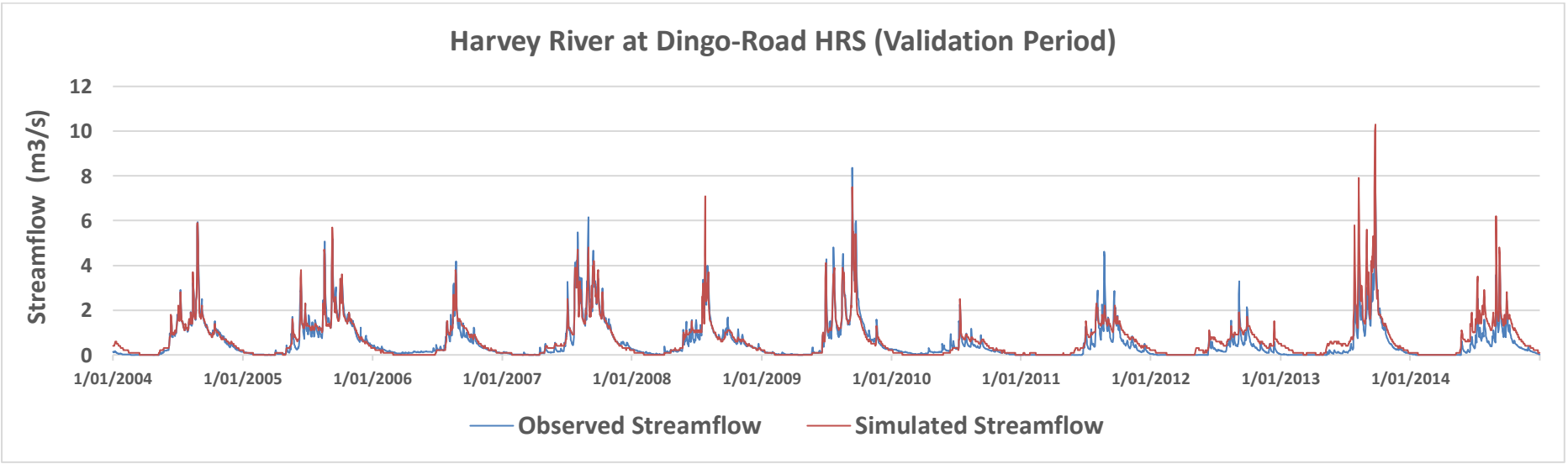
Harvey River at Dingo-Road HRS (Validation Period)
Streamflow (m3/s)
12
10
8
6
4
2
0
1/01/2004
1/01/2005
1/01/2006
1/01/2007
1/01/2008
1/01/2009
1/01/2010
1/01/2011
1/01/2012
1/01/2013
1/01/2014
Observed Streamflow
Simulated Streamflow

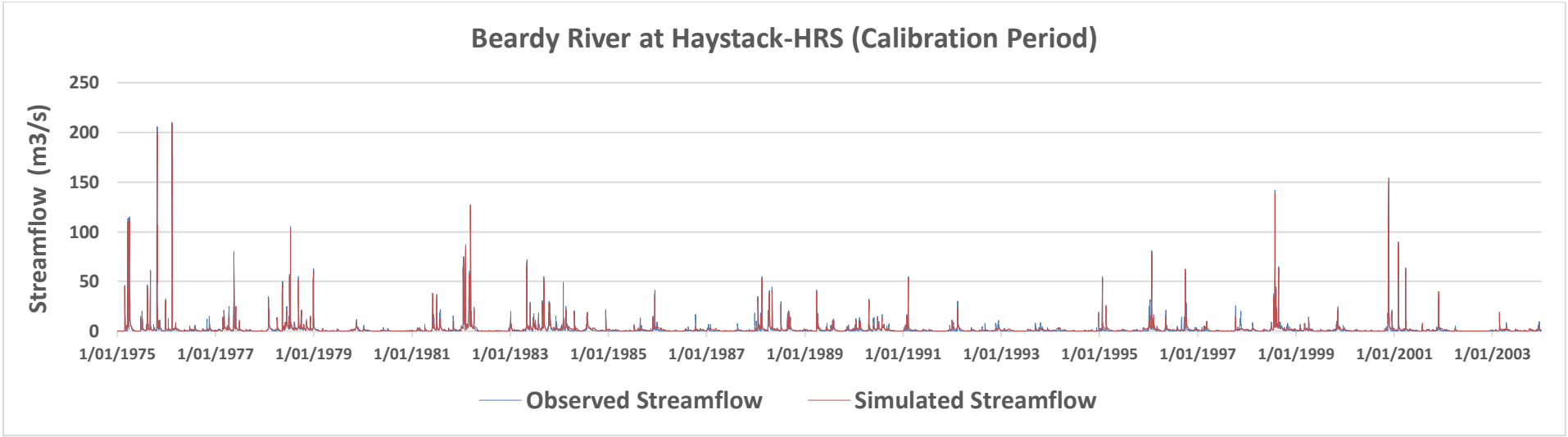
Beardy River at Haystack-HRS (Calibration Period)
Streamflow (m3/s)
250
200
150
100
50
0
1/01/1975
1/01/1977
1/01/1979
1/01/1981
1/01/1983
1/01/1985
1/01/1987
1/01/1989
1/01/1991
1/01/1993
1/01/1995
1/01/1997
1/01/1999
1/01/2001
1/01/2003
Observed Streamflow
Simulated Streamflow

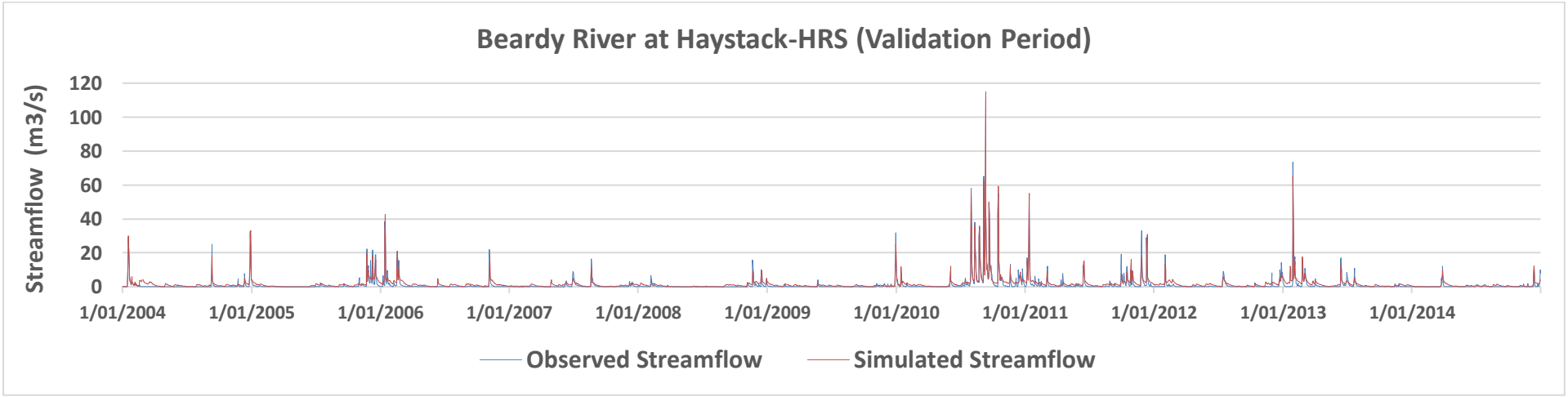
Beardy River at Haystack-HRS (Validation Period)
Streamflow (m3/s)
120
100
80
60
40
20
0
1/01/2004
1/01/2005
1/01/2006
1/01/2007
1/01/2008
1/01/2009
1/01/2010
1/01/2011
1/01/2012
1/01/2013
1/01/2014
Observed Streamflow
Simulated Streamflow

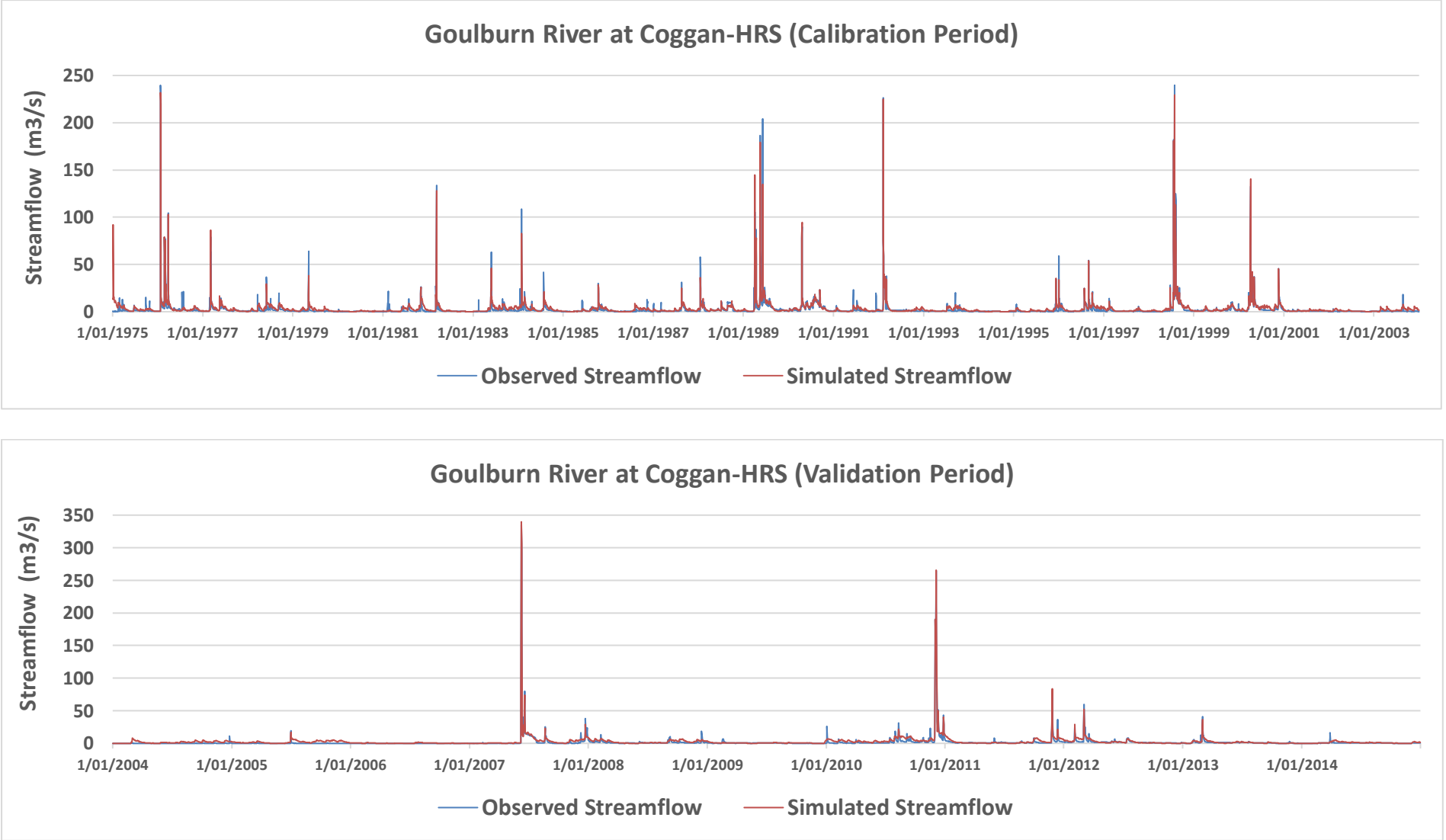

Figure 6.5 Daily observed and simulated streamflow at the three HRSs for the calibration and validation periods

6.4.2 Future climate predictions

To investigate the effect of warmer climate on the magnitude and the seasonal and annual distributions of runoff, two different climate change scenarios of a warmer environment (RCP4.5 and RCP8.5) were taken into consideration. Future climate series of rainfall, temperature and potential evapotranspiration across the three contributing catchments were compared with the baseline climate, and the changes in mean annual values are presented in Table (6.7). The ensemble mean of the 8-GCMs shows a decline in mean annual rainfall and an increase in temperature and potential evapotranspiration values across the three contributing catchments during the mid and late of the 21st century under the two climate scenarios. A graphical comparison of mean annual rainfall between the baseline and the scenarios of the future periods across the three contributing catchments is presented in Figure (6.6). For the Harvey River catchment, the mid-century rainfall is projected to decline by 6.6% and 9.2% under the scenarios RCP4.5 and RCP 8.5 respectively (Figure 6.6). By the late-century, the rainfall decline is projected to reach 7.5% and 11.2% under the same scenarios correspondingly. For the Beardy River catchment, the rainfall reduction during the mid-century is anticipated to be 3.2% and 5.8% for the RCP4.5 and RCP8.5 scenarios respectively (Figures 6.6). Towards the end of the century, there could be a further reduction of 9% and 1.4% in mean annual rainfall under the same scenarios correspondingly. Similarly, the mid-century rainfall across the Goulburn River catchment is projected to decline by 4.4% and 6.9% under the RCP4.5 and RCP8.5 scenarios respectively. While the late-century rainfall decline is projected to reach 5.6% and 7.8% under both scenarios correspondingly.

Table 6.7 Changes in mean annual climate of the future scenarios relative to the baseline period across the three studied catchments. (The values of the RCPs represent the ensemble mean of 8-GCMs)

	Variable	Baseline climate (1982-2014)	Changes in mean annual values compared to the baseline period			
			(2046-2065)		(2080-2099)	
Harvey River catchment			**RCP 4.5**	**RCP 8.5**	**RCP 4.5**	**RCP 8.5**
	P (mm/year)	980	-6.6%	-9.2%	-7.5%	-11.2%
	T (C°)	16.7	+0.5 °C	+0.8 °C	+0.7 °C	+1.2 °C
	PE (mm/year)	1500	+8.6%	+10.7%	+13.3%	+14.3%
	Variable	**Baseline climate (1975-2014)**	**Changes in mean annual values compared to the baseline period (%)**			
			(2046-2065)		**(2080-2099)**	
Beardy River catchment			**RCP 4.5**	**RCP 8.5**	**RCP 4.5**	**RCP 8.5**
	P (mm/year)	765	-3.2%	-5.8%	-9.0%	-1.4%
	T (C°)	16.0	+0.5 °C	+0.9 °C	+0.6 °C	+1.4 °C
	PE (mm/year)	1600	+9.2%	+10%	+12.6%	+14%
Goulburn River catchment	P (mm/year)	640	-4.4%	-6.9%	-5.6%	-7.8%
	T (C°)	16.5	+0.7 °C	+0.8 °C	+0.7 °C	+1.5 °C
	PE (mm/year)	1540	+8.8%	+9.4%	+10.7%	+13.8%

Note: (+) means increase, (-) means decrease

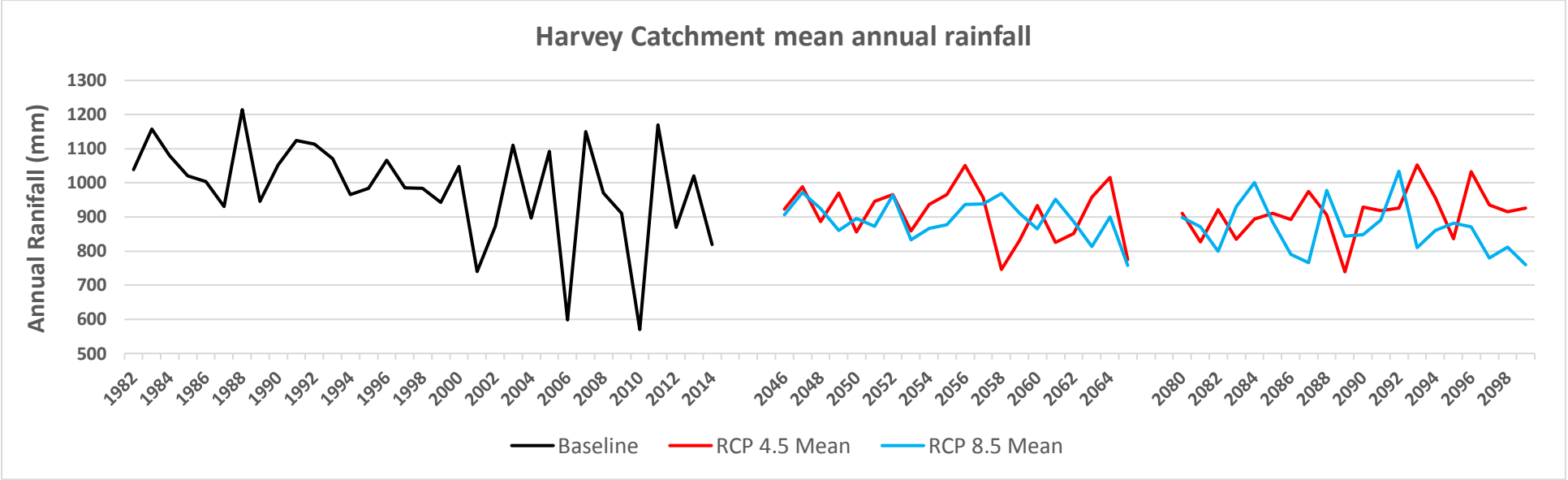
Harvey Catchment mean annual rainfall
Annual Ranifall (mm)
1300
1200
1100
1000
900
800
700
600
500
1982 1984 1986 1988 1990 1992 1994 1996 1998 2000 2002 2004 2006 2008 2010 2012 2014
2046 2048 2050 2052 2054 2056 2058 2060 2062 2064
2080 2082 2084 2086 2088 2090 2092 2094 2096 2098
Baseline
RCP 4.5 Mean
RCP 8.5 Mean

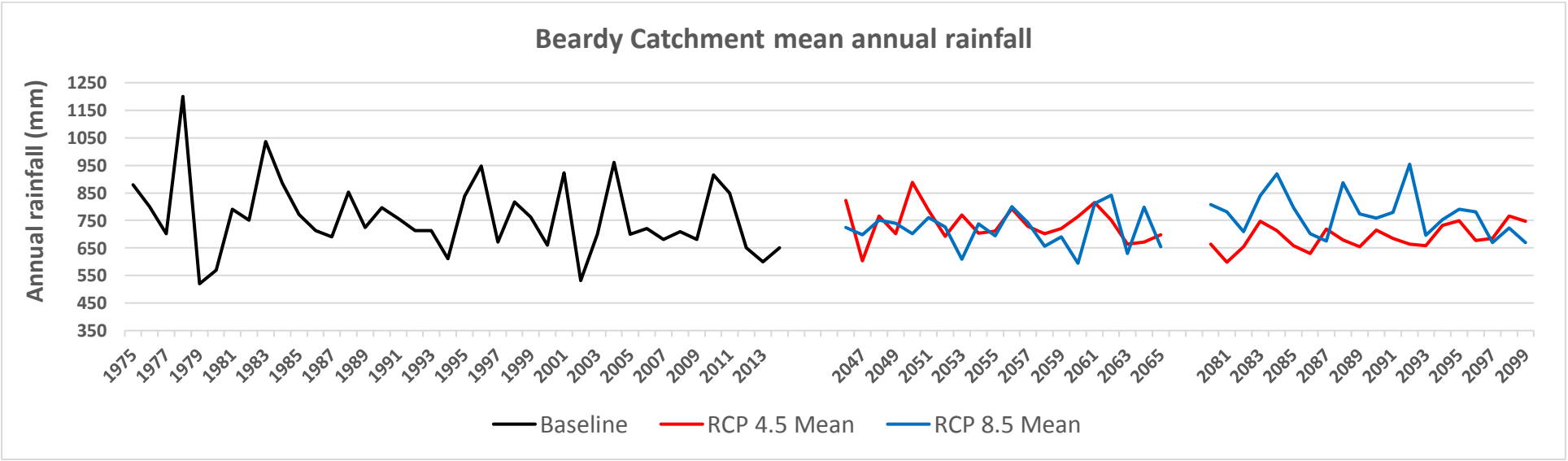
Beardy Catchment mean annual rainfall
Annual rainfall (mm)
1250
1150
1050
950
850
750
650
550
450
350
1975 1977 1979 1981 1983 1985 1987 1989 1991 1993 1995 1997 1999 2001 2003 2005 2007 2009 2011 2013
2047 2049 2051 2053 2055 2057 2059 2061 2063 2065
2081 2083 2085 2087 2089 2091 2093 2095 2097 2099
Baseline
RCP 4.5 Mean
RCP 8.5 Mean

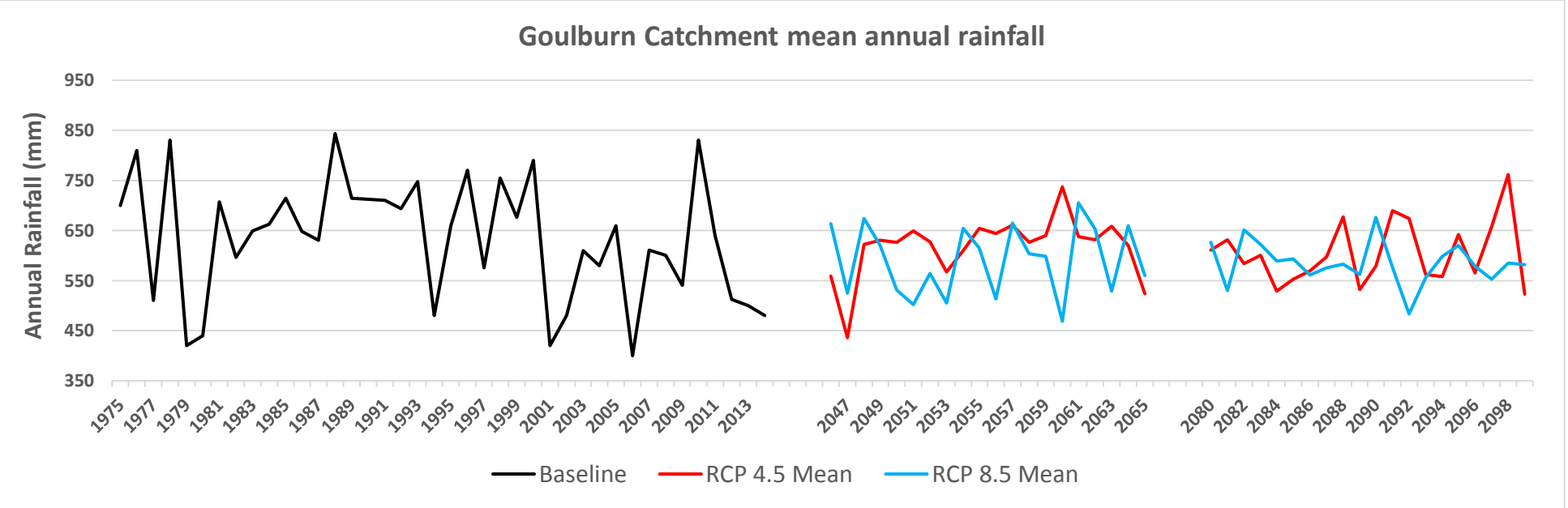

Figure (6.6) A comparison between the annual mean rainfall during the baseline and the scenarios of the future periods across the three contributing catchments. (The simulated rainfall is the ensemble mean of 8-GCMs).

For the three contributing catchments, the reduction in mean annual rainfall could be attributed to the fact that the whole distribution is shifted to lower values by the mid and late of the current century. Another possible explanation for the decline in rainfall amount is the lack of high-intensity rainfall events during the future periods. On the other hand, potential evapotranspiration across the three contributing catchments is anticipated to increase under all scenarios during the future periods relative to the baseline period (Table 6.7). This could be a consequence of the expected rise in mean annual temperature in the future. As the temperature is projected to rise, additional energy is available for driving soil water and intercepted water for evaporation or transpiration. For the Harvey River catchment, the increase in potential evapotranspiration during the future periods ranged between 8.6% and 14.3% under the two climate scenario. While for the Beardy-River catchment, the increase in potential evapotranspiration ranged between 9.2% and 14.0% under the same scenarios of the two future periods. Similarly, there could be an increment of 8.8-13.8% in potential evapotranspiration across the Goulburn River catchment during the future periods under the two studied scenarios. Therefore, the combined impact of rainfall reduction and potential evapotranspiration increase in the mid and late-century could adversely affect the future streamflow across the contributing catchments of the three HRSs.

6.4.3 Future runoff projections

After the successful calibration and validation processes, the BTOPMC-model forced with the ensemble mean of the downscaled future climate series to simulate the future daily streamflow at the three HRSs for the mid and late of the century. The model also forced with the downscaled climate data from the baseline periods to simulate the daily streamflow at the three HRSs for a control run to be compared with the future streamflow. The differences between the two simulations represent the projected impact of climate change on the hydrological system of the contributing catchments. A recent study by Vaze et al., (2010) explained that the process-based simulation models calibrated over a period of more than 20 years can be used effectively in impact assessment studies, conditioned that the mean annual rainfall in the simulated period should not be more than 15% drier or 20% wetter than the calibration period. As the future projected mean annual rainfall across the three contributing catchments is within the above limits relative to the observed mean annual rainfall over the calibration periods (Table 6.7), then the calibrated BTOPMC-model can be used confidently to project streamflow responses of the three catchments to changes in the future climate inputs. The variations of

annual mean streamflow statistics of the future climate scenarios relative to the control run at the three HRSs are presented in Table (6.8). Figure (6.7) illustrates a graphical comparison between the control run and the simulated mean annual streamflow of the future scenarios at the three HRSs. While Figure (6.8) shows the 25th and 75th streamflow percentile statistics at the three HRSs for the mid and late century under the RCP4.5 and RCP8.5.

Table (6.8) Changes in annual mean streamflow statistics (m^3/s) of the future climate scenarios relative to the control run at the three HRSs. The values of all RCPs represent the ensemble mean of 8-GCMs

HRSs	Variable	Control run (1982-2014)	Changes in mean annual runoff compared to the control run (%)			
			(2046-2065)		(2080-2099)	
			RCP 4.5	RCP 8.5	RCP 4.5	RCP 8.5
Harvey River at Dingo Road	Q Min.	0.20	-10	-10	-5	-10
	Q25	0.5	-17	-30	-50	-50
	Q50	0.9	-33	-39	-44	-61
	Q75	1.2	-38	-44	-54	-62
	Q Max.	1.9	-20	-18	-26	-34
	Q Mean	0.95	-26	-32	-42	-53
Beardy River at Haystack	Q Min.	0.5	-4	-4	-6	-6
	Q25	0.85	-6	-11	-9	-10
	Q50	1.4	-4	-14	--21	-8
	Q75	2.2	-4	-13	-32	-21
	Q Max.	6.6	-23	-39	-21	-27
	Q Mean	1.7	-10	-19	-25	-15
Goulburn River at Coggan	Q Min.	0.8	-6	-33	-22	-28
	Q25	2.0	-28	-47	-40	-51
	Q50	2.9	-17	-41	-41	-48
	Q75	5.5	-49	-43	-49	-52
	Q Max.	7.5	-19	-42	-35	-45
	Q Mean	3.1	-6	-33	-22	-28

Note: (-) means decrease.

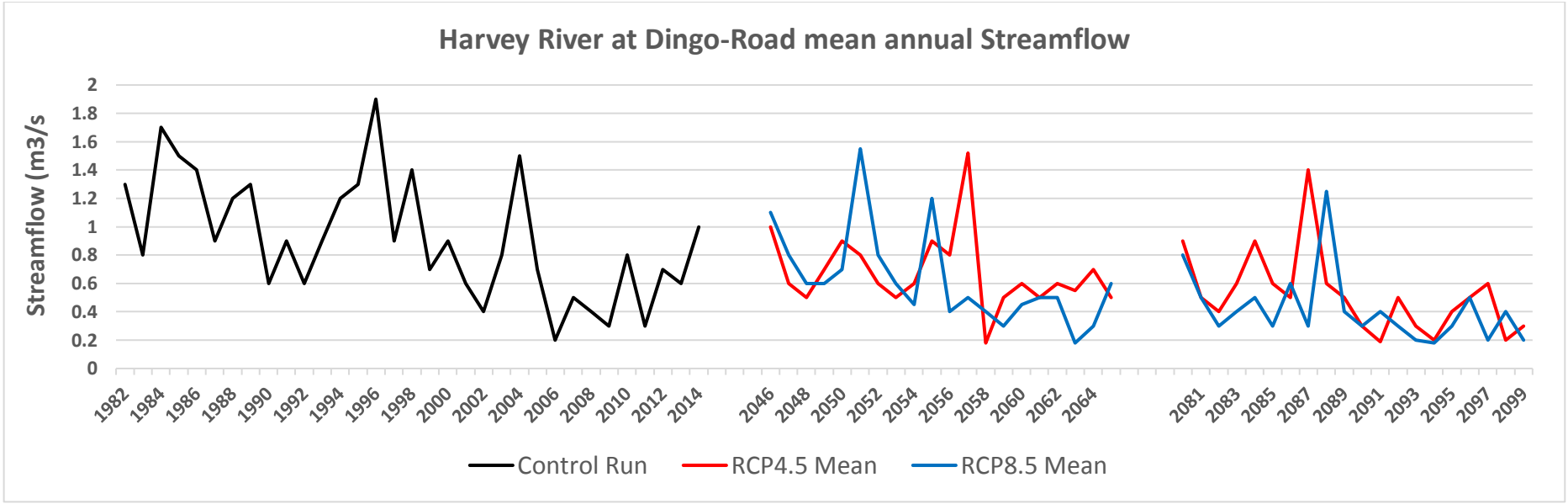
Harvey River at Dingo-Road mean annual Streamflow
Streamflow (m3/s
2
1.8
1.6
1.4
1.2
1
0.8
0.6
0.4
0.2
0
1982 1984 1986 1988 1990 1992 1994 1996 1998 2000 2002 2004 2006 2008 2010 2012 2014
2046 2048 2050 2052 2054 2056 2058 2060 2062 2064
2081 2083 2085 2087 2089 2091 2093 2095 2097 2099
Control Run
RCP4.5 Mean
RCP8.5 Mean

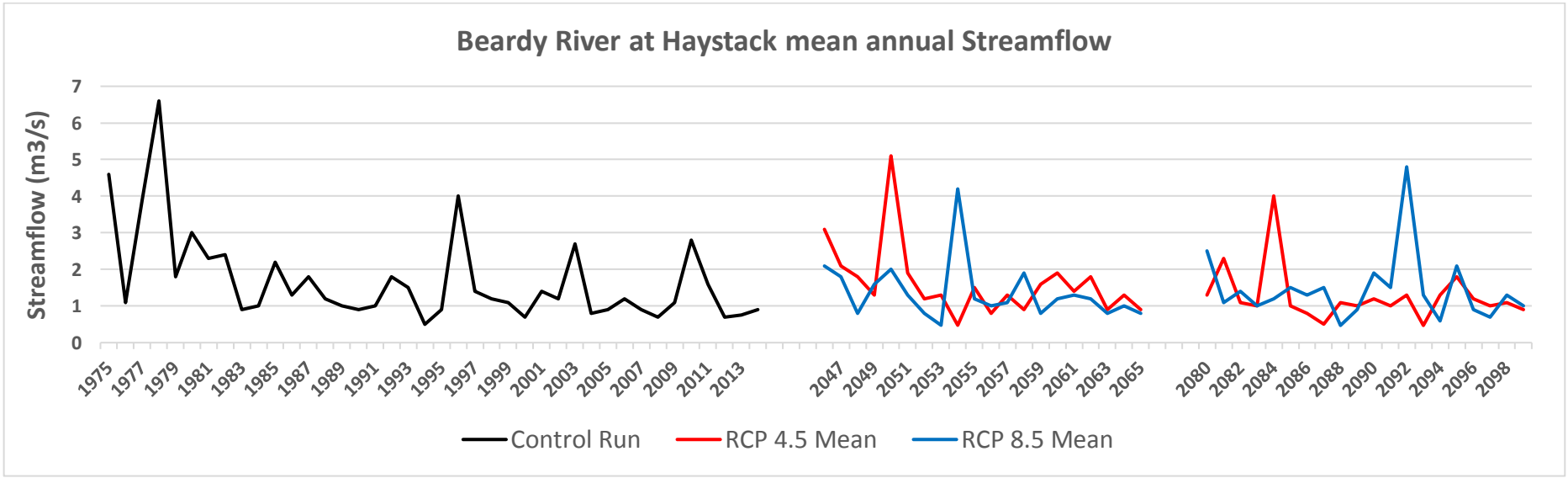
Beardy River at Haystack mean annual Streamflow
Streamflow (m3/s)
7
6
5
4
3
2
1
0
1975 1977 1979 1981 1983 1985 1987 1989 1991 1993 1995 1997 1999 2001 2003 2005 2007 2009 2011 2013
2047 2049 2051 2053 2055 2057 2059 2061 2063 2065
2080 2082 2084 2086 2088 2090 2092 2094 2096 2098
Control Run
RCP 4.5 Mean
RCP 8.5 Mean

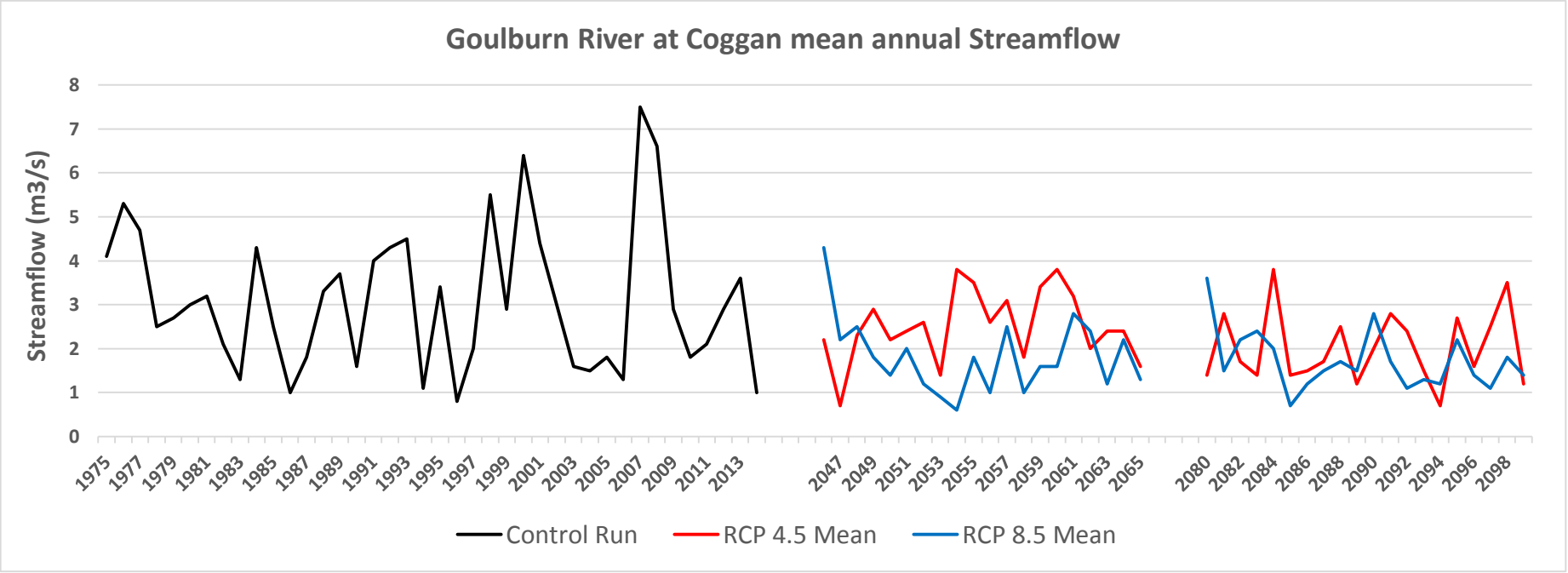

Figure (6.7) Annual mean streamflow variations of the future climate scenarios relative to the control run. The average simulated discharge is the ensemble mean of 8-GCMs.

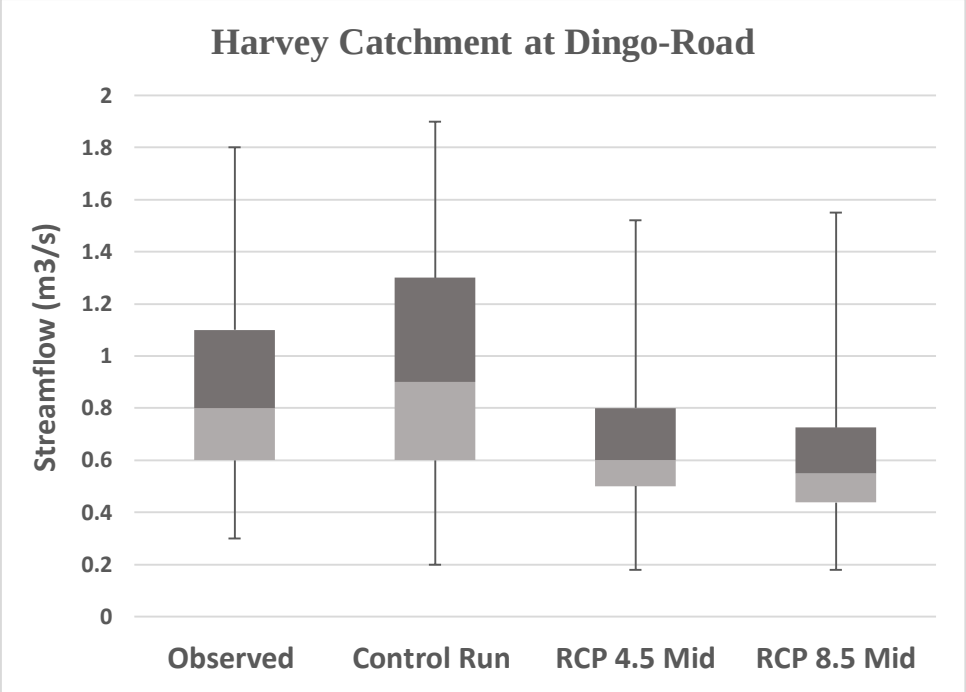
Harvey Catchment at Dingo-Road
Streamflow (m3/s)
2
1.8
1.6
1.4
1.2
1
0.8
0.6
0.4
0.2
0
Observed
Control Run
RCP 4.5 Mid
RCP 8.5 Mid

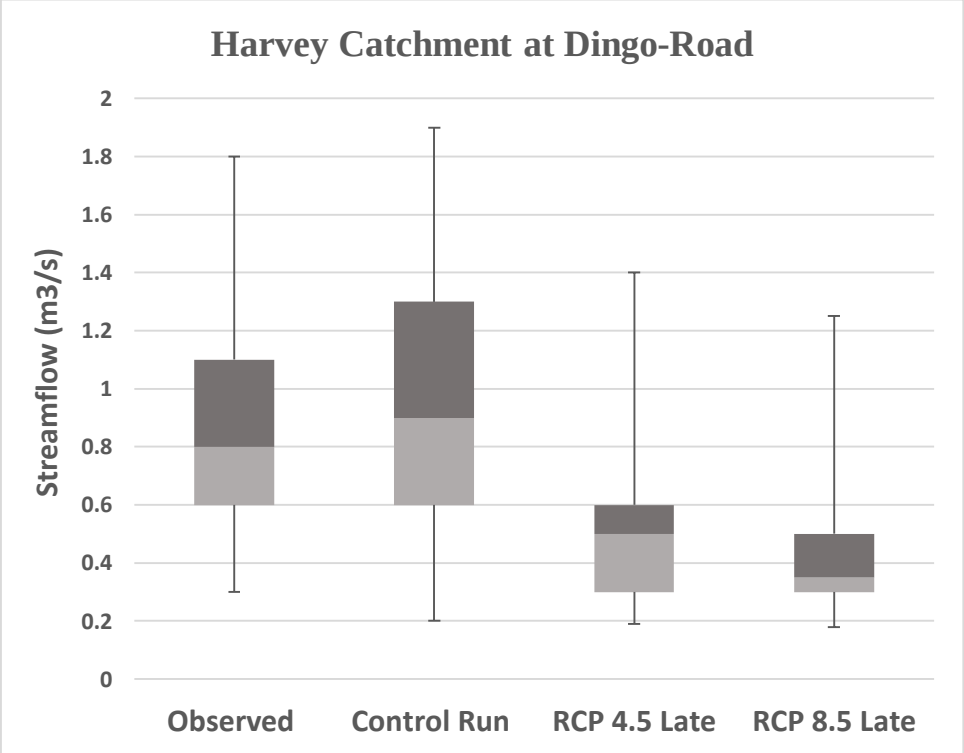
Harvey Catchment at Dingo-Road
Streamflow (m3/s)
2
1.8
1.6
1.4
1.2
1
0.8
0.6
0.4
0.2
0
Observed
Control Run
RCP 4.5 Late
RCP 8.5 Late

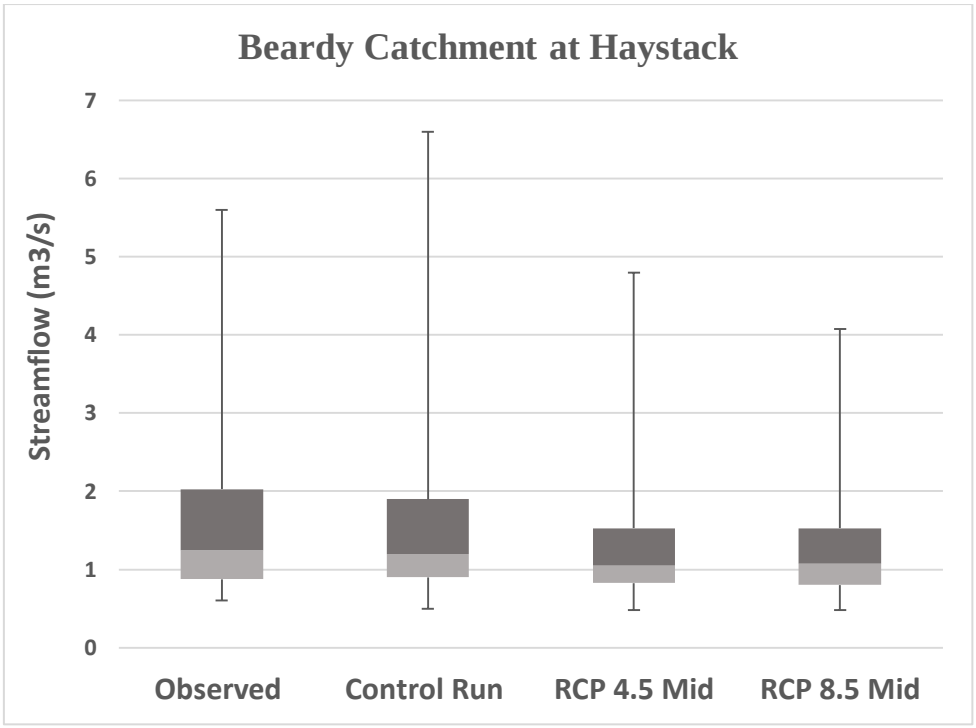
Beardy Catchment at Haystack
Streamflow (m3/s)
7
6
5
4
3
2
1
0
Observed
Control Run
RCP 4.5 Mid
RCP 8.5 Mid

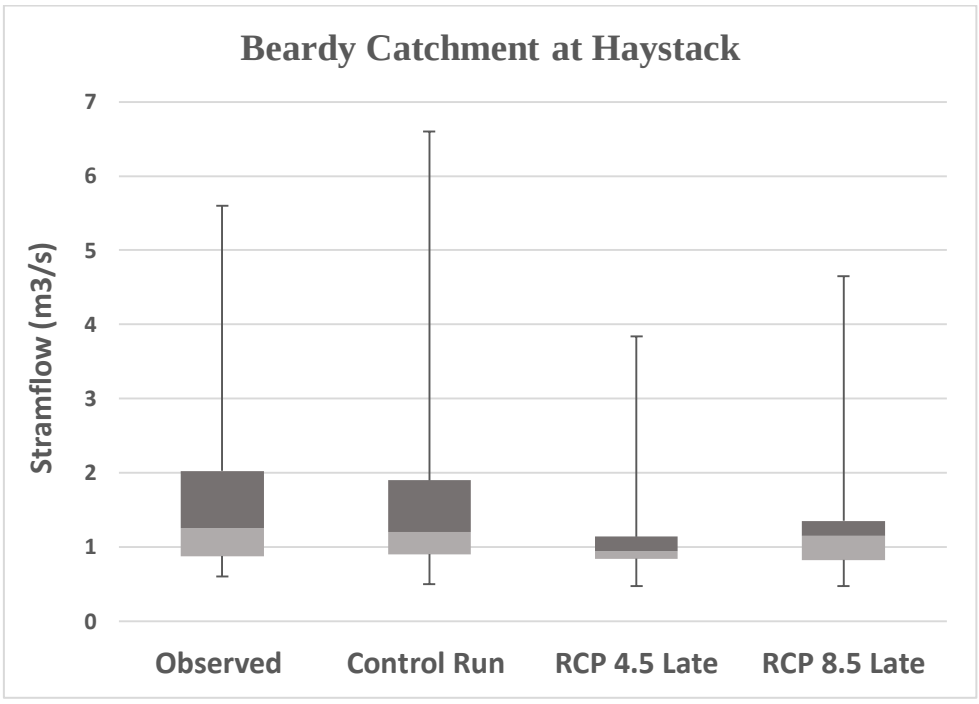
Beardy Catchment at Haystack
Stramflow (m3/s)
7
6
5
4
3
2
1
0
Observed
Control Run
RCP 4.5 Late
RCP 8.5 Late

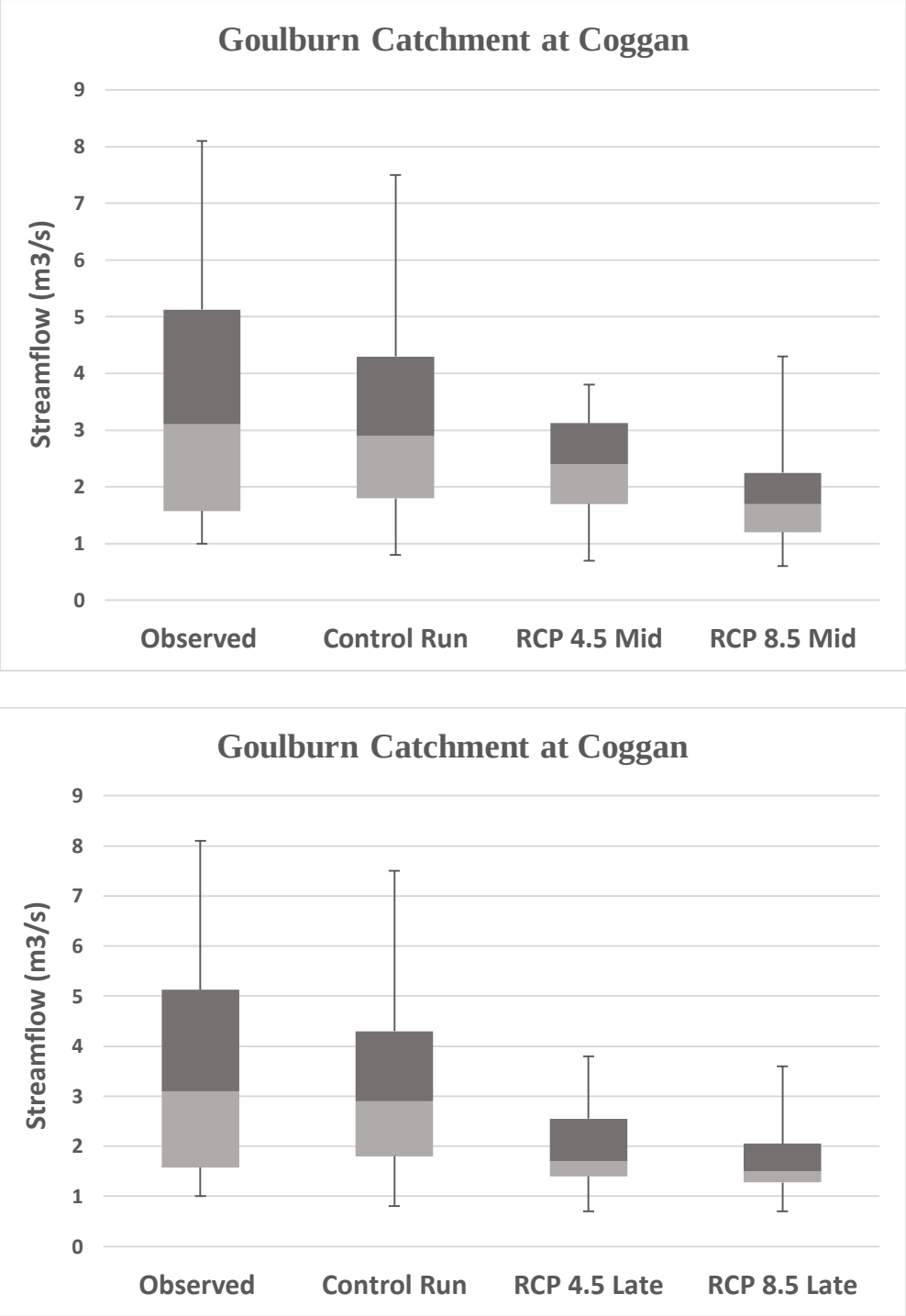

Figure (6.8) the 25th and 75th percentiles of annual mean streamflow at the three HRSs for the observed, baseline and future periods. The bars represent the errors in the minimum and maximum annual streamflow percentiles. The simulated streamflow of the control run and the future periods is the ensemble mean of 8-GCMs.

Table (6.8) and Figures (6.7) clearly show the response of the contributing catchments to the predicted impact of climate change through the decline in all future streamflow statistics measured at the three HRSs. The decline in streamflow trends could be attributed to the rainfall reduction during the mid and late of the century, as well as the increase in potential evapotranspiration across the three catchments.

At Dingo-Road HRS, a considerable streamflow reduction (especially during the late-century) is projected in the contributing catchment under the RCP4.5 and RCP8.5 climate scenarios compared to the control run. During the mid-century, the mean annual streamflow is projected to decrease by 26% and 32% under the RCP4.5 and RCP8.5 respectively. By the end of the century, the mean annual streamflow reduction is anticipated to reach 42% and 53% for the same scenarios correspondingly. The minimum streamflow statistics (expressed as Q_{min} and Q_{25}) also show decreasing tendencies during the future period ranged between 5% and 50% under the two scenarios (Figure 6.8). Similarly, the maximum streamflow statistics (expressed as Q_{75} and Q_{max}) are also anticipated to decline with a range of 20% and 62% under both scenarios during the mid and late-century (Figure 6.8). The step-change analysis of the observed mean annual streamflow at Dingo Road HRS showed a declining trend over the time. The long-term annual streamflow trend has noticeably declined since the early 1970s until 1993 (the step-change year) after which the median annual streamflow has reduced from around 36 GL per water year to 23 GL per water year (Figure 5.9).

At Haystack HRS, the future streamflow in the contributing catchment is also projected to decrease under the two studied scenarios relative to the control run (Table 6.8). The mid-century mean annual streamflow is projected to decrease by 10% and 19% under the RCP4.5 and RCP8.5 respectively. By the end of the century, there could be a further reduction in mean annual streamflow of 25% and 15% under the same scenarios correspondingly. The minimum flows (Q_{min} and Q_{25}) are also projected to decline with a range of (4-11%) during the mid and late of the current century under both scenarios. Similarly, the maximum flows (Q_{max} and Q_{75}) are also expected to decrease with a range of (2.2%-39%) under both scenarios during the future periods (Table 6.8). The step-change analysis of the long-term mean annual streamflow at Haystack HRS has also shown a reduction trend over the time (Figure 6.9). Since the early 1970s, the median annual streamflow has declined from 50 GL per water year to around 35 GL per water year after year of step-change (2000).

At Coggan HRS, the future streamflow is also anticipated to decrease in the contributing catchment relative to the control run (Table 6.8). For the mid-century, the mean annual streamflow is projected to decline by 6% and 33% under the scenarios RCP4.5 and RCP8.5 respectively. By the end-century, the anticipated decline in mean annual streamflow is projected to reach 22% and 28% under the same scenarios correspondingly. The minimum flows (Q_{min} and Q_{25}) also show high reduction tendencies under both scenarios ranged between 6% and 51% during the future periods relative to the control run (Table 6.8). Alike, the maximum flows (Q_{max}. and Q_{75}) also reviled substantial negative trends under the two scenarios ranged between 19% and 52% during the mid and late-century compared to the control run (Table 6.8). The step-change analysis of the observed mean annual streamflow at Coggan HRS revealed a decreasing trend over the time. The long-term annual streamflow trend has declined since the early 1950s until the year of step change (1978) after which the median annual streamflow has reduced to the half (from around 80 GL per water year to 40 GL per water year) (Figure 6.9).

Finally, as the future runoff in the contributing catchments is anticipated to be less than the historical runoff, as in the case of chapter five, so please refer to section (5.4.3) for further discussion about the possible consequences of this reduction in the future runoff on the flow regime of the three catchments.

6.5 Summary and Conclusion

This study presents an assessment of the impacts of climate change on future streamflow of three contributing catchments of the Australian Hydrologic Reference Stations; including Harvey River catchment in Western Australia, Beardy and Goulburn catchments in New South Wales. The Australian HRSs network represents an important source of high-quality continuous streamflow data across the continent that enables better analysis of the long-term streamflow trends. A physically-based distributed hydrological model (BTOPMC) is applied to perform the hydrological modelling in the study area. The model was properly calibrated and validated prior to the streamflow projection based on the daily observed hydro-meteorological data from the contributing catchments and the spatially distributed monthly average potential evapotranspiration calculated from the Shuttleworth–Wallace method. The high performance of the calibrated model at daily scale justifies its applicability to assess the impacts of climate variability on the hydrology of the corresponding catchments. Two periods were selected to represent the future climate status including the mid (2046-2065) and late

(2080-2099) of the 21st century. Future climatic series at monthly scale were extracted from a multi-model ensemble of eight GCMs of the CMIP5 under two Representative Concentration Pathways (RCP4.5 and RCP8.5) which belongs to the IPCC (AR5). The global-scale monthly outputs were then downscaled by using a Statistical Downscaling Model developed by the Australian Bureau of Meteorology (BoM-SDM). The quality of future climate data has been checked with higher priority by the Australian-BOM before inputting them into the BTOPMC model for a local-scale impact assessment. Almost all GCMs predict decline tendencies in mean annual rainfall and an increase in temperature and potential evapotranspiration across the studied catchments in the future. The calibrated BTOPMC model was then forced with the ensemble mean of the downscaled daily rainfall and temperature from the baseline (control run) and the future periods to simulate the daily streamflow at the three HRSs. The results of hydrological modelling reveal decline tendencies in the future streamflow measured at the three HRSs under the two studied scenarios relative to the control run.

At Dingo-Road HRS of Harvey River catchment, the mid-century mean annual streamflow is projected to decline by 26% and 32% under the RCP4.5 and RCP8.5 scenarios respectively following a decline of 6.6% and 9.2% in mean annual rainfall. By the late-century, there could be a 42% and 53% decline in mean annual streamflow under the same scenarios correspondingly following a decline of 7.5% and 11.2% in mean annual rainfall. At Haystack HRS of Beardy River catchment, the mid-century mean annual streamflow is also projected to decline by 10% and 19% under the RCP4.5 and RCP8.5 scenarios respectively following a decline of 3.2% and 5.8% in mean annual rainfall. By the late century, there could also be a 25% and 15% decline in mean annual streamflow under the same scenarios correspondingly following a decline of 9% and 1.4% in mean annual rainfall. Similarly, at Coggan HRS of Goulburn River catchment, the mid-century mean annual streamflow is expected to decline by 6% and 33% under the RCP4.5 and RCP8.5 scenarios following a decline of 4.4% and 6.9% in mean annual rainfall. Toward the end of the century, the mean annual rainfall is anticipated to decrease by 5.6% and 7.8% under the scenarios RCP4.5 and RCP8.5 respectively, and the corresponding decline in mean annual streamflow is projected to reach 22% and 28%.

In conclusion, the results of this study specify that the potential changes in streamflow due to climate change could be very significant. The projected streamflow reduction would probably impose additional burdens on the currently available surface water resources and would influence the environmental and ecological communities in the contributing catchments. Thus,

options for additional water supply sources and adaptive responses would be essential in the future to support the economic and population development and to maintain sustainable ecological communities. The current findings could provide a theoretical basis to the communities and decision makers to manage the usage of future water resources in the contributing catchments taking into account the expected streamflow reduction.

Chapter 7

A comparison of conceptual versus distributed hydrological modelling across three catchments of the Australian HRSs network

7.1 Introduction

There is a continuing debate in the hydrological modelling research area on whether or not physically based distributed models better capture recorded streamflow than conceptual lumped models approaches do. In the current research, the ability of two characteristically different hydrological models, a conceptual lumped model and a physically based distributed model (HBV and BTOPMC) was assessed to represent the observed streamflow and to simulate the impact of future climate changes on the hydrological behaviour of three unregulated local catchments of the Australian HRSs. Chapters five and six show the detailed application of these two models as separate case studies. The selected catchments almost represent a range of climatic conditions and biophysical characteristics (e.g., latitude, longitude, elevation, land use type and soil type) across the Australian continent. Therefore, it is highly valuable to assess the applicability of both models to represent the observed discharge and to simulate the future runoff at the HRSs. To fairly compare the behaviour of the two hydrological models, precisely the same forcing data applied to the distributed model was used to force the conceptual model but as lumped input. Linde et al., (2008) explained that the forcing data has a significant effect on model performance, regardless of the kind of model structure. Hence, the quality of the observed data has been checked carefully, and the regression relationships between the neighbouring stations were used to fill the very few missing data.

This chapter mainly compares and evaluates the outcome of the application of two different modelling concepts and interprets the results of these two models in different hydrological environments.

7.2 Results of hydrological daily rainfall-runoff simulation (modelling performance during the calibration and validation periods)

To evaluate the performance of the two hydrological models across the studied catchments, simulation results from both models during the calibration and validation periods were assessed and compared. As mentioned earlier, the same observed hydro-meteorological data from the three contributing catchments were used to calibrate and validate the conceptual and distributed hydrological models. The only difference between the observed forcing data is the values of Potential Evapotranspiration (PE). The long-term observed monthly mean values were used in the conceptual modelling. Whereas the global monthly data (Table 6.1) was adopted to force the Shuttleworth-Wallace model to calculate the PE values in the distributed modelling. The two models were also calibrated and validated over the same time periods, and the manual calibration was used to optimize the parameters of the two hydrological models.

The goodness-of-fit statistics resulting from the comparison of the observed and simulated discharges based on the optimized parameters of the two hydrological models are illustrated in Table (7.1). Nash-Sutcliffe efficiency (NSE), relative volume error (VE) and the coefficient of determination (R^2) (Equations 4.1, 4.2 and 4.3) were used for the conceptual modelling. While Nash-Sutcliffe Efficiency (NSE) and Volume Ratio (VR) (Equations 4.1 and 6.1) were used in the distributed modelling. It indicates that both models performed well with an acceptable goodness-of-fit. Figure 7.1 also shows a graphical comparison between the observed and simulated discharges resulting from both hydrological models at the three HRSs (for a specified period of two-years each). The visual inspection of the hydrographs specifies that the two models are good at producing the observed daily scale streamflow. In addition, the two models were validated using independent hydrometeorological data during the period (2005-2014), and the goodness-of-fit results were also satisfied (Table 7.1).

Table (7.1) Modelling performance during the calibration and verification periods at the three HRS based on the two modelling approaches

	Hydrologic Reference Stations	Calibration			Validation		
		NSE	VE (%)	R^2	NSE	VE (%)	R^2
Conceptual modelling approach	Harvey River at Dingo Road	0.87	-4.2	0.83	0.85	4.4	0.81
	Beardy River at Haystack	0.92	-3.9	0.91	0.90	-4.1	0.89
	Goulburn River at Coggan	0.9	3.8	0.85	0.88	4.2	0.82

	Hydrologic Reference Stations	Calibration		Validation	
		NSE	VR (%)	NSE	VR
Distributed modelling approach	Harvey River at Dingo Road	0.76	96.2	0.74	114.3
	Beardy River at Haystack	0.79	97.6	0.77	109.3
	Goulburn River at Coggan	0.83	102.4	0.8	107.6

However, the modelling results from Table 7.1 revealed that the conceptual model performs better than the distributed model in capturing the observed streamflow across the three contributing catchments. The values of Nash-Sutcliffe efficiency (NSE) in the conceptual modelling approach are better than those values obtained from the distributed hydrological modelling. The results also specified that the peak and low discharges are well captured by the conceptual model than the distributed model (Figure 7.1). This implies that the simple structure of the HBV model, which normally requires fewer input data, can represent the hydrological behaviour of the catchments better than the more complicated structure of the BTOPMC model which usually involves more input data. An additional consideration is that simpler hydrological models that are requiring less complex calibration are preferred over the more complex and demanding models if only streamflow is of interest, and not the spatial patterns of runoff generating processes.

Based on the above analysis, the general performance of the two models was relatively sensible in simulating the historical runoff volume at the three HRSs. The analysis of the results shows that there are no large differences in the modelling performance of the two models. On the basis of model performances, it seems that the conceptual and distributed hydrological models almost perform similarly across the studied catchments. Therefore, both hydrological models can be used effectively for climate scenario quantification to assess the impacts of future climate changes on the hydrological behaviour of the corresponding catchments of the three HRSs. Hence, both models were forced with the ensemble mean of the downscaled climate outputs of rainfall and temperature from the eight-GCMs of the CMIP5 model to simulate the future daily streamflow at the three HRSs.

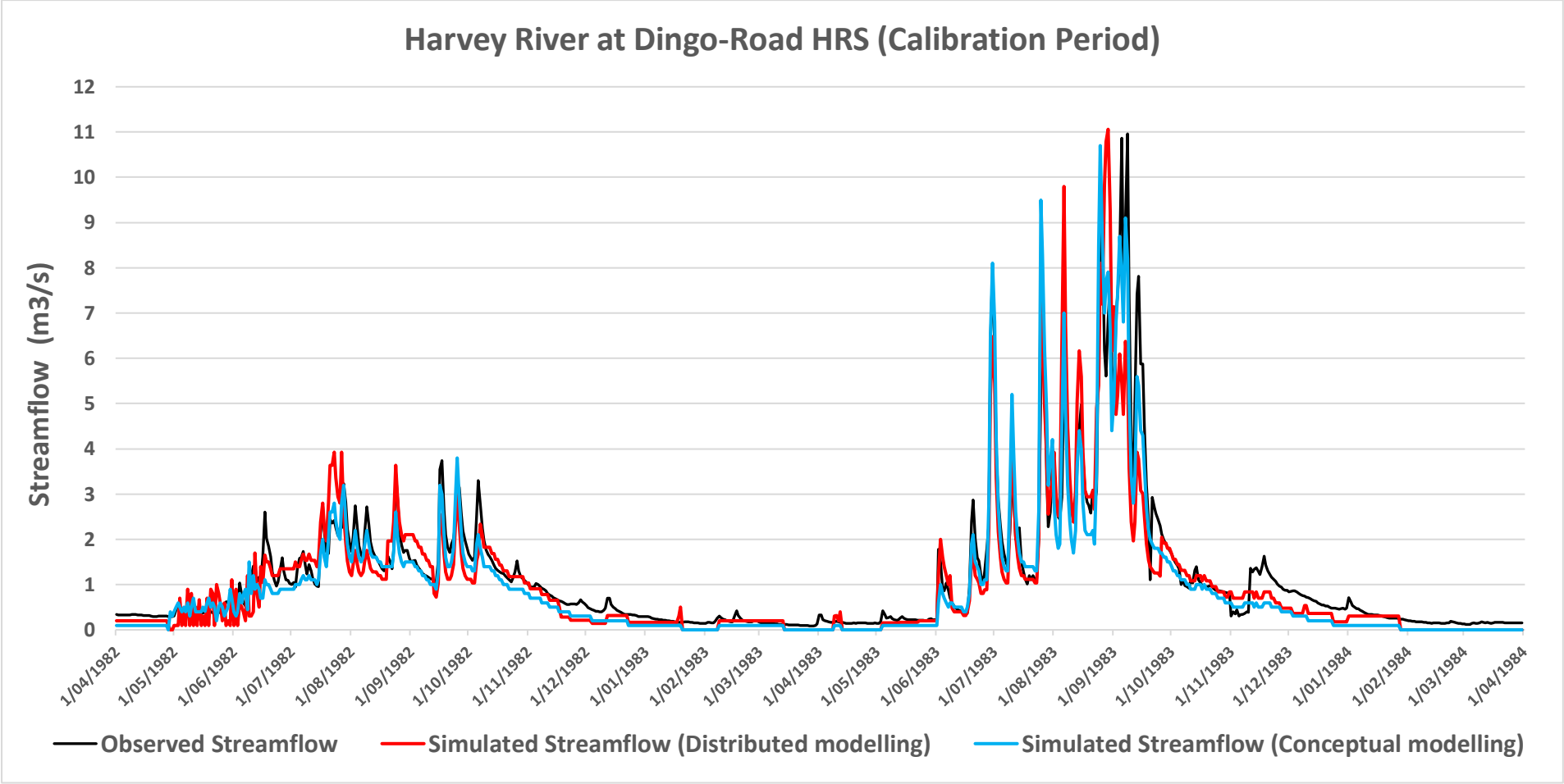
Harvey River at Dingo-Road HRS (Calibration Period)
Streamflow (m3/s)
12
11
10
9
8
7
6
5
4
3
2
1
0
1/04/1982
1/05/1982
1/06/1982
1/07/1982
1/08/1982
1/09/1982
1/10/1982
1/11/1982
1/12/1982
1/01/1983
1/02/1983
1/03/1983
1/04/1983
1/05/1983
1/06/1983
1/07/1983
1/08/1983
1/09/1983
1/10/1983
1/11/1983
1/12/1983
1/01/1984
1/02/1984
1/03/1984
1/04/1984
Observed Streamflow
Simulated Streamflow (Distributed modelling)
Simulated Streamflow (Conceptual modelling)

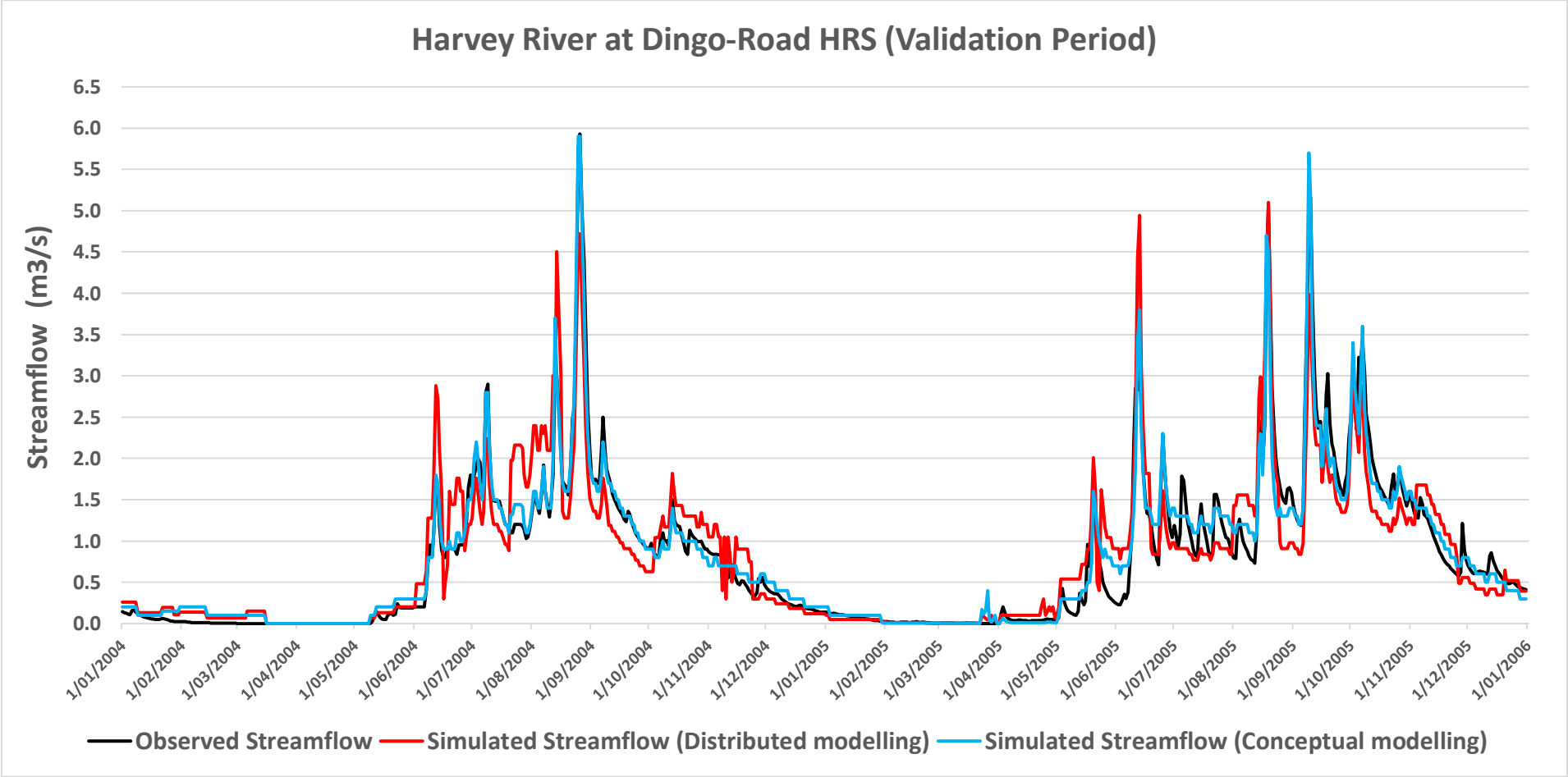
Harvey River at Dingo-Road HRS (Validation Period)
Streamflow (m3/s)
6.5
6.0
5.5
5.0
4.5
4.0
3.5
3.0
2.5
2.0
1.5
1.0
0.5
0.0
1/01/2004
1/02/2004
1/03/2004
1/04/2004
1/05/2004
1/06/2004
1/07/2004
1/08/2004
1/09/2004
1/10/2004
1/11/2004
1/12/2004
1/01/2005
1/02/2005
1/03/2005
1/04/2005
1/05/2005
1/06/2005
1/07/2005
1/08/2005
1/09/2005
1/10/2005
1/11/2005
1/12/2005
1/01/2006
Observed Streamflow
Simulated Streamflow (Distributed modelling)
Simulated Streamflow (Conceptual modelling)

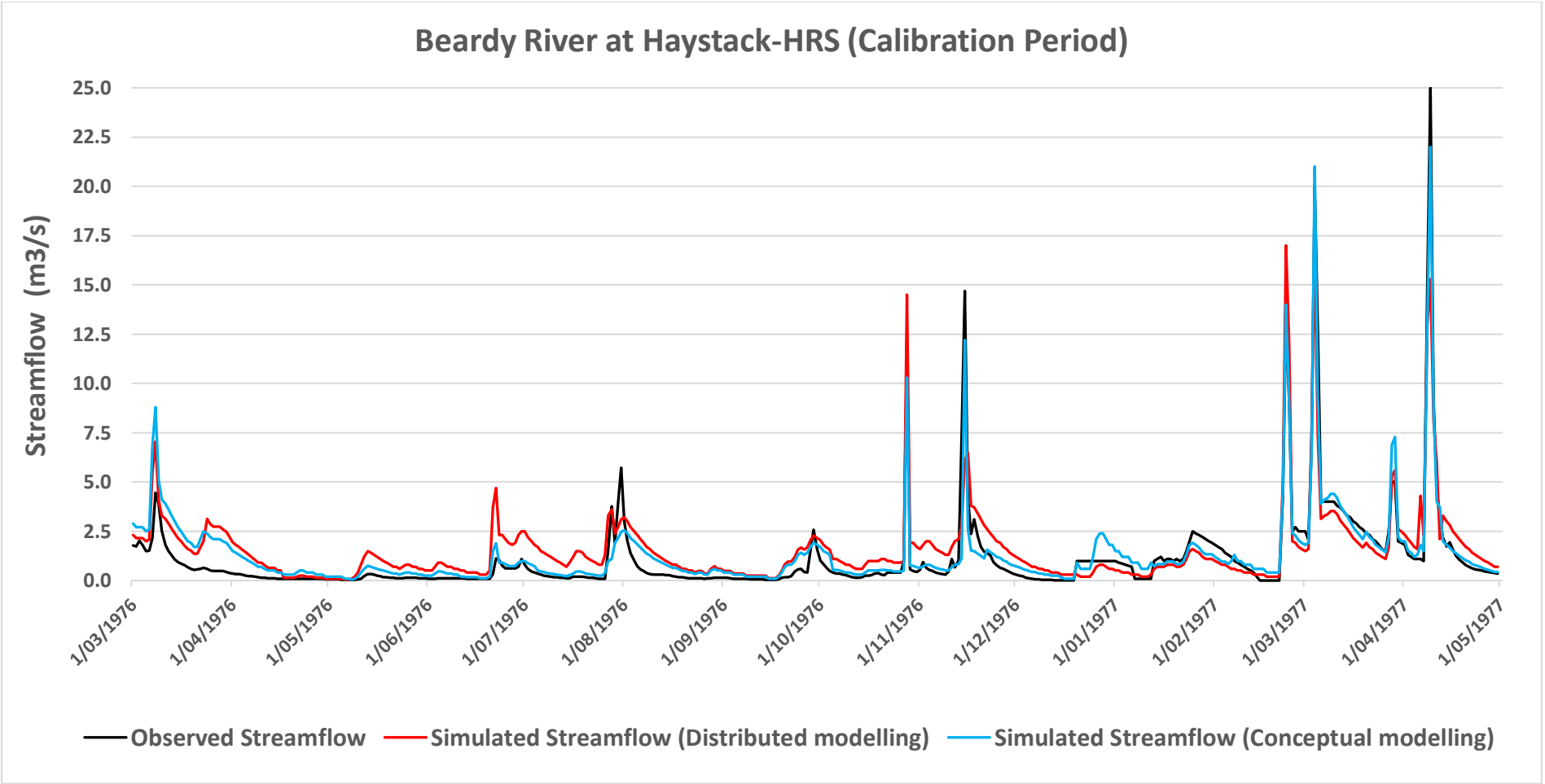
Beardy River at Haystack-HRS (Calibration Period)
Streamflow (m3/s)
25.0
22.5
20.0
17.5
15.0
12.5
10.0
7.5
5.0
2.5
0.0
1/03/1976
1/04/1976
1/05/1976
1/06/1976
1/07/1976
1/08/1976
1/09/1976
1/10/1976
1/11/1976
1/12/1976
1/01/1977
1/02/1977
1/03/1977
1/04/1977
1/05/1977
Observed Streamflow
Simulated Streamflow (Distributed modelling)
Simulated Streamflow (Conceptual modelling)

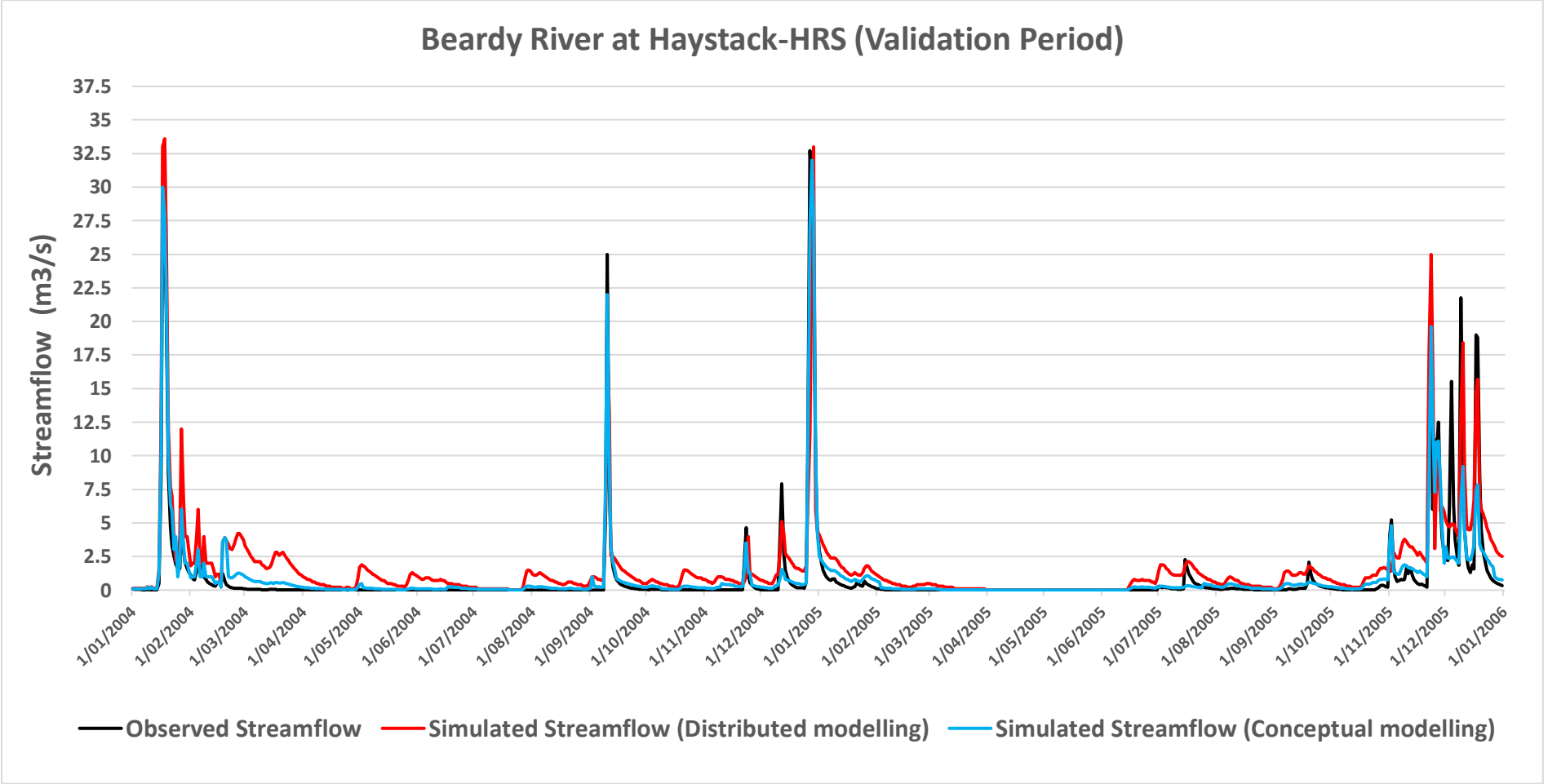
Beardy River at Haystack-HRS (Validation Period)
Streamflow (m3/s)
37.5
35
32.5
30
27.5
25
22.5
20
17.5
15
12.5
10
7.5
5
2.5
0
1/01/2004
1/02/2004
1/03/2004
1/04/2004
1/05/2004
1/06/2004
1/07/2004
1/08/2004
1/09/2004
1/10/2004
1/11/2004
1/12/2004
1/01/2005
1/02/2005
1/03/2005
1/04/2005
1/05/2005
1/06/2005
1/07/2005
1/08/2005
1/09/2005
1/10/2005
1/11/2005
1/12/2005
1/01/2006
Observed Streamflow
Simulated Streamflow (Distributed modelling)
Simulated Streamflow (Conceptual modelling)

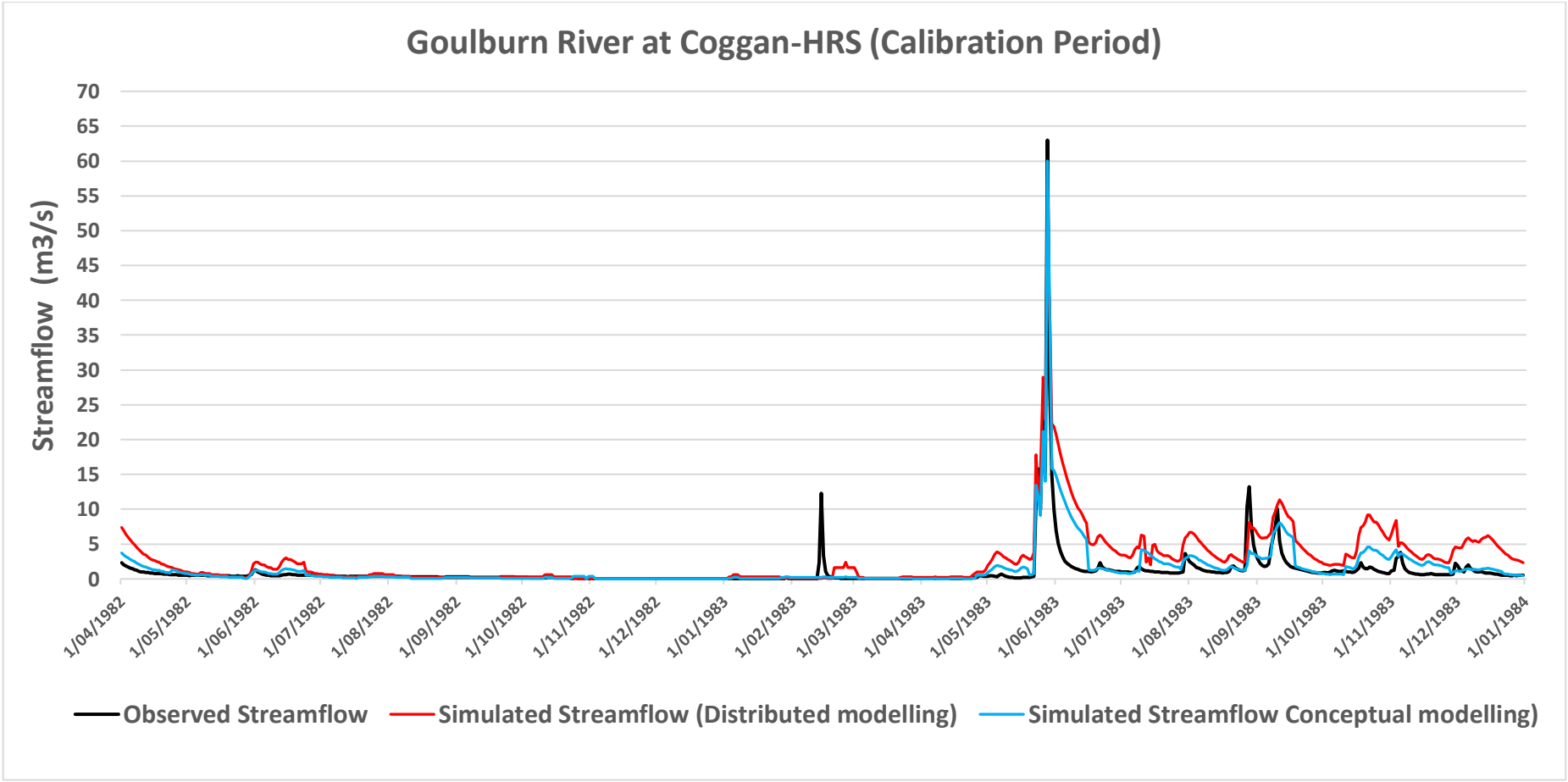
Goulburn River at Coggan-HRS (Calibration Period)
Streamflow (m3/s)
70
65
60
55
50
45
40
35
30
25
20
15
10
5
0
1/04/1982
1/05/1982
1/06/1982
1/07/1982
1/08/1982
1/09/1982
1/10/1982
1/11/1982
1/12/1982
1/01/1983
1/02/1983
1/03/1983
1/04/1983
1/05/1983
1/06/1983
1/07/1983
1/08/1983
1/09/1983
1/10/1983
1/11/1983
1/12/1983
1/01/1984
Observed Streamflow
Simulated Streamflow (Distributed modelling)
Simulated Streamflow Conceptual modelling)

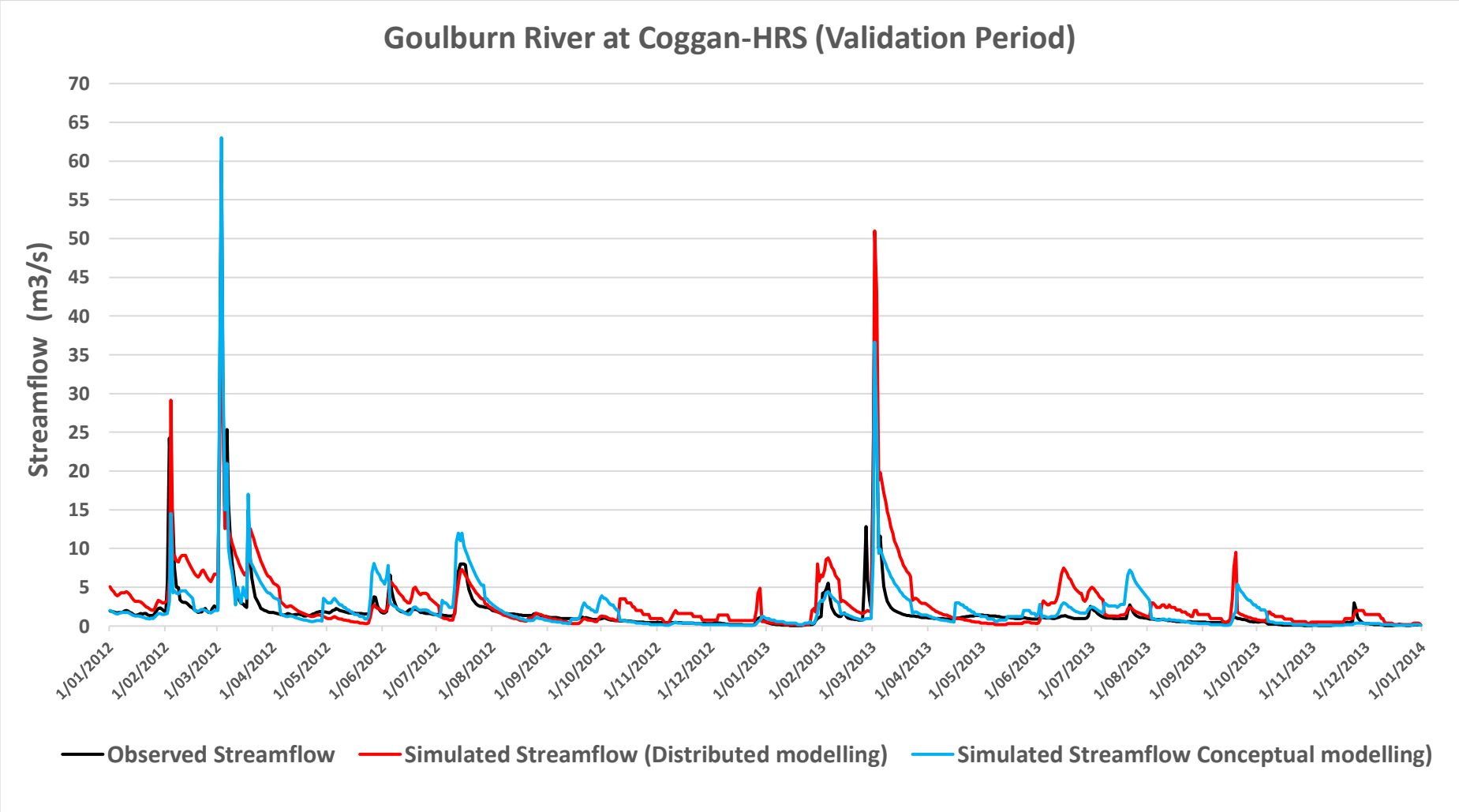

Figure (7.1) Daily observed and simulated streamflow (from the two hydrological models) at the three HRSs for the calibration and validation periods

7.3 Comparison of modelling results and catchments hydrological behaviour under climate change scenarios

To study the hydrologic behaviour of the three contributing catchments under the scenarios of climate change, the two hydrological models were forced with the same climate outputs, the ensemble mean of the eight-GCMs, but as lumped and distributed modes for the HBV and BTOPMC models respectively. The key reason was to fairly compare the behaviour of the two models under changing climate conditions and to explore any changes in the future direction of streamflow at the studied catchments. The climate change impacts on future streamflow were analysed by comparing the future monthly mean simulations (seasonal streamflow) of the two models for the mid and late of the century with the control run (Figure 7.2). Furthermore, the changes in annual mean streamflow statistics of the future climate scenarios (RCP4.5 and RCP8.5) relative to the control run at the three HRSs were also compared and presented in Tables 5.5 and 6.8. It shows that the future streamflow simulated by the two models tends to decrease across the three contributing catchments under both climate scenarios, regardless of the magnitude, relative to the control run.

At Dingo-Road HRS, the HBV model shows a shift in the wet season streamflow from (July-September) in the baseline period (control run) to (October-December) under the scenarios of future climate (Figure 7.1 a and b). While the monthly mean streamflow simulated by the BTOPMC model tends to keep the same temporal distribution as in the baseline period. The peak flows simulated by the two hydrological models indicate reduction tendencies for both scenarios; however, the changes are slightly higher for the HBV model (-29%-56%) than for the BTOPMC model (-26%-53%) especially for the mid-century (Figure 7.1 a and b). The low flows, particularly the period from January to June, are also expected to decline in the future with high reduction tendencies projected by the HBV model than the BTOPMC model. These findings specify that the uncertainty resulting from using two structurally distinctive hydrological models cannot be ignored. That is to say that even though the input data are same, different hydrological models provide different streamflow outputs because of differences in model structures. The shift in seasonal streamflow, projected by the HBV model, could be related to the shift in future rainfall patterns.

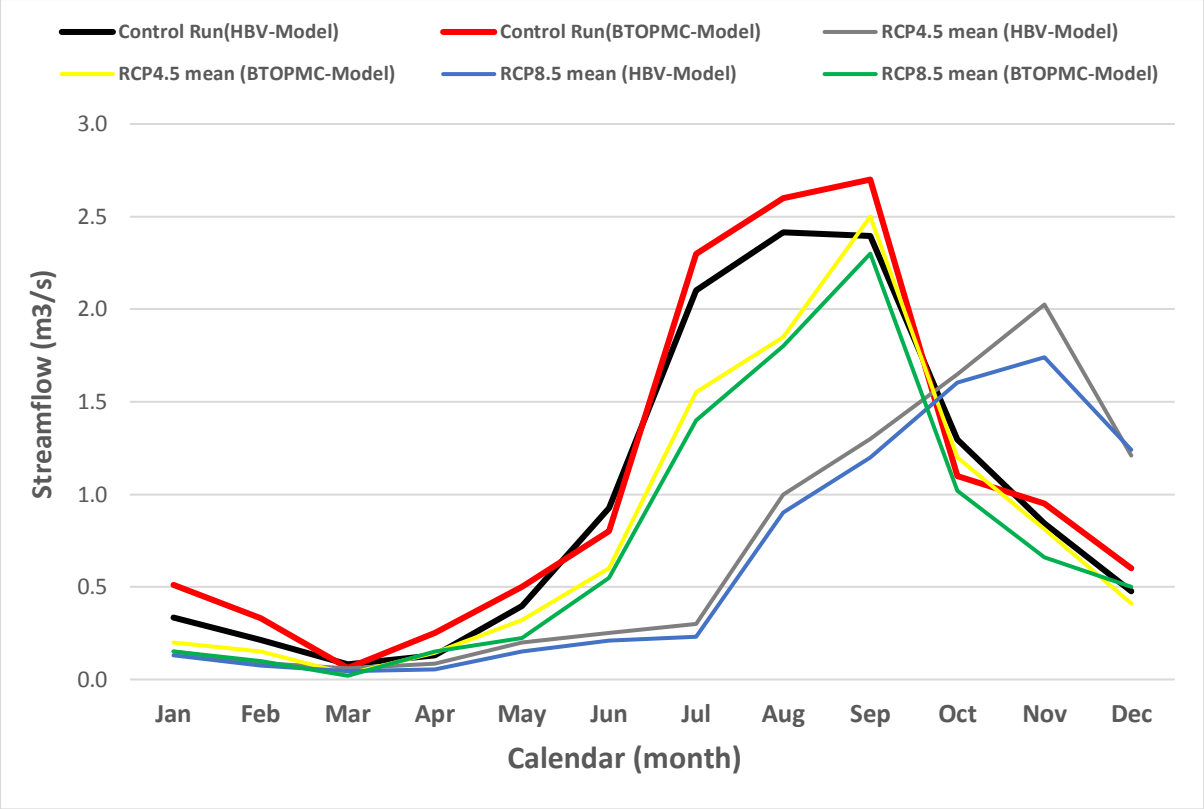

(a) Harvey catchment at Dingo-Road HRS (Mid-century)

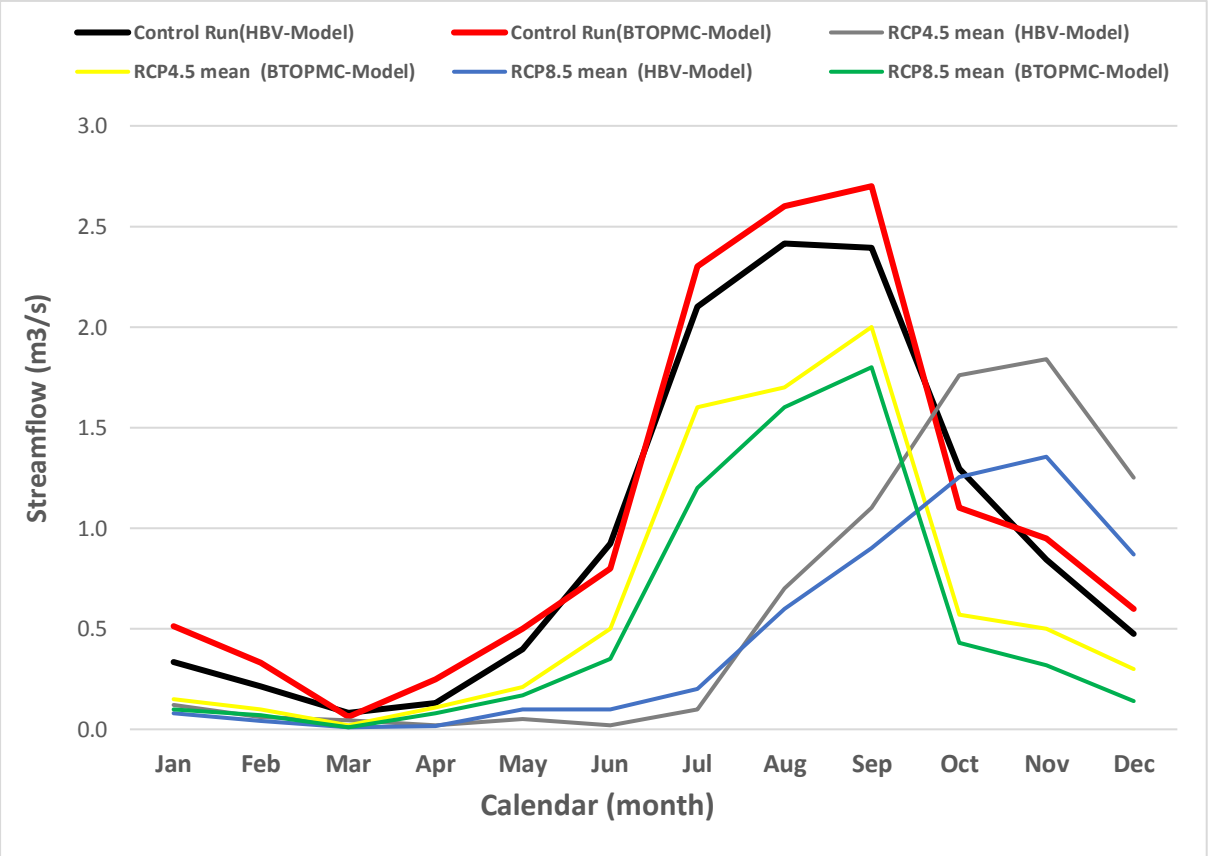

(b) Harvey catchment at Dingo-Road HRS (Late-century)

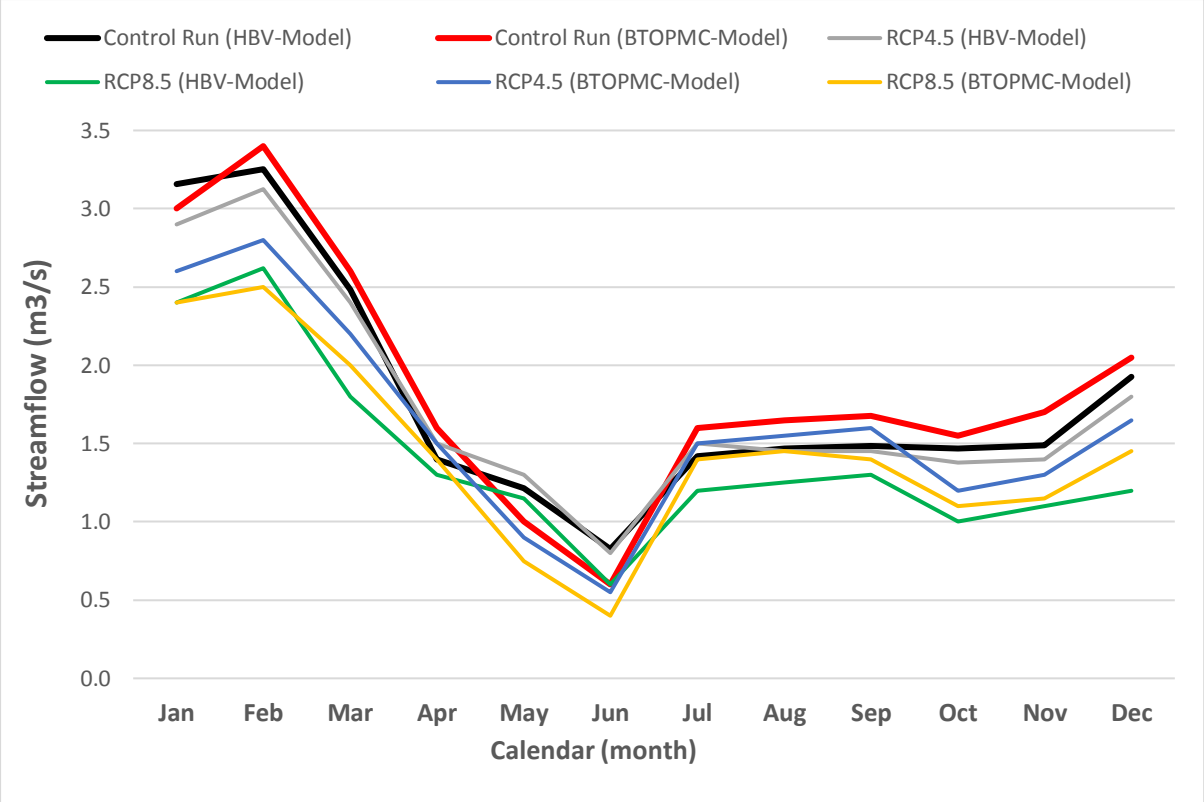

(c) Beardy catchment at Haystack HRS (Mid-century)

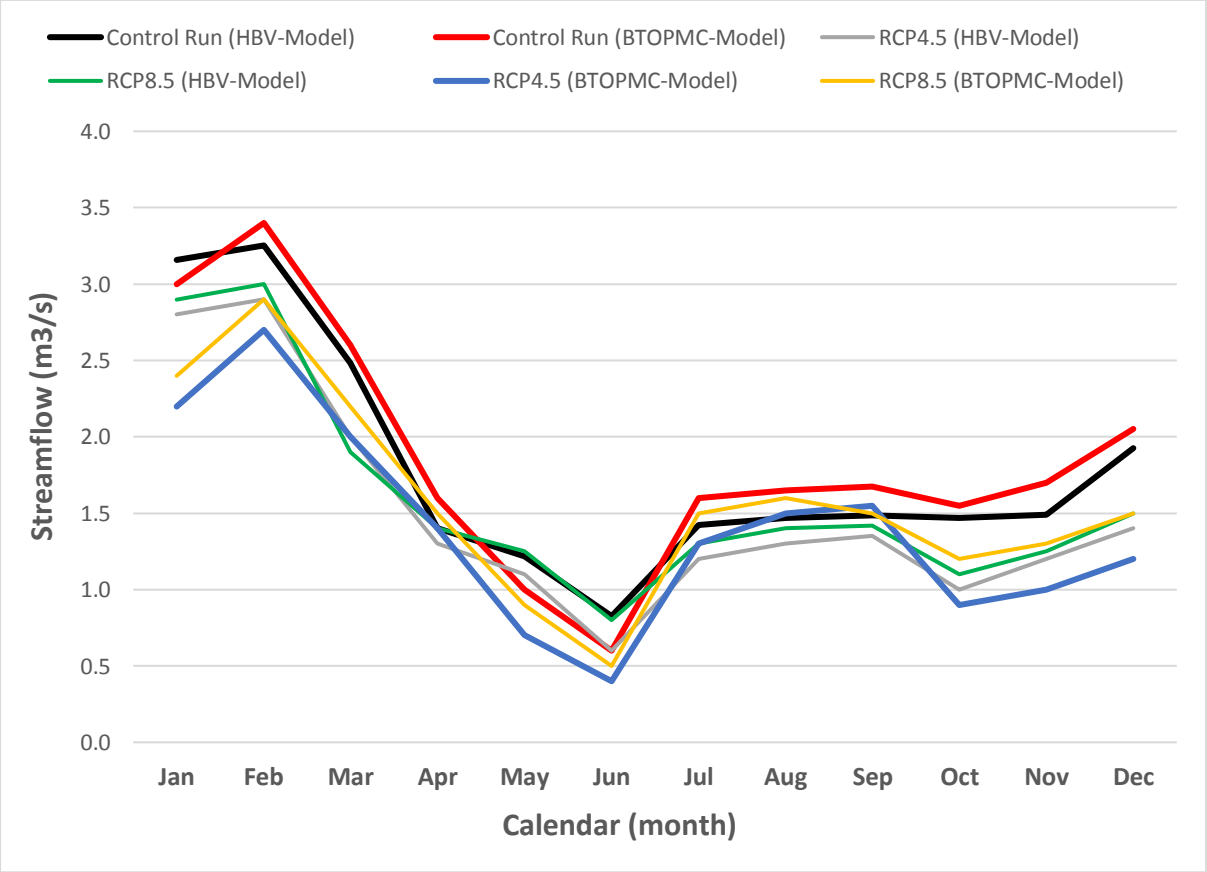

(d) Beardy catchment at Haystack HRS (Late-century)

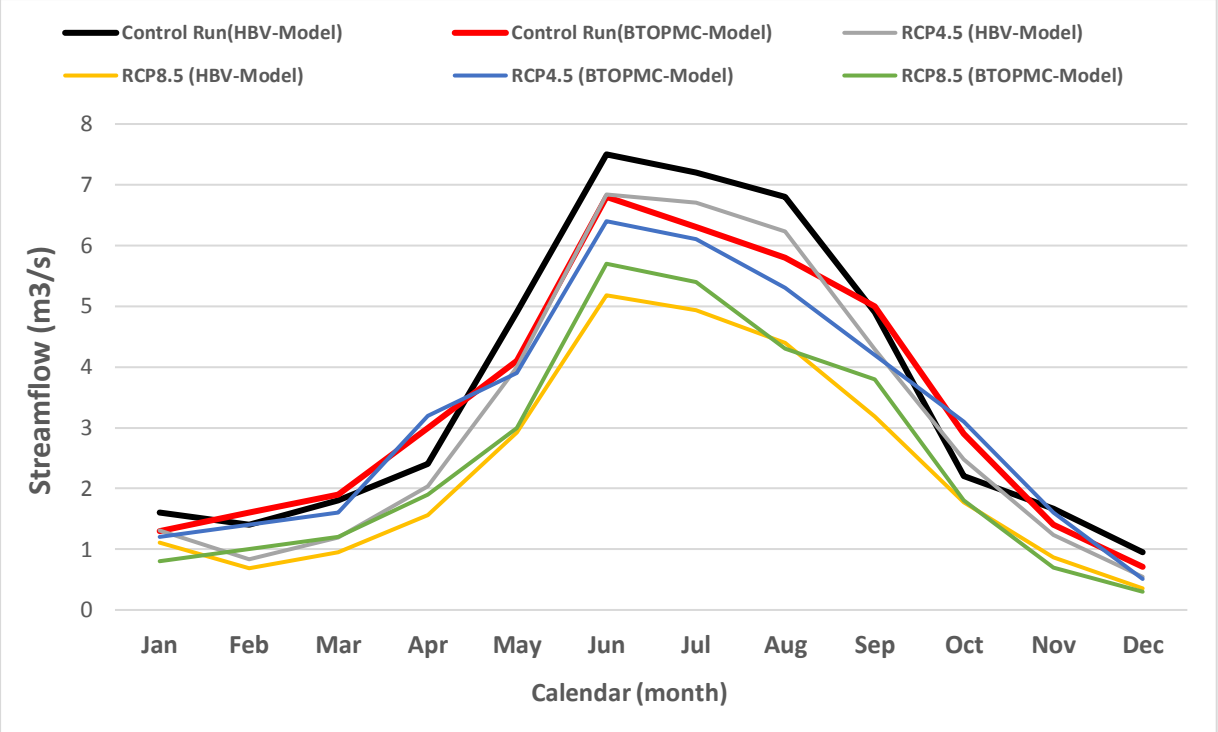

(e) Goulburn catchment at Coggan HRS (Mid-century)

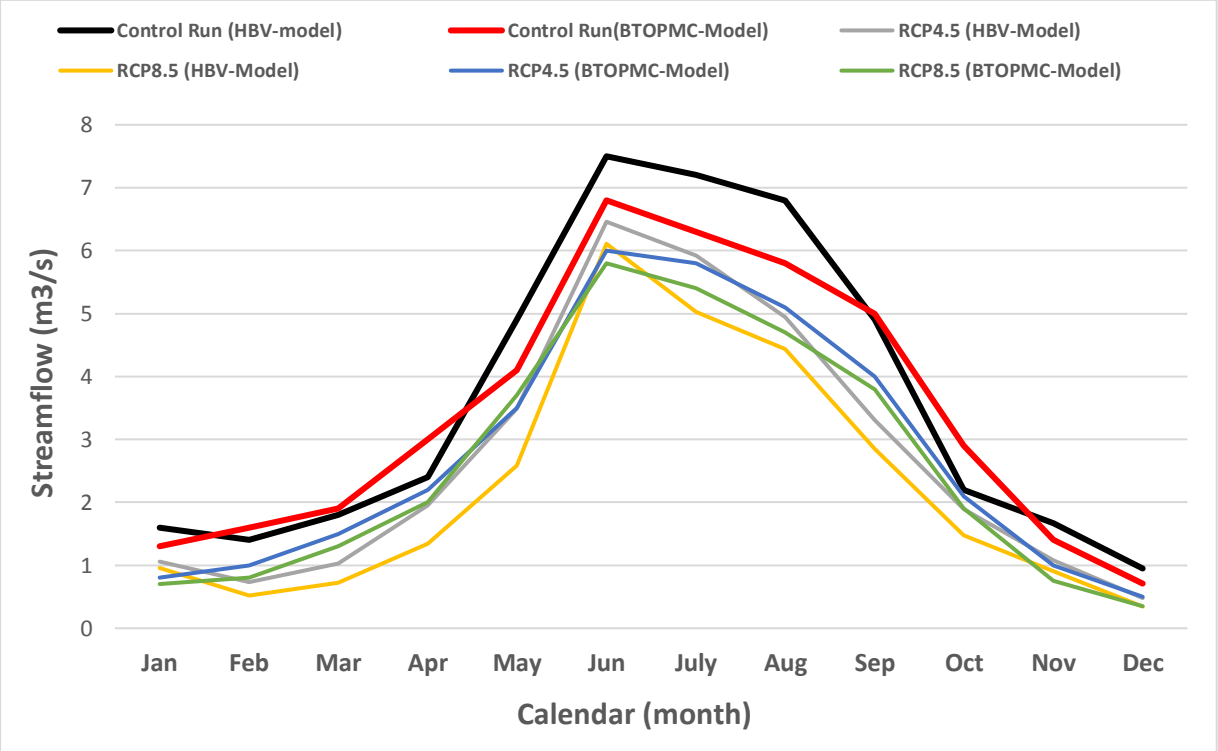

(f) Goulburn catchment at Coggan HRS (Late-century)

Figure (7.2) A comparison between the control run and the future monthly mean streamflow simulated by the two hydrological models

At Haystack HRS, the behaviour of the two hydrological models is almost the same, and showing a clear reduction in the overall future streamflow of the wet and dry seasons (Figure 7.1 c and d). However, the BTOPMC model predicts slightly higher reduction tendencies than the HBV model, specifically for the RCP4.5 scenario during the mid and late of the century. The seasonal distribution of the future streamflow simulated by the two models also tends to follow the same temporal distribution as in the baseline period. Nevertheless, the decline in the wet season's flow (October-March) is higher than the dry seasons (April-September) which show insignificant changes (Figure 7.1 c and d). This indicates that the streamflow during the wet season is more sensitive to climate change than the total annual streamflow.

The attitude of the two hydrological models is also relatively similar at Coggan HRS on Goulburn River. The wet and dry seasons streamflow are expected to decline in the future under both climate scenarios (Figure 7.1 e and f). In contrary to the case of Haystack HRS, the streamflow reduction tendencies are higher as simulated by the HBV model than by the BTOPMC model. However, the seasonal distribution of the future streamflow simulated by the two models tends to follow the same temporal distribution as in the baseline period.

7.4 Impacts of future climate changes on annual streamflow and its implications on Eco-hydrology in the studied catchments

Proper understanding the nature of human–hydrology interactions at the local-scale system is essential for a sustainable management of freshwater resources (Elshafei et al., 2014). It is widely agreed that climate change can have a critical influence on many regions around the world (Solomon et al., 2007), especially in arid and semiarid regions such as Australia, which suffers serious water deficiencies. Freshwater is almost a scarce source in Australia (Arthington and Pusey, 2003), making water resources ecological management a crucial social, economic and political issue. It is expected that future climatological alterations of precipitation, temperature, evapotranspiration and the frequency of extreme weather events will affect many physical and biological processes in many Australian local watersheds (McVicar et al., 2010). Consequently, this can alter the amount and spatial and temporal distributions of water that flows into downstream rivers and estuaries. An integrated signal of ecosystem function can be achieved from the water streams that drain catchments (Pourmokhtarian et al., 2017). Therefore, streamflow statistics at regulated catchments can be used effectively to assess disruption in upland terrestrial ecosystems.

Evaluating the effects of streamflow variation on ecology and other water-related environment is widely studied in the eco-hydrology research field. Eco-hydrology is an interdisciplinary theme that emphases on connections between ecosystems and hydrological processes (Zalewski, 2002). Climate change and human activities have had a significant impact on the eco-hydrological cycle and freshwater system (Peng et al., 2013). Variations of climate conditions can directly affect the vegetation, ecology and the hydrology of a watershed. As vegetation and hydrology are strongly connected, alterations in vegetation conditions themselves can also affect hydrology. Therefore, changes in climatic status can alter the hydrology both directly through the water supply demands, and indirectly through climate-induced changes in vegetation water use. Effective long-term water management strategies at local-scale require an appropriate understanding of the eco-hydrological processes of a catchment. Eco-hydrologic alterations resulting from changing climate conditions can alter the status of streamflow, evapotranspiration, surface storage, and soil dampness and directly affecting the region's biota and habitat (Guo et al., 2014). As the vast majority of climate models predict a drier future climate across the south-eastern and south-western parts of the Australian continent (Chiew et al., 2014), alterations in the economy, ecosystem and the quality of life are also expected. Therefore, it is crucial to understand various potential water-related challenges such as the shortage in freshwater resources, environmental protection and ecological balance (Xu et al., 2013; Zhang et al., 2008).

Annual streamflow is a crucial aspect of water resources management (Peng et al., 2013). The measurements of streamflow at controlled watersheds provide an effective assessment of the disturbance in upland terrestrial ecosystems. It has been shown in the previous chapters that the future annual streamflow, simulated by the HBV and BTOPMC hydrological models, at the gauging stations of the studied catchments is expected to decrease under all future climate scenarios relative to the baseline simulation, except for the Richmond catchment during the near future period which shows a slight increment. The decline of annual streamflow could exacerbate the water scarcity problem in these catchments. Based on the outcome of this study, the results of conceptual and distributed models, eco-hydrological applications of the hydrological modelling results from the studied catchments are discussed and highlighted below.

At Harvey River catchment, the expected streamflow decline, measured at Clifton Park and Dingo Road gauging stations, will possibly reduce the flows received by the Peel-Harvey Estuary (total area of 133 km^2). The Harvey River discharges directly to the Harvey Estuary, therefore any reduction in the flow amount of the River will badly affect the quantities of water received by the Estuary. As the depth of the Estuary is quite shallow (up to 2m for the deepest point), and more than 50% of its area has a depth of only 0.5m (Kelsey et al., 2010), this will affect the aquatic life and the environmental status of the lagoon. The estuary is an internationally important habitat for waterbirds and migratory wading birds, in which tens of thousands of waterbirds gather annually with more than 80 species (Environmental Protection Authority, 2008). The growing environmental and economic importance of the estuary (such as water demands for drinking and agricultural production, parasite control, commercial fishing, foreshore development and access, boat use and moorings and jetties) have placed additional burdens on the estuarine system. Furthermore, the projected reduction in the flow amount of the Harvey River would also reduce the quantities of water received by the Stirling and Harvey Reservoirs which represent the main water supply sources to the Perth Metropolitan. As the population and the economic development in Perth and its outskirts is in continuous growth, this would increase the competition for the currently available water resources in the area. Therefore, options for additional water supply sources in the future would be necessary to support the economic and population development in the area.

On the other hand, the anticipated streamflow reduction at the outlet of the Richmond River catchment, measured at Casino gauging station, will negatively impact the future water resources in the catchment especially with the continuous population growth in line with the highly intensive agricultural lands and tourist places. Significant attention is required to preserve the extensive wetland complexes in the lower Richmond River, such as Tuckean swamp on the Richmond floodplain and Ballina Nature Reserve which protects wide areas of mangroves and saltmarsh communities, from the risk of streamflow reduction. Thus, long-term development plans in the area should take into consideration the potential future climate change. This requires sustainable and efficient water management strategies to be applied in the catchment to overcome the problem of water scarcity.

The Beardy River region is rich in rare flora and fauna and some rare plants such as the MacNutt's wattle, velvet wattle and Torrington pea. The region also supports a variety of endangered birds such as the glossy black-cockatoo, brown treecreeper, swift parrot, and a few

marsupials, including the spotted-tailed quoll and squirrel glider (NSW government, the Office of Environment and Heritage, 2016). Therefore, the expected streamflow reduction would adversely impact the environmental and ecological communities of the Beardy River system particularly the Beardy River Hill Catchment. On the other hand, Goulburn River is the right bank tributary to the Hunter-River in NSW, Australia. It drains approximately 50% of the Hunter catchment and donates nearly quarter of the mean Hunter River flow. Water in the Hunter basin is the main source for power generation, irrigation and agriculture, stock manufacturing, coal mining and public water supplies. As the Goulburn River flow is projected to decrease due to future climate changes, this would impose further limitations on the surface water supply systems in the Hunter River basin.

7.5 Summary and Conclusions

To investigate the effectiveness of hydrological models in climate scenario studies, the HBV and BTOPMC hydrological models were compared by assessing their behaviour for simulating the historical streamflow and catchment hydrological response to climate change across three contributing catchments of the Australian HRSs. These models have different structures, and there is almost no agreement in the rainfall-runoff modelling research area on the best preferable model structure. The same observed hydro-meteorological data from the three contributing catchments were used to calibrate and validate the two hydrological models, and various performance criteria were used to assess the modelling performance. The simulated peak and low flows were also compared. Moreover, the same forcing climate data of the RCP4.5 and RCP8.5 scenarios, for the baseline and future periods, were used to force the two hydrological models to assess the impact of climate change on future streamflow.

Results of historical streamflow simulation show that the conceptual model performs better than the distributed model on a daily basis across the three contributing catchments. It seems that the conceptual model is more robust when performing in the calibration and validation periods because it produces Nash-Sutcliffe efficiency (NSE) values that are better than those values obtained from the distributed hydrological modelling (Table 7.1). The conceptual model also captured the timing and magnitude of peak flows better than the distributed model (Figure 7.1). The distributed model generally overestimated the majority of low flows, whereas the HBV model relatively tends to overestimate some of the low flows.

Regarding the future streamflow simulation, the performance of the two models was relatively compatible in the overall direction of change, irrespective of the magnitude, and inconsistent regarding the change in the direction of high and low flows for both future climate scenarios. Both models predicted a decline in wet and dry seasons streamflow across the three contributing catchments. At Haystack and Coggan HRSs, the future monthly mean streamflow distribution, simulated by the two models under both climate scenarios, follows the same patterns of the baseline period. But, at Dingo-Raod HRS, the HBV model shows a shift of the peak season from July–September in the base period to October–December for future climate scenarios (Figure 7.2 a and b).

Overall, both hydrological models, assessed in this study, are found suitable for streamflow simulations in climate change scenarios as they produced comparable results. However, the conceptual HBV model could be considered more suitable than the distributed BTOPMC model for streamflow simulations as it requires fewer input data which is an advantage in data-sparse regions. Furthermore, conceptual models are preferred over the distributed models in situations when only streamflow is of interest, as in the case of this study, and not the spatial patterns of runoff generating processes. However, if the assessment of climate change impacts on water balance components is the main concern, then, the impact on interflow conditions may be better described by using the physically based distributed models.

In conclusion, as the main interest of this study is to investigate how likely the future streamflow of three Australian HRSs will be impacted due to the changes in climatological status, then, the priority is given to the conceptual modelling as its overall performance was highly satisfied and seems to be more robust than distributed modelling. The conceptual model properly represented the extreme events, which increase the possibility of reliable representation of future streamflow due to the shifts in extreme events of future climate. Furthermore, the more accurate and complicated calculation process of potential evapotranspiration (Shuttleworth-Wallace method) by the distributed modelling did not improve the modelling performance even in the dry periods when the volume of evaporation is highly significant in the water balance. Finally, the short computation time of the conceptual modelling, compared to the distributed modelling, makes it more appropriate for long-term streamflow simulation under the various scenarios of future climate.

The hydrological result of this study will provide a theoretical basis to the local management authorities to make scientific and rational control measures and response plans which allow

them to manage the usage of future water resources in the study area. The impacts of climate change may influence human water use and the stability of the ecosystem. More attention and effort should be allocated to future water resources management and ecosystem planning in the study regions. Further research on feedbacks of vegetation, water balance, processes that directly influence plant performance and the ecological effects of weather extremes to improve climate change projections on hydrology and ecosystems will be useful in the sustainable management of catchment water resources in the future.

Chapter 8

Summary, Conclusions and Recommendations

8.1 Summary

In this study, the impact of climatic changes on the future hydrological behaviour and surface water sustainability was assessed for some local catchments within the southeastern and southwestern parts of Australia. Five catchments corresponding to five rivers were selected including Harvey River and Richmond River local catchments in Western Australia and three contributing catchments of the Australian Hydrologic Reference Stations namely Harvey River at Dingo Road HRS, Beardy River at Haystack HRS and Goulburn River at Coggan HRS. The study includes the application of two distinctively different hydrological models, the HBV conceptual model and the BTOPMC distributed model to perform the hydrological modelling. The same observed hydro-meteorological data from the contributing catchments were used to calibrate and validate the two hydrological models before the runoff simulation. The long-term observed monthly mean values of Potential Evaporation (PE) were adopted in the conceptual modelling, while the PE values in the distributed modelling were calculated using the Shuttleworth-Wallace model by utilizing the global monthly data. The two models were calibrated and validated with acceptable modelling performance which demonstrates the ability of the models to simulate the future streamflow at the catchments' outlet.

Future climate series of rainfall and temperature were extracted from a variety of Global Climate Models (GCMs) from the Coupled Model Intercomparison Project phase 3 and 5 (CMIP3 and CMIP5) of the Intragovernmental Panel on Climate Change (IPCC) Fourth and Fifth Assessment Reports (AR4 and AR5). Three future time periods including the near future (2016-2035), mid (2046-2065) and late (2080-2099) of the current century were selected to represent the future climatic conditions. A control run, with different baseline climate periods, was used to represent the current climate status. Also, three CO_2 emission scenarios of low, medium and high (A2, A1B and B1 for the AR4) and (RCP2.6, RCP4.5 and RCP8.5 for the AR5) were used to assess the impact of climate change on catchments' future streamflow. The local scale future climate conditions were computed by utilising two statistical downscaling

methods including LARS-WG 5.5 and the Bureau of Meteorology statistical downscaling model. The performance and accuracy of the downscaling methods were highly reasonable and demonstrated its ability to simulate the future climate signals at the catchment scale.

In the beginning, the historical climate change patterns in the studied catchments were analysed using the temporal change of climate over the past decades. Then the impact of future climate changes on the daily, seasonal and annual streamflow of the catchments was investigated. Almost all GCMs' scenarios predict a slight increase in the annual mean rainfall during the beginning of the century and a decrease in the mid and late-century. While the temperature and Potential Evapotranspiration (PE) are expected to increase under all scenarios during the future periods. Predicted future annual mean streamflow simulated by the two hydrological models shows positive trends during the near-future and negative trends in the mid and late century under all scenarios compared to the control run.

8.2 Conclusions

Following are the summarized conclusions of this research study:

1. The trend analysis of the annually observed streamflow confirmed evidence of changes in hydrological responses consistent with observed changes in climate over the past decades.
2. The modelling results at the three HRSs revealed that the conceptual (HBV model) performs better than the distributed (BTOPMC model) in capturing the observed streamflow across the three contributing catchments. This implies that the simple structure of the conceptual model, which normally requires fewer input data, can represent the hydrological behaviour of the catchments better than the more complicated structure of the distributed model which usually involves more input data.
3. Overall, the general performance of the two models was relatively sensible for predicting runoff volume at the three HRSs. Both models predicted a decline in the wet and dry seasons streamflow across the three contributing catchments. The analysis of the results also shows that there are no large differences in the modelling performance of the two models. Anyway, the priority of hydrological modelling is given to the HBV as its overall performance was highly satisfied and seems to be more robust than BTOPMC model.
4. The study highlighted the similar outcomes with other previous studies that have been conducted in many south-western and south-eastern Australian catchments and revealed noticeable rainfall-runoff reduction tendencies.

5. The outcomes of this assessment specify that the potential changes in streamflow due to changing climate conditions could be very significant. The projected streamflow reduction would probably impose additional burdens on the currently available surface water resources and would influence the environmental and ecological communities in the contributing catchments. Options for additional water supply sources and adaptive responses would be essential in the future to support the economic and population development in the catchments and to maintain sustainable ecological communities.
6. The findings could assist the authorities and communities of the studied River catchments to manage the usage of future water resources in the area such as irrigation, industrial and domestic water supply and even drinking water supply taking into consideration the low flow situation.

8.3 Recommended future works

The outcomes of the present study confirmed the robustness and reliability of the two hydrological models to simulate the future streamflow in the studied catchments. However, there are still many issues to be investigated in future research. Following is a brief recommendation for further research work;

1. The HRSs network represents 'living-gauges' that enable the long-term streamflow monitoring and climate-change adaptation in Australia. In this research study, only three contributing catchments corresponding to three HRSs were taken into account due to the time limitation. Substantially increase the number of the contributing catchments will help in exploring any novel future spatial or temporal patterns/trends that previous studies may have missed.
2. The previous hydrological research in Australia used a variety of conceptual models to examine the impacts of future climate changes on water sustainability. As the HBV model has proved its well performance in Europe, Asian Pacific, and also in this study, it is recommended to apply the HBV model in future hydrological studies in Australia.
3. Combining the outputs of hydrological modelling with ecological models is highly recommended to predict the Ecohydrological impact of future climate changes on the ecosystem of the studied catchments.
4. The attention of future research should also focus on feedbacks of vegetation, water balance, processes that directly influence plant performance and on the ecological effects of weather extremes to improve climate change projections on hydrology and ecosystems.

References

Abebe, N. A., Ogden, F. L., & Pradhan, N. R. (2010). Sensitivity and uncertainty analysis of the conceptual HBV rainfall–runoff model: Implications for parameter estimation. Journal of Hydrology, 389(3), 301-310.

Abbott, M. B., Bathurst, J. C., Cunge, J. A., O'Connell, P. E., and Rasmussen, J. (1986). An introduction to the European Hydrological System—Systeme Hydrologique Europeen, "SHE", 1: History and philosophy of a physically-based, distributed modelling system. *Journal of Hydrology 87* (1-2), 45-59.

Alkaeed, O., Flores, C., Jinno, K., & Tsutsumi, A. (2006). Comparison of several reference evapotranspiration methods for Itoshima Peninsula area, Fukuoka, Japan. Memoirs of the Faculty of Engineering, Kyushu University, 66(1), 1-14.

Al-Safi, H. I. J., Sarukkalige, P. R. (2017 a). Potential Climate Change Impacts on the Hydrological System of the Harvey River Catchment. World Academy of Science, Engineering and Technology, International Journal of Environmental, Chemical, Ecological, Geological and Geophysical Engineering, 11(4), 296-306.

Al-Safi, H. I. J., Sarukkalige, P. R. (2017b). Assessment of future climate change impacts on hydrological behavior of Richmond River Catchment. Water Science and Engineering, 10(3), 197-208.

Al-Safi, H. I. J., Sarukkalige, P. R. (2017 c). Assessment of climate change impacts on the variability of future streamflow in a selected contributing catchment of the Australian Hydrologic Reference Stations. In: the proceeding of the 16th World Water Congress "Bridging Science and Policy". Cancun, Mexico, pp. 1-19.

Ao T. Q., Yoshitani J, Takeuchi K, Fukami K, Mutsura T, Ishidaira H. (2003). Effects of sub-basin scale on runoff simulation in distributed hydrological model: BTOPMC. In Weather Radar Information and Distributed Hydrological Modeling, TachikawaY,Vieux BE,Georgakakos KP, Nakakita E (eds). IAHS Publ. no. 282; 227–234.

Ao, T. Q. (2000). Development of a Distributed Hydrological Model for Large River Basins and Its Application to Southeast Asian Rivers. Ph. D. Dissertation. Kofu, Japan: University of Yamanashi.

Arnold JG, Srinivasan R, Muttiah RS, Williams JR (1998). Large area hydrologic modeling and assessment part I: model development. J Am Water Resour Assoc 34:73–89.

Arthington AH, Pusey BJ (2003) Flow restoration and protection in Australian rivers. River Res Appl 19:377–395.

Badrzadeh, H. (2014). River flow forecasting using an integrated approach of wavelet multi-resolution analysis and computational intelligence techniques.

Bao, H. J., Wang, L. L., Li, Z. J., Zhao, L. N., & Zhang, G. P. (2010). Hydrological daily rainfall-runoff simulation with BTOPMC model and comparison with Xin'anjiang model. Water Science and Engineering, 3 (2), 121-131.

Bari, M., Amirthanathan, G., & Timbal, B. (2010). Climate change and long term water availability in South-Western Australia-an experimental projection. Climate Change 2010: Practical Responses to Climate Change, 180.

Barron, O., Crosbie, R., Charles, S., Dawes, W., Ali, R., Evans, W, Cresswell, R., Pollock, D., Hodgson, G., Currie, D., Mpelasoka, F., Pickett, T., Aryal, S., Donn, M., and Wurcker, B. (2011). Climate change impact on groundwater resources in Australia. Waterlines Report (67).

Bates, B., Kundzewicz, Z. W., Wu, S., Palutikof, J. (2008). Climate change and water. Intergovernmental Panel on Climate Change (IPCC). http://digital.library.unt.edu/ark:/67531/metadc11958/.

Betts R. A., Boucher O., Collins M., Cox P.M., Falloon P. D., Gedney N., Hemming D. L., Huntingford C., Jones C. D., Sexton D. M. H., Webb W. J. (2007). Projected increase in continental runoff due to plant response to increasing carbon dioxide. Nature 448(7157):1037–1041.

Beven K. J., Kirkby MJ. (1979). A physically based, variable contributing area model of hydrology. Hydrological Science-Bulletin 24 (1): 43–69.

Beven, K. J. (2001). Rainfall-Runoff Modelling The Primer. John Wiley & Sons, Lancaster, UK.

Bergstrom, S., (1976). Development and application of a conceptual runoff model for Scandinavian catchments. SMHI RH07, Norrk6ping.

Bergstrom, S., (1995). The HBV model (Chapter 13, pp. 443-476), in: Singh, V.P. (ed.) Computer models of watershed hydrology, Water Res. Pub., Highlands Ranch, Colorado, U.S.A., 1130 pp.

Bian, H., Lü, H., Sadeghi, A. M., Zhu, Y., Yu, Z., Ouyang, F, Su, J. & Chen, R. (2017). Assessment on the Effect of Climate Change on Streamflow in the Source Region of the Yangtze River, China. Water, 9(1), 70.

Boughton, W. C. (2004). The Australian water balance model. Environmental Modelling and Software, 19, 943-956.

Beven, K. J. (2011). Rainfall-runoff modelling: the primer. John Wiley & Sons.

Bouaziz, L., Sperna Weiland, F., Beersma, J. & Buiteveld, H. (2014). New insights for the hydrology of the Rhine based on the new generation climate models. In: EGU General Assembly Conference, 27 April–2 May, Vienna, Austria.

Brown, S. C., Versace, V. L., Lester, R. E., & Walter, M. T. (2015). Assessing the impact of drought and forestry on streamflows in south-eastern Australia using a physically based hydrological model. *Environmental earth sciences*, *74*(7), 6047-6063.

Bureau of Meteorology-BoM, (2017). http://www.bom.gov.au/water/hrs/. (Accessed 10th April 2017).

Bureau of Meteorology-BoM, (2015). Hydrologic Reference Stations. Water information.

Burnash, R. J. C., Ferral, R. L. & McGuire, R. A. (1973). A Generalised streamflow simulation system–conceptual modelling for digital computers. Joint Federal and State River Forecast Centre, Sacramento, Technical Report, 204.

Cai, W. & Cowan, T. (2008). Dynamics of late autumn rainfall reduction over south-eastern Australia. Geophysical Research Letters, 35. http://dx.DOI:10.1029/2008GL033727.

Calver, A., and Wood, W. L. (1995). The institute of hydrology distributed model. Singh, V. P. ed., Computer Models of Watershed Hydrology, 595-626. Highlands Ranch, CO: Water Resources Publications.

Chartres, C., & Varma, S. (2010). *Out of water: from abundance to scarcity and how to solve the world's water problems*: FT Press.

Charles, S. P., Bates, B. C., Smith, I. N., Hughes, J. P. (2004). Statistical downscaling of daily precipitation from observed and modelled atmospheric fields. Hydrological Processes, 18(8), 1373-1394. http://dx.DOI:10.1002/hyp.1418.

Charles, S., Silberstein, R., Teng, J., Fu, G., Hodgson, G., Gabrovsek, C., Cai, W. (2010). Climate analyses for south-west Western Australia. A Report to the Australian Government from the CSIRO South-West Western Australia Sustainable Yields Project. ISSN 1835-095X.

Cheng, L., Zhang, L., Wang, Y.-P., Yu, Q., Eamus, D., & O'Grady, A. (2014). Impacts of elevated CO 2, climate change and their interactions on water budgets in four different catchments in Australia. Journal of Hydrology, 519, 1350-1361.

Chau, K., Wu, C., & Li, Y. (2005). Comparison of Several Flood Forecasting Models in Yangtze River. Journal of Hydrologic Engineering, 10(6), 485-491. http://doi:10.1061/(ASCE)1084-0699(2005)10:6(485).

Chiew, F. H. S., and T. A. McMahon (2002). Modelling the impacts of climate change on Australian streamflow, Hydrol. Processes, 16, 1235–1245, doi:10.1002/hyp.1059.

Chiew, F. H. S., Potter, N. J., Vaze, J., Petheram, C., Zhang, L., Teng, J., & Post, D. A. (2014). Observed hydrologic non-stationarity in far south-eastern Australia: implications for modelling and prediction. Stochastic Environmental Research and Risk Assessment, 28(1), 3-15.

Chiew, F., Teng, J., Vaze, J., Post, D., Perraud, J., Kirono, D., & Viney, N. (2009). Estimating climate change impact on runoff across southeast Australia: Method, results, and implications of the modeling method. *Water Resources Research, 45*(10).

Clarke, R. T. (1973). A review of some mathematical models used in hydrology, with observations on their calibration and use. Journal of hydrology, 19(1), 1-20. http://dx.doi.org/10.1016/0022-1694(73)90089-9.

Commonwealth Scientific and Industrial Research Organisation and Australian Bureau of Meteorology (2007). Climate change in Australia, technical report, Melbourne, Victoria, Australia.

Commonwealth Scientific and Industrial Research Organisation and Australian Bureau of Meteorology (2015). Climate Change in Australia Information for Australia's Natural Resource Management Regions: Technical Report, CSIRO and Bureau of Meteorology, Australia.

Collier, M. A., Jeffrey, S. J., Rotstayn, L. D., Wong, K. K., Dravitzki, S. M., Moseneder, C., ... & El Zein, A. (2011, December). The CSIRO-Mk3. 6.0 Atmosphere-Ocean GCM: participation in CMIP5 and data publication. In International Congress on Modelling and Simulation–MODSIM.

Coulibaly, P. (2008). Multi-model approach to hydrologic impact of climate change. From Headwaters to the Ocean, Hydrological Change and Water Management-Hydrochange, 249-255.

Crawford, N. H., & Linsley, R.K. (1966). Digital simulation in hydrology: Stanford watershed model IV. Technical report No. 39, Department of Civil engineering. Stanford University: 210.

Dawson, C. W., & Wilby, R. L. (2001). Hydrological modelling using artificial neural networks. Progress in Physical Geography, 25(1), 80-108.

Dehghan, Z., Fathian, F., Eslamian, S., (2018). Climate Change Impact on Agriculture and Irrigation Network, In Climate Change-Resilient Agriculture and Agroforestry: Ecosystem Services and Sustainability, by Paula Cristina Castro, Anabela Marisa Azul,Walter Leal Filho, and Ulisses M. Azeiteiro, Climate Change Management Book Series, Springer.

De Jager, C., Usoskin, I.G. (2006). On possible drivers of sun-induced climate change. J. Atmos. Solar-Terres. Phys. 68, 2053–2060.

Demaria, E. M. C., Maurer, E. P., Thrasher, B., Vicuña, S., & Meza, F. J. (2013). Climate change impacts on an alpine watershed in Chile: Do new model projections change the story? Journal of hydrology, 502, 128-138.

Deng, Z., Qiu, X., Liu, J., Madras, N., Wang, X., & Zhu, H. (2016). Trend in frequency of extreme precipitation events over Ontario from ensembles of multiple GCMs. Climate dynamics, 46(9-10), 2909-2921.

Department of Primary Industries, Water, NSW. (2016). http://www.water.nsw.gov.au/watermanagement/catchments/richmond-catchment. (Accessed 20 October 2016).

Doorenbos, J. and Pruitt, W. O. (1977). Guidelines for predicting crop water requirements. FAO Irrigation and Drainage Paper, 24, 144 pp.

Driessen, T. L. A., Hurkmans, R. T. W. L., Terink, W., Hazenberg, P., Torfs, P. J. J. F., Uijlenhoet, R. (2010). The hydrological response of the Ourthe catchment to climate change as modelled by the HBV model. Hydrology and Earth System Sciences, 14(4), 651-665.

Du J, Rui H, Zuo T, LiQ, Zheng D, ChenA, Xu CY. (2013). Hydrological simulation by SWAT model with fixed and varied parameterization approaches under land use change. Water Resour Manag 27(8):2823–2838.

Durrant, J., & Byleveld, S. (2009). Streamflow trends in south-west Western Australia, Surface water hydrology series–Report no. HY32, Department of Water, Government of Western Australia.

Elshafei, Y., Sivapalan, M., Tonts, M., & Hipsey, M. R. (2014). A prototype framework for models of socio-hydrology: identification of key feedback loops and parameterisation approach. Hydrology and Earth System Sciences, 18(6), 2141-2166.

Environmental Protection Authority. (2008). Water Quality Improvement Plan for the Rivers and Estuary of the Peel-Harvey System - Phophorus Management, Environmental Protection Authority, Perth, Western Australia.

Falkenmark M, Chapman T (eds). (1989). Comparative Hydrology. UNESCO: France.

FAO/IIASA/ISRIC/ISSCAS/JRC. (2012). “Harmonized World Soil Database,” version 1. 2, FAO, Rome, Italy and IIASA, Laxenburg, Austria.

Fowler, H., Blenkinsop, S., & Tebaldi, C. (2007). Linking climate change modelling to impacts studies: recent advances in downscaling techniques for hydrological modelling. International Journal of climatology, 27(12), 1547-1578.

Fu, G., Charles, S. P., & Chiew, F. H. (2007). A two-parameter climate elasticity of streamflow index to assess climate change effects on annual streamflow. Water Resources Research, 43(11).

Garrote, L., and Bras, R. L. (1995). A distributed model for real-time flood forecasting using digital elevation models. Journal of Hydrology, 167(1-4), 279-306. http://doi:10.1016/0022-1694(94)02592-Y.

Gassman PW, Reyes MR, Green CH, Arnold JG (2007). The soil and water assessment tool: historical development, applications, and future research directions. Trans ASABE 50:1211–1250.

Geris, J., Tetzlaff, D., Seibert, J., Vis, M., & Soulsby, C. (2015). Conceptual modelling to assess hydrological impacts and evaluate environmental flow scenarios in montane river systems regulated for hydropower. River Research and Applications, 31(9), 1066-1081.

Gordon, H. B., O'Farrell, S. P. (1997). Transient climate change in the CSIRO coupled model with dynamic sea ice. Monthly Weather Review, 125(5), 875-908. http://dx.doi.org/10.1175/1520-0493(1997)125<0875:TCCITC>2.0.CO;2.

Gosain, A. K., Mani, A. & Dwivedi, C. (2009). Hydrological modeling review. Climawater, Report No. 1.

Green D., Ali A., Petrovic J., Burrell M., Moss P. (2012). Water resource and management overview: Border Rivers Catchment. NSW Department of Primary Industries, Sydney.

Green CH, Tomer MD, Luzio MD, Arnold JG. (2006). Hydrologic evaluation of the soil and water assessment tool for a large tile-drained watershed in Iowa. American Society of Agricultural and Biological Engineers 49 (2): 413–422.

Grillakis, M. G., Tsanis, I. K., & Koutroulis, A. G. (2010). Application of the HBV hydrological model in a flash flood case in Slovenia. Natural Hazards and Earth System Sciences, 10(12), 2713.

Grillakis, M. G., Koutroulis, A. G., & Tsanis, I. K. (2011). Climate change impact on the hydrology of Spencer Creek watershed in Southern Ontario, Canada. Journal of Hydrology, 409(1), 1-19.

Gunawardhana, L. N., Al-Rawas, G. A., Kazama, S., & Al-Najar, K. A. (2015). Assessment of future variability in extreme precipitation and the potential effects on the wadi flow regime. Environmental monitoring and assessment, 187(10), 1-19.

Guo, B., Zhang, J., Gong, H., & Cheng, X. (2014). Future climate change impacts on the ecohydrology of Guishui River Basin, China. Ecohydrology & Hydrobiology, 14(1), 55-67.

Hapuarachchi HAP, Takeuchi K, Zhou M, Kiem AS, Georgievski M, Magome J, Ishidaira H. (2008). Investigation of the Mekong River basin hydrology for 1980–2000 using the YHyM. Hydrological Processes 22(9): 1246–1256.

Hargreaves, G. H., and Samani, Z. A. (1985). Reference crop evapotranspiration from temperature. Applied Engineering Agric., 1(2), 96-99.

Hartmann, C.L.A.D.L.; Brönnimann, S.; Dentener, F.J.; Dlugokencky, E.J.; Easterling, D.R.; Kaplan, A.; Soden, B.J. IPCC (2013), Climate Change 2013, in the Physical Science Basis, Working Group I Contribution to the Fifth Assessment Report of the Intergovernmental Panel on Climate Change; Cambridge University Press: Cambridge, UK, 2014.

Huang, M., & Liang, X. (2006). On the assessment of the impact of reducing parameters and identification of parameter uncertainties for a hydrologic model with applications to ungauged basins. Journal of hydrology, 320(1–2), 37-61. http://dx.doi.org/10.1016/j.jhydrol.2005.07.010.

Hughes, D. A., Kingston, D. G., & Todd, M. C. (2011). Uncertainty in water resources availability in the Okavango River basin as a result of climate change. Hydrology and Earth System Sciences, 15(3), 931-941. http://dx.doi:10.5194/hess-15-931-2011.

Indian Ocean Climate Initiative. (2002). Climate variability and change in south west Western Australia. Indian Ocean Climate Initiative Panel, Perth.

Intergovernmental Panel on Climate Change (IPCC), (2000). Special Report on Emission Scenarios, Cambridge University Press, Cambridge, UK, 570 pp.

Intergovernmental Panel on Climate Change (IPCC), (2007). The physical science basis – summary for policymakers. Contribution of WGI to the Fourth Assessment Report of the Intergovernmental Panel on Climate Change. http://www.ipcc.ch/ipccreports/ar4-wg1.htm.

Intergovernmental Panel on Climate Change (IPCC), (2011). 30-Year means of the CRU data. Available online at: http://www.ipccdata.org/obs /get_30yr_means.html, retrieved on 14th March 2017.

Islam, S. A., Bari, M. A., Anwar, A. H. M. F. (2014). Hydrologic impact of climate change on Murray Hotham catchment of Western Australia: a projection of rainfall-runoff for future water resources planning. Hydrology and Earth System Sciences Discussions, 10(10), 12027-12076. http://dx.doi:10.5194/hess-18-3591-2014.

Jakeman, A., Littlewood, I., Whitehead, P. (1990). Computation of the instantaneous unit hydrograph and identifiable component flows with application to two small upland catchments. J. Hydrol. 117, 95–123.

Jarvis A, Reuter HI, Nelson A, Guevara E. (2008). Hole-filled seamless SRTM data V4, International Centre for Tropical Agriculture (CIAT). Available online at: http://srtm.csi.cgiar.org/, retrieved on 14th March 2017.

Jia, Q. Y., & Sun, F. H. (2012). Modeling and forecasting process using the HBV model in Liao river delta. Procedia Environmental Sciences, 13, 122-128.

Kebede, A., Diekkrüger, B., & Moges, S. A. (2014). Comparative study of a physically based distributed hydrological model versus a conceptual hydrological model for assessment of climate change response in the Upper Nile, Baro-Akobo basin: a case study of the Sore watershed, Ethiopia. International Journal of River Basin Management, 12(4), 299-318.

Kelsey, P., Hall, J., Kretschmer, P., Quinton, B., & Shakya, D. (2010). Hydrological and nutrient modelling of the Peel-Harvey catchment: Water Science Technical Series, Report.

Krogh, M., Dorani, F., Foulsham, E., Mcsorley, A. & Hoey, D. (2013). Hunter catchment salinity assessment. Final Report. NSW Environment Protection Authority. Final Advice, 1.

Kundzewicz, Z. W., Mata, L. J., Arnell, N. W., Doll, P., Kabat, P., Jimenez, B., Miller, K. A., Oki, T., Sen, Z., Shiklomanov, I. (2007). Freshwater resources and their management. Cambridge University Press.

Liang, X., Lettenmaier, D. P.,Wood, E. F., and Burges, S. J. (1994). A simple hydrologically based model of land surface water and energy fluxes for general circulation models, J. Geophys. Res., 99(D7), 14 415–14 428.

Lidén, R., & Harlin, J. (2000). Analysis of conceptual rainfall–runoff modelling performance in different climates. Journal of Hydrology, 238(3), 231-247.

Lindström, G., Johansson, B., Persson, M., Gardelin, M., & Bergström, S. (1997). Development and test of the distributed HBV-96 hydrological model. Journal of Hydrology, 201(1), 272-288.

Littlewood, I.G., Down, K., Parker, J.R., Post, D.A. (1997). IHACRES Version 1.0 User Guide. Institute of Hydrology, Wallingford, U.K. 97 pp.

Liu, Y., Brown, J., Demargne, J., & Seo, D.-J. (2011). A wavelet-based approach to assessing timing errors in hydrologic predictions. Journal of hydrology, 397(3–4), 210-224. http://dx.doi.org/10.1016/j.jhydrol.2010.11.040.

Li, Z. J., Cheng, Y., and Xu, P. Z. (2006a). Application of GIS-based hydrological models in humid watersheds. Water for Life: Surface and Ground Water Resources, Proceedings of the 15th APD-IAHR & ISMH, 685-690. Madras.

Li, Z. J., Zhang, K. (2008). Comparison of three GIS-based hydrological models. Journal of Hydrologic Engineering, 13(5), 364-370. http://doi:10.1061/(ASCE)1084-0699(2008)13:5(364).

Lu, M.J., Koike, T., Hayakawa, N. (1989). Development of a Precipitation-Runoff Model Corresponding to Distributed Hydrological Information (in Japanese), PhD Thesis, Nagaoka University, pp. 34–35.

Liu, Z., and Todini, E. (2002). Towards a comprehensive physically-based rainfall-runoff model. Hydrology and Earth System Sciences, 6(5), 859-881.

Maleksaeidi, H., Keshavarz, M., Karami, E., Eslamian, S., (2017). Climate Change and Drought: Building Resilience for an Unpredictable Future, Ch. 9 in Handbook of Drought and Water Scarcity, Vol. 2: Environmental Impacts and Analysis of Drought and Water Scarcity, Ed. by Eslamian S. and Eslamian F., Francis and Taylor, CRC Press, USA, 163-186.

Manandhar, S., Pandey, V. P., & Kazama, F. (2013). Climate change and adaptation: an integrated framework linking social and physical aspects in poorly-gauged regions. Climatic change, 120(4), 727-739.

McCarthy, J. J. (2001). Climate change 2001: impacts, adaptation, and vulnerability: contribution of Working Group II to the third assessment report of the Intergovernmental Panel on Climate Change: Cambridge University Press.

McFarlane, D., Stone, R., Martens, S., Thomas, J., Silberstein, R., Ali, R., Hodgson, G. (2012). Climate change impacts on water yields and demands in south-western Australia. Journal of Hydrology, 475, 488-498. http://dx.doi.org/10.1016/j.jhydrol.2012.05.038.

McVicar, T. R., Donohue, R. J., O'Grady, A. P., & Li, L. T. (2010). The effects of climatic changes on plant physiological and catchment ecohydrological processes in the high-rainfall catchments of the Murray-Darling Basin: A scoping study. Prepared for the Murray-Darling Basin Authority (MDBA) by the Commonwealth Scientific and Industrial Research Organization (CSIRO) Water for a Healthy Country National Research Flagship, MDBA, Canberra, ACT, Australia.

Michaels, P.J. (2005). The Prediction of Distortion of Global Warming by Scientists, Politicians and the Media. Cato Institute.

Minville, M., Brissette, F., & Leconte, R. (2008). Uncertainty of the impact of climate change on the hydrology of a nordic watershed. Journal of hydrology, 358(1), 70-83. http://dx.doi.org/10.1016/j.jhydrol.2008.05.033.

Moss, R. H., Edmonds, J. A., Hibbard, K. A., Manning, M. R., Rose, S. K., Van Vuuren, D. P., . . . Kram, T. (2010). The next generation of scenarios for climate change research and assessment. Nature, 463(7282), 747-756.

Murphy, B. F., & Timbal, B. (2008). A review of recent climate variability and climate change in south-eastern Australia. International Journal of climatology, 28(7), 859-879.

Nash, J. E., & Sutcliffe, J. V. (1970). River flow forecasting through conceptual models part I—A discussion of principles. Journal of hydrology, 10(3), 282-290. http://dx.doi:10.1016/0022-1694(70)90255-6.

Nawarathna, N. B., Ao, T., Kazama, S., Sawamoto, M., & Takeuchi, K. (2001). Influence of human activities on the BTOPMC model runoff simulations in large-scale watersheds. In PROCEEDINGS OF THE CONGRESS-INTERNATIONAL ASSOCIATION FOR HYDRAULIC RESEARCH (pp. 93-99).

Nayak, P. C., Sudheer, K. P., Rangan, D. M., & Ramasastri, K. S. (2005). Short-term flood forecasting with a neuro-fuzzy model. Water Resources Research, 41(4), W04004. http://doi:10.1029/2004wr003562.

Nazif, S. and Tavakolifar, H., Eslamian, S., 2017, Climate Change Impact on Urban Water Deficit, Ch. 5 in Handbook of Droughtand Water Scarcity, Vol. 2: Environmental Impacts and Analysis of Drought and Water Scarcity, Ed. by Eslamian S. and Eslamian F., Francis and Taylor, CRC Press, USA, 81-106.

Normand, S., Konz, M., & Merz, J. (2010). An application of the HBV model to the Tamor Basin in Eastern Nepal. Journal of Hydrology and Meteorology, 7(1), 49-58.

NSW Department of Infrastructure, Planning and Natural Resources. (2002). Geomorphic Categorisation of Streams in the Wybong Creek Catchment. Australia.

NSW government, the office of Environment and Heritage, (2016). http://www.environment.nsw.gov.au/threatenedSpeciesApp/cmaSearchResults.aspx?SubCmaId=122. (Accessed 6th December 2016).

Nunez, M., McGregor, J. L. (2007). Modelling future water environments of Tasmania, Australia. Climate Research: Interactions of Climate with Organisms, Ecosystems, and Human Societies, 34(1), 25-37. http://dx.doi:10.3354/cr034025.

O'Connell, P. E. (1970). River flow forecasting through conceptual models part II - The Brosna catchment at Ferbane. Journal of hydrology, 10(4), 317-329.

O'Connor K. M. (2006). River flow forecasting. In River basin modelling for flood risk mitigation: Taylor & Francis.

Onyutha, C., Tabari, H., Rutkowska, A., Nyeko-Ogiramoi, P., & Willems, P. (2016). Comparison of different statistical downscaling methods for climate change rainfall projections over the Lake Victoria basin considering CMIP3 and CMIP5. Journal of Hydro-environment Research, 12, 31-45.

Osman, Y., Al-Ansari, N., Abdellatif, M., Aljawad, S. B., & Knutsson, S. (2014). Expected future precipitation in central Iraq using LARS-WG stochastic weather generator. Engineering, 6(13), 948.

Peel-Harvey Catchment Council (2012). Adapting to climate change in the Peel region: Improving local government emergency management and biodiversity conservation services. A report by Kim Byrnes to the PHCC, edited by Andrew Del Marco, Mandurah, Western Australia.

Phan, T. T. H., Sunada, K., Oishi, S., & Sakamoto, Y. (2010). River discharge in the Kone River basin (Central Vietnam) under climate change by applying the BTOPMC distributed hydrological model. Journal of Water and Climate Change, 1(4), 269-279.

Peng, H., Jia, Y., Qiu, Y., Niu, C., & Ding, X. (2013). Assessing climate change impacts on the ecohydrology of the Jinghe River basin in the Loess Plateau, China. Hydrological sciences journal, 58(3), 651-670.

Perrin, C., Michel, C., Andréassian, V. (2003). Improvement of a parsimonious model for streamflow simulation. J. Hydrol. 279 (1–4), 275–289.

Photiadou, C., van den Hurk, B., van Delden, A., & Weerts, A. (2016). Incorporating circulation statistics in bias correction of GCM ensembles: hydrological application for the Rhine basin. Climate Dynamics, 46(1-2), 187-203.

Pittock, A. B. (2003). Climate change: an Australian guide to the science and potential impacts. Published by the Australian Greenhouse Office, the lead Australian Government agency on greenhouse matters.

Piotrowski, A. P., & Napiorkowski, J. J. (2011). Optimizing neural networks for river flow forecasting-Evolutionary Computation methods versus the Levenberg–Marquardt approach. Journal of Hydrology, 407(1–4), 12-27. http://dx.doi.org/10.1016/j.jhydrol.2011.06.019.

Pourmokhtarian, A., Driscoll, C. T., Campbell, J. L., Hayhoe, K., Stoner, A. M., Adams, M. B., Burns, D., Fernandez, I., Mitchell, M. & Shanley, J. B. (2017). Modeled ecohydrological responses to climate change at seven small watersheds in the northeastern United States. Global change biology, 23(2), 840-856.

Power, S., Sadler, B., & Nicholls, N. (2005). The influence of climate science on water management in Western Australia: Lessons for climate scientists. Bulletin of the American Meteorological Society, 86(6), 839.

Praskievicz, S., Chang, H. (2009). A review of hydrological modelling of basin-scale climate change and urban development impacts. Progress in Physical Geography, 33(5), 650-671. http://dx.doi:10.1177/0309133309348098.

Refsgaard, J. C. (1997). Parameterisation, calibration and validation of distributed hydrological models. Journal of hydrology, 198(1–4), 69-97. http://dx.doi.org/10.1016/S0022-1694(96)03329-X.

Refsgaard, J. C., Storm, B. (1995). MIKE SHE. In V. P. Singh, Computer models in hydrology (pp. 809-846), Water Resources Publications. Colorado, USA.

Santer, B.D., Wigley, T.M.L., Simmons, A.J. (2004). Identification of anthropogenic climatic change using a second-generation reanalysis. J. Geophys. Res.-Atmos. 109, D21104.

Scafetta, N., West, B.J. (2006). Phenomenological solar contribution to the 1900–2000 global surface warming. Geophys. Res. Lett. 33. http://dx.doi.org/10.1029/2005GL025539.

Seibert, J. (2005). HBV light version 2. User's manual. Stockholm University.

Seiler, K.P., GU, W.Z., Stichler, W. (2008). Transient response of groundwater systems to climate changes. In: Dragoni, W., Sukhija, B.S. (Eds.), Climate Change and Groundwater. Geological Society, London, Special Publication, pp. 288.

Semenov, M. A., Barrow, E. M. (1997). Use of a stochastic weather generator in the development of climate change scenarios. Climatic change, 35(4), 397-414. http://dx.DOI:10.1023/A:1005342632279.

Semenov, M. A., Barrow, E. M., & Lars-Wg, A. (2002). A stochastic weather generator for use in climate impact studies. User's manual, Version, 3.

Semenov, M. A., Stratonovitch, P. (2010). Use of multi-model ensembles from global climate models for assessment of climate change impacts. Climate research, 41(1), 1-14. http://dx.doi:10.3354/cr00836.

Sene, K. (2010). Hydrometeorology: Forecasting and applications: Springer. http://dx.doi.org/10.1007/978-90-481-3403-8.

Shi, P., Zhou, M., Qu, S., Chen, X., Qiao, X., Zhang, Z., & Ma, X. (2013). Testing a conceptual lumped model in karst area, Southwest China. Journal of Applied Mathematics.

Silberstein, R. P., Aryal, S. K., Durrant, J., Pearcey, M., Braccia, M., Charles, S. P., McFarlane, D. J. (2012). Climate change and runoff in south-western Australia. Journal of Hydrology, 475, 441-455. http://dx.doi:10.1016/j.jhydrol.2012.02.009.

Silva GHAC, Magome J, Ishidaira H. (2010). Application of YHyM/BTOPMC to assess hydrological response of Gin River baisn at southern Sri Lanka. In Platform Presentation Proceedings of The 8th International Symposium on South East Asian Water Environment 8:10–17.

Singer, S.F., Avery, D.T. (2006). Unstoppable Global Warming: Every 1500 Years. Rowman and Littlefield Publishers, Inc., Lanham MD.

Singh P, Bengtsson L. (2005). Impact of warmer climate on melt and evaporation for the rainfed, snowfed and glacier fed basins in the Himalayan region. Journal of Hydrology 300: 140–154.

Shrestha S, Bastola S, Babel MS, Dulal KN, Magome J, Hapuarachchi HAP, Kazama F, Ishidaira H, Takeuchi K. (2007). The assessment of spatial and temporal transferability of a physically based distributed hydrological model parameters in different physiographic regions of Nepal. Journal of Hydrology 347: 153–172.

Sperna Weiland, F., Buishand, A., Kraaijenbrink, P., Ruiter, A., van Pelt, S., Schellekens, J. & Beersma, J. (2013). Assessment of future changes in Meuse discharge extremes. In: In: EGU General Assembly Conference, 27 April–2 May, Vienna, Austria.

Solomon, S., Qin, D., Manning, M., Chen, Z., Marquis, M., Averyt, K., Tignor M. and Miller, H. (2007). Contribution of working group I to the fourth assessment report of the intergovernmental panel on climate change, 2007: Cambridge University Press, Cambridge.

South West Attraction. (2017). http://www.southwestattractions.com.au/harvey-dam-2.html. Accessed on April 2, 2017.

Stanhill, G., (2007). A perspective on global warming, dimming and brightening. EOS 88, 58–59.

Stern, N. (2007). Stern review: the economics of climate change. Available at http://www.hmtreasury.gov.uk/d/ExecutiveSummary.pdf. Accessed 9 March 2017.

Sugawara, M. (1979). Automatic calibration of the tank model. Hydrological Sciences Bulletin, 24(3), 375-388.

Sun, W., Wang, J., Li, Z., Yao, X., & Yu, J. (2014). Influences of climate change on water resources availability in Jinjiang Basin, China. The Scientific World Journal, 2014. http://dx.doi.org/10.1155/2014/908349.

Surfleet, C. G., Tullos, D., Chang, H., & Jung, I. W. (2012). Selection of hydrologic modelling approaches for climate change assessment: A comparison of model scale and structures. Journal of Hydrology, 464, 233-248. http://dx.doi.org/10.1016/j.jhydrol.2012.07.

Swedish Meteorological and Hydrological Institute (SMHI), 2012. Integrated Hydrological Modelling System (IHMS). User Manual, Version 6.3.

Svensmark, H. (2007). Cosmoclimatology: a new theory emerges. Astronom. Geophys. 48, 1.18–1.24.

Szépszó, G., Lingemann, I., Klein, B. & Kovács, M. (2014). Impact of climate change on hydrological conditions of Rhine and Upper Danube rivers based on the results of regional climate and hydrological models. Natural Hazards, 72(1), 241–262.

Takeuchi K, Ao TQ, Ishidaira H. (1999). For hydro-environmental simulation of a large ungauged basinintroduction of block-wise use of TOPMODEL and Muskingum-Cunge method. Hydrological Sciences Journal 44(4): 633–646.

Takeuchi, K., Hapuarachchi, P., Zhou, M., Ishidaira, H., & Magome, J. (2008). A BTOP model to extend TOPMODEL for distributed hydrological simulation of large basins. Hydrological Processes, 22 (17), 3236-3251.

Taylor, K. E., Stouffer, R. J., & Meehl, G. A. (2012). An overview of CMIP5 and the experiment design. Bulletin of the American Meteorological Society, 93(4), 485.

Teng, J., Vaze, J., Chiew, F.H.S., Wang, B., Perraud, J.M. (2012a). Estimating the relative uncertainties sourced from GCMs and hydrological models in modeling climate change impact on runoff. J. Hydrometeorol. 13(1), 122e139. https://doi.org/10.1175/JHM-D-11-058.1.

Teng, J., Chiew, F., Vaze, J., Marvanek, S., Kirono, D. (2012b). Estimation of climate change impact on mean annual runoff across continental Australia using Budyko and Fu equations and hydrological models. Journal of Hydrometeorology, 13(3), 1094-1106. http://dx.DOI:10.1175/JHM-D-11-097.1.

Teutschbein, C., & Seibert, J. (2012). Bias correction of regional climate model simulations for hydrological climate-change impact studies: Review and evaluation of different methods. Journal of Hydrology, 456, 12-29.

Timbal, B. (2004). Southwest Australia past and future rainfall trends. Climate Research, 26(3), 233-249.

Timbal, B. and Jones, D. (2008). Future projections of winter rainfall in southeast Australia using a statistical downscaling technique. Climate Change 86, 165–187. http://dx.DOI:10.1007/s10584-007-9279-7.

Timbal, B., P. Hope and S. Charles. (2008a). Evaluating the consistency between statistically downscaled and global dynamical model climate change projections, J. Climate, 21(22), 6052-6059. http://dx.doi.org/10.1175/2008JC LI2379.1.

Timbal. B., McAvaney, B. (2001). An analogue-based method to downscale surface air temperature: application for Australia. Clim Dyn 17:947–963.

Timbal, B., Li, Z., & Fernandez, E. (2008). The Bureau of meteorology statistical downscaling model graphical user interface: user manual and software documentation. Centre for Australian Weather and Climate Research.

Todini, E. (1988). Rainfall-runoff modeling - Past, present and future. Journal of hydrology, 100(1–3), 341-352. doi: http://dx.doi.org/10.1016/0022-1694(88)90191-6.

Todini, E. (1996). The ARNO rainfall-runoff model. Journal of Hydrology 175 (1-4), 339-382.

Todini, E., Ciarapica, L. (2001). The TOPKAPI model. Singh, V. P., and Frevert, D. K., eds., Mathematical Models of Large Watershed Hydrology. Littleton: Water Resources Publications, LLC.

Turner, M., Bari, M., Amirthanathan, G., & Ahmad, Z. (2012). Australian network of hydrologic reference stations-advances in design, development and implementation. In Hydrology and Water Resources Symposium 2012 (p. 1555). Engineers Australia.

United States Geological Survey (USGS). (2011). Global Land Cover Characteristics Data Base Version 2.0. Available online at: http://landcover.usgs.gov/landcoverdata.php, retrieved on 14th March 2017.

U.S. Army Corps of Engineers. (2015). Hydrologic Modeling System (HEC-HMS) Application Guide: Version 4.0; Institute for Water Resources, Hydrologic Engineering Center: Devis, CA, USA.

Vaze, J., Davidson, A., Teng, J., & Podger, G. (2011). Impact of climate change on water availability in the Macquarie-Castlereagh River Basin in Australia. Hydrological Processes, 25(16), 2597-2612.

Vaze, J., Jorda, P., Beecham, R., Frost, A. Summerell, G. (2012). Guidelines for rainfall-runoff modelling: Towards best practice model application. eWater cooperative research centre. ISSN- 978-1-921543-51-7.

Vaze, J., Post, D., Chiew, F., Perraud, J.-M., Viney, N., Teng, J. (2010). Climate non-stationarity–validity of calibrated rainfall–runoff models for use in climate change studies. Journal of Hydrology, 394(3), 447-457. http://dx.doi:10.1016/j.jhydrol.2010.09.018.

Vaze, J., Teng, J. (2011). Future climate and runoff projections across New South Wales, Australia: results and practical applications. Hydrological Processes, 25(1), 18-35. http://dx.DOI:10.1002/hyp.7812.

Wang, G. Q., Zhou, M. C., Takeuchi, K., and Ishidaira, H. (2007a). Improved version of BTOPMC model and its application in event-based hydrologic simulations. Journal of Geographical Sciences, 17(1), 73-84. http://doi:10.1007/s11442-007-0073-2.

Water and Rivers Commission. (2000). Stirling Dam Catchment Area Water Source Protection Plan: Perth Metropolitan and Harvey Town Water Supply, Water and Rivers Commission, Water Resource Protection Series No WRP 34.

Whitehead, P. G., Wilby, R. L., Battarbee, R. W., Kernan, M., Wade, A. J. (2009). A review of the potential impacts of climate change on surface water quality. Hydrological Sciences Journal, 54(1), 101-123. http://dx.doi.org/10.1623/hysj.54.1.101.

Wigmosta, M. S., Vail, L. W., and Lettenmaier, D. P. (1994). A distributed hydrology-vegetation model for complex terrain. Water Resources Research, 30(6), 1665-1679.

Wilks, D. S., & Wilby, R. L. (1999). The weather generation game: a review of stochastic weather models. Progress in Physical Geography, 23(3), 329-357. http://dx.doi:10.1177/030913339902300302.

Xu, Y.P., Zhang, X.J., Ran, Q.H., Tian, Y. (2013). Impact of climate change on hydrology of upper reaches of Qiantang River. Journal of Hydrology 483, 51–60.

Yang, D., Herath, S., and Musiake, K. (2002). A hillslope-based hydrological model using catchment area and width functions. Hydrological Sciences Journal, 47(1), 49-65. http://doi:10.1080/02626660209492907.

Yao, C., Li, Z. J., Bao, H. J., and Yu, Z. B. (2009). Application of a developed Grid-Xin'anjiang model to Chinese watersheds for flood forecasting purpose. Journal of Hydrologic Engineering, 14(9), 923-934. http://doi:10.1061/(ASCE)HE.1943-5584.0000067.

Yu, P. S., Yang, T. C., Kuo, C. M., Tseng, H. W., & Chen, S. T. (2014). Climate Change Impacts on Streamflow Drought: A Case Study in Tseng-Wen Reservoir Catchment in Southern Taiwan. Climate, 3(1), 42-62.

Yu, Z. (2000). Assessing the response of subgrid hydrologic processes to atmospheric forcing with a hydrologic model system. Global and Planetary Change, 25(1-2), 1-17.

Zalewski, M. (2002). Ecohydrology—the use of ecological and hydrological processes for sustainable management of water resources. Hydrological Sciences Journal, 47 (5), 823–832. http://dx.doi.org/10.1080/02626660209492.

Zareeian, M.J., Eslamian, S., Gohari, A., and Adamowski, J. (2017). The Effect of Climate Change on Watershed Water Balance, inMathematical Advances Towards Sustainable Environmental Systems, Ed. by Furze, J.N., Swing, K., Gupta, A.K., McClatchey, R.,Reynolds, D., Springer International Publishing, Switzerland, 215-238.

Zareian, Z., Eslamian, S., (2018). Using of Optimization Strategy for Reducing Water Scarcity in the Face of Climate Change, In Climate Change-Resilient Agriculture and Agroforestry: Ecosystem Services and Sustainability, by Paula Cristina Castro, Anabela Marisa Azul, Walter Leal Filho, and Ulisses M. Azeiteiro, Climate Change Management Book Series, Springer.

Zeng, X., Kiviat, K. L., Sakaguchi, K., & Mahmoud, A. M. A. (2012). A toy model for monthly river flow forecasting. Journal of Hydrology, 452–453(0), 226-231. http://dx.doi.org/10.1016/j.jhydrol.2012.05.053.

Zhang, L.P., Chen, X.F., Zhao, Z.P., Hu, Z.F. (2008). Progress in Study of Climate Change Impacts on Hydrology and Water Resources. Process in Geography 27 (3) 60–67.

Zhang R, Santos CAG, Moreira M, Freire PK, Corte-Real J. (2013). Automatic calibration of the SHETRAN hydrological modelling system using MSCE. Water Resour Manag 27(11):4053–4068.

Zhang, S. X., Bari, M., Amirthanathan, G., Kent, D., MacDonald, A., & Shin, D. (2014a). Hydrologic reference stations to monitor climate-driven streamflow variability and trends. In Hydrology and Water Resources Symposium 2014 (p. 1048). Engineers Australia.

Zhang, S. X., Amirthanathan, G. E., Bari, M., Laugesen, R., Shin, D, Kent, D., MacDonald, A., Turner, M. & Tuteja, N. K. (2016). How streamflow has changed across Australia since 1950's: evidence from the network of Hydrologic Reference Stations. Hydrology and Earth System Sciences, 20(9), 3947.

Zhang, Y., Vaze, J., Chiew, F. H., Teng, J., & Li, M. (2014). Predicting hydrological signatures in ungauged catchments using spatial interpolation, index model, and rainfall–runoff modelling. Journal of hydrology, 517, 936-948.

Zhou MC, Ishidaira H, Hapuarachchi HP, Magome J, Takeuchi K. (2006). Adaptive Muskingum-Cunge routing method for distributed hydrological modeling in large river basins. 3rd APHW Conference, 16–18 October 2006, Bangkok, Thailand.

Zhao, R. J. (1992). The Xin'anjiang model applied in China. Journal of Hydrology, 135(1-4), 371-381. http://doi:10.1016/0022-1694(92)90096-E.

Zorita, E., Von Storch, H. (1999). The analog method as a simple statistical downscaling technique: comparison with more complicated methods. Journal of climate, 12(8), 2474-2489.